TerraNotes Ltd GEOPHYSICS ©TerraNotes Ltd 2007-2013

Geophysical Interpretation of the Rory Claim Group, Yukon

Prepared for

Guyana Precious Metals Inc.

Prepared by

Volkan Tuncer, P. Geo.

Lei Sha, P. Geo.

Michael Moore, G.I.T.

Julien Lambert, C.E.O.

03 Jan 2013

Executive Summary

©TerraNotes Ltd 2007-2013

The airborne magnetic and frequency domain EM (DIGHEM) survey, commissioned by Coronation Minerals Inc. (now Guyana Precious Metals Inc. as filed in the Whitehorse Mining Recorders office in August, 2008), was acquired over the Rory claim group in Yukon forms the basis of this interpretation work. The DIGHEM data were analyzed, mapped and interpreted using the TerraNotes WorkFlow™. Over 300 geophysical maps were produced. This report presents the 123 most significant maps with their description and main findings. The other maps are provided in Appendix. The maps are also provided in a separate folder in jpeg/png formats. Overall findings are as follows:

Magnetics

- High magnetic anomalies are interpreted as the ultramafic rocks and the gabbro intrusion.
- Weak magnetic anomalies are amplified and interpreted. Most of these anomalies are interpreted as mafic rocks of the Nicolai formation or as conduit/feeder zones.
- The contact zones of all the magnetic structures are delineated to reveal the possible Ni-Cu-PGE mineralization zones.

Electromagnetics

- The EM conductors are identified and integrated both visually and mathematically with the topography and magnetic maps. Strong bedrock conductors were separated from the near-surface weaker conductors.

Integration of geophysics and geochemistry

- Coincident magnetic and conductive zones are selected as high priority targets for Ni-Cu-PGE mineralization. This coincidence resembles the Wellgreen mineralization.
- Based on Copper and Nickel anomalies in soil, the northern Rory and gabbroic intrusion area are found to be interesting for further exploration. These high magnetic anomalies are selected as secondary targets.

Regions of Interest

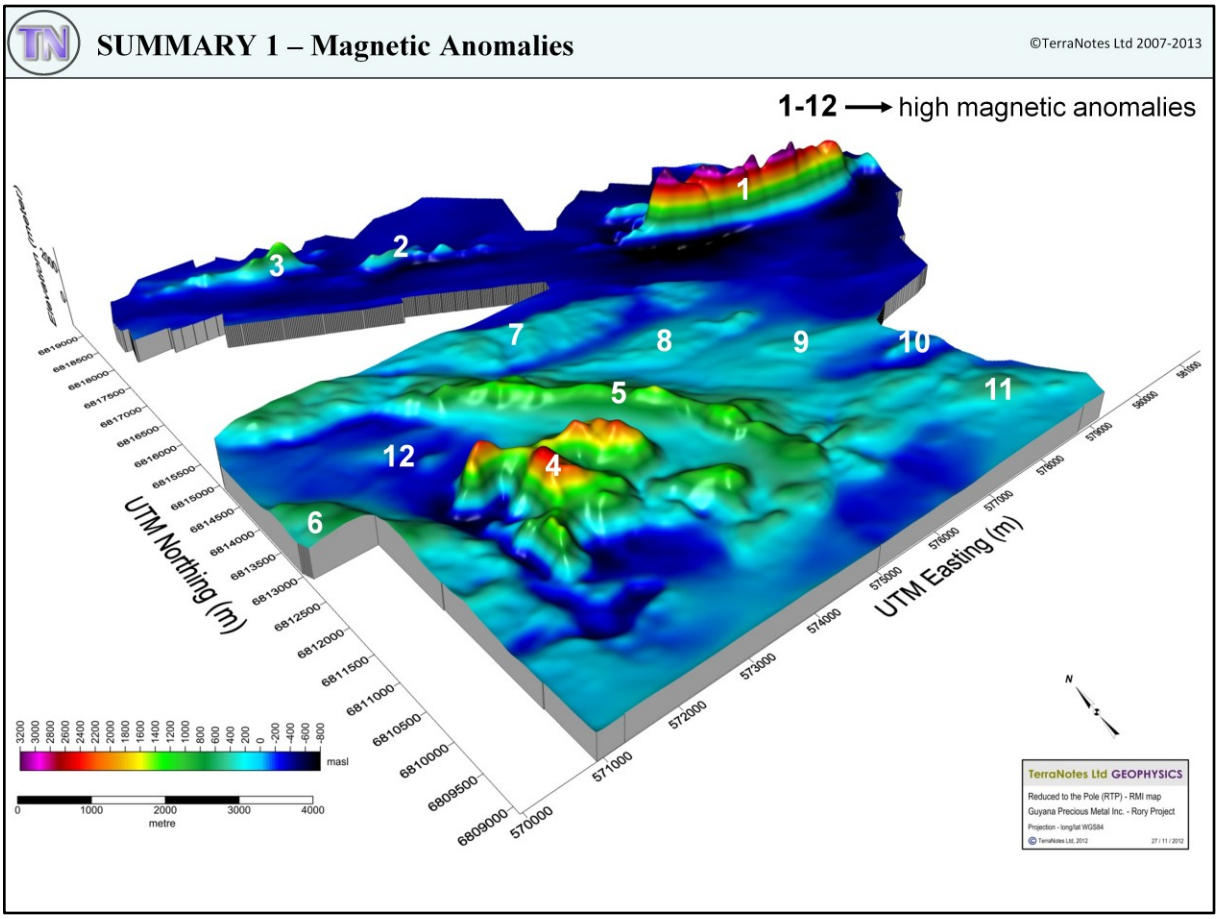
- A total of sixteen (16) Regions of Interest (ROI) have been selected for further Ni-Cu-PGE exploration. These ROIs are classified into three groups according to their conductive and magnetic properties.
- ROI-1 and -2 are interpreted as the most important coincident magnetic and EM anomalies.

Recommendations for further analysis of the geophysical and geochemical data are proposed including the production of detailed maps for each ROI as they may play a crucial role in the design of the drilling grids and the collar placements.

Table of contents

©TerraNotes Ltd 2007-2013

Summary 4
Introduction: Claim Group Location and Geology 13
Topography: Digital Elevation Model 19
Magnetic Data 23
Collected Data and Corrections 23
Amplifications 32
Electromagnetic Data 40
Collected EM Data 40
Calculated Apparent Resistivities 49
Calculated Apparent Depths 53
Comparative Amplifications 57
Amplifications 62
Soil Geochemistry Overlays: Cu and Ni Overlays 81
Integration of Soil Geochemistry with Geophysics: Ternary Geochemistry and Geophysics Maps 90
3-Dimensional Integration of Geophysical Data: Topography, Magnetics, and Electromagnetics 101
Analysis and Interpretation of Selected Profiles 113
Regions of Interest 128
Conclusions and Recommendations 153
Conclusions 154
Recommendations 155
Copyright 156
Disclaimer 157
Appendices 158
Appendix A: Separation of Magnetic Field (Regional and Local) 158
Appendix B: List of Figures 168
Appendix C: List of Claims 172
Certificate of Qualified Person 176

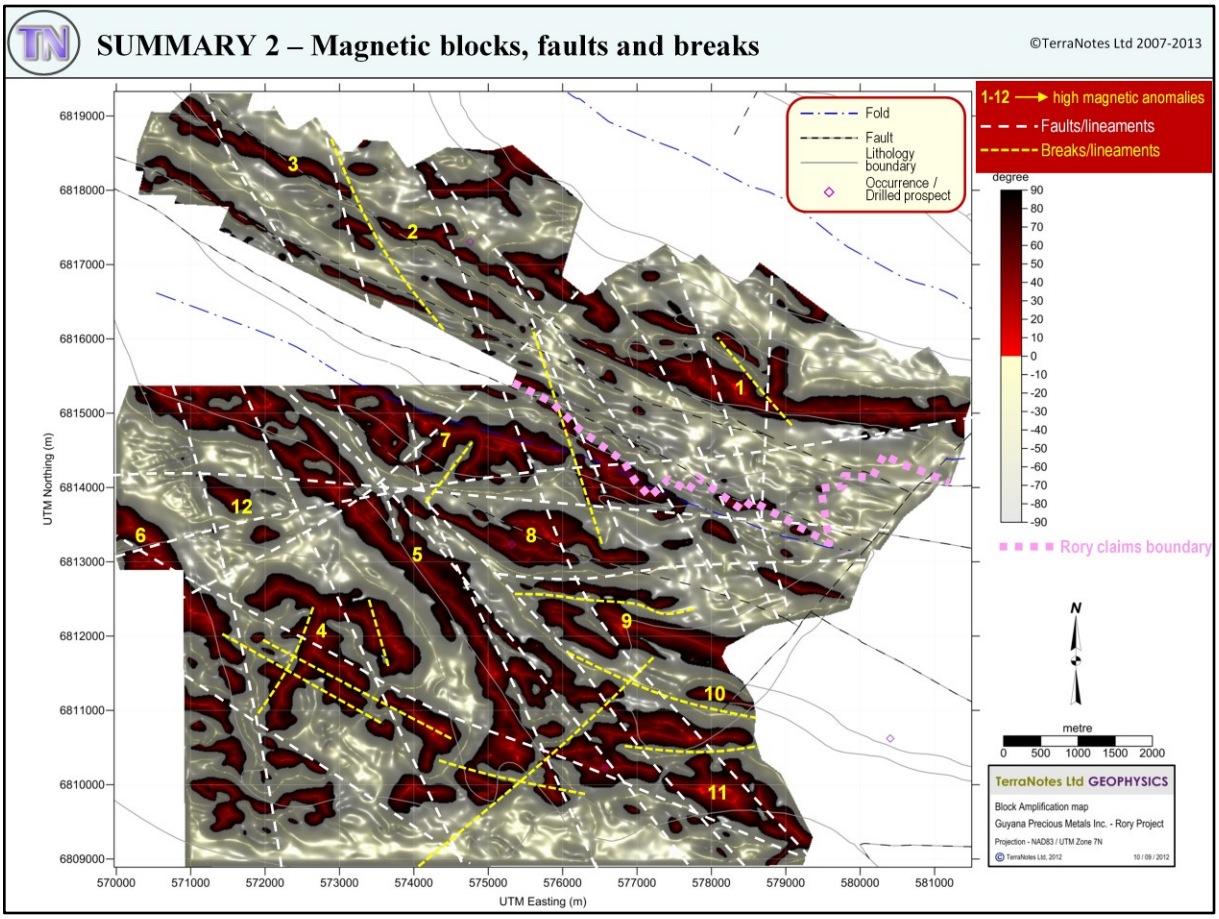


SUMMARY 1 – Magnetic Anomalies

The strength of the magnetic Anomalies 1 through 12 are visible in the map above.

Anomalies 1 and 5 are strong anomalies with linear characteristics. Other linear characteristic anomalies can be listed as Anomalies 2, 3, 9 and 10.

The other anomalies have more elliptical shapes, the strongest of which is Anomaly 4. Anomaly 4 may represent a gabbro intrusion, whereas the other elliptical anomalies (7–11) may represent the Nicolai formation.



SUMMARY 2 – Magnetic blocks, faults and breaks

It is known that the economic Cu-Ni and PGE mineralization occurs at the basal contact of the red area in Anomaly 1. Hence the red colour anomalies may be of interest for further Cu-Ni and PGE exploration.

The yellow letters mark the significant magnetic anomalies.

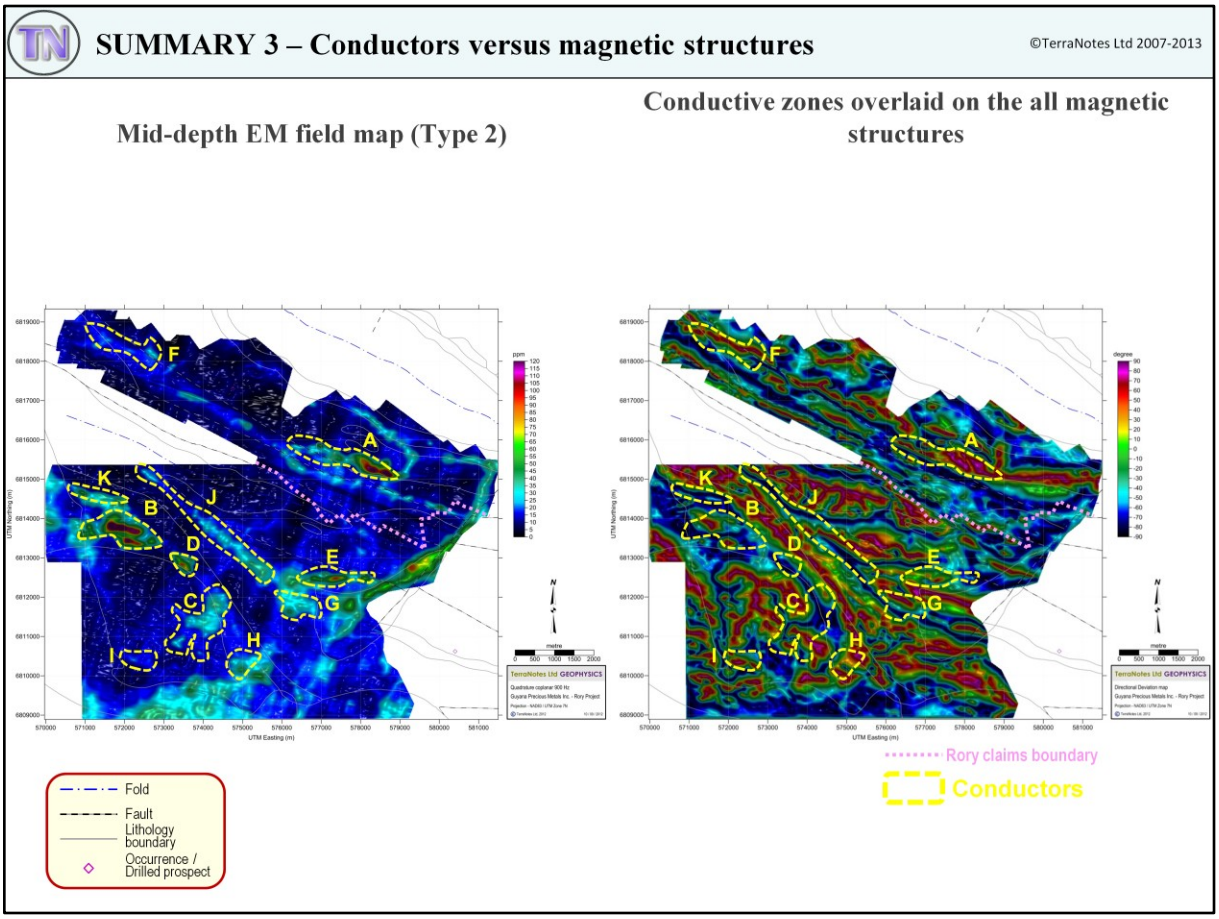
Please note that magnetite, pyrrhotite, ilmenite and/or franklinite may be present within the red blocks since they exhibit high magnetism. Pyrrhotite particularly is very important for Cu-Ni and PGE exploration. It is interpreted that magnetic Anomalies 1, 9, and 12 may contain conductive and magnetic pyrrhotite.

The dashed white lines indicate the continuous fault-like low magnetic lineaments.

The dashed yellow lines indicate the short distance, non-continuous low magnetic breaks.

The pink dotted line approximately separates the Rory claims from the other claims.

The location of the faults and breaks (white and yellow dashed lines) fit well with the shape of the anomalies.



SUMMARY 3 – Conductors versus magnetic structures

The dashed polygons and the letters delineate the significant conductive zones that are observed in the left map. The conductive zones that are thought to be associated with topographical features were not marked in the above maps.

Anomaly A coincides with the high magnetic structure and may be associated with Cu-Ni-PGE mineralization.

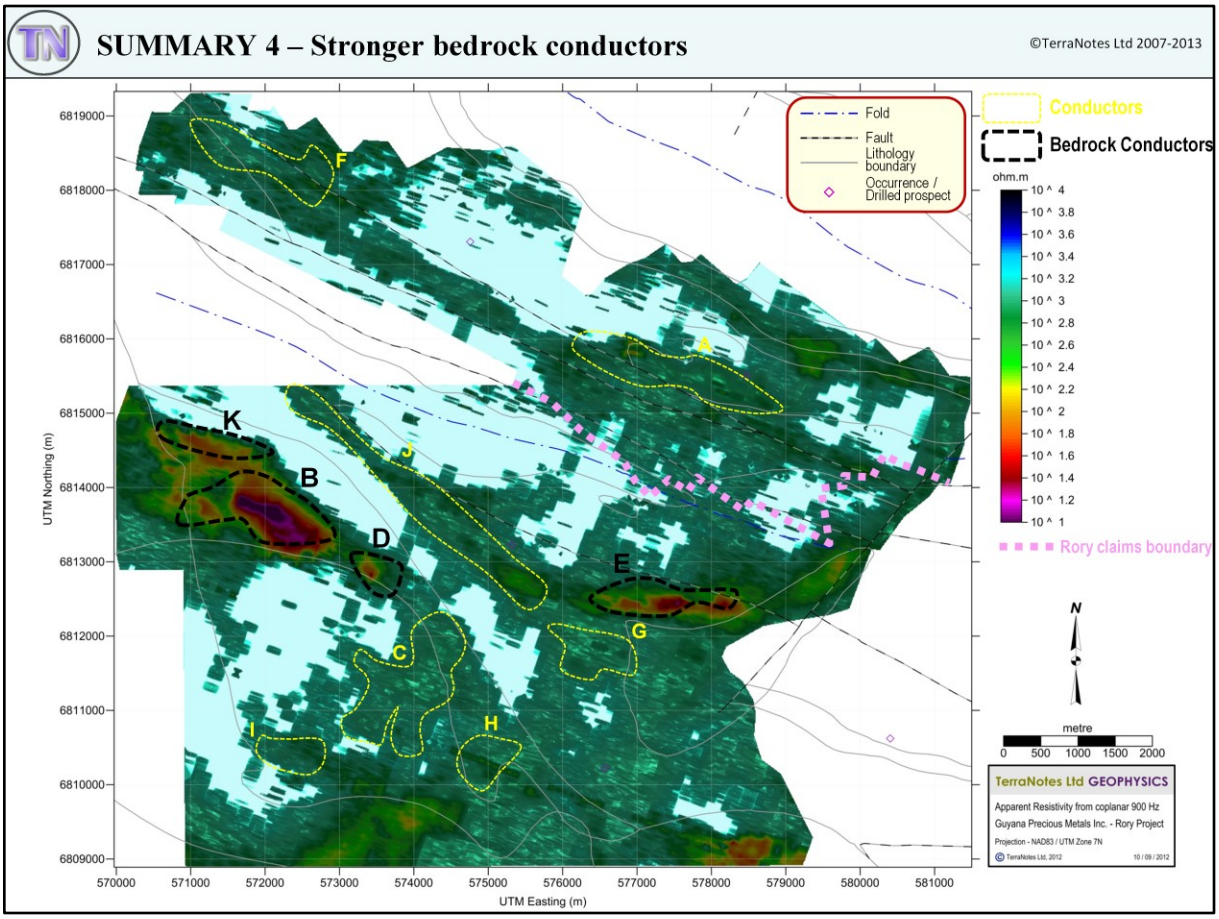
Anomaly B also coincides with the high magnetic structure and it might be associated with Cu-Ni-PGE mineralization.

Anomaly E also coincides with the high magnetic structure and may be associated with Cu-Ni-PGE mineralization.

Anomaly F also coincides with the high magnetic structure and may be associated with Cu-Ni-PGE mineralization.

Anomaly I, which does not show very strong bedrock conductor characteristics, also coincides with the high magnetic structure and may be associated with Cu-Ni-PGE mineralization.

The rest of the conductors (C, D, G, H, J and K) seem to coincide with the low magnetic zones and structures. They may indicate non-magnetic sulphides, graphitic conductors, alterations, or other conductive geological formations.



SUMMARY 4 – Stronger bedrock conductors

The black dashed polygons indicate the interpreted bedrock conductors. Anomaly B is very strong conductor with less than 10 Ω·m resistivity. Anomaly E become stronger conductor (~10 Ω·m) with depth as well.

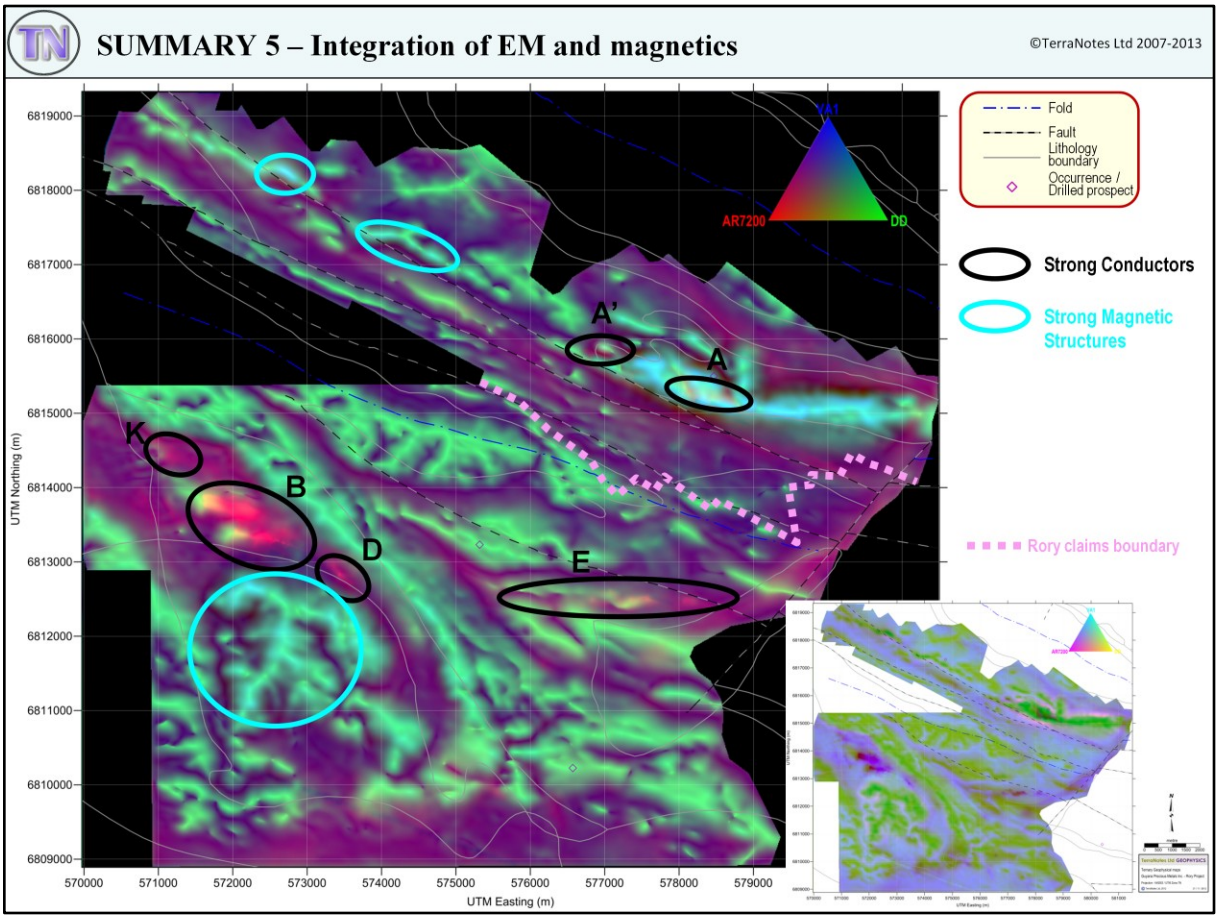
Since Anomaly B and E are associated with weak to intermediate magnetic anomalies, they may indicate sulphide mineralization that could be associated with Cu-Ni-PGE mineralization.

Anomaly K occurs on a low magnetic zone immediately east of a very weak magnetic anomaly. It could be sulphide or graphite mineralization.

Anomaly D also occurs on a low magnetic trend between two magnetic highs. It could be a graphitic conductor, but sulphide possibility for this location should also be investigated.

Other conductive anomalies (A, C, F, G, H, I, and J) give a non-anomalous background resistivity around 1000 Ω·m. It is either because the susceptibility effect increases the resistivity (i.e. Anomaly A and F) or they are surficial conductors and their resistivity is increasing with depth at these locations, although the overall background resistivity decrease with depth.

Fugro's algorithm could not calculate the apparent resistivity of the very resistive zones (see flat lying cyan colour zones).



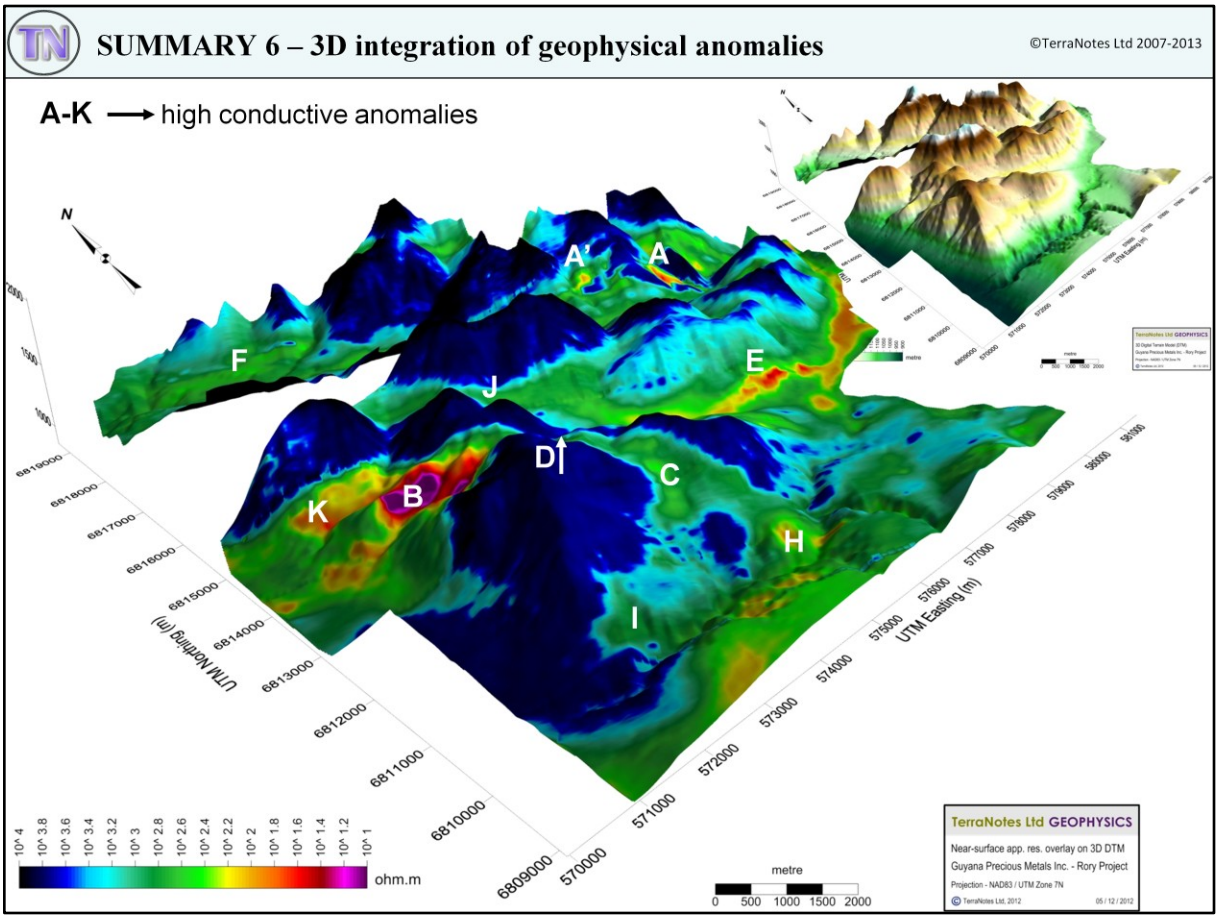
SUMMARY 5 – Integration of EM and magnetics

The black ellipses (Anomalies B, D, E, and K) exhibit brighter yellow-red anomalies near the cyan-green anomalies which indicate coincident magnetic and conductive anomalies. Hence, they are the first priority targets for further Cu-Ni-PGE exploration.

The difference is observed in the Wellgreen area (A and A'). The magnetic structure is very strong (as the cyan colour suggests) and the conductor beneath this structure is observed in the near-surface.

The strong conductors may be more visible in the CMY colour map (inset map at the bottom right) with dark (almost black colour) anomalies. Particularly A, A', two anomalies in B, and E are clearer in the inset map.

The cyan ellipses mark the other cyan anomalies which may indicate the ultramafic intrusions in the north (in the Arch claims) and the interpreted gabbro intrusion in the southwest.

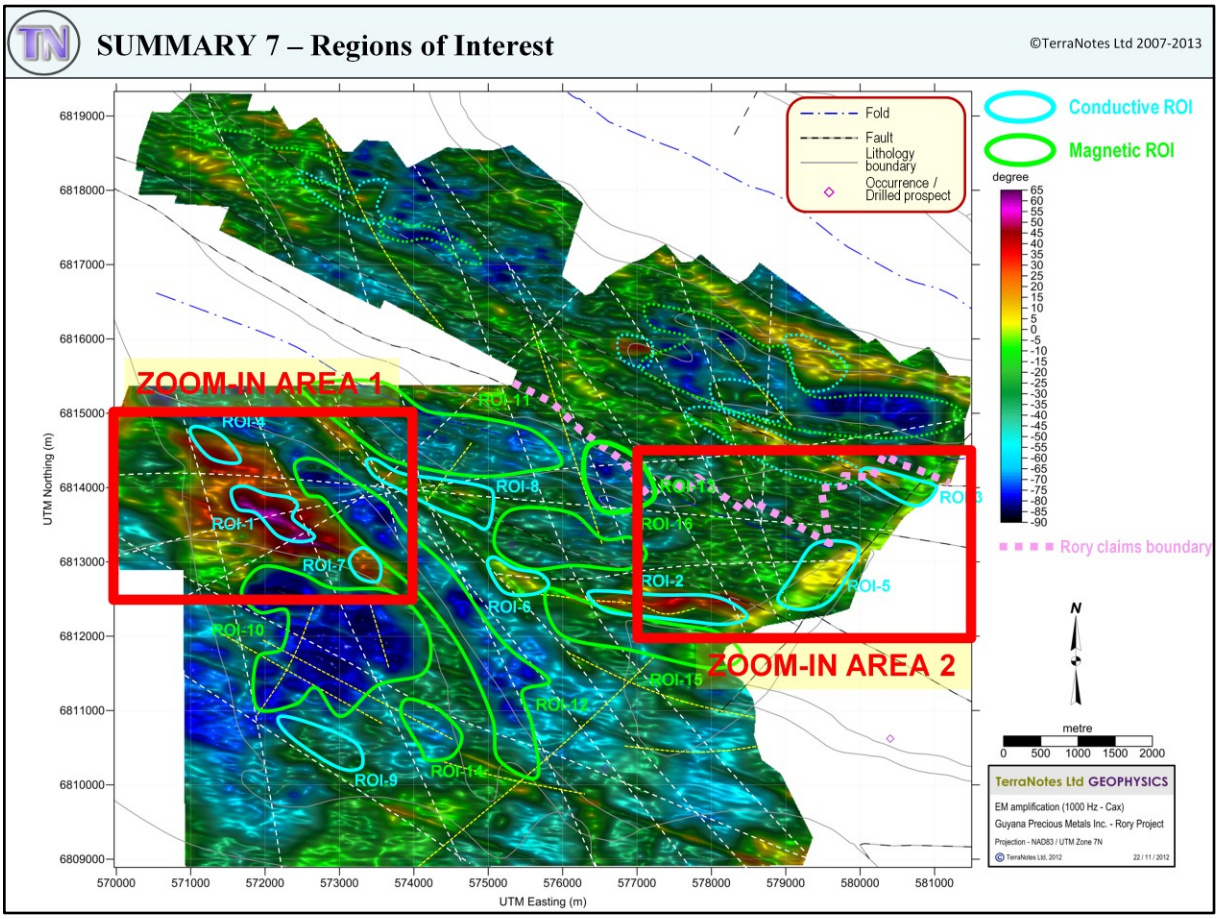


SUMMARY 6 – 3D integration of geophysical anomalies

As can be seen from the map above, the most conductive zones are located on the high topographic areas or on the flanks of these areas. Hence, they should not be due to the erosions by rivers, creeks, etc.

On the other hand, weaker conductive trends are following the creeks and valleys and are probably due to transported sediments. These anomalies are identified throughout the report.

The letters above indicate the locations of the previously identified conductive anomalies. Please note that Anomaly D is not visible since it is located behind the hill.



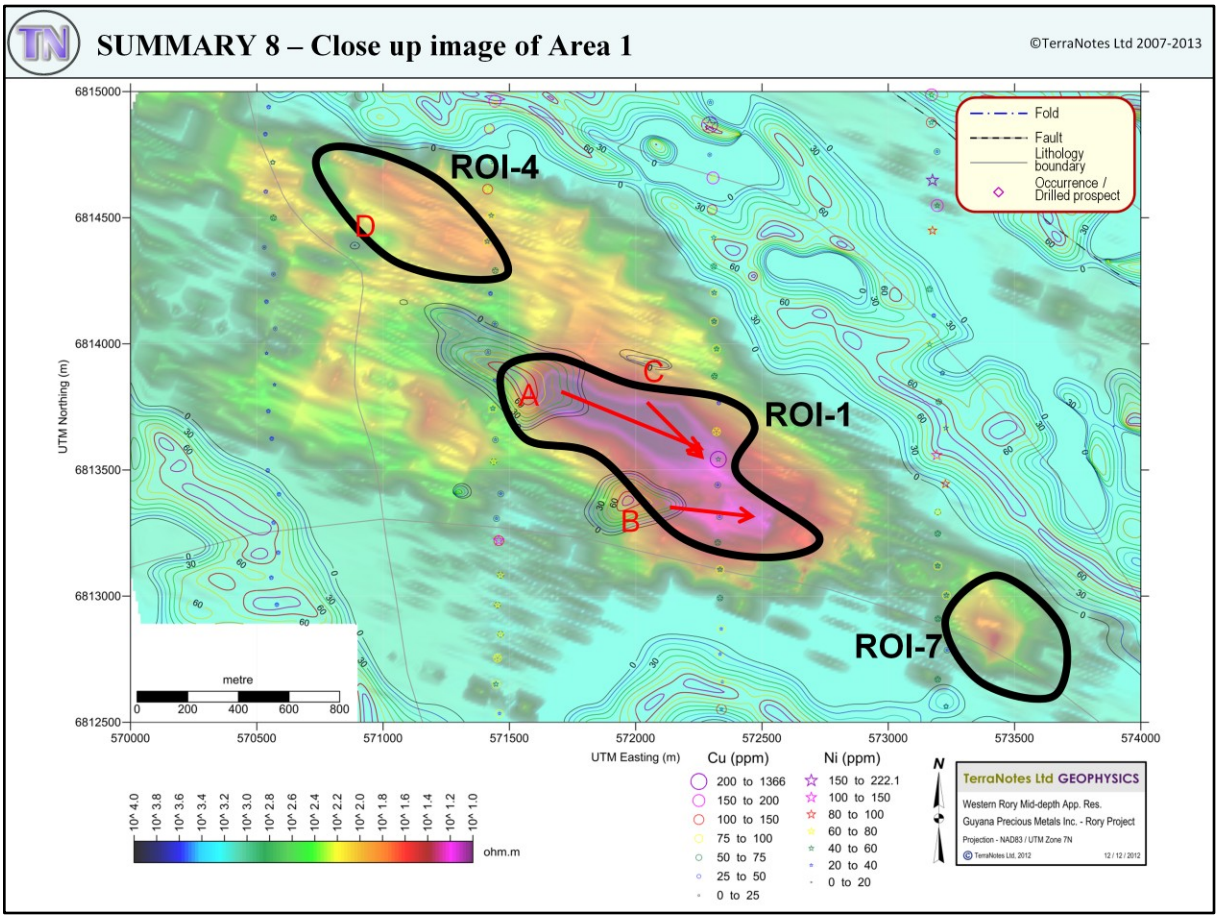
SUMMARY 7 – Regions of Interest

A total of sixteen (16) Regions of Interest (ROI) have been selected for further exploration. These ROIs are classified as: 1) conductive (first nine, indicated by cyan polygons) or 2) magnetic (remaining seven, indicated by green polygons).

Outside the Rory claim group, 5 EM anomalies and two magnetic anomalies were selected as further ROI in the Wellgreen and Arch properties.

As seen above, ROI-1 and ROI-2 are the strongest EM anomalies. All the cyan anomalies show some degree of high EM conductivity. The green ROI exhibit low conductivity and high susceptibility. Hence, deep penetrating EM methods are recommended to assess what is beneath the green ROI.

ROI-1 and ROI-2 are selected as the most important coincident magnetic and EM anomalies. Close-up maps and interpretation are given in the vicinity of these ROI as marked by the red boxes (see Summary-8 and Summary-9). The red boxes mark two crucial areas for possible Cu-Ni-PGE mineralization.



SUMMARY 8 – Close up image of Area 1 that includes ROI-1, -4 and -7.

The contours indicate the high magnetic anomalies of the magnetic structures map to evaluate the relationship between the EM conductors and magnetic anomalies.

The black polygons indicate ROI-1, -4, and -7.

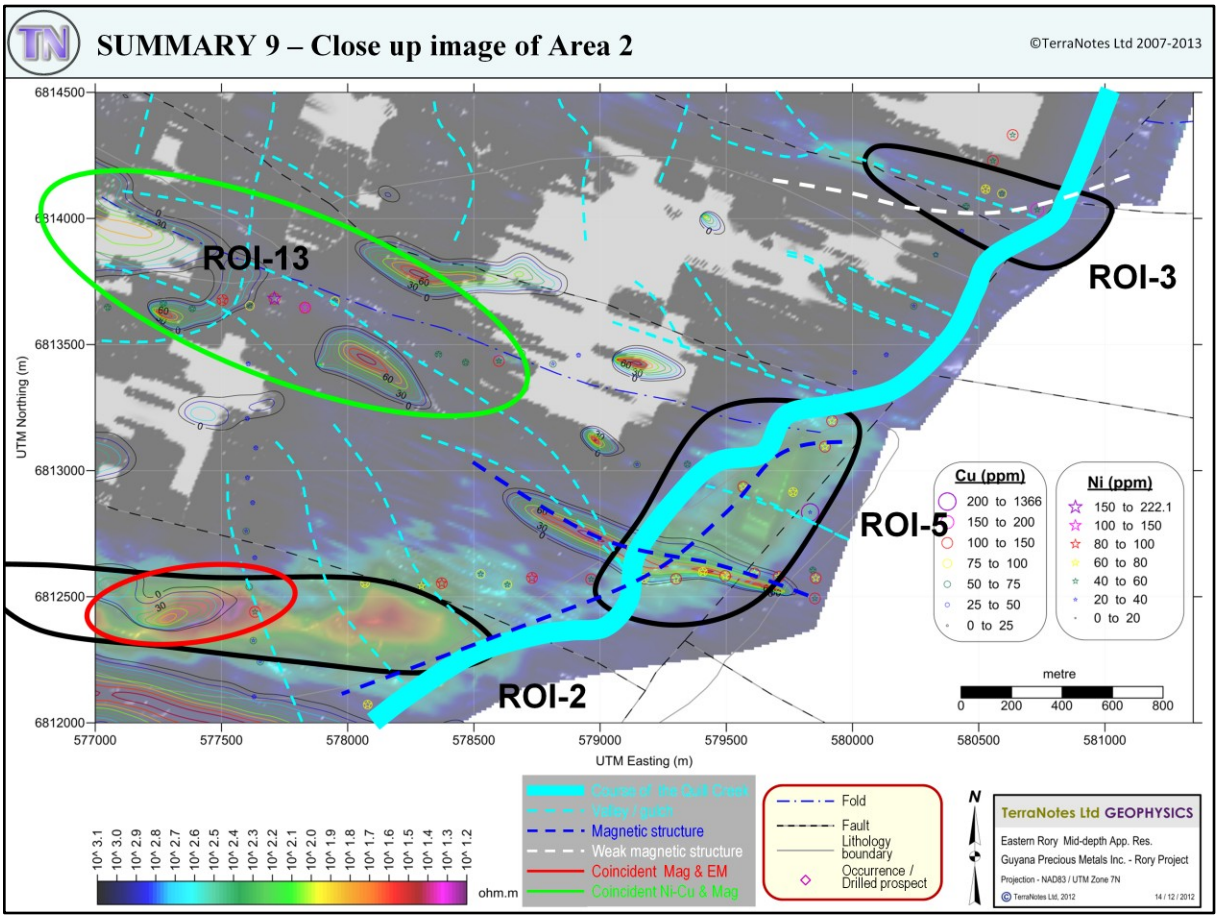
ROI-1 exhibits three different conductive trends immediately below the surface. The red arrows show the orientation of these trends. The letters mark the locations of the weaker magnetic highs (coloured contours) deduced from the magnetic amplification maps. Therefore, the conductive trends (red arrows) may represent the sulphide mineralization at the contact of the interpreted conduits. Because, each arrow is associated with one weak magnetic anomaly (A, B or C).

The conductive trends that seem to be coming from magnetic anomalies A and C appear to merge at mid-depth. The conductive zone from magnetic anomaly A appears to extend deeper.

Copper value in soil is very anomalous (> 200 ppm) where the two red arrows from magnetic Anomalies A and C merge (see purple circle). The Ni value in the soil at the same location is between 40 and 60 ppm (the small green star within the purple circle). Immediately north of that point (yellow marks), the soil contains 75-100 ppm Cu and 60-80 ppm Ni.

ROI-4 is associated with a very weak magnetic anomaly which is not shown here, whereas ROI-7 occurs in a low magnetic zone.

On the other hand, more anomalous Cu and Ni in soil is found on the more resistive zones in the north. Deep penetrating geophysical EM methods should be used in this area to thoroughly evaluate its potential.



SUMMARY 9 – Close up image of Area 2 that includes ROI-2, -3, -5 and -13.

The contours indicate the high magnetic anomalies from the magnetic structures map to evaluate the relationship between the EM conductors and magnetic anomalies.

The black polygons indicate ROI-2, -3, -5, and -13.

The thick cyan line indicates the course of Quill Creek and the thin, dashed cyan lines mark significant valleys that have been observed on the DTM map.

The dashed white line indicates a very weak magnetic trend within ROI-3.

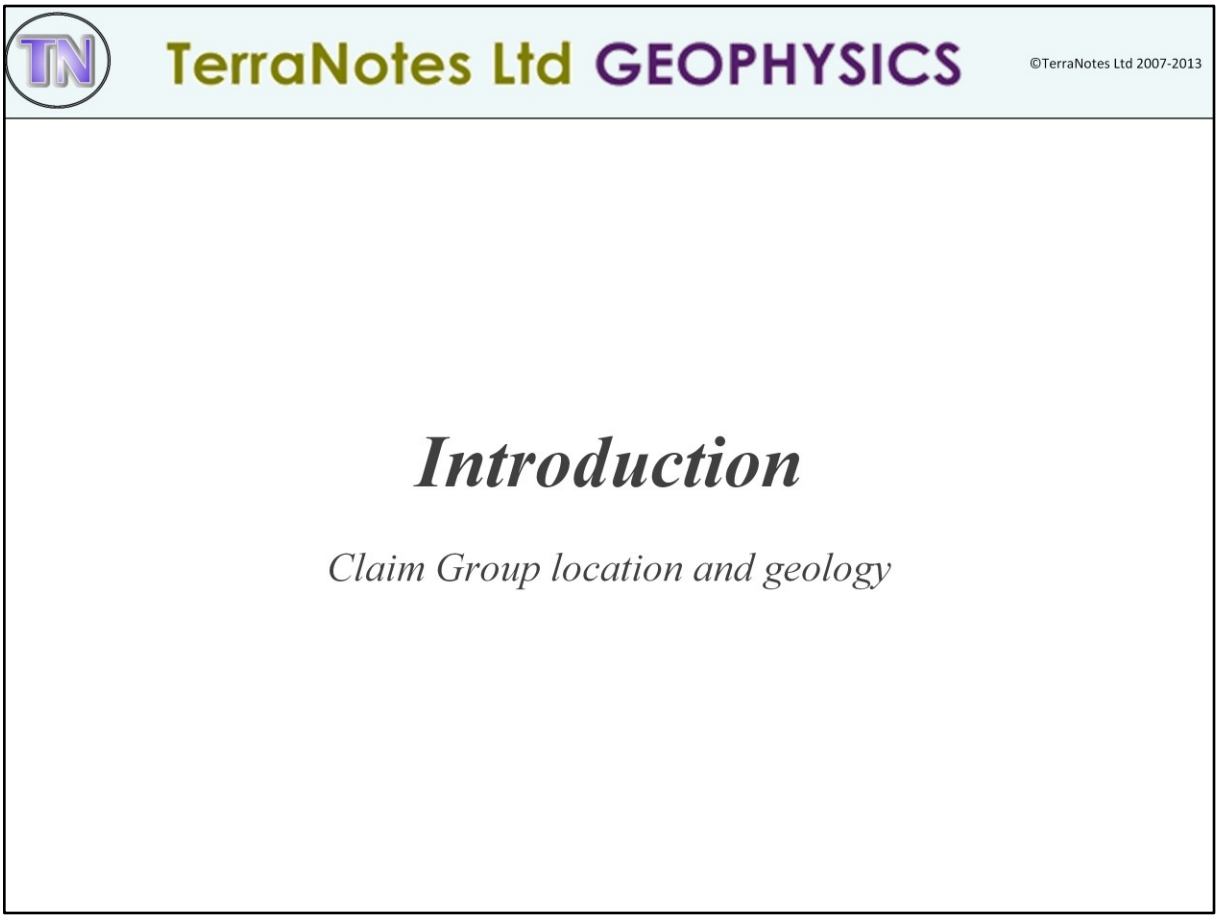
The dashed blue lines indicate weak magnetic trends in ROI-5.

The red ellipse indicates the weak magnetic anomaly coincident with the strong mid-depth conductor in ROI-2. The resistivity value is approximately 15 Ω·m (~10^1.2), which is low enough to say it could be a sulphide mineralization. Hence, the red ellipse area is the high priority target for further Ni-Cu mineralization. The mineralization may also extend to the further east and further west (not shown above).

The conductor within ROI-3 completely disappeared. Only at the western extension there is a weakly conductive zone. Since the conductivity decreased with depth it is probably a surficial conductor.

The conductivity at ROI-5 also decreases with depth. It is less than 100 Ω·m near the surface but more than 200 Ω·m at mid-depth. Therefore, this might be a weak conductor at near surface due to an alteration. This possible alteration should be investigated further if it is associated with Ni-Cu mineralization.

ROI-13 is a high magnetic anomaly with embayments similar to the Wellgreen deposit and exhibits elevated Ni and Cu levels in the soil. However, there is no coincident conductive zone at this location.


TerraNotes Ltd GEOPHYSICS
©TerraNotes Ltd 2007-2013
Introduction
Claim Group location and geology

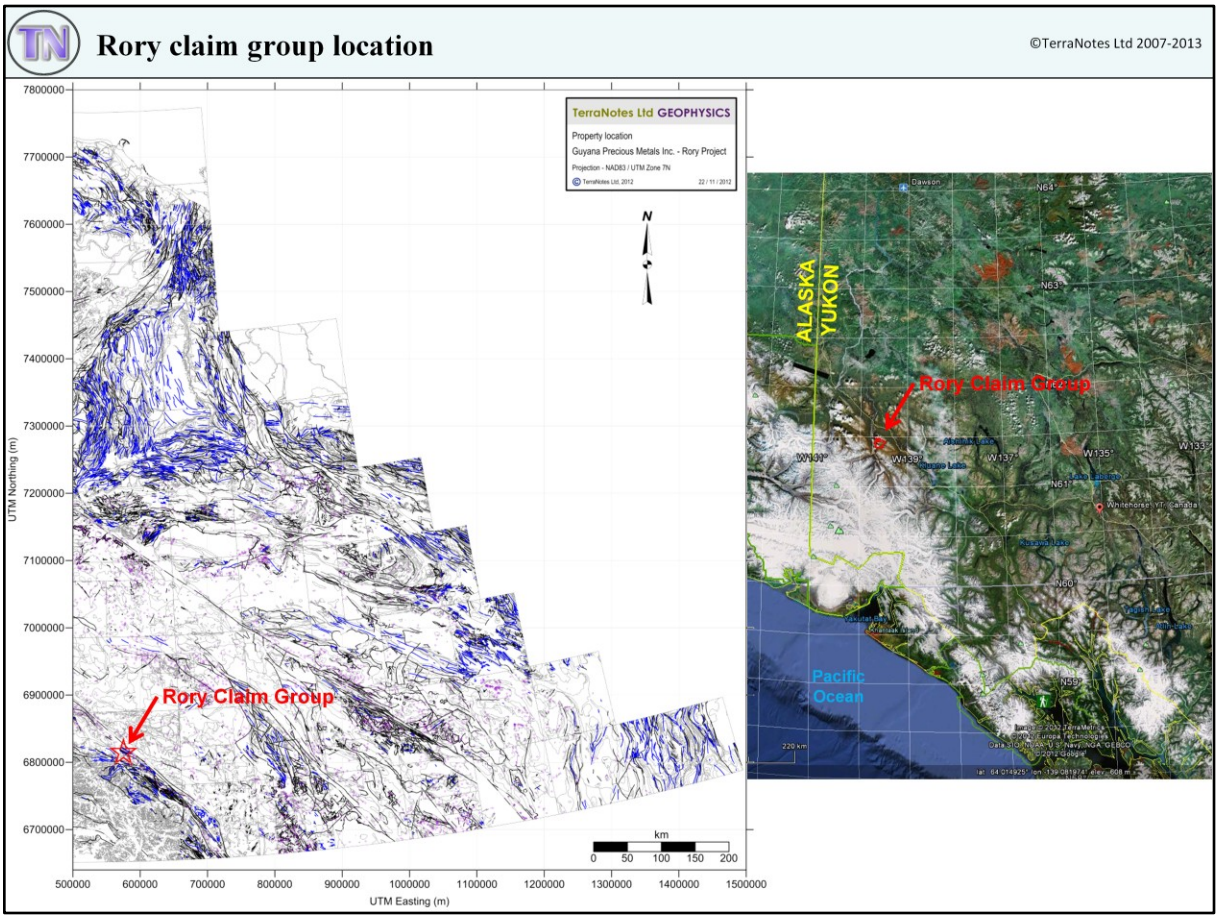


Figure 1. Location of the claim group. The left panel shows the geological features of the Yukon Territory. The red star indicates the location of the Rory claims. The right panel is the Google Earth image of the survey area. The red polygon indicates the location of the Rory claims.

Main Findings

Rory claim group is located in the southwest corner of the Yukon Territory (see red star on the left panel).

The straight line distance from the Alaskan border in the west is approximately 70 km and from the Pacific Ocean (Yakutat Bay) in the south it is approximately 150 km.

The Alaska Highway (1) provides an access to the Rory claims through the Quill Creek junction. The highway distance from Whitehorse, Yukon, is approximately 315 km, and from Anchorage, Alaska, is approximately 845 km.

Rory is located on the Kluane Ranges. The Kluane Ranges are bounded by the Saint Elias Mountains in the south, which is seen in white on the Google Earth image due to several glaciers. The Kluane Ranges is bounded with Shakwak Trench in the north. The Kluane Ranges are mentioned as the host of possible economic Ni-Cu and platinum group element (PGE) mineralization in the geological literature.

The Rory claim group is also located ~8 km north of the Kluane National Park and Reserve of Canada.

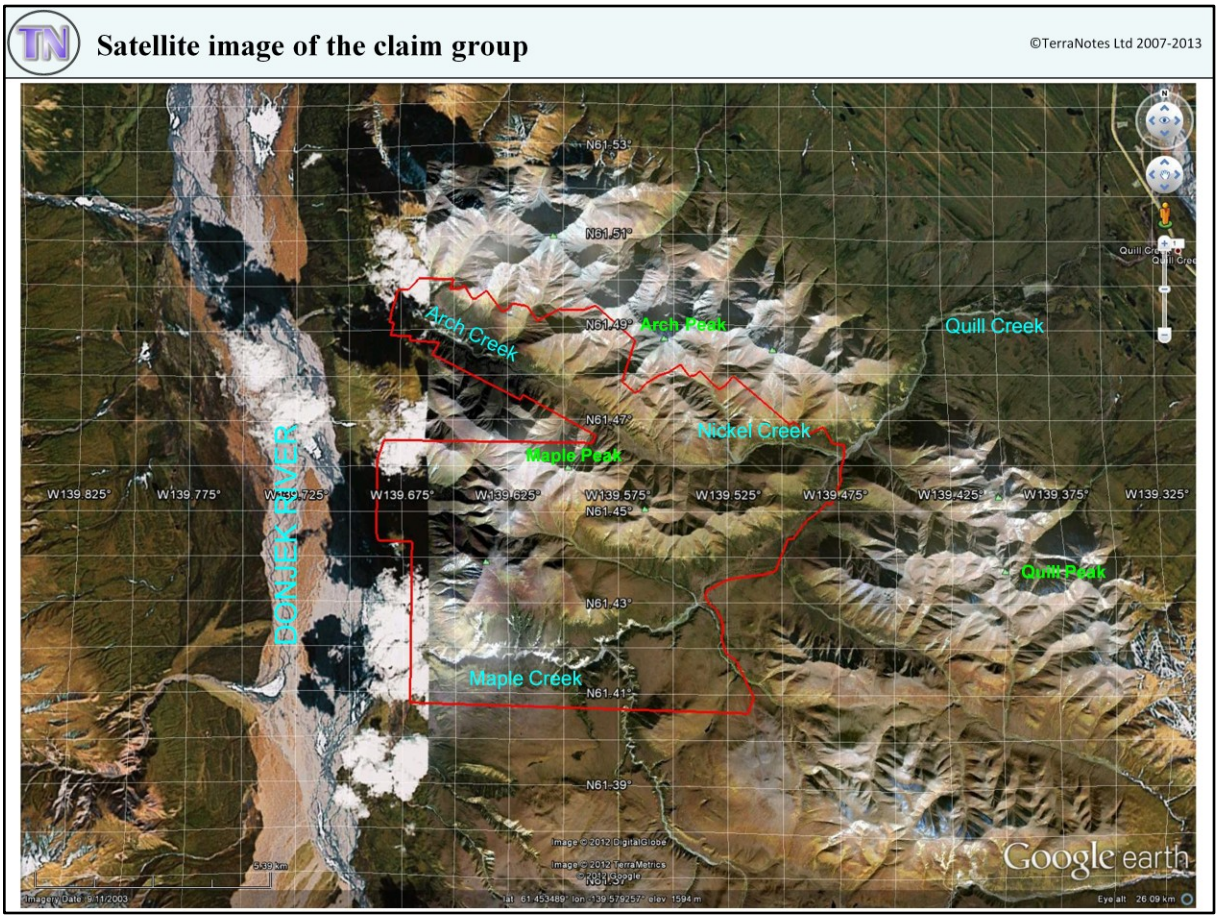


Figure 2. Satellite image of the claim group (modified from Google Earth). The map above shows the close up satellite image of the survey area. The red polygon outlines the boundary of the current airborne survey.

Main Findings

The survey area is located on a variable elevation zone with several peaks and valleys. Maple Creek, Nickel Creek, and Arch Creek are situated within the survey area and appear to branch from Quill Creek in the east and flow into Donjek River in the west.

The Maple Peak, the Maple Peak SE, and the Maple Peak SW are situated within the survey area (green triangles).

The Arch Peak, the Arch Peak E, and the Arch Peak NW are located immediately north of the survey area.

The Quill Peak and the Quill Peak N are located in the east of the survey area.

Rory claims information

©TerraNotes Ltd 2007-2013

- The Rory claim group is consist of 265 claims.

Grant Number	: YC65957 – YC66221
Claim Label	: Rory 1 – Rory 265
Claim Name	: Rory
Tenure Type	: Quartz
Regulation Type	: Q
Tenure Status	: Active
Claim Number	: 1-265
Owner	: Guyana Precious Metals Inc. (formerly Coronation Minerals Inc. – 100%)
Staking Date	: 09/30 – 10/01 2007
Recorded Date	: 10/03 2007
Expiry Date	: 10/03 2013
District	: Whitehorse
NTS Map #	: 115G05 – 115G06

Source: Yukon Geological Survey (http://mapservices.gov.yk.ca/YGS/WebMap.aspx)

The information about the claims of interest for this report is given above. Two thirds of the airborne geophysical data covers these 265 claims as well as the neighbouring claims to the north (Wellgreen and Arch). The details can be found in the following sections.

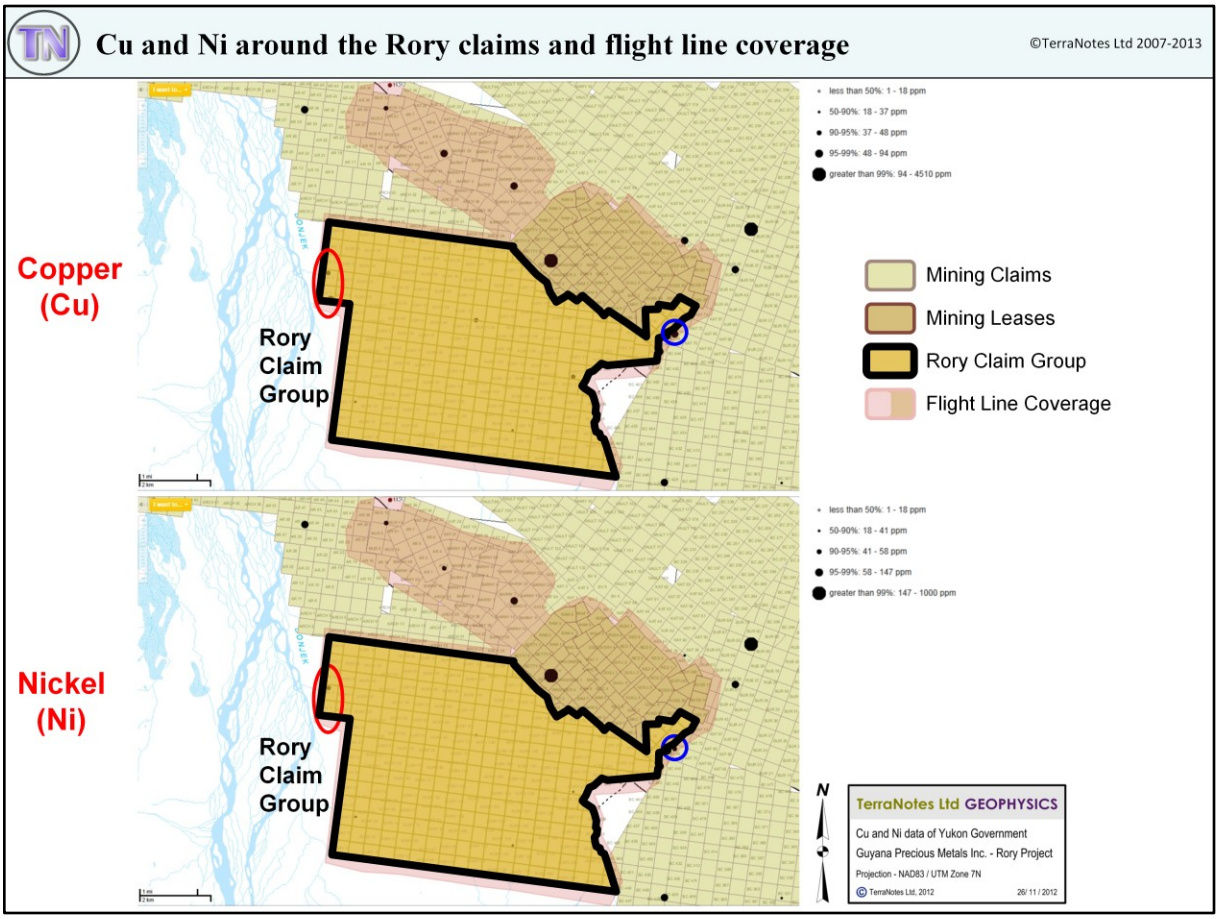


Figure 3. Copper and nickel potential of the Rory claims. The maps above show the flight line coverage with the "Quartz" claims of Yukon Geological Survey. The black dots indicate the known Cu content in the top panel and the known Ni content in the bottom panel. The red/pink shaded polygon indicates the flight line coverage of the DIGHEM Airborne survey. The dark yellow zone, outlined with the thick black polygon, indicates the Rory claim group (1-265), which is the main interest of this geophysical interpretation document. The dark brown polygons indicate the Mining Leases, which cover the known Nickel deposit named Wellgreen. DIGHEM survey covers this zone to see the geophysical signatures above a known deposit. The lighter green-brown polygons indicate the other mining ("Quartz") claims, in the vicinity of the Rory claim group. Part of the northwestern claims were covered by the DIGHEM survey. This is called the Arch property. It was included in the survey to observe possible continuation of the Wellgreen deposit in the northwest direction.

Main Findings

The highest Ni and Cu occurrence is located within the Mining Lease in the vicinity of the Wellgreen deposit. In the east (outside) and northwest (Arch property), there are intermediate to high Ni and Cu occurrences.

Ni abundance is generally low within the Rory claims, except for the western part where it is intermediate (18-41 ppm). Cu, on the other hand, has an intermediate abundance throughout the Rory claim group. The red ellipses show where there is coincident intermediate levels of Ni and Cu.

The blue circles indicate another high Cu and intermediate Ni occurrence at the border of the claims.

Please note that NW is the identified direction of the Ni mineralization at Wellgreen.

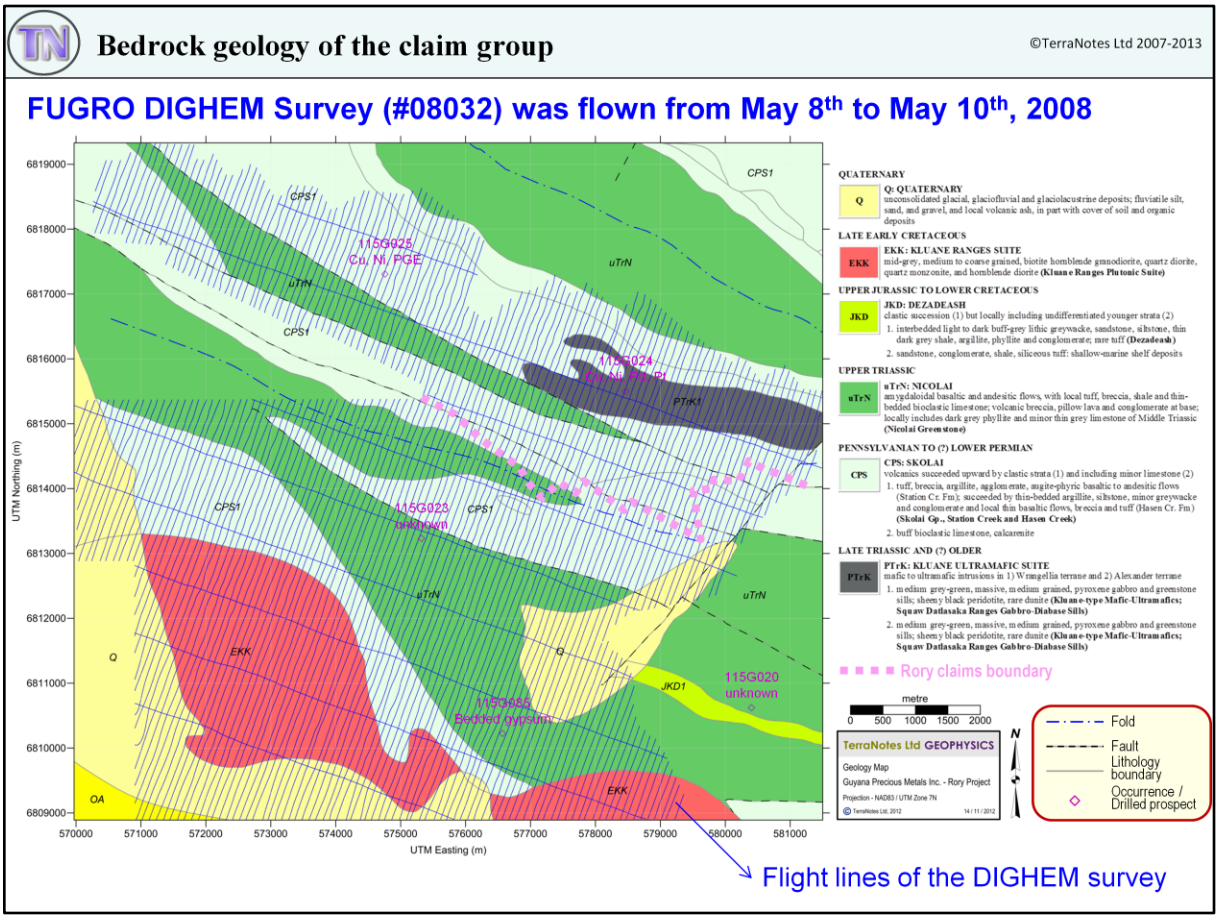


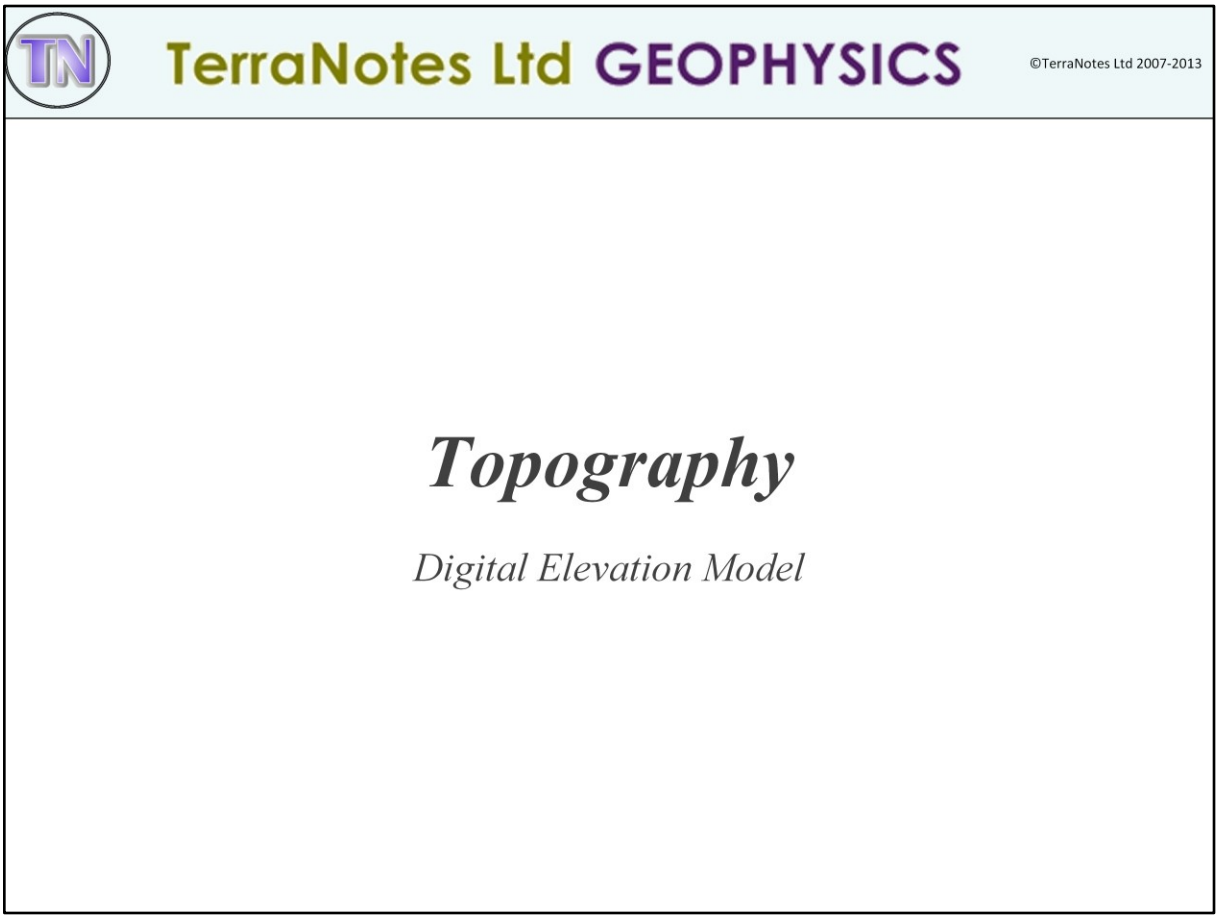
Figure 4. A map of the bedrock geology of the survey area with blue lines indicating the flight lines of Fugro's DIGHEM survey. The airborne survey (#08032) was flown from May 8th to May 10th, 2008. Please refer to the legend on the right for the details of the geological formations. Pink diamond shapes mark mineral occurrences of YGS. The gray polygons indicate the boundaries of the geological formations. The dashed black lines indicate the faults/shears and the dashed blue lines indicate fold axes.

Main Findings

The known Ni-Cu and PGE deposits are situated on the Triassic formations, which are shown in dark green (Nicolai), light green (Skolai) and dark gray (Kluane ultramafic suite). For example, the Wellgreen deposit occurs at the contact between Skolai formation and Kluane ultramafic suite.

The pink dotted line approximately separates the Rory claims from the other claims. As seen in the map above, there is no known ultramafic rock in the Rory portion.

There are known Cu-Ni-PGE occurrences in the north. Unknown Cu-Ni-PGE occurrences may also exist in the south. In addition to these, there is a bedded gypsum showing in the south.


TerraNotes Ltd GEOPHYSICS
©TerraNotes Ltd 2007-2013
Topography
Digital Elevation Model

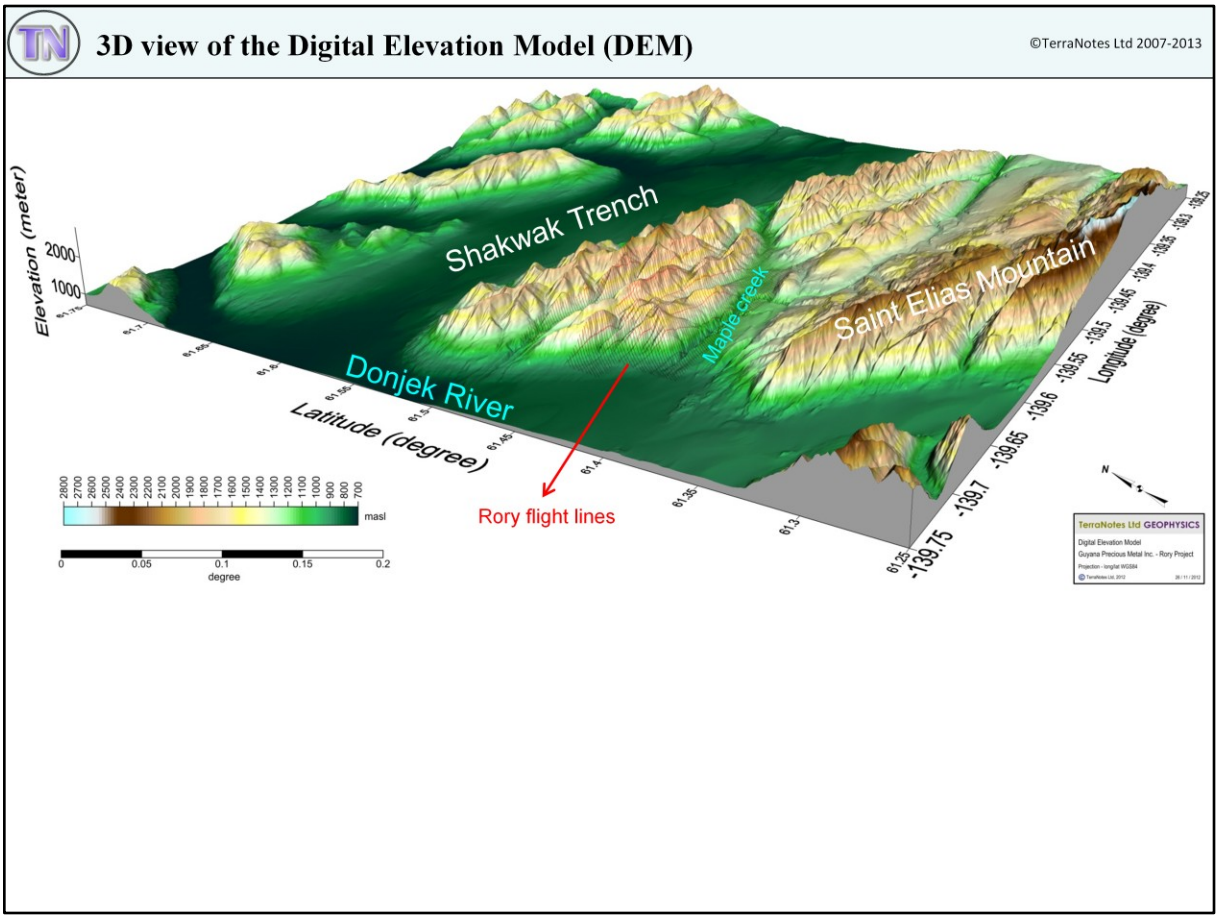


Figure 5. The three-dimensional (3D) view of the Digital Elevation Model (DEM), obtained from Canadian Government. The red lines, overlaid on the DEM surface between Shakwak Trench and Maple Creek, indicate the flight lines of the DIGHEM survey.

Main Findings

The Shakwak Trench in the north, the Donjek River in the west, and Maple Creek in the south are the three main low elevation zones in the map above. These three low elevation zones bound the Rory claim group.

The rest of the area has a high elevation, including the Rory claim group, with very rugged topographical features.

The difference between the lowest (Donjek River) and the highest elevations (Saint Elias Mountains) is approximately 2100 metres.

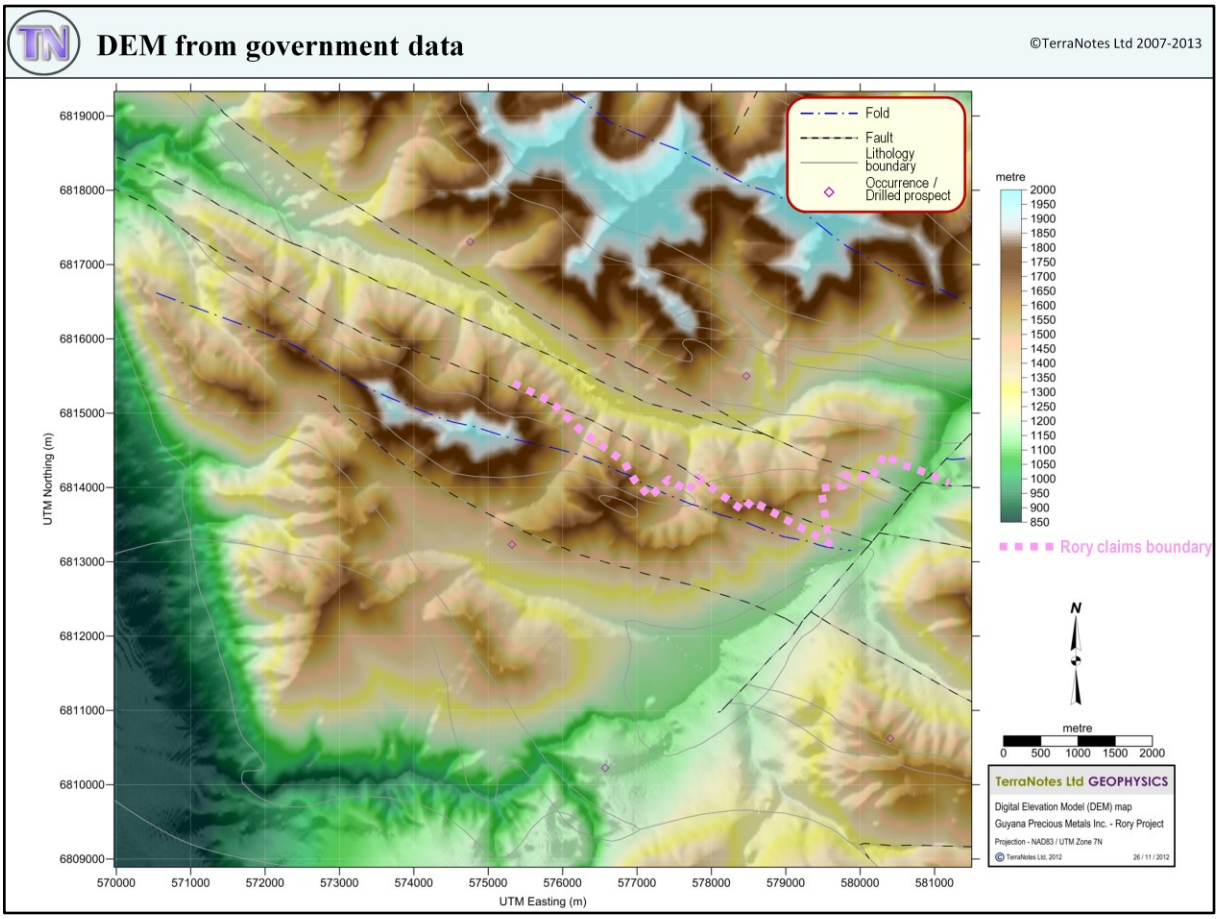


Figure 6. 2D view of the DEM. This map is same as the previous map (Figure 5) with a top view. This map is for comparison with the airborne elevation map to observe if there is a coordinate shift in the data. The pink diamonds indicate mineral occurrences of YGS. The gray polygons indicate the boundaries of the geological formations. The dashed black lines indicate the faults/shears and the dashed blue lines indicate fold axes.

Please refer to the next map for this Quality Assurance / Quality Control (QA/QC) analysis.

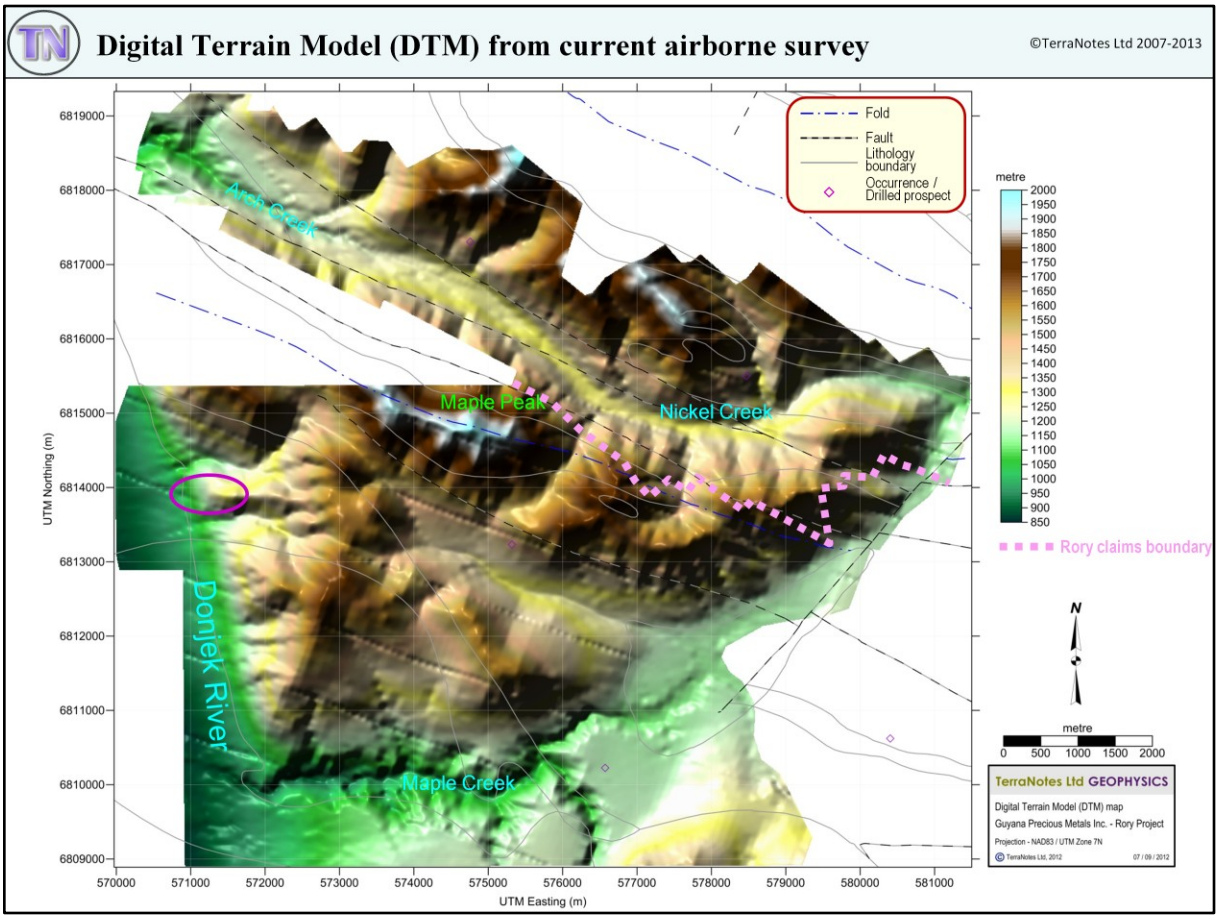


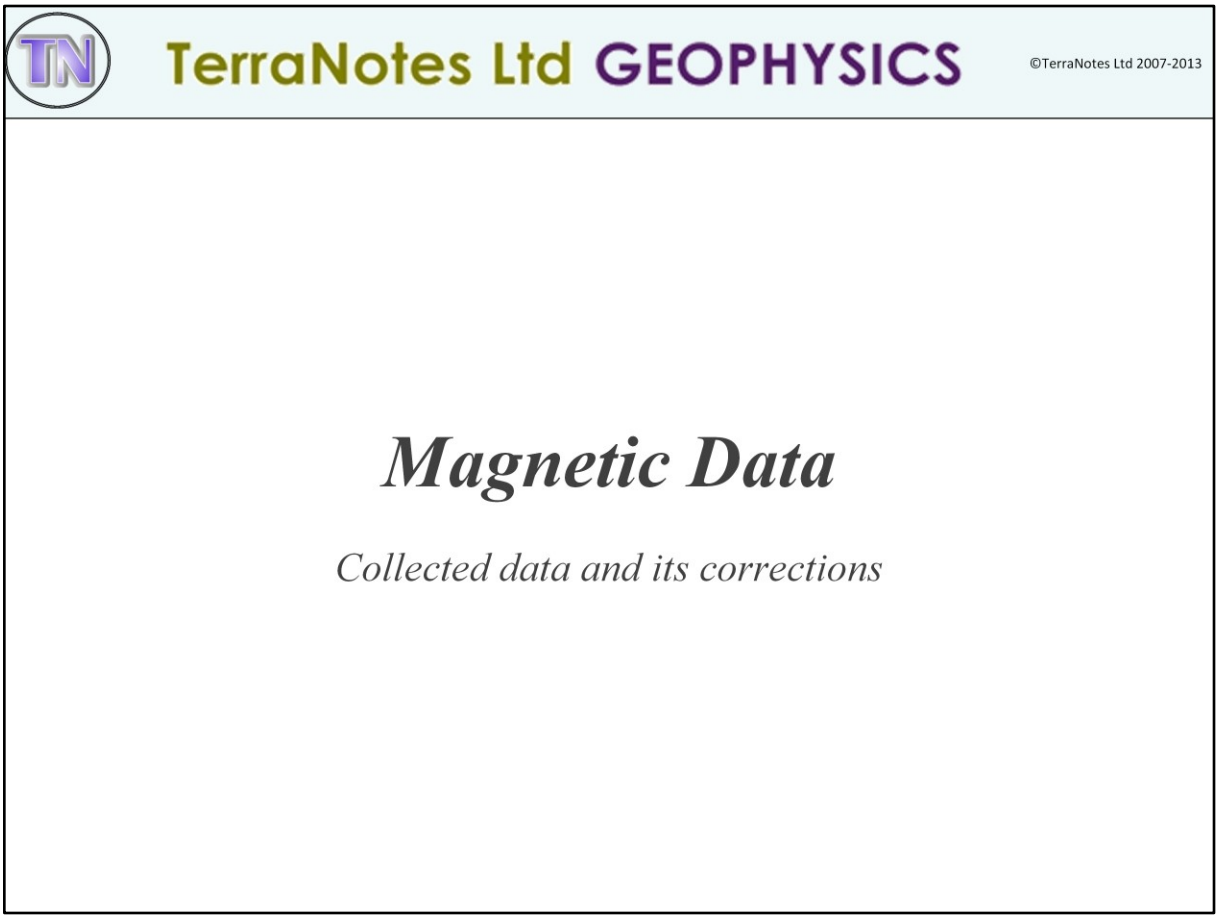
Figure 7. Digital Terrain Model (DTM) from current airborne survey. This map shows the DTM which is obtained from the GPS measurement of the airborne survey. The pink diamonds indicate mineral occurrences of YGS. The gray polygons indicate the boundaries of the geological formations. The dashed black lines indicate the faults/shears and the dashed blue lines indicate fold axis. The pink dotted line approximately separates the Rory claims from the other claims.

Main Findings

When compared with the government DEM map (Figure 6), all the topographic features are the same, suggesting that there is no major coordinate shift in the airborne dataset.

The creeks, rivers, and peaks can be well defined with this topography map.

The difference between the highest elevation (Maple Peak) and the lowest elevation (Donjek River) is approximately 1150 m. These points are within 4km of each other confirming how steep the topography is. Even within 1 km of the hill with the most gentle slope (pink ellipse), there is a 400 m elevation difference.


TerraNotes Ltd GEOPHYSICS
©TerraNotes Ltd 2007-2013
Magnetic Data
Collected data and its corrections

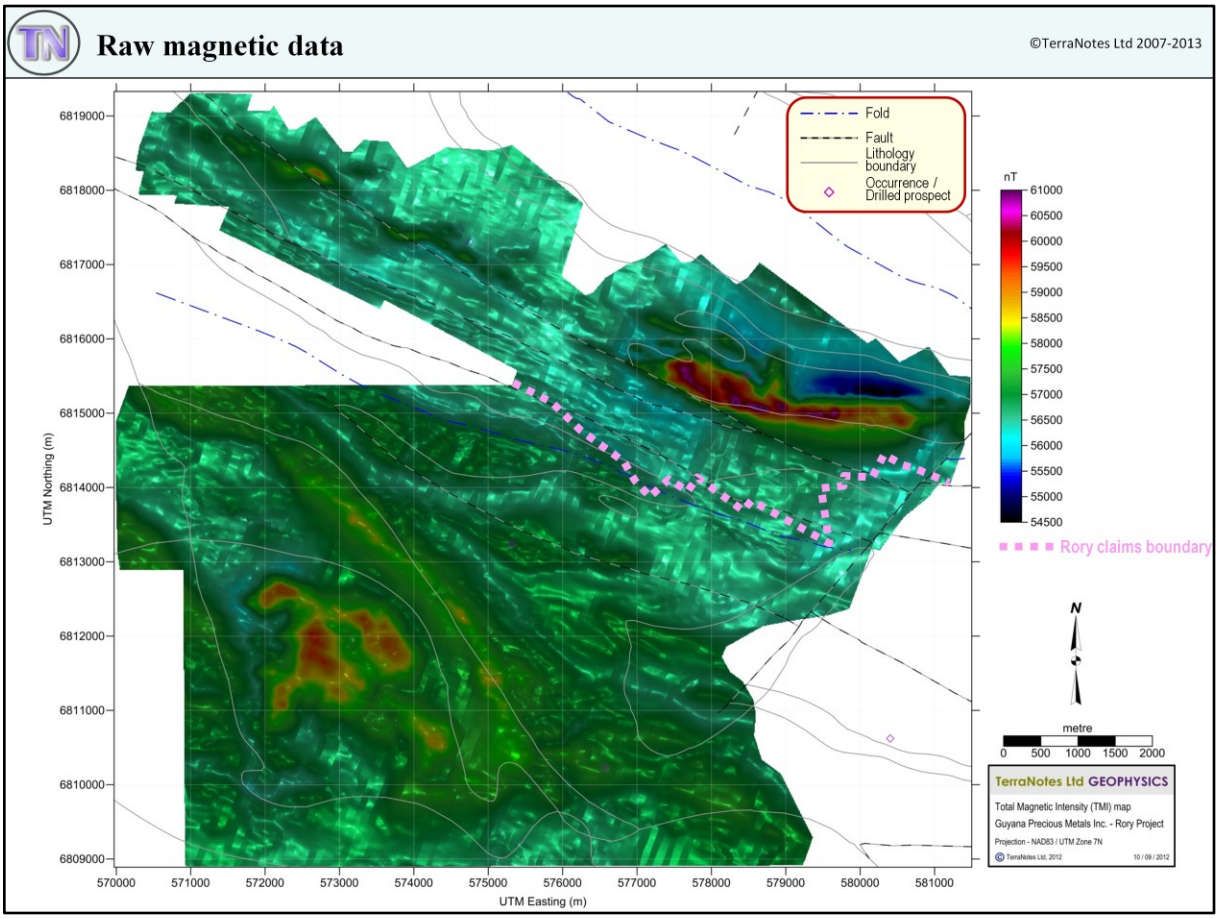


Figure 8. The measured raw magnetic data (total magnetic intensity [TMI]) that was acquired by the Fugro Airborne Surveys. The warm colours indicate the high magnetic zones and the cool colours indicate the low magnetic zones. The pink diamonds indicate mineral occurrences of YGS. The gray polygons indicate the boundaries of the geological formations. The dashed black lines indicate the faults/shears and the dashed blue lines indicate fold axes. The pink dotted line approximately separates the Rory claims from the other claims.

The Rory claim group is very magnetically active since the difference between the high and low magnetic zones reaches 6500 nT.

Several corrections are required to produce the final magnetic data and these corrections are shown in the next three figures.

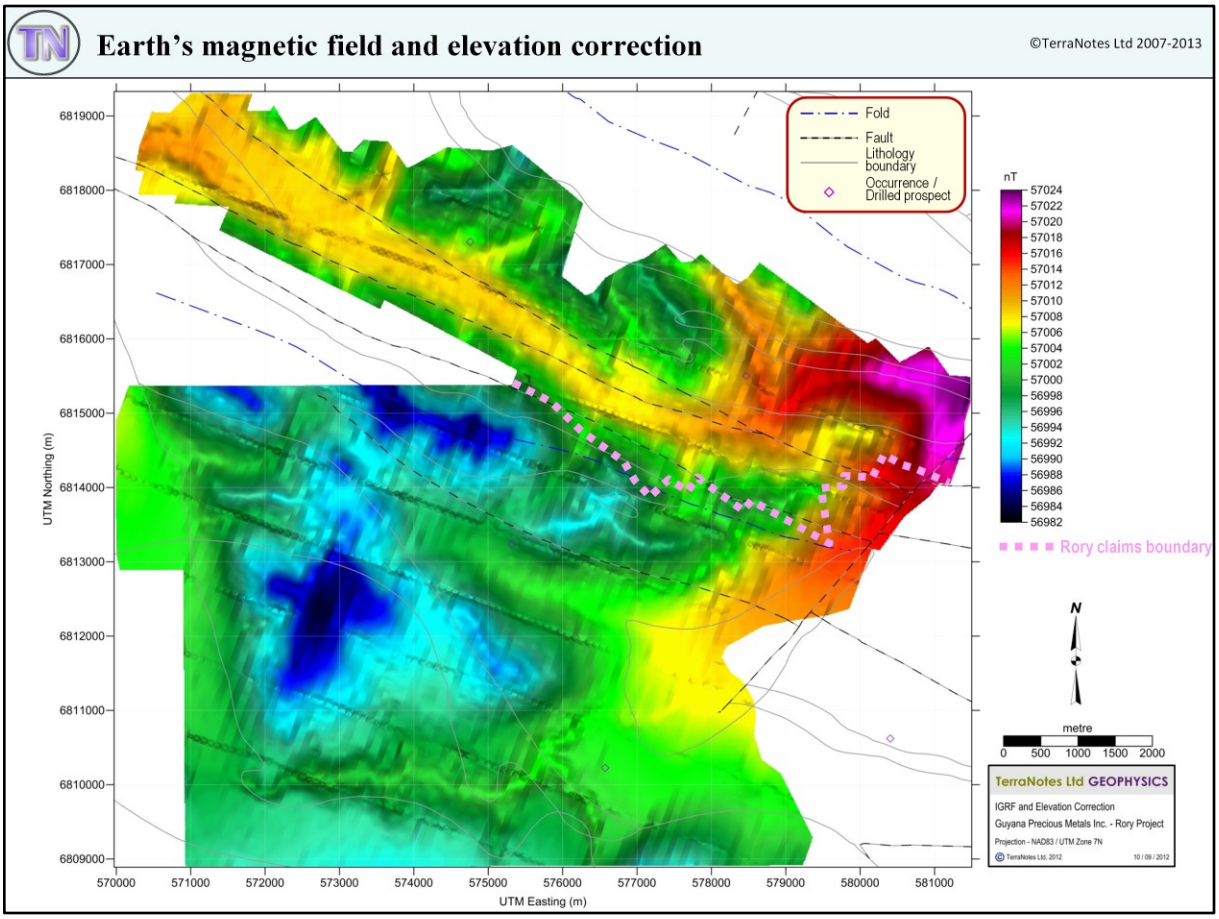


Figure 9. Earth's magnetic field caused by the its outer core, which is not of interest for mineral exploration, must be removed from the raw magnetic data. This field due to Earth's outer core is called the International Geomagnetic Reference Field (IGRF). The effect of the distance between the helicopter and the topographic surface has also been included in the IGRF calculation. The pink diamonds indicate mineral occurrences of YGS. The gray polygons indicate the boundaries of the geological formations. The dashed black lines indicate the faults/shears and the dashed blue lines indicate fold axes. The pink dotted line approximately separates the Rory claims from the other claims.

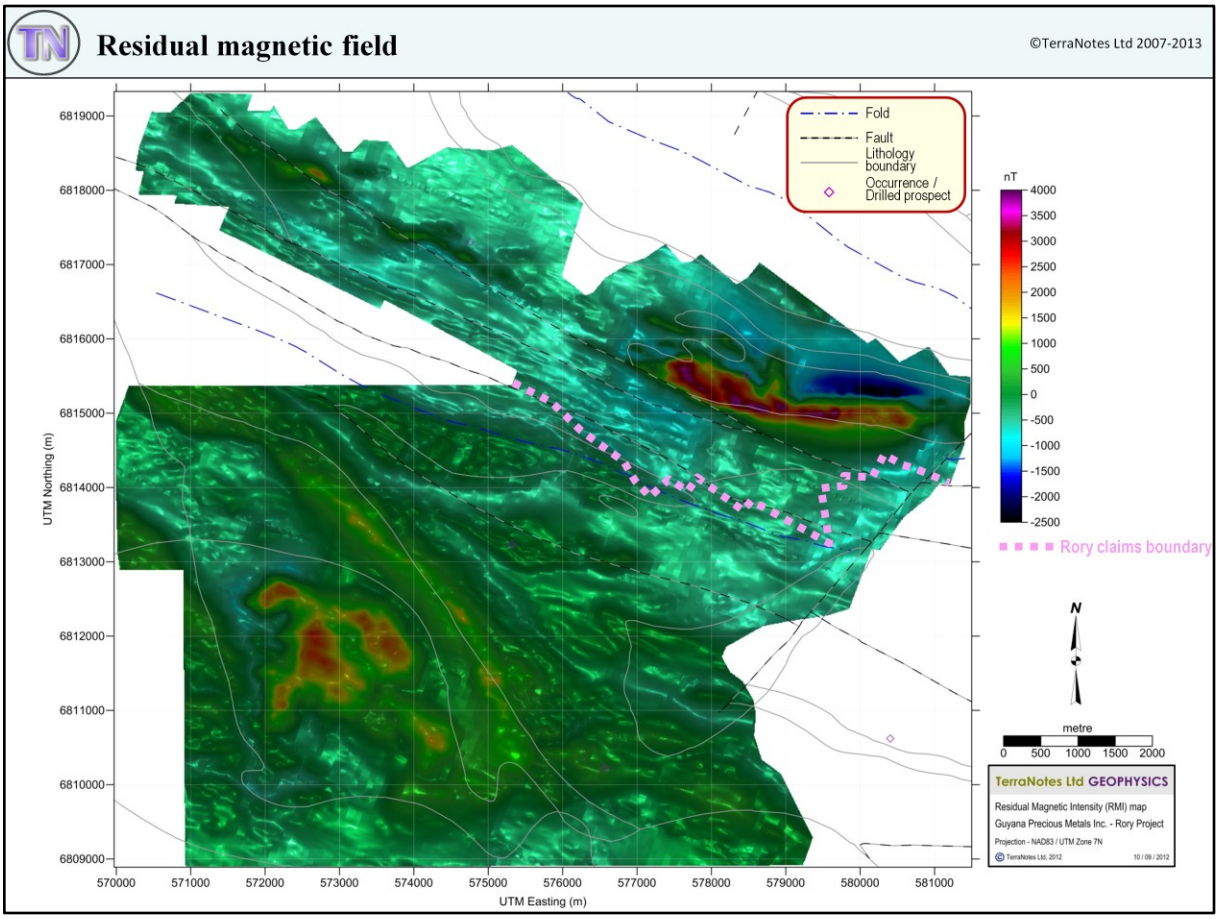


Figure 10. The residual magnetic intensity (RMI), which is obtained through removing the IGRF and elevation effect from the TMI. The pink diamonds indicate mineral occurrences of YGS. The gray polygons indicate the boundaries of the geological formations. The dashed black lines indicate the faults/shears and the dashed blue lines indicate fold axes. The pink dotted line approximately separates the Rory claims from the other claims.

Before further interpretation, an additional correction is required (see next figure).

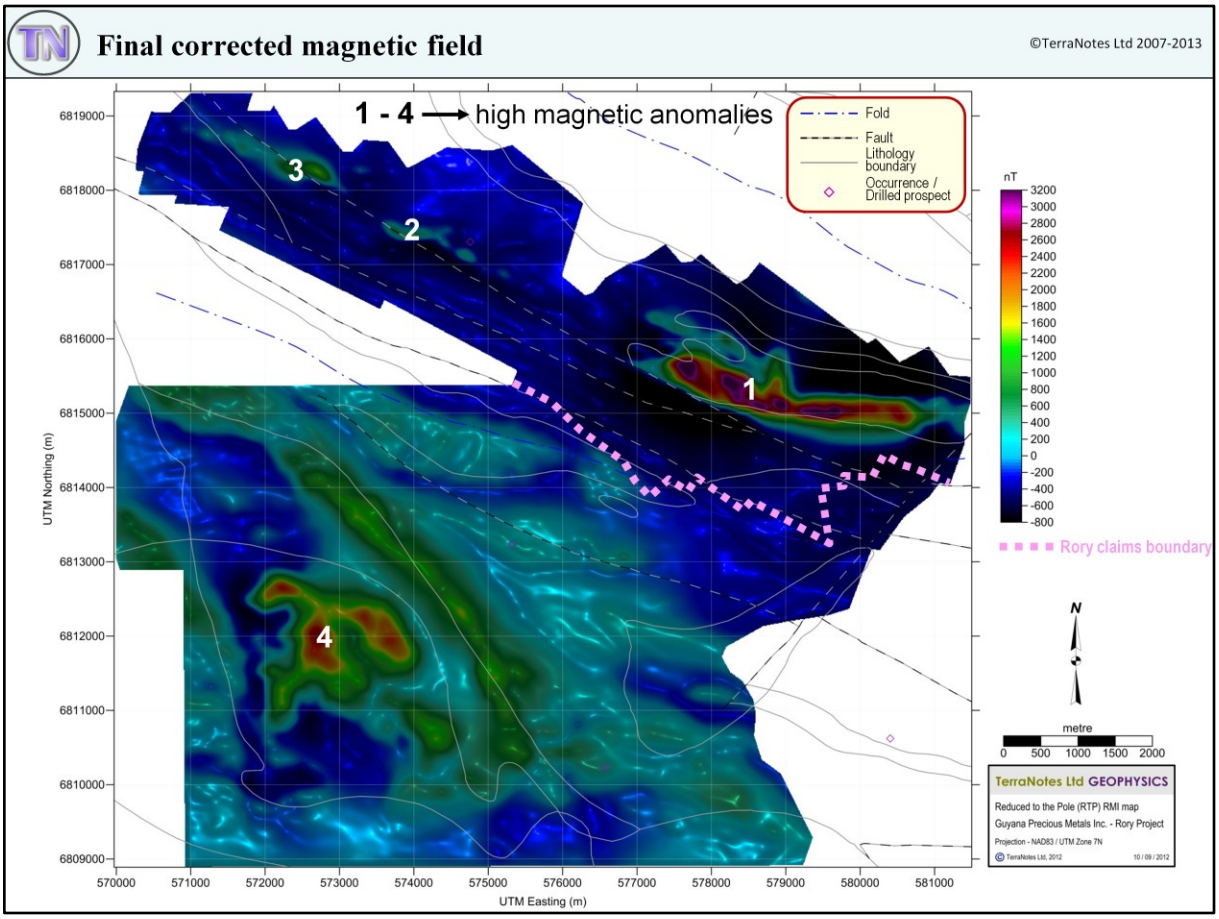


Figure 11. The final corrected magnetic data called Reduced-to-the-Pole Residual Magnetic Intensity (RTP-RMI). The RMI map (Figure 10) is corrected for its geographical location and de-noised to obtain the map above. The pink diamonds indicate mineral occurrences of YGS. The gray polygons indicate the boundaries of the geological formations. The dashed black lines indicate the faults/shears and the dashed blue lines indicate fold axes. The pink dotted line approximately separates the Rory claims from the other claims.

Main Findings

The highest magnetic zone (Anomaly 1) in the vicinity of Wellgreen deposit occurs in the NE. Anomaly 1 is due to the Kluane Ultramafic Suite (PTrK) seen in the geology map (Figure 4). In this part of the survey area, both Nikolai and Skolai formations (see Figure 4) are non-magnetic.

Anomalies 2 and 3 seem to occur on the contact between Nikolai and Skolai and could be independent from those formations. Since they are oriented in the same direction as Anomaly 1, Anomalies 2 and 3 may indicate similar ultramafic rocks. Thus, they should be of interest for further exploration. As a matter of fact, Airways, the drilled prospect of YGS (115G025) with anomalous Cu-Ni-PGE, is located near Anomaly 2 (see pink diamond).

The Anomaly 4 is coincident with the Kluane Ranges Plutonic Suite (EKK) of felsic to intermediate rocks (see Figure 4). This level of magnetism (up to 2600 nT) is unusually high for this type of rocks, indicating that this high magnetic anomaly may have another source which should be examined with ground geophysics, ground truthing, or drilling. Israel et al. (2004)* observed pyroxene diorite and gabbro within EKK formation around Duke River, so gabbro, which is found to be related with the Ni-Cu-PGE mineralization, could be the reason for the high magnetism in Anomaly 4.

** **Israel S., A. Tizzard, and J. Major, 2005,** Bedrock geology of the Duke River area, parts of NTS 115G/2,3,4,6 and 7, southwestern Yukon,* Yukon Exploration and Geology 2005

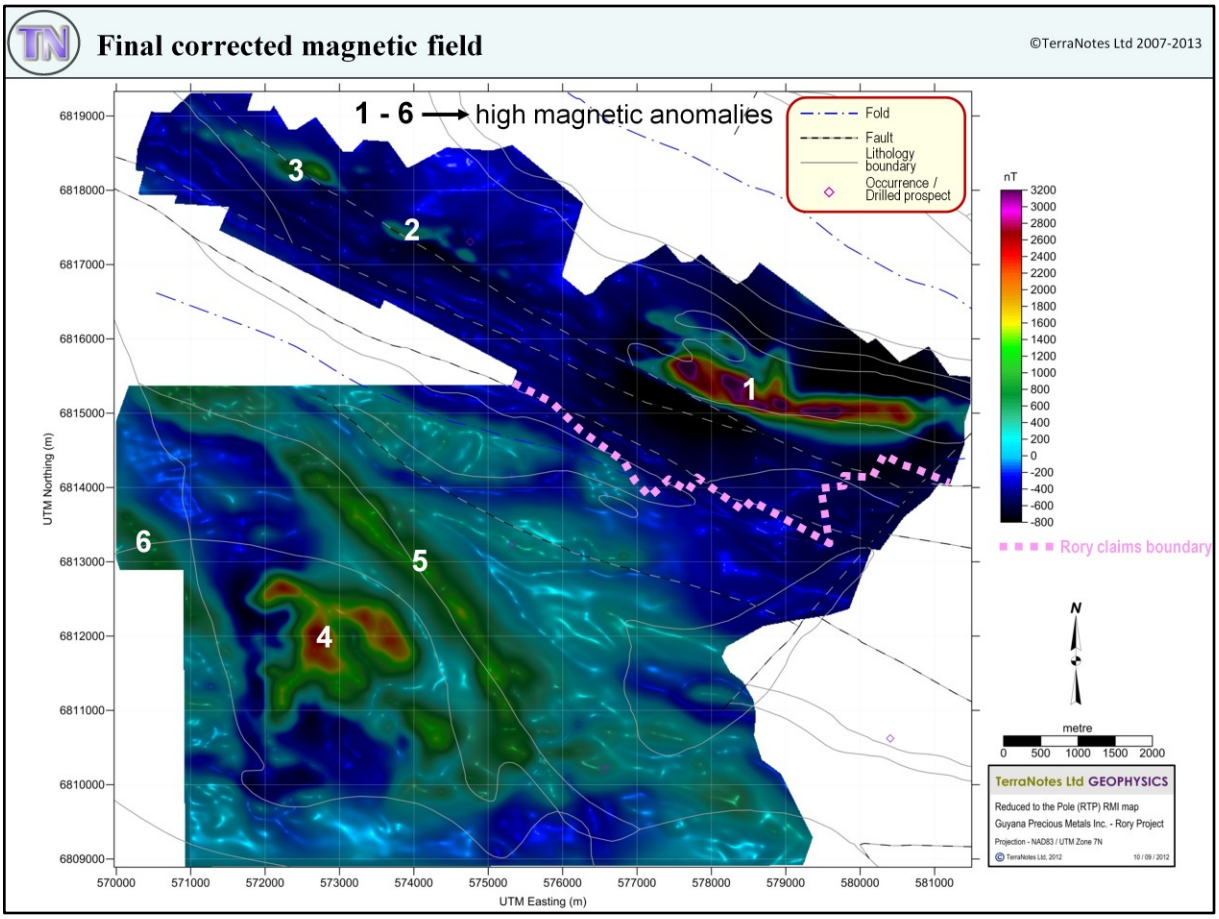


Figure 11 *CONTINUED*. Final corrected magnetic field.

Main Findings

The Anomaly 5 seems to occur in the contact zone between Nicolai and Skolai formations. A phenomenon similar to Anomalies 2 and 3 may be the source of this anomaly. More ultramafic rocks may be formed in this contact zone.

The intermediate (cyan) to high (green) magnetic anomalies within the southern part of the Rory claims represent the Nicolai formation because these anomalies seem to coincide with the Nicolai formation in the geology map. In this case, we may separate Nicolai formation from the Skolai formation using magnetic anomalies.

Both interpretations above might be valid for this part. It could also be that the intermediate magnetic anomalies (cyan anomalies in the eastern Rory) represent the Nicolai formation and the high magnetic anomaly (Anomaly 5) represents the ultramafic suite.

Anomaly 6 is coincident with the Quaternary deposits, so this magnetic anomaly should represent a bedrock unit beneath the Quaternary deposit.

The Skolai formation seems to exhibit a low magnetic intensity throughout the whole claim group.

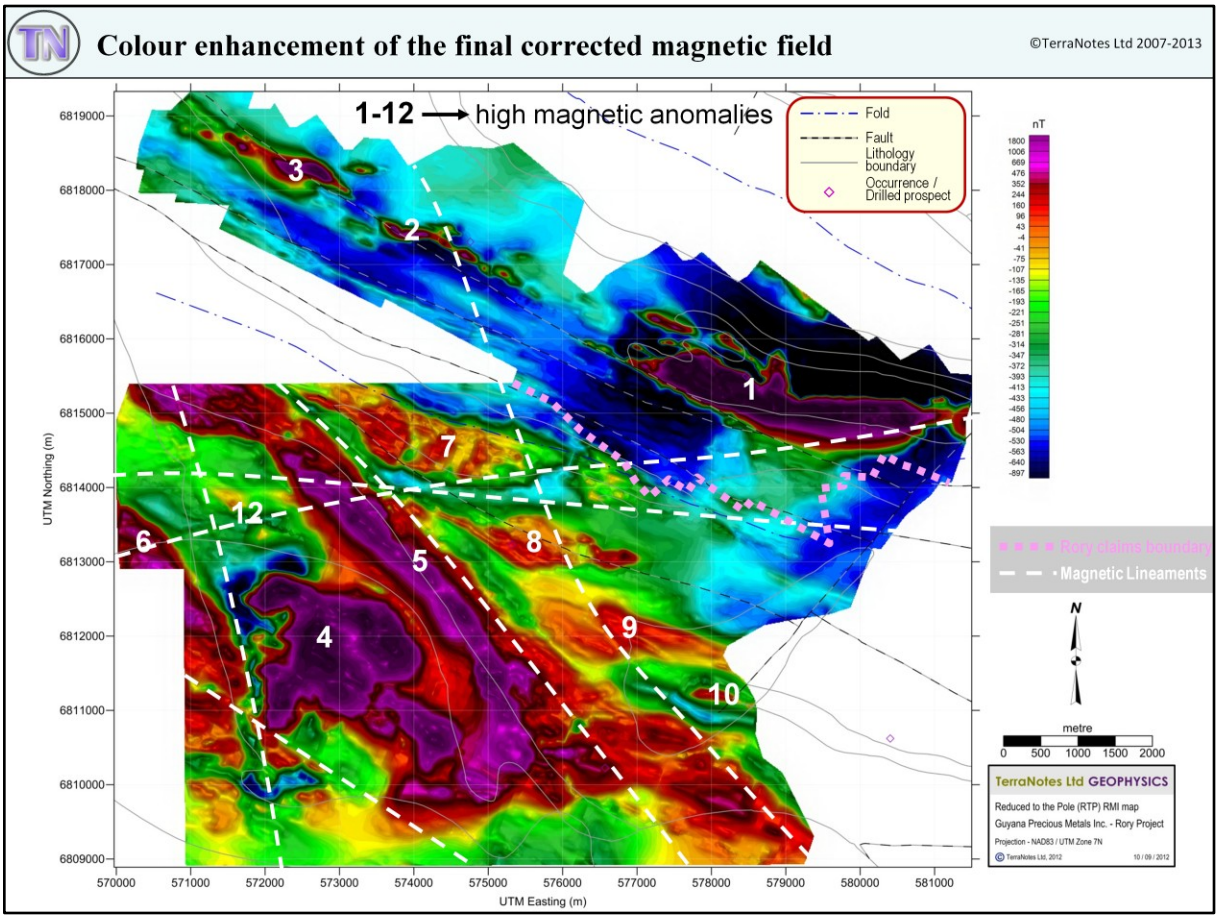


Figure 12. Colour enhancement of the final corrected magnetic field. This map is same as Figure 11 but the colours are enhanced using statistical methods to observe more details about the intermediate and weak magnetic anomalies. The pink diamonds indicate mineral occurrences of YGS. The gray polygons indicate the boundaries of the geological formations. The dashed black lines indicate the faults/shears and the dashed blue lines indicate fold axes. The pink dotted line approximately separates the Rory claims from the other claims.

Main Findings

As seen in the figure above, Anomalies 1-6 are illustrated with the purple colour indicating high magnetic anomalies.

Anomalies 7-12 can be observed in this map as intermediate (red) to weak (yellow) magnetic anomalies, and these anomalies might be of interest if they also show high conductivity (or low resistivity). They may represent the Nikolai formation.

The white dashed lines indicate the interpreted fault-like structures that break the high magnetic anomalies. More lineaments may be found in the amplification images of the magnetic field (see next section).

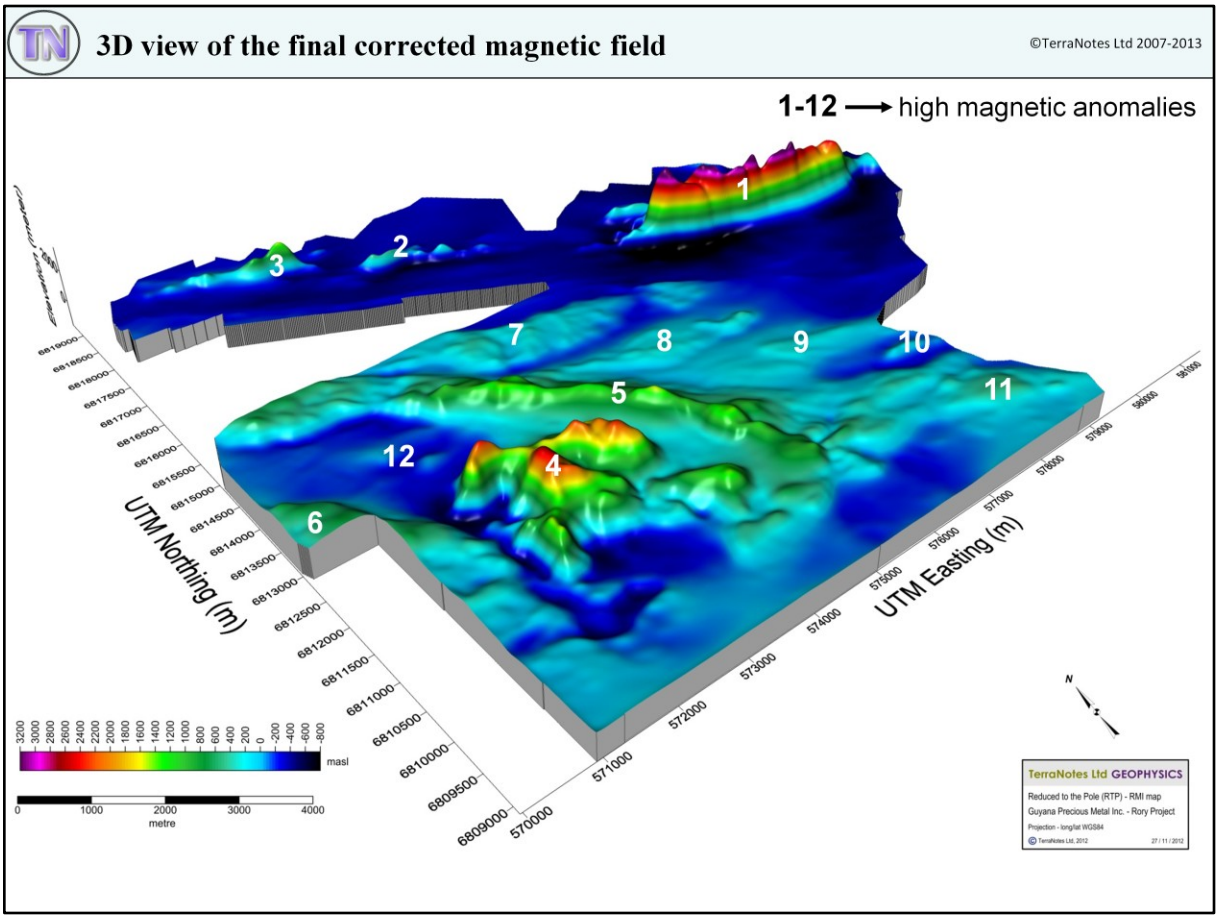


Figure 13. This map is same corrected magnetic field as Figure 11 but in 3D to better observe some of the details.

Main Findings

The strength of Anomalies 1-12 can be seen better in this figure than the previous one.

Anomalies 1 and 5 are strong anomalies with linear characteristics. Anomalies 2, 3, 9 and 10 also exhibit linear characteristics.

Other anomalies have more elliptical shapes, the highest anomaly is Anomaly 4. Anomaly 4 may represent a gabbro intrusion, whereas the other elliptical shape anomalies (7–11) may represent the Nikolai formation.

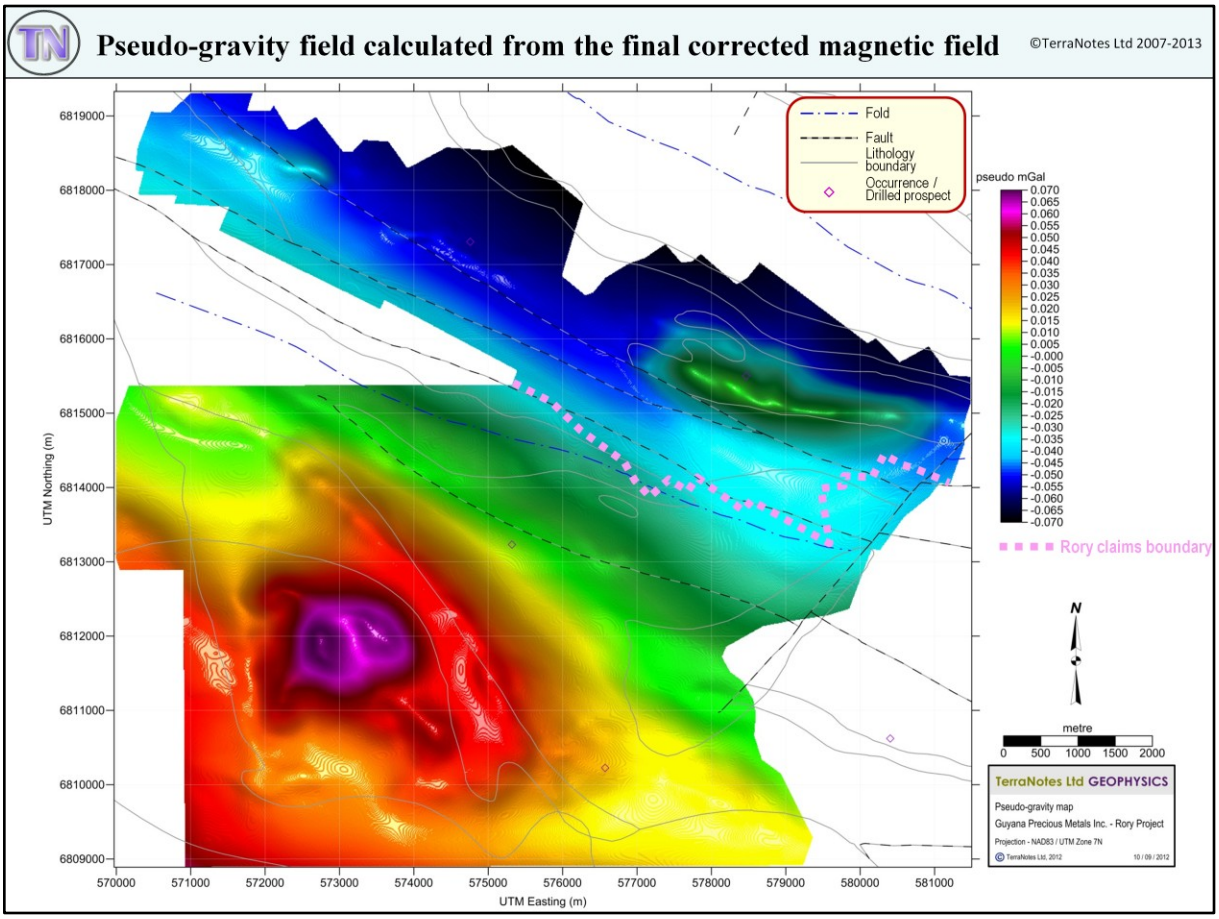
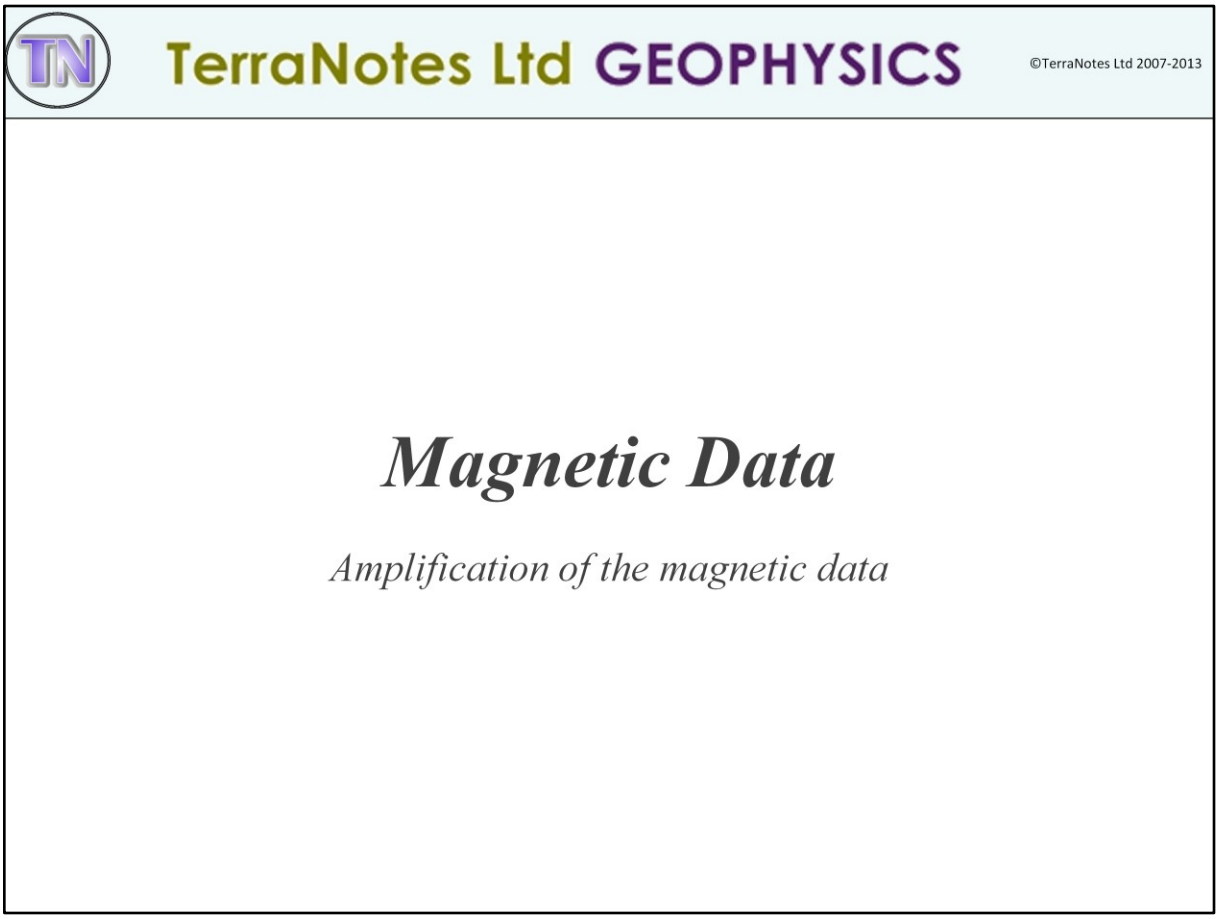


Figure 14. Pseudo-gravity field calculated from the final corrected magnetic field. The pink diamonds indicate mineral occurrences of YGS. The gray polygons indicate the boundaries of the geological formations. The dashed black lines indicate the faults/shears and the dashed blue lines indicate fold axes. The pink dotted line approximately separates the Rory claims from the other claims.

Main Findings

The pseudo-gravity represents the regional behaviour of the magnetic field data. The Skolai and Nikolai formations have higher magnetic susceptibilities in the Rory claims than in the Wellgreen and Arch portions of the survey area.

The highest anomaly occurs beneath the Kluane Ranges Plutonic Suite (EKK – see Figure 4). The source of this anomaly could be gabbro and it should be investigated further to see if it could be related to Cu-Ni and PGE mineralization.


TerraNotes Ltd GEOPHYSICS
©TerraNotes Ltd 2007-2013
Magnetic Data
Amplification of the magnetic data

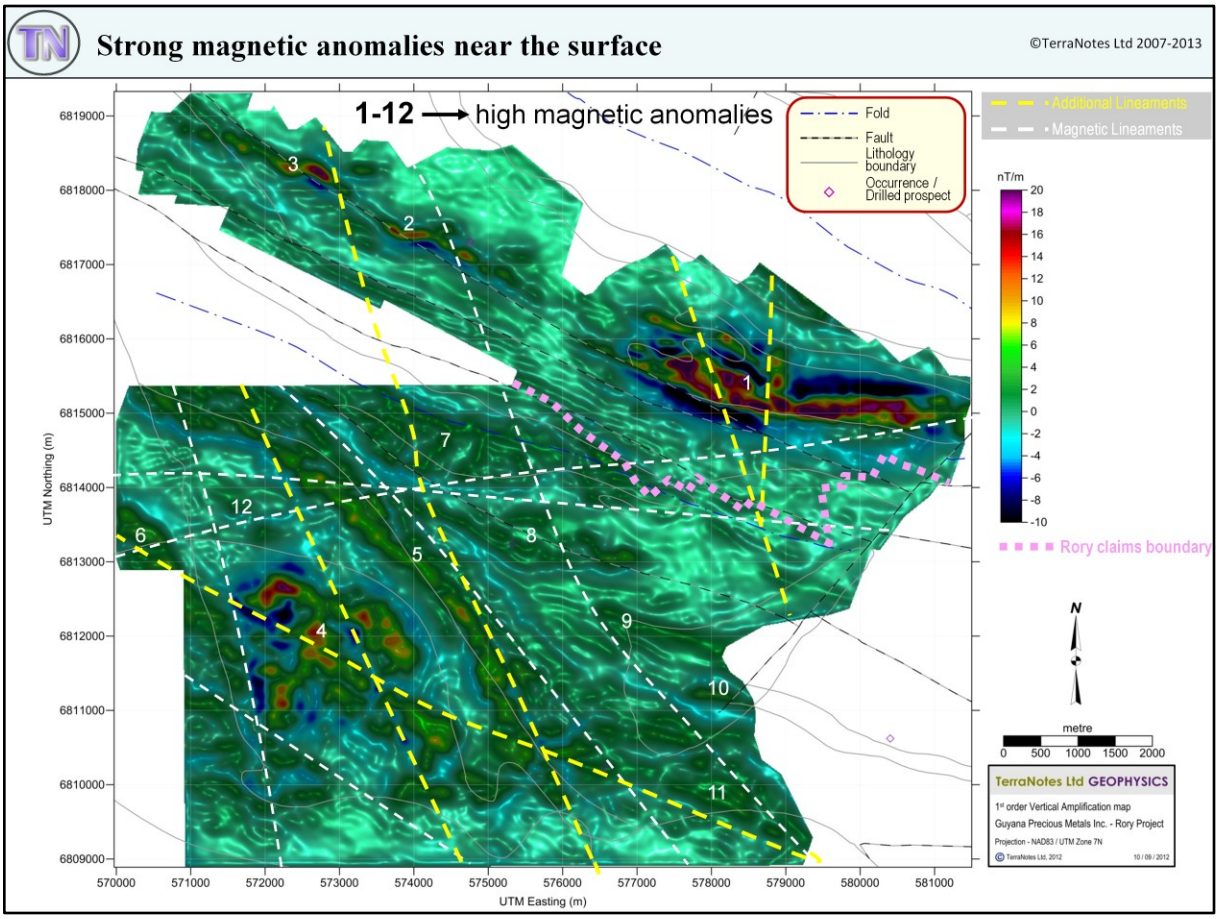


Figure 15. Amplification of the strong, near-surface magnetic anomalies and their detailed structure. The pink diamonds indicate mineral occurrences of YGS. The gray polygons indicate the boundaries of the geological formations. The dashed black lines indicate the faults/shears and the dashed blue lines indicate fold axes. The pink dotted line approximately separates the Rory claims from the other claims. The previously identified anomalies and faults were marked with numbers and white dashed lines, respectively.

Main Findings

The details of the magnetic anomalies can be observed in the map above, including the shallower magnetic anomalies observed in Figure 11. The details of the high magnetic Anomalies 1, 2, 3 and 4 in particular are very clear.

The details of the weaker anomalies can also be observed within the Anomalies 7, 8 and 9. These details will be more visible in the following figures.

The yellow dashed lines indicate additional fault-like magnetic lineaments. These lineaments might be associated with the Cu-Ni and PGE mineralization. For example, the eastern lineaments form an embayment in the area within Anomaly 1 showing the highest magnetic intensities and it is known from the geological literature that the Wellgreen deposit occurred within this embayment or one with similar characteristics.

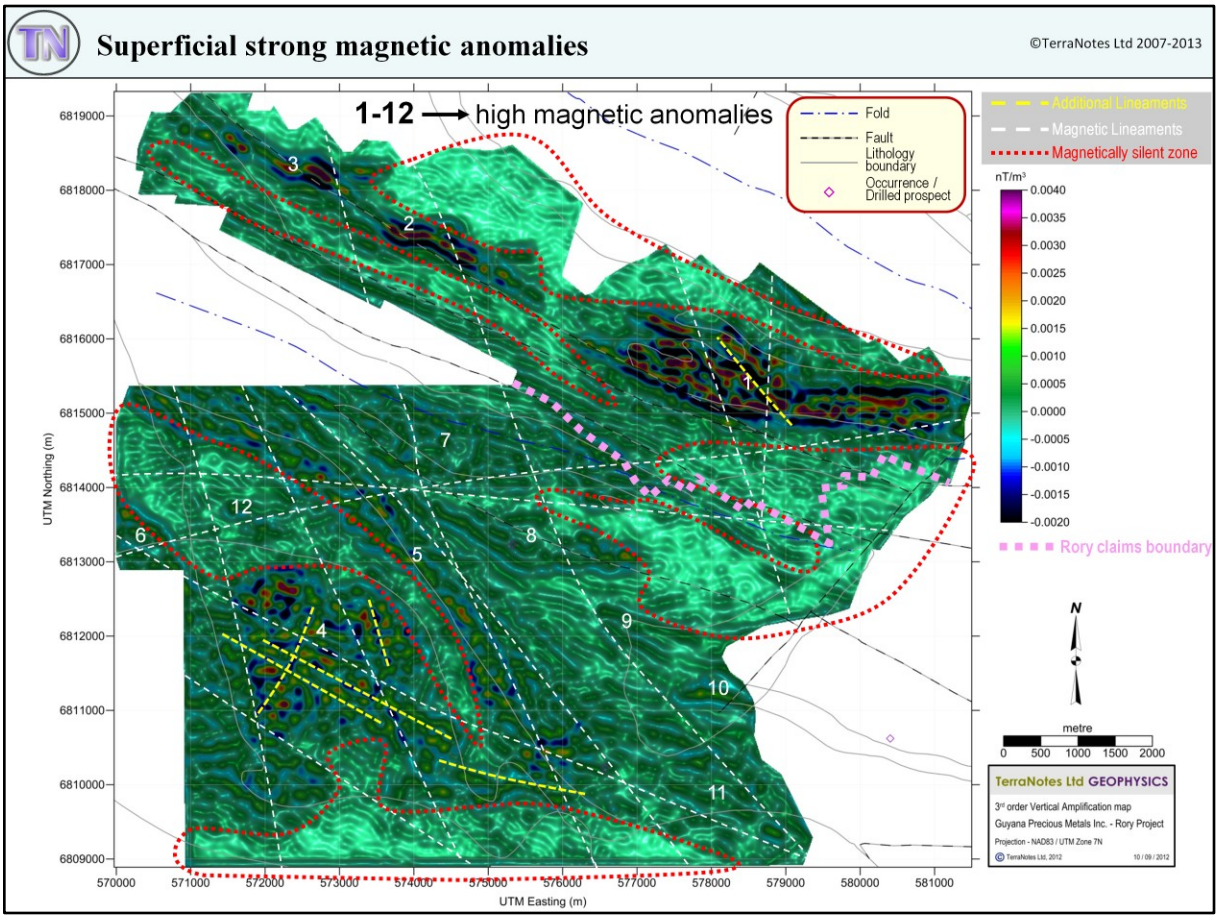


Figure 16. The third order vertical amplification, which accentuates more surficial and local scale contributions from the magnetic field at the expense of deeper and more regional magnetic anomalies. The pink diamonds indicate mineral occurrences of YGS. The gray polygons indicate the boundaries of the geological formations. The dashed black lines indicate the faults/shears and the dashed blue lines indicate fold axes. The pink dotted line approximately separates the Rory claims from the other claims. The previously identified fault-like lineaments are marked with white dashed lines and the previously identified anomalies are marked with numbers.

Main Findings

The details of the high magnetic Anomalies 1, 2, 3, 4 and 5 are very clear.

The yellow dashed lines indicate the local scale breaks/faults that are not continuous throughout the claim group.

The dotted red polygons delineate the magnetically silent zones with less variable bright green colour. Most of these zones, except the southern-most one, coincide with the Skolai formation (CPS1 – see Figure 4). A magnetic intrusion in the Skolai formation may form a region of interest similar to the Wellgreen deposit, such as Anomaly 12.

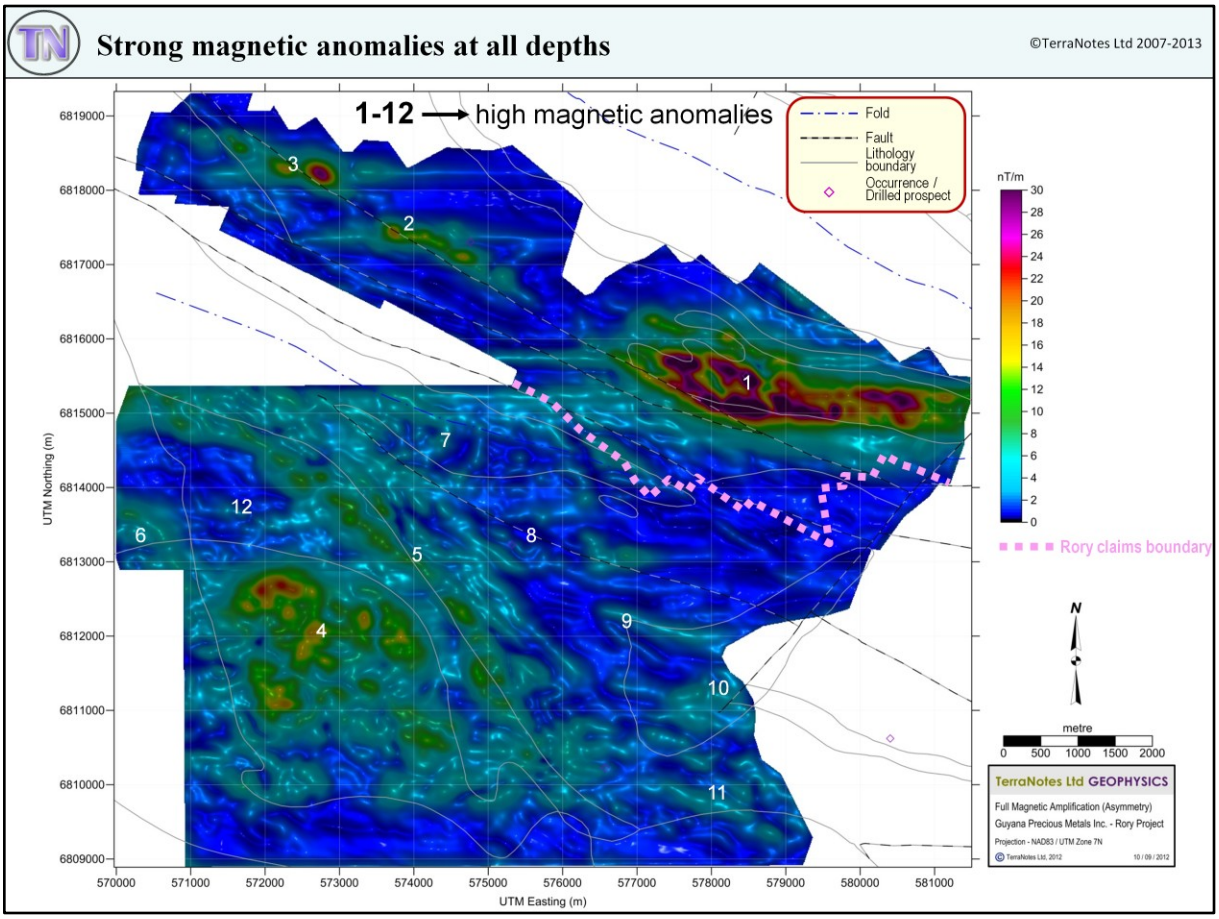


Figure 17. The strong magnetic features from near surface to greater depths. The pink diamonds indicate mineral occurrences of YGS. The gray polygons indicate the boundaries of the geological formations. The dashed black lines indicate the faults/shears and the dashed blue lines indicate fold axes. The pink dotted line approximately separates the Rory claims from the other claims. The previously identified anomalies are marked with numbers.

Main Findings

Anomalies 1, 2, 3, 4 and 5 are the strongest anomalies.

The intermediate anomalies (7 and 8) almost disappeared in the map above. This observation may suggest weak magnetic properties of a thicker geological formation. This could be due to a lithology, most likely due to Nicolai formation.

Other intermediate magnetic anomalies (6, 9, 10, and 11) form linear shaped anomalies which may indicate magnetic mineral deposition which may be associated with the Cu-Ni-PGE mineralization. Anomaly 9, found on the contact zone between Nicolai and Quaternary, forms an interesting shape, which may be related to the mineralization.

The Anomaly 12, which was weak, is still visible in the map above, suggesting a magnetic mineral deposit that may be associated with Ni-Cu-PGE mineralization.

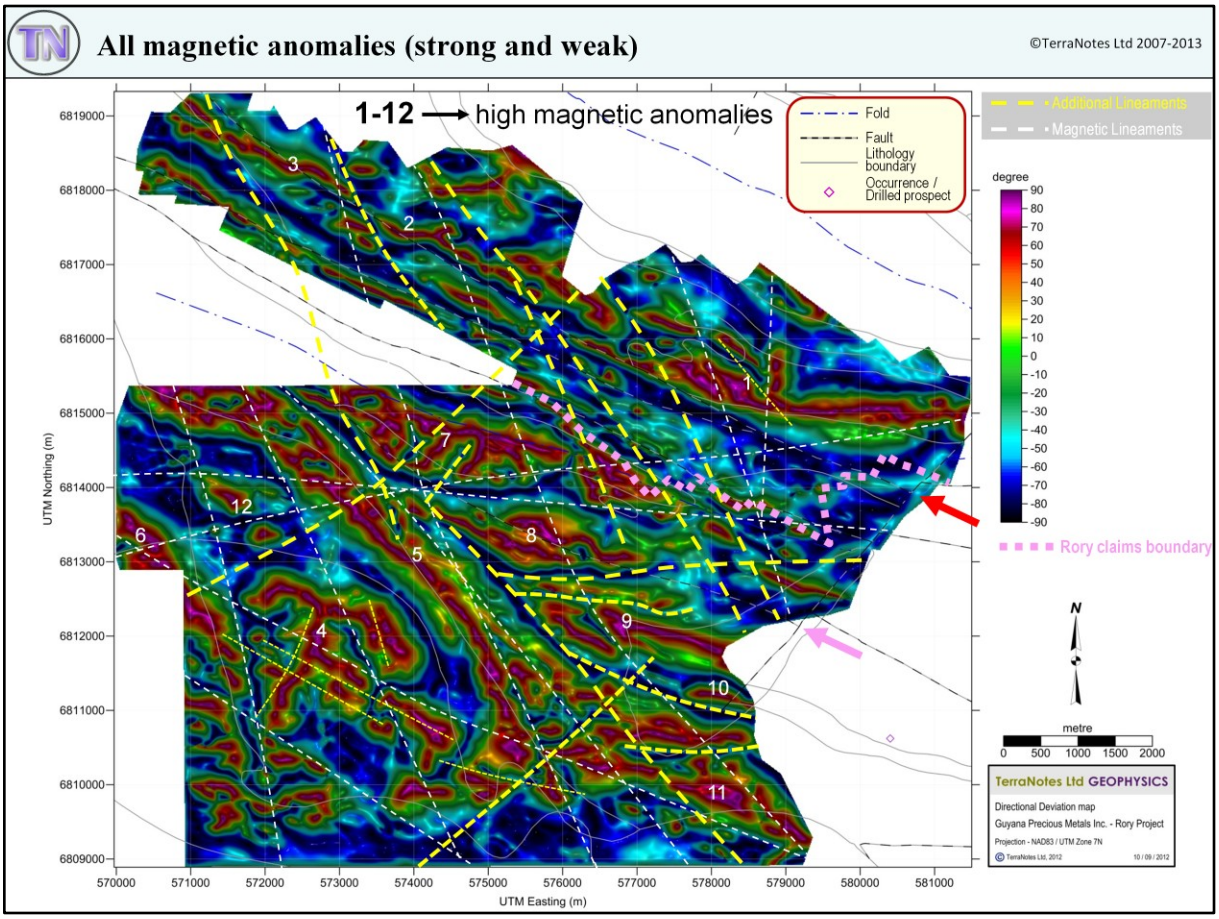


Figure 18. All magnetic structures, including the weak and deep anomalies, displayed at the same level as the strong and near surface anomalies. The pink diamonds indicate mineral occurrences of YGS. The gray polygons indicate the boundaries of the geological formations. The dashed black lines indicate the faults/shears and the dashed blue lines indicate fold axes. The pink dotted line approximately separates the Rory claims from the other claims. The previously identified anomalies, faults, and local breaks are marked with numbers, white dashed lines, and thin yellow dashed lines, respectively.

Main Findings

This map shows all the magnetic anomalies and how they are connected to each other. For example, the continuation from Anomaly 1 to Anomalies 2 and 3 is very clear in this figure.

No connection, however, was observed from Anomaly 1 to the NE corner of the Rory claims.

This map confirms all the previous findings of the magnetic interpretation in Figures 11-17, as well as the faults that are drawn from Yukon government data (dashed black-gray lines). For example, the northern fault (see red arrow) bounds the southern part of Anomalies 1, 2 and 3 perfectly. The fault line which divides Anomaly 8 in two pieces (see pink arrow), also matches very well with the details in the magnetic map above. This indicates that the government maps contain enough details to be used in local interpretation.

The thick yellow dashed lines indicate the additional fault-like structures and breaks that are deduced form this map.

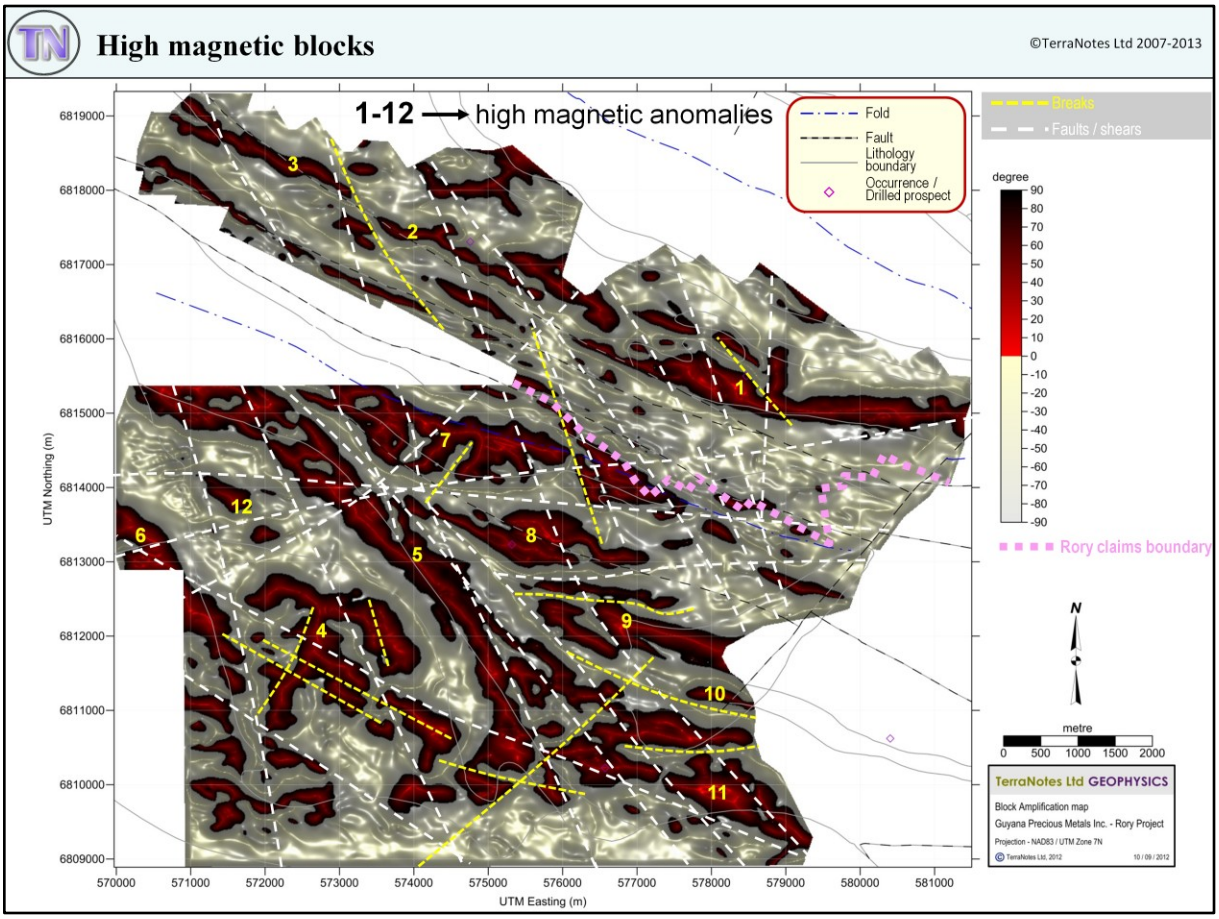


Figure 19. A simplified version of the map of the high magnetic blocks (see pink anomalies in Figure 18) in red. Bright red areas indicate the high magnetic anomalies and the darker red areas delineate the edges of these anomalies. The pink diamonds indicate mineral occurrences of YGS. The gray polygons indicate the boundaries of the geological formations. The dashed black lines indicate the faults/shears and the dashed blue lines indicate fold axes. The pink dotted line approximately separates the Rory claims from the other claims. The previously identified anomalies, faults, and local breaks are marked with numbers, thin white dashed lines, and thin yellow dashed lines, respectively.

Main Findings

It is interpreted that the economic Cu-Ni and PGE mineralization occurs within or in contact with the red area in Anomaly 1. This indicates that the red areas may be of interest for further Cu-Ni and PGE exploration.

Please note that magnetite, pyrrhotite, ilmenite, and franklinite may be present within the red blocks since they exhibit high magnetism.

The location of the faults and breaks (white and yellow dashed lines) fit well with the shapes of the anomalies.

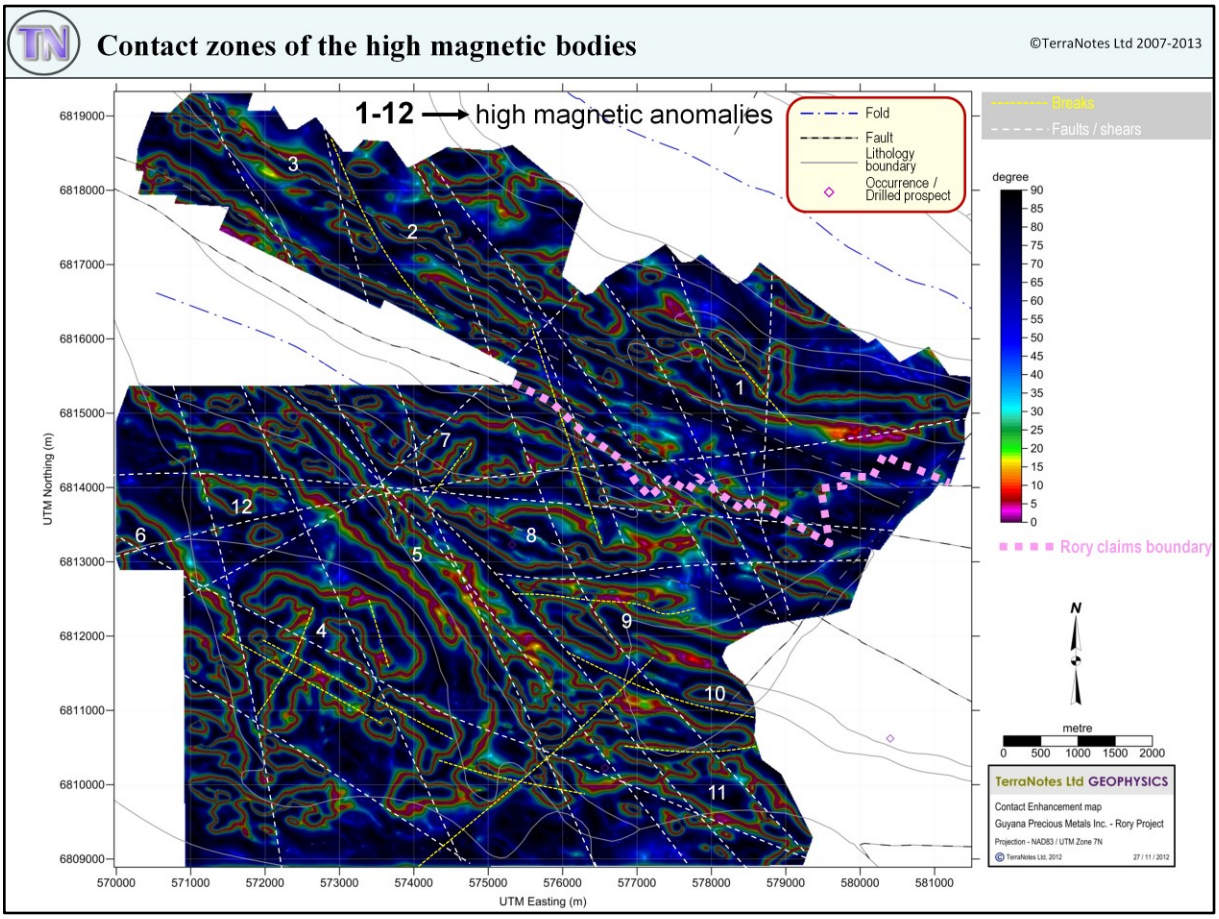


Figure 20. Contact enhancement map, which visualizes the contact zones of the high magnetic blocks. The pink diamonds indicate mineral occurrences of YGS. The gray polygons indicate the boundaries of the geological formations. The dashed black lines indicate the faults/shears and the dashed blue lines indicate fold axes. The pink dotted line approximately separates the Rory claims from the other claims. The previously identified anomalies, faults, and local breaks are marked with numbers, thin white dashed lines, and thin yellow dashed lines, respectively.

Main Findings

The red anomalies indicate the contact zones of the high magnetic structures at all depths.

This map can be very helpful during the placement of a drill hole targeting the contact zones of the highly magnetic structures. After locating a zone of interest from previous maps and the associated contact zone above, a drill collar could easily be placed outside the contact zone in order to drill through it and the source of the magnetic anomaly.

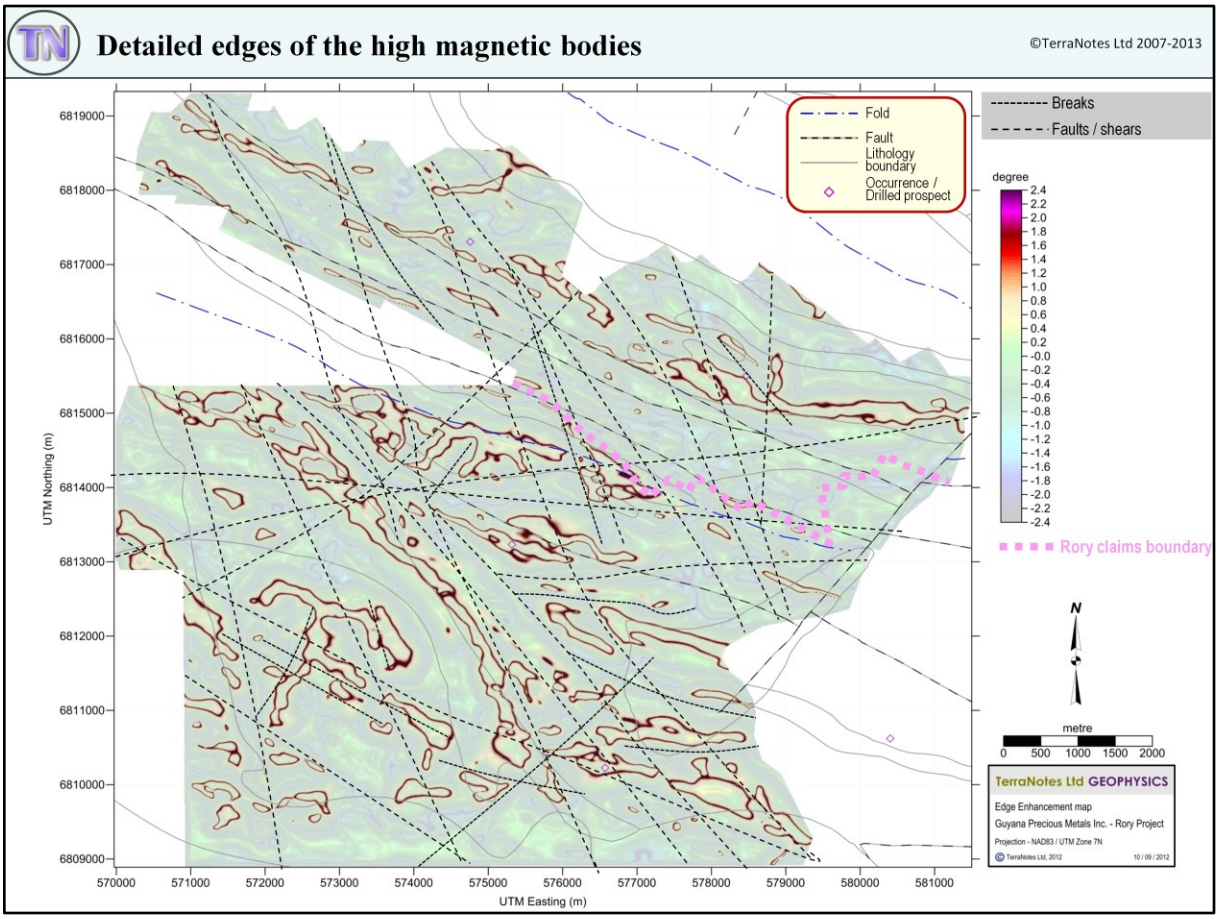
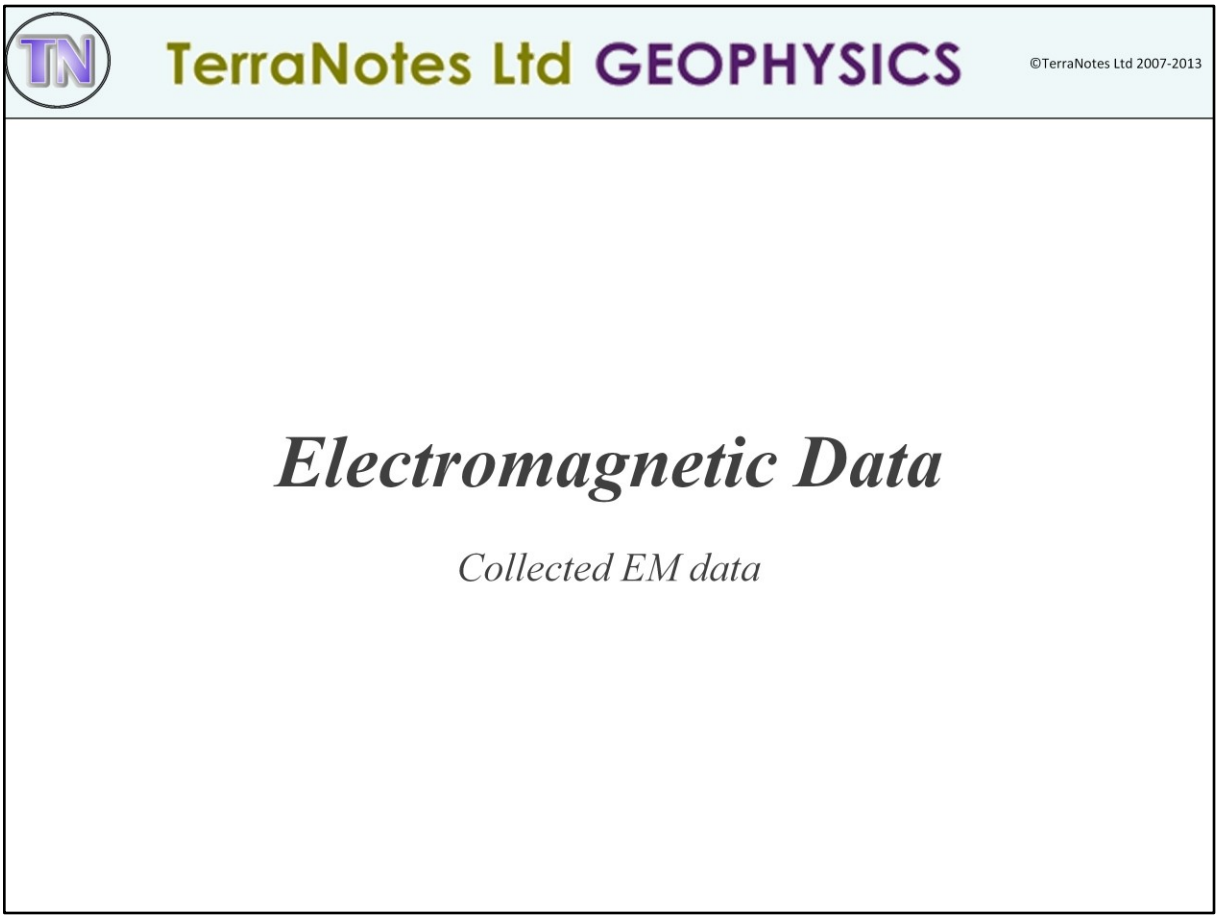


Figure 21. The detailed edges of the high magnetic blocks indicated by dark red polygons. It will be very useful in the later stages of the exploration, such as sampling, drilling, and mining. The pink diamonds indicate mineral occurrences of YGS. The gray polygons indicate the boundaries of the geological formations. The dashed black lines indicate the faults/shears and the dashed blue lines indicate fold axes. The pink dotted line approximately separates the Rory claims from the other claims. The previously identified faults are marked with black dashed lines.

Main Findings

It is expected that the most magnetic mineralization occurs within the dark red polygons.


TerraNotes Ltd GEOPHYSICS
©TerraNotes Ltd 2007-2013
Electromagnetic Data
Collected EM data

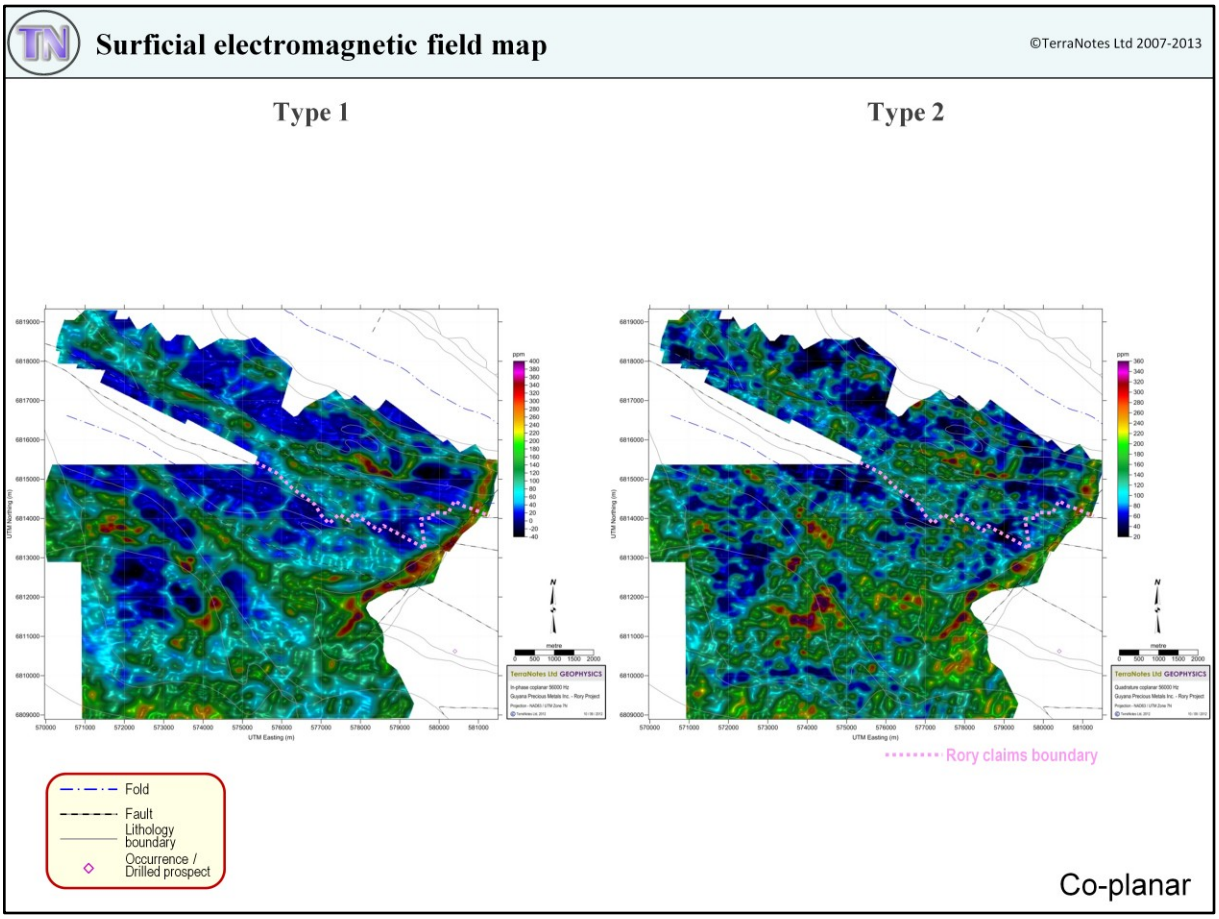


Figure 22. The left panel shows the highest frequency (56000 Hz) in-phase EM data, which reflects the surficial conductivity structure. The right panel shows the same frequency quadrature EM data which also reflects the surficial conductivity structure. The pink diamonds indicate mineral occurrences of YGS. The gray polygons indicate the boundaries of the geological formations. The dashed black lines indicate the faults/shears and the dashed blue lines indicate fold axes. The pink dotted line approximately separates the Rory claims from the other claims.

Main Findings

The warm coloured zones indicate the high conductivity and the cool coloured zones indicate high resistivity.

The in-phase and quadrature components are similar to each other, which suggest a similar conductivity and magnetic structure at the surface. This was expected for the high frequency data.

Since this data reflects the surficial structures, the anomalous areas in the map above may be associated with the topographic features. For example, conductive sediment along the creeks and valleys may be responsible for some of the conductive anomalies. To eliminate the topographical effect, we have compared the in-phase data with the DTM map (see Figure 23).

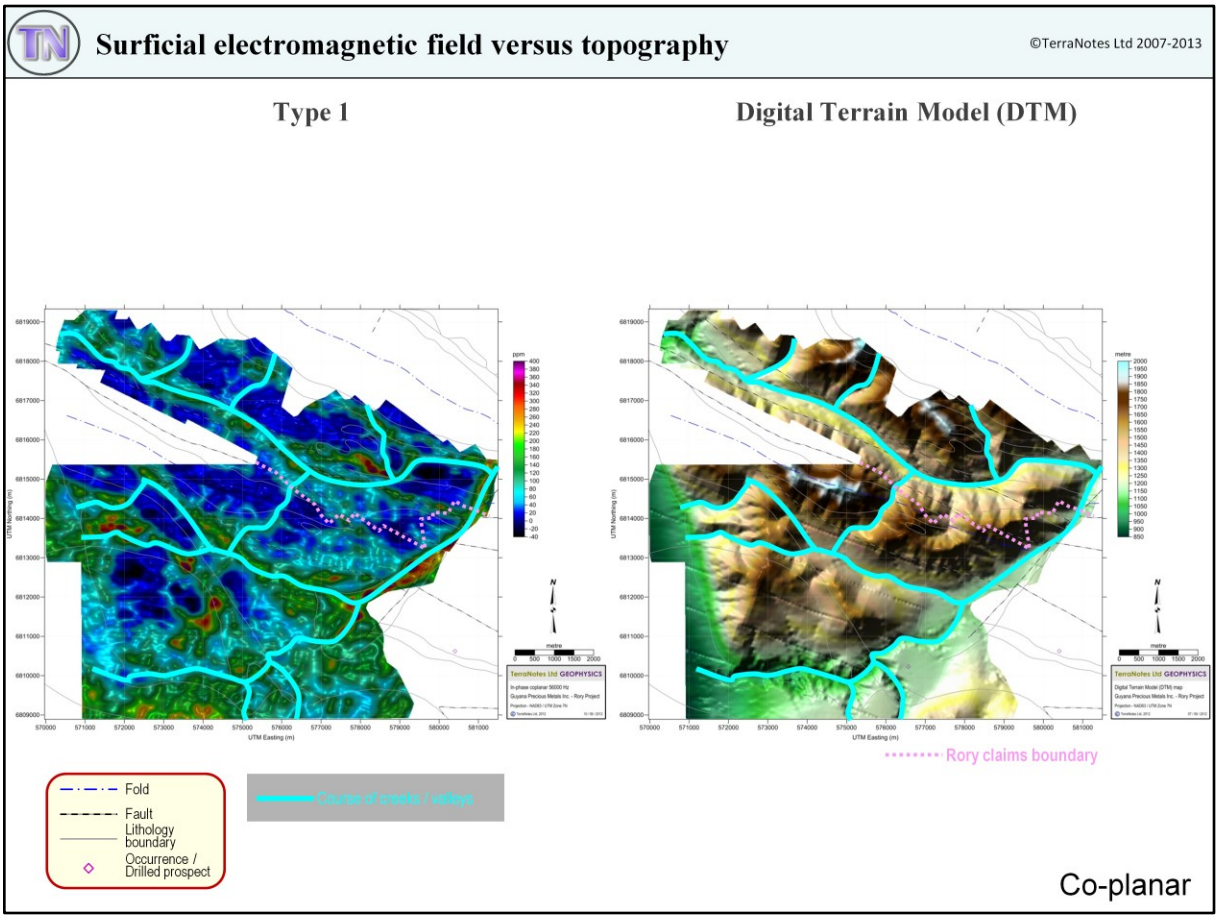


Figure 23. The left panel shows the highest frequency (56000 Hz) in-phase EM data which reflects the surficial conductivity structure. The right panel shows the DTM. The pink diamonds indicate mineral occurrences of YGS. The gray polygons indicate the boundaries of the geological formations. The dashed black lines indicate the faults/shears and the dashed blue lines indicate fold axes. The pink dotted line approximately separates the Rory claims from the other claims.

Main Findings

The thick cyan lines mark the creeks and valleys deduced from the DTM map (right panel). The same polygons are overlaid on the in-phase map (left panel) to mask the EM conductors due to topographical features.

The linear conductor in the north appears to follow the Nickel and Arch creeks. However, there are still other conductors that exist to the north of the creek in the elevated areas. The strongest conductor in this area seems to be related to the Wellgreen deposit.

A zone to the south of Maple Creek is also conductive and could be due to sediment deposition on a flat lying topography.

The stronger conductors in the central zone seem to be independent of the topographic features and may be related to the magnetic structures. In order to evaluate these anomalies, the in-phase map must be compared to the magnetic map (see Figure 24).

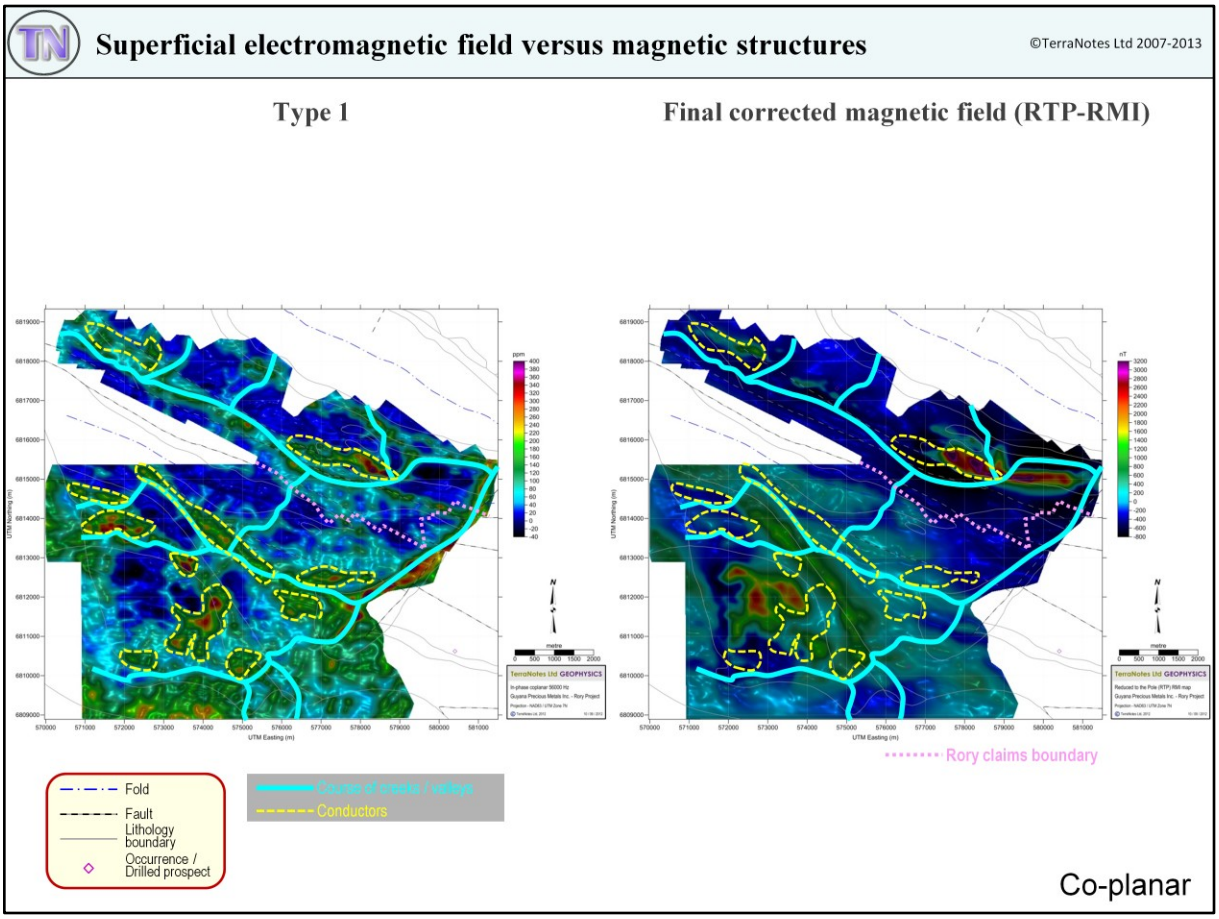


Figure 24. The left panel shows the highest frequency (56000 Hz) in-phase EM data which reflects the surficial conductivity structure. The right panel shows the final corrected magnetic field (RTP-RMI) map. The pink diamonds indicate mineral occurrences of YGS. The gray polygons indicate the boundaries of the geological formations. The dashed black lines indicate the faults/shears and the dashed blue lines indicate fold axes. The pink dotted line approximately separates the Rory claims from the other claims. The cyan lines mark the position of the creeks and valleys.

Main Findings

The dashed yellow polygons indicate the conductive structures that are independent from the topographical features in the left panel of this figure.

These polygons are also overlaid on the RTP-RMI map (right panel) to investigate if these conductors are associated with magnetic structures.

As seen in the maps above, only the Wellgreen conductor is associated with a strong magnetic anomaly. The rest of the conductive anomalies are related to intermediate or low intensity magnetic zones.

Further comparative interpretation of EM conductors with medium to high magnetic structures will reveal additional Cu-Ni-PGE targets.

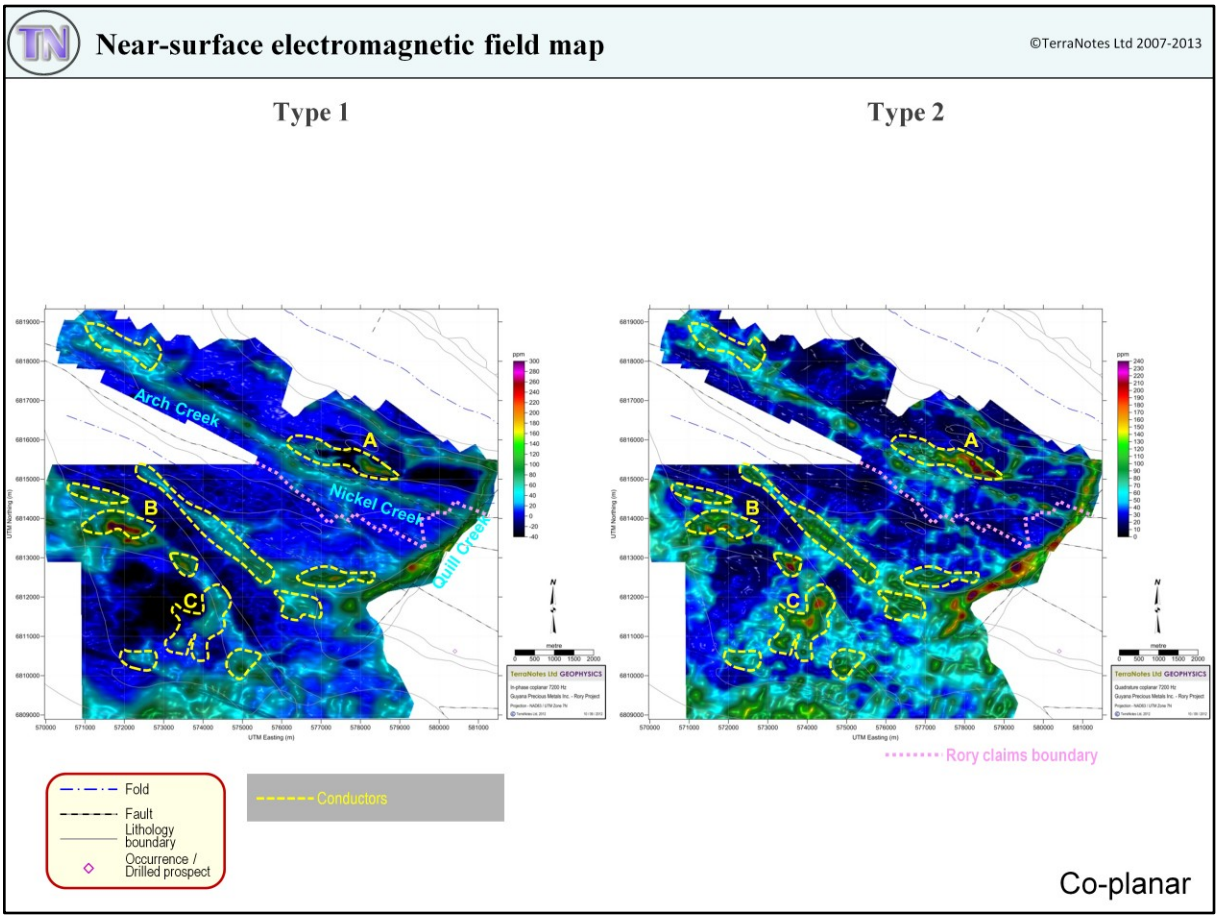


Figure 25. The left panel shows the high frequency (7200 Hz) in-phase EM data, which reflects the near-surface conductivity structure. The right panel shows the same frequency quadrature EM data, which also reflects the near-surface conductivity structure. The pink diamonds indicate mineral occurrences of YGS. The gray polygons indicate the boundaries of the geological formations. The dashed black lines indicate the faults/shears and the dashed blue lines indicate fold axes. The pink dotted line approximately separates the Rory claims from the other claims.

Main Findings

The near surface maps show the same conductive structures as the surficial maps (Figure 22).

The difference occurs in the Wellgreen area and in the west. The Wellgreen conductor (A) becomes weaker in the In-phase component while the Quadrature component becomes stronger. The western conductor (B) also get stronger in in-phase component and begins to appear in the Quadrature component.

The conductor C, in the south, also becomes weaker in both In-phase and Quadrature component, which may suggest a superficial conductor or conductive overburden.

The effect of Quill, Nickel, and Arch Creeks is still visible at near surface maps, particularly on in-phase component.

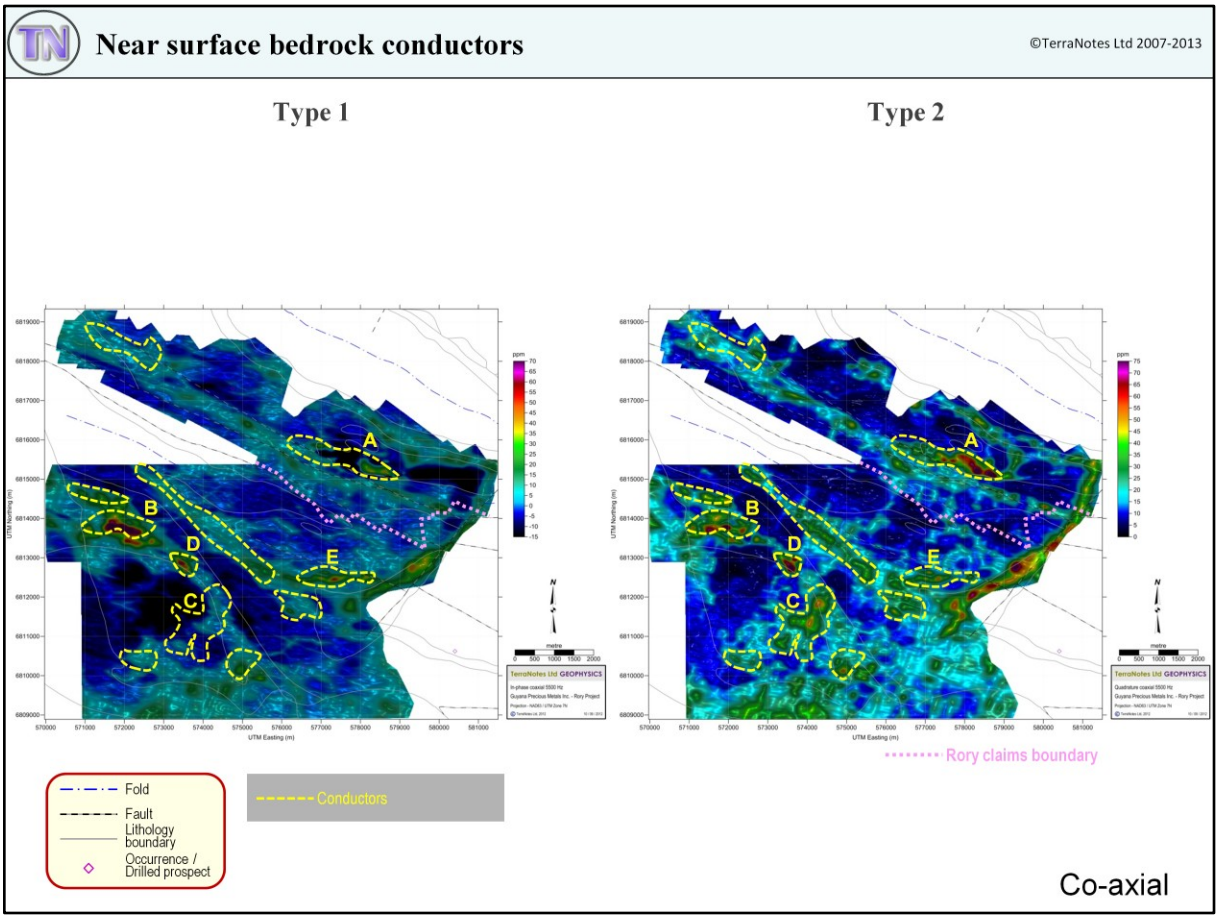


Figure 26. The left panel shows the mid-frequency (5500 Hz) in-phase EM data, which reflects the near-surface conductivity structure. The right panel shows the mid-frequency (5500 Hz) quadrature EM data which also reflects the near-surface conductivity structure. These maps show the EM data from a co-axial transmitter and receiver while the previous maps show the EM data from co-planar a transmitter and receiver. Co-axial data is more sensitive to discrete conductors such as vertical sheets which may represent the bedrock conductors such as sulphidic or graphitic body. Co-planar data is more sensitive to broader conductors such as geological formations, conductive overburdens, etc. The pink diamonds indicate mineral occurrences of YGS. The gray polygons indicate the boundaries of the geological formations. The dashed black lines indicate the faults/shears and the dashed blue lines indicate fold axes. The pink dotted line approximately separates the Rory claims from the other claims.

Main Findings

Conductors B, D, and E become stronger in the co-axial component, which may suggest a more discrete conductive body in comparison to other conductors. Anomaly B particularly becomes very strong.

Anomaly A begins to disappear in the in-phase component. This is called the susceptibility effect. The high magnetic susceptibility in the ultramafic rocks masks the conductive anomaly in the in-phase data (left panel), but it still exist in the quadrature data (right panel).

A similar phenomenon may be occurring at the location of Anomaly C since the quadrature component is stronger than the in-phase component.

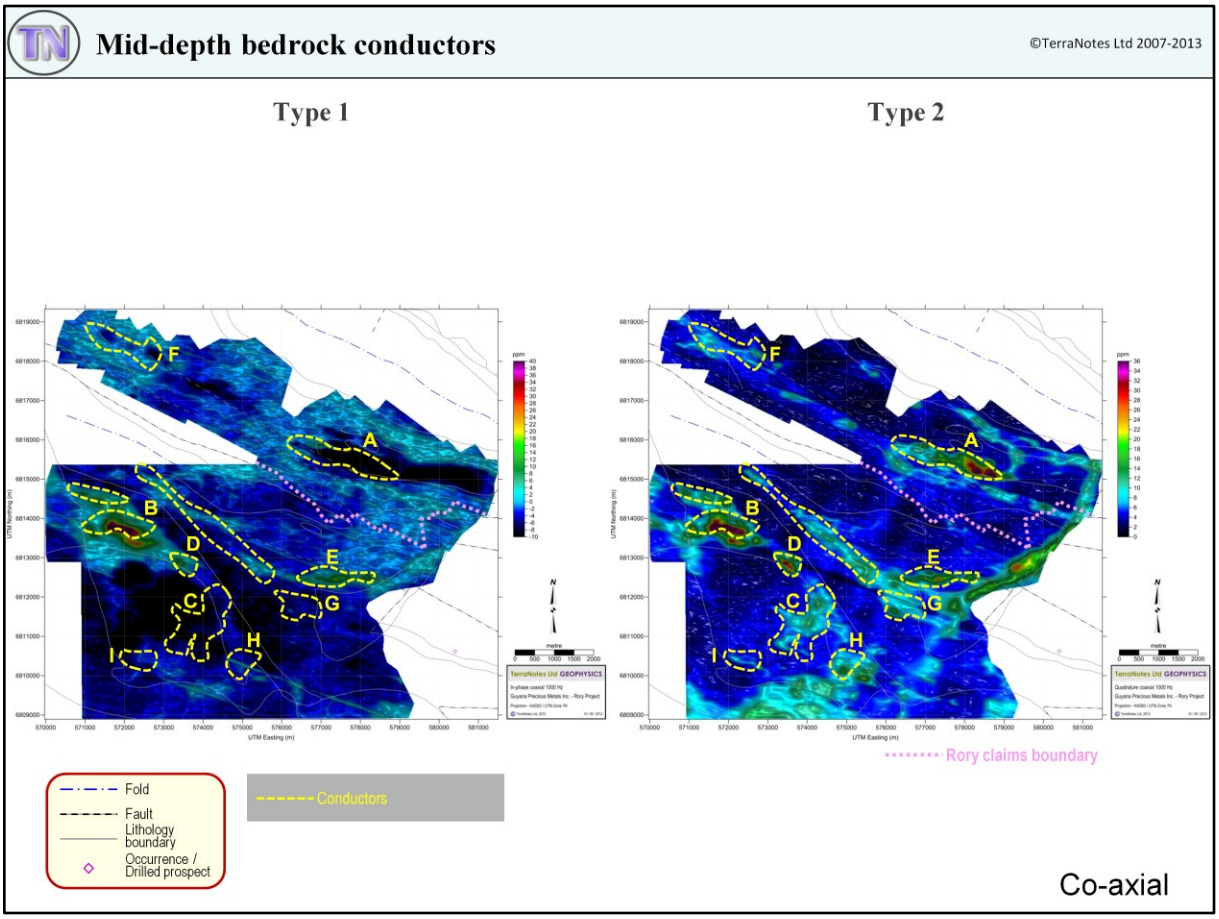


Figure 27. The left panel shows the lower frequency (1000 Hz) in-phase EM data, which reflects the mid-depth conductivity structure. The right panel shows the lower frequency (1000 Hz) quadrature EM data, which also reflects the mid-depth conductivity structure. This map also shows co-axial data, which is more sensitive to discrete bedrock conductors such as vertical sulphide bodies. The pink diamonds indicate mineral occurrences of YGS. The gray polygons indicate the boundaries of the geological formations. The dashed black lines indicate the faults/shears and the dashed blue lines indicate fold axes. The pink dotted line approximately separates the Rory claims from the other claims.

Main Findings

The Wellgreen conductor (A) totally disappeared from the in-phase component due to high magnetic susceptibility of ultramafic rocks. The Quadrature component still shows a strong anomaly, suggesting a very strong bedrock conductor at this location.

Phenomena similar to Anomaly A can be observed at Anomalies C and F. Anomalies G, H, and I also show similar characteristics but more weakly.

The dark blue zones of the in-phase map (left panel) also indicates the high magnetic intensity zones with higher susceptibilities.

The topographic effects due to creeks and valleys are no longer present in the mid-depth maps.

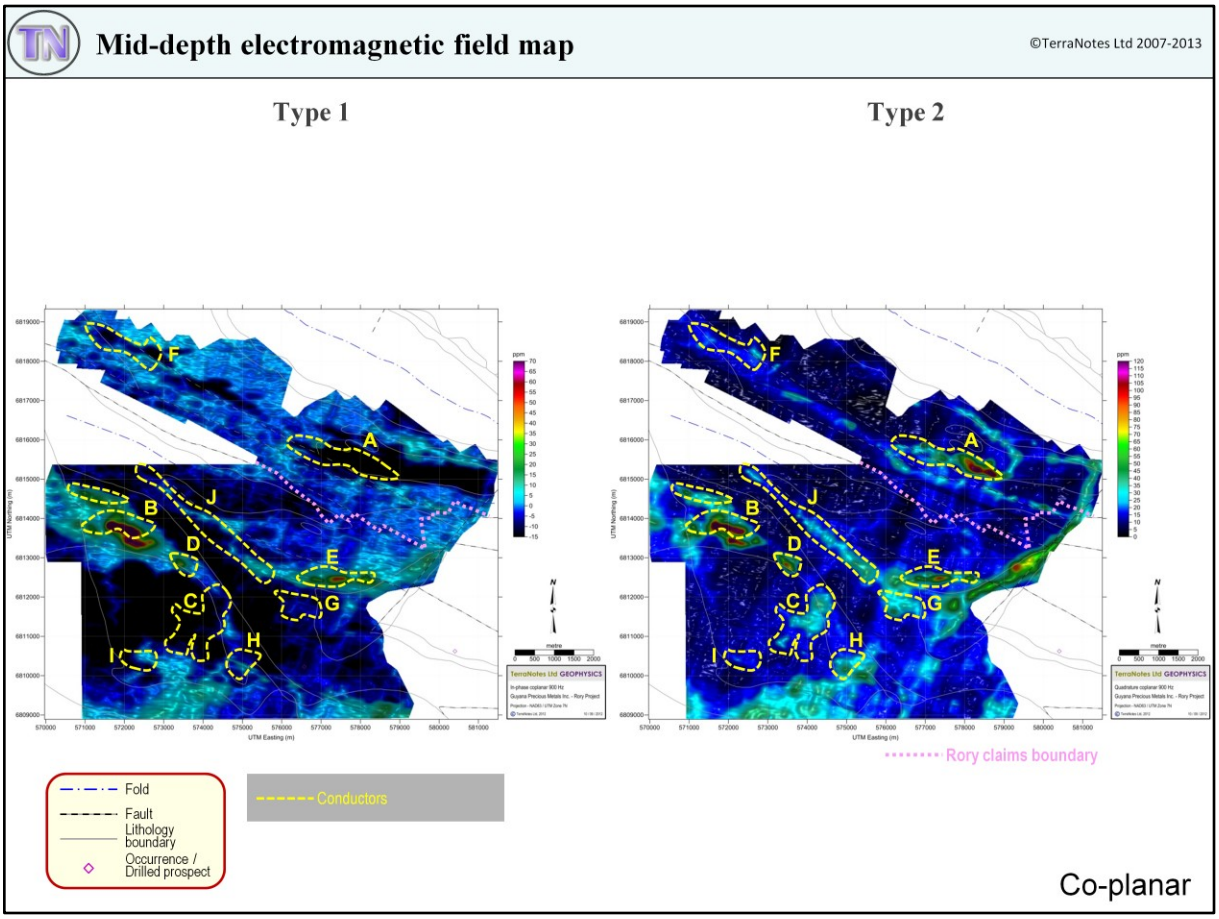


Figure 28. The left panel shows the lowest frequency (900 Hz) in-phase EM data, which reflects the mid-depth conductivity structure. The right panel shows the lowest frequency (900 Hz) quadrature EM data, which also reflects the mid-depth conductivity structure. This map shows co-planar data as opposed to the co-axial data shown in Figures 26 and 27. Co-planar data is more sensitive to broad conductors such as geological formations. The pink diamonds indicate mineral occurrences of YGS. The gray polygons indicate the boundaries of the geological formations. The dashed black lines indicate the faults/shears and the dashed blue lines indicate fold axes. The pink dotted line approximately separates the Rory claims from the other claims.

Main Findings

The bedrock conductor characteristics can be observed at Anomalies A, B, D, E, and F.

Anomalies C, H, and I seem to be broader conductors that may be related to geological formations or alterations.

Anomalies G and J have more complex characteristics and may be either bedrock conductors or conductive alterations.

Please note that conductive alterations may also indicate association with mineralization.

Anomalies A, C, and F appear to exhibit strong susceptibility effect in the in-phase component.

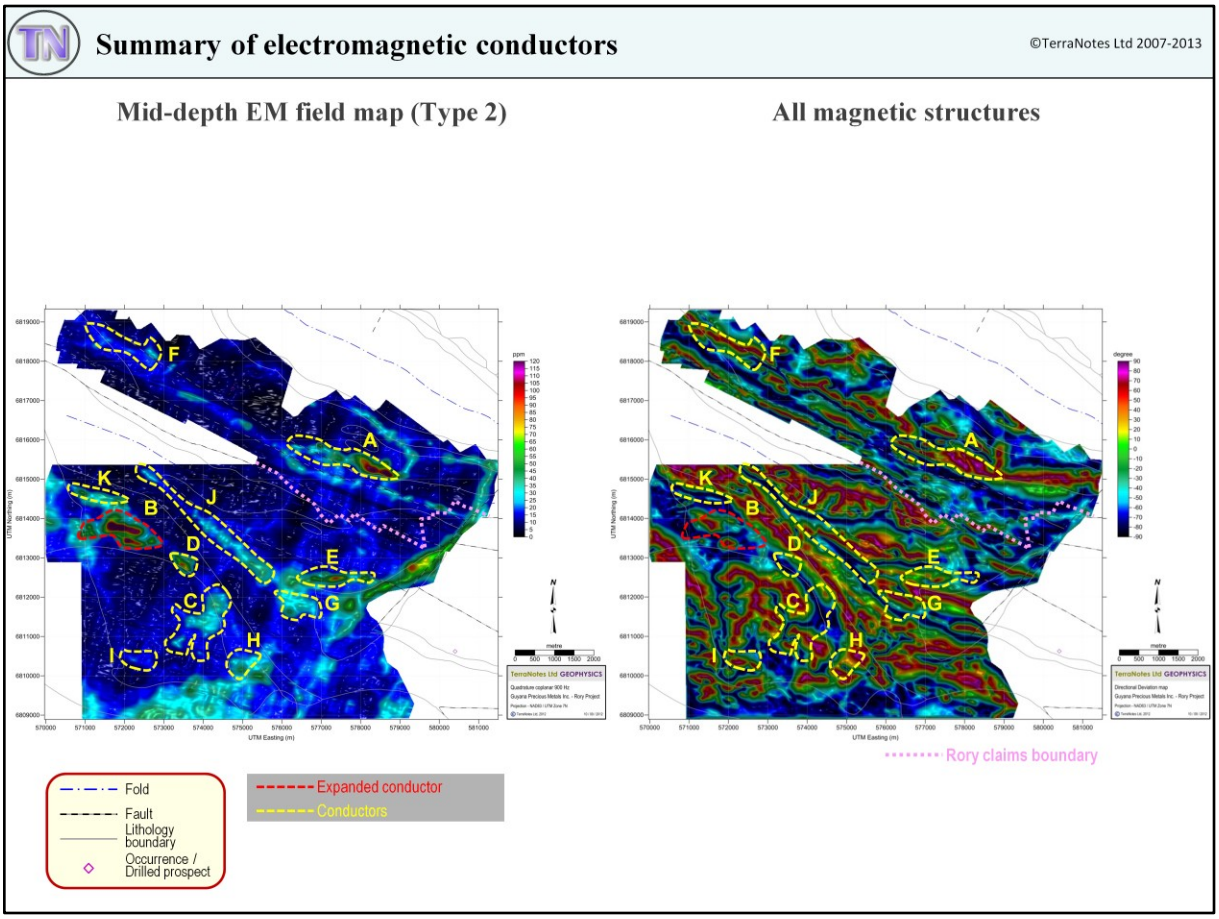


Figure 29. The left panel shows the lowest frequency (900 Hz) quadrature EM data, which reflects the mid-depth conductivity structure. The right panel shows all of the magnetic structures deduced from the directional deviation map. The pink diamonds indicate mineral occurrences of YGS. The gray polygons indicate the boundaries of the geological formations. The dashed black lines indicate the faults/shears and the dashed blue lines indicate fold axes. The pink dotted line approximately separates the Rory claims from the other claims.

Main Findings

Anomaly A coincides with the high magnetic structure and may be associated with Cu-Ni-PGE mineralization.

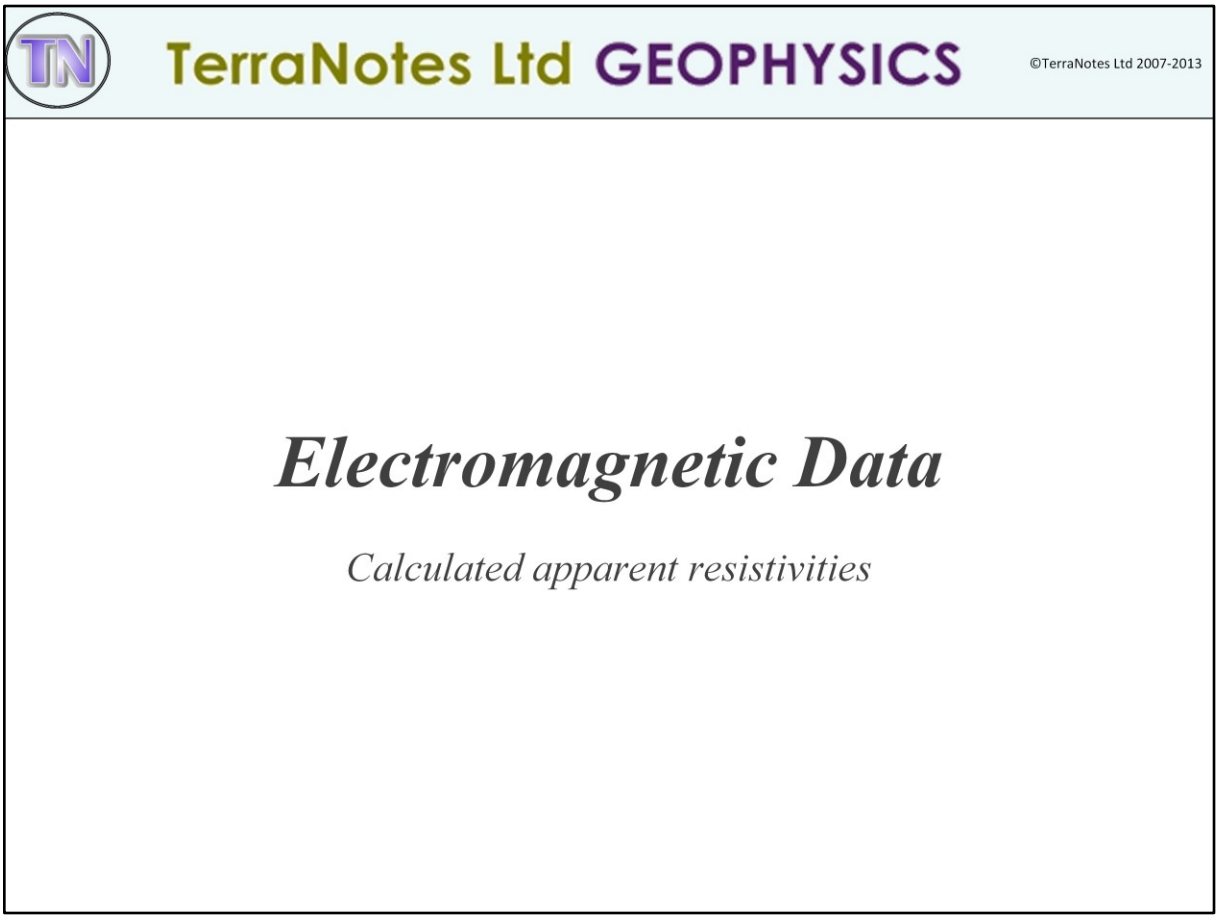
Anomaly B, which was extended more than the previous maps as shown with red dashed line, coincides with the high magnetic structure and may be associated with Cu-Ni-PGE mineralization.

Anomaly E coincides with the high magnetic structure and may be associated with Cu-Ni-PGE mineralization.

Anomaly F coincides with the high magnetic structure and may be associated with Cu-Ni-PGE mineralization.

Anomaly I, which does not show very strong bedrock conductor characteristics, also coincides with the high magnetic structure and may be associated with Cu-Ni-PGE mineralization.

The rest of the conductors (C, D, G, H, J, and K) appears to coincide with the low magnetic zones and structures and may indicate graphitic conductors, alterations, or geological formations.


TerraNotes Ltd GEOPHYSICS
©TerraNotes Ltd 2007-2013
Electromagnetic Data
Calculated apparent resistivities

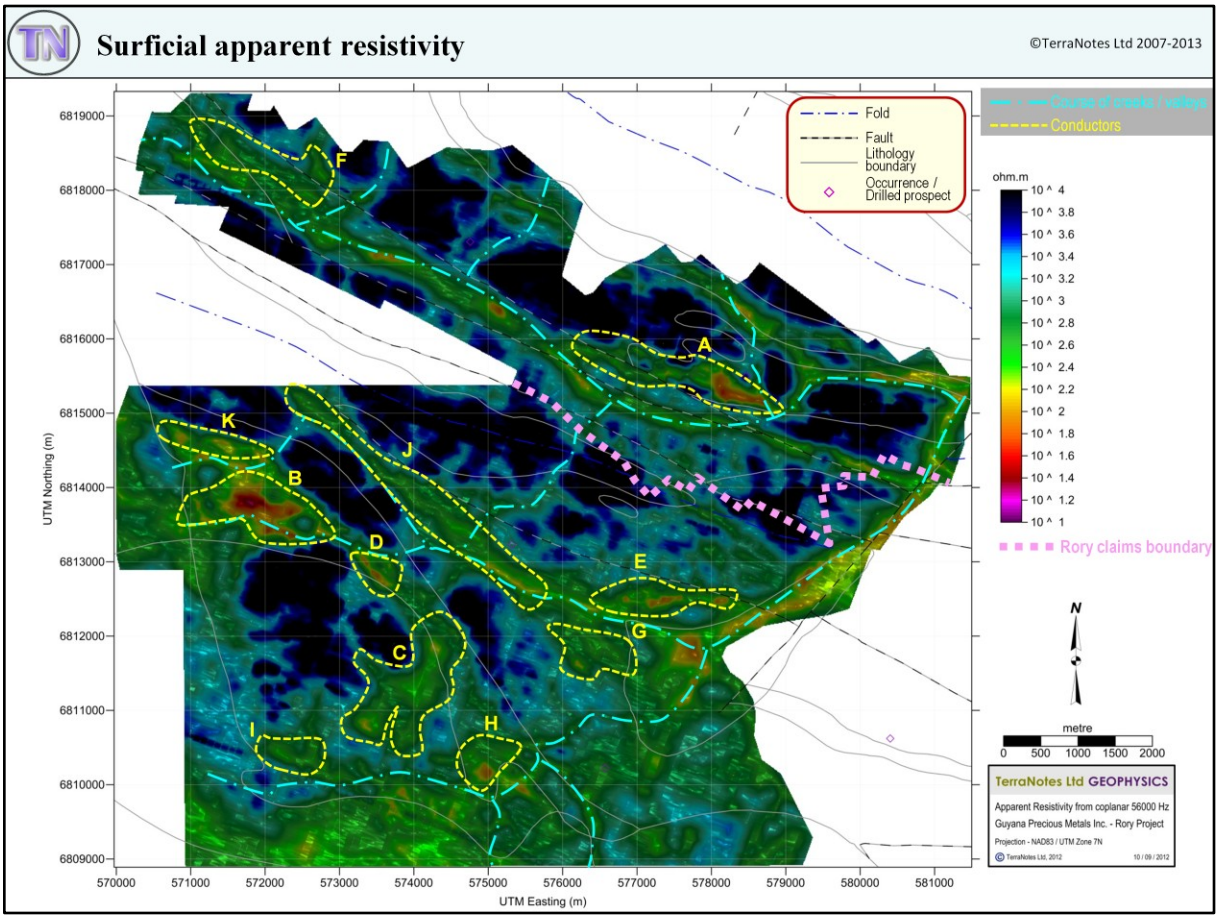


Figure 30. The calculated apparent resistivity using co-planar 56000 Hz data, which represents the surficial resistivity structures. The dash-dotted cyan lines indicate the location of creeks and valleys. The dashed yellow polygons and yellow letters mark the previously interpreted conductors. The pink diamonds indicate mineral occurrences of YGS. The gray polygons indicate the boundaries of the geological formations. The dashed black lines indicate the faults/shears and the dashed blue lines indicate fold axes. The pink dotted line approximately separates the Rory claims from the other claims.

Main Findings

Resistivity mapping is particularly useful where broad or flat-lying conductors are of interest, such as clay alteration, and it can be used to discriminate the conductor types. For example, discrete conductors will appear as narrow anomalies while the broad conductors will be wide. Also, resistivity mapping is not affected by the altitude variations, meaning that it only reflects anomalies due to resistivity changes.

All the previously identified conductors (yellow dashed polygons) are seen as the conductive zones in this figure.

Only anomalies A, B, D, E, and K are observed as narrow conductors with low resistivity (less than 100 Ω·m), meaning that they may represent bedrock conductors.

Since conductors D and K are mainly located on a low magnetic zone at a contact with a high magnetic zone, there is a slight chance that these conductors might be due to graphite rather than sulphide. Similar conclusions might be drawn for Conductors B and E, but they are less likely to be graphite.

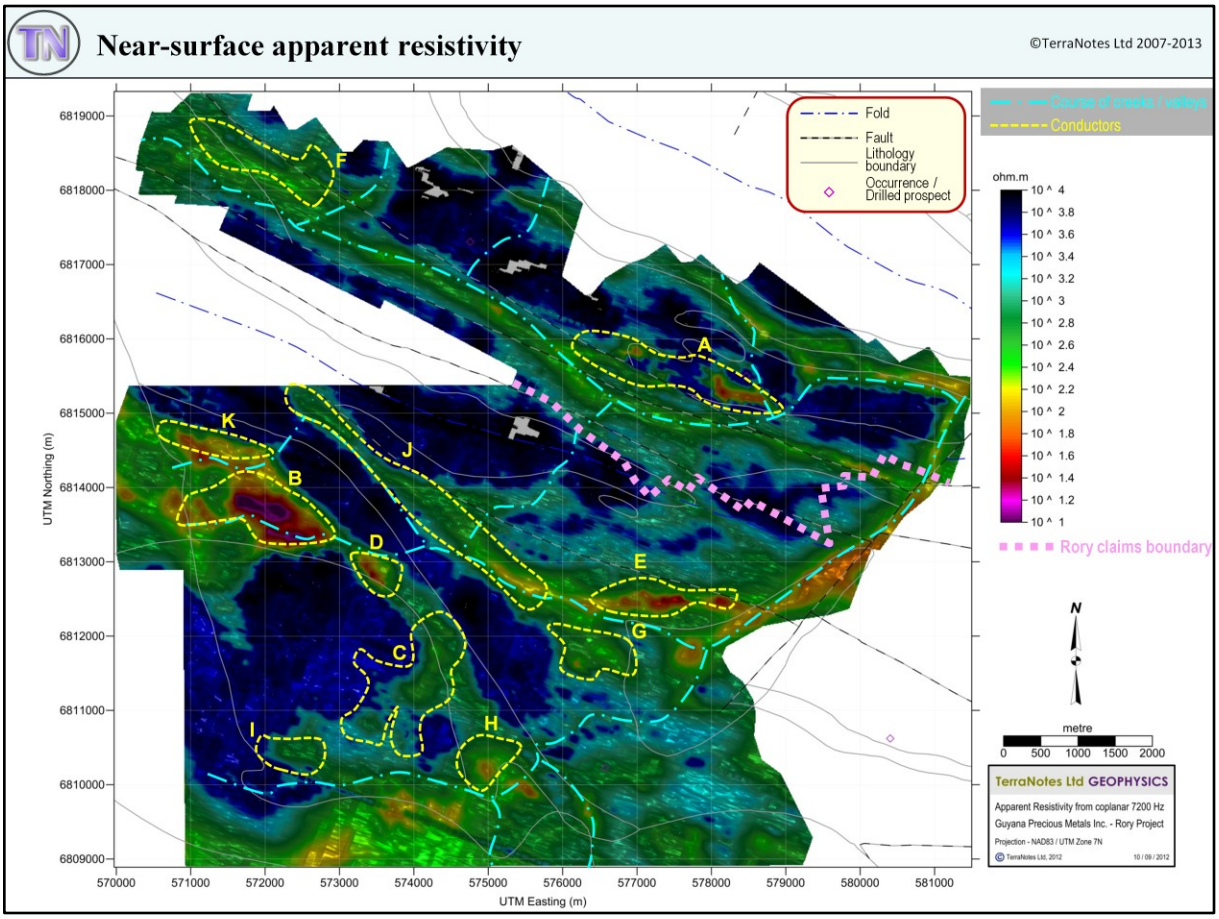


Figure 31. The calculated apparent resistivity using co-planar 7200 Hz data, which represents the near-surface resistivity structure. The dash-dotted cyan lines indicate the location of creeks and valleys. The dashed yellow polygons and yellow letters mark the previously interpreted conductors. The pink diamonds indicate mineral occurrences of YGS. The gray polygons indicate the boundaries of the geological formations. The dashed black lines indicate the faults/shears and the dashed blue lines indicate fold axes. The pink dotted line approximately separates the Rory claims from the other claims.

Main Findings

Anomalies B, D, E, and K appear stronger in this map than in Figure 30 whereas Anomaly A's strength remains the same.

All these four anomalies (B, D, E, and K) are situated on the Skolai formation (see Figure 4). It appears that the background conductive zone exactly coincides with the Skolai formation (CPS1). The Skolai formation consist of tuff, breccia, argillite, agglomerate, augite-phyric basaltic to andesitic flows (Station Creek Formation); and thin-bedded argillite, siltstone, minor graywacke and conglomerate, local thin basaltic flows, breccia, and tuff (Hasen Creek Formation). Among all these rock types, only argillite can be somewhat conductive with a minimum of 20 Ω·m resistivity. However, Anomalies B, D, E, and K are narrow, local anomalies within the broad conductive zone. Anomaly B is particularly anomalous with a resistivity less than 10 Ω·m. Thus, these anomalies could be bedrock conductors resulting from sulphide mineralization.

The high resistivity zones (dark blue) exhibit resistivity of ~10000 Ω·m. The Nicolai formation (uTrN), Kluane Ranges Suite (EKK), and Quaternary (Q) formations coincide with these zones (see Figure 4).

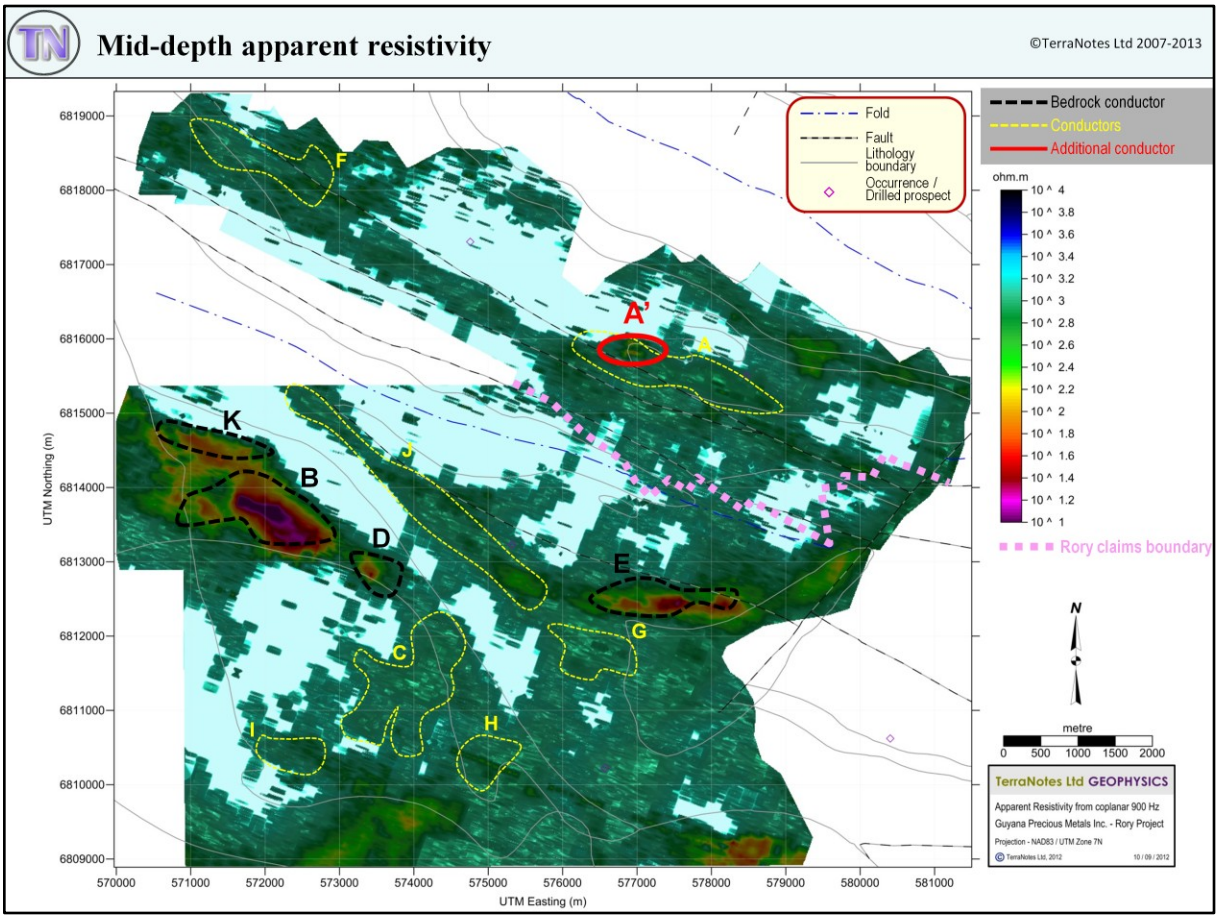


Figure 32. The calculated apparent resistivity using co-planar 900 Hz data, which represents the mid-depth resistivity structure. The dashed yellow polygons and yellow letters mark the previously interpreted conductors. The pink diamonds indicate mineral occurrences of YGS. The gray polygons indicate the boundaries of the geological formations. The dashed black lines indicate the faults/shears and the dashed blue lines indicate fold axes. The pink dotted line approximately separates the Rory claims from the other claims.

Main Findings

The black dashed polygons indicate the interpreted bedrock conductors. Anomaly B is still a very strong conductor with less than 10 Ω·m resistivity. Anomaly E becomes a stronger conductor (~10 Ω·m) with increasing depth as well.

Since Anomaly B and E are associated with weak to intermediate magnetic anomalies, they may indicate sulphide mineralization that could be associated with Cu-Ni-PGE mineralization.

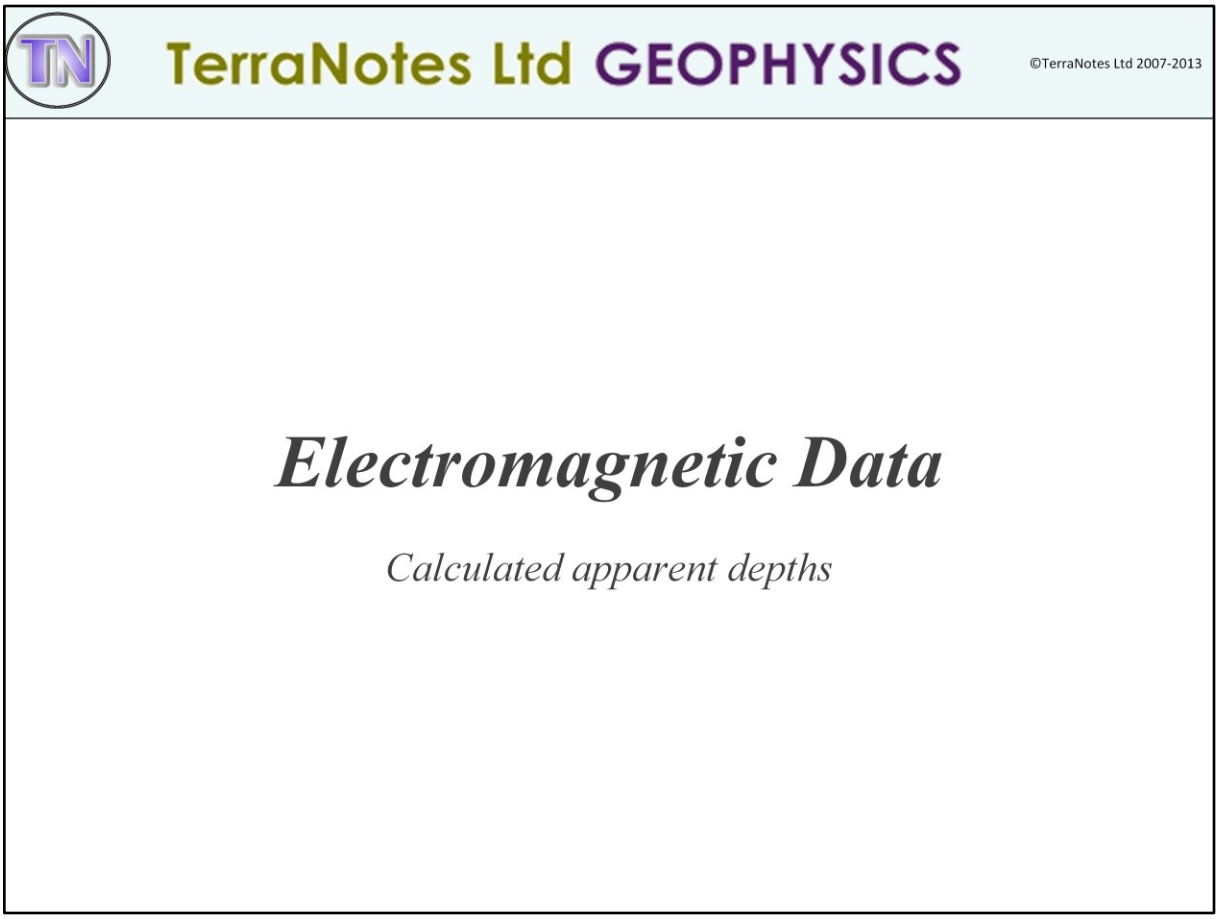
Anomaly K occurs on a low magnetic zone immediately east of very weak magnetic anomaly and, therefore, could be a sulphide or graphite mineralization.

Anomaly D also occurs on a low magnetic trend in between two magnetic highs and could be a graphitic conductor. However, a sulphide possibility for this location should also be investigated.

Other anomalies (A, C, F, G, H, I, and J) give a non-anomalous background resistivity around 1000 Ω·m. This may be due to a susceptibility effect increasing the resistivity (i.e. Anomaly A and F) or the anomalies being due to surficial conductors. If the latter is the case, the resistivity of the sources of these anomalies increases with depth while the overall background resistivity decreases with depth.

Fugro's algorithm could not calculate the apparent resistivity of the very resistive zones (see flat lying cyan zones).

The red ellipse shows the only conductive zone with a double peak, indicating a thin vertical conductor.


TerraNotes Ltd GEOPHYSICS
©TerraNotes Ltd 2007-2013
Electromagnetic Data
Calculated apparent depths

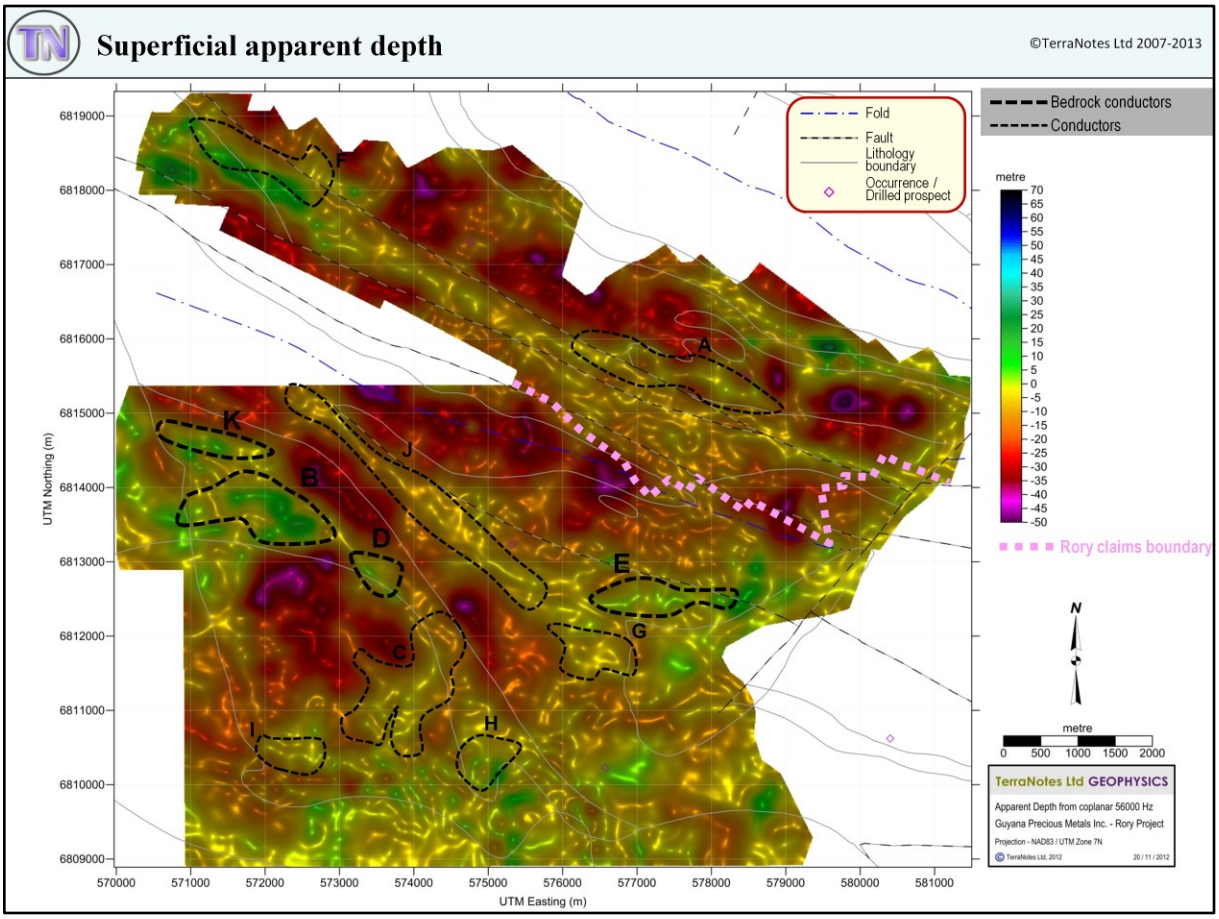


Figure 33. The calculated apparent depth using co-planar 56000 Hz data, which arises from surficial sources. The dashed black polygons and letters mark the previously interpreted conductors. The pink diamonds indicate mineral occurrences of YGS. The gray polygons indicate the boundaries of the geological formations. The dashed black lines indicate the faults/shears and the dashed blue lines indicate fold axes. The pink dotted line approximately separates the Rory claims from the other claims.

Special Note: Positive apparent depth indicates resistive top layer with conductive bottom layer, whereas the negative apparent depth indicates conductive top layer with resistive bottom layer.

Main Findings

Since we are interested in bedrock conductors, the positive apparent depths are of interest for further exploration. These are indicated by green and blue anomalies. As seen in the map above, only Anomalies B, D, E, and K are slightly above 0 m apparent depth in the surficial calculation.

The pink colour anomalies indicate zones that become more resistive with increasing depth.

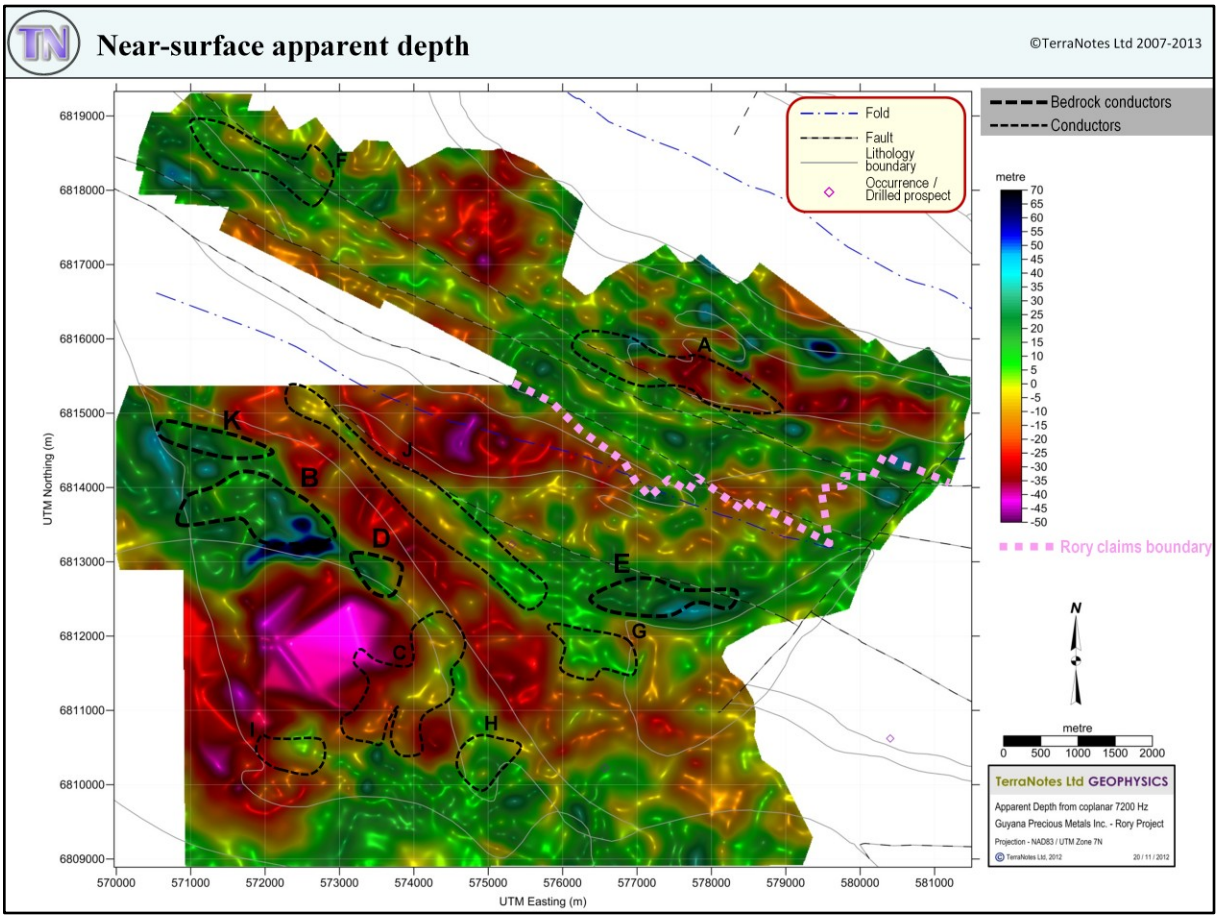


Figure 34. The calculated apparent depth using co-planar 7200 Hz data, which arises from near-surface sources. The dashed black polygons and letters mark the previously interpreted conductors. The pink diamonds indicate mineral occurrences of YGS. The gray polygons indicate the boundaries of the geological formations. The dashed black lines indicate the faults/shears and the dashed blue lines indicate fold axes. The pink dotted line approximately separates the Rory claims from the other claims.

Special Note: Positive apparent depth indicates resistive top layer with conductive bottom layer, whereas the negative apparent depth indicates conductive top layer with resistive bottom layer.

Main Findings

Anomalies B, D, E, and K are slightly above 0 m apparent depth, indicating the possibility of bedrock conductors.

Anomalies F, G, and H seem to have positive apparent depths as well, which indicates decreasing resistivity with depth.

The ultramafic rock beneath Anomaly A, which exhibits negative apparent depths, becomes more resistive with depth. This was expected due to the susceptibility effect.

Anomalies C, I, and J appear to become more resistive with depth, as indicated by the negative apparent depths.

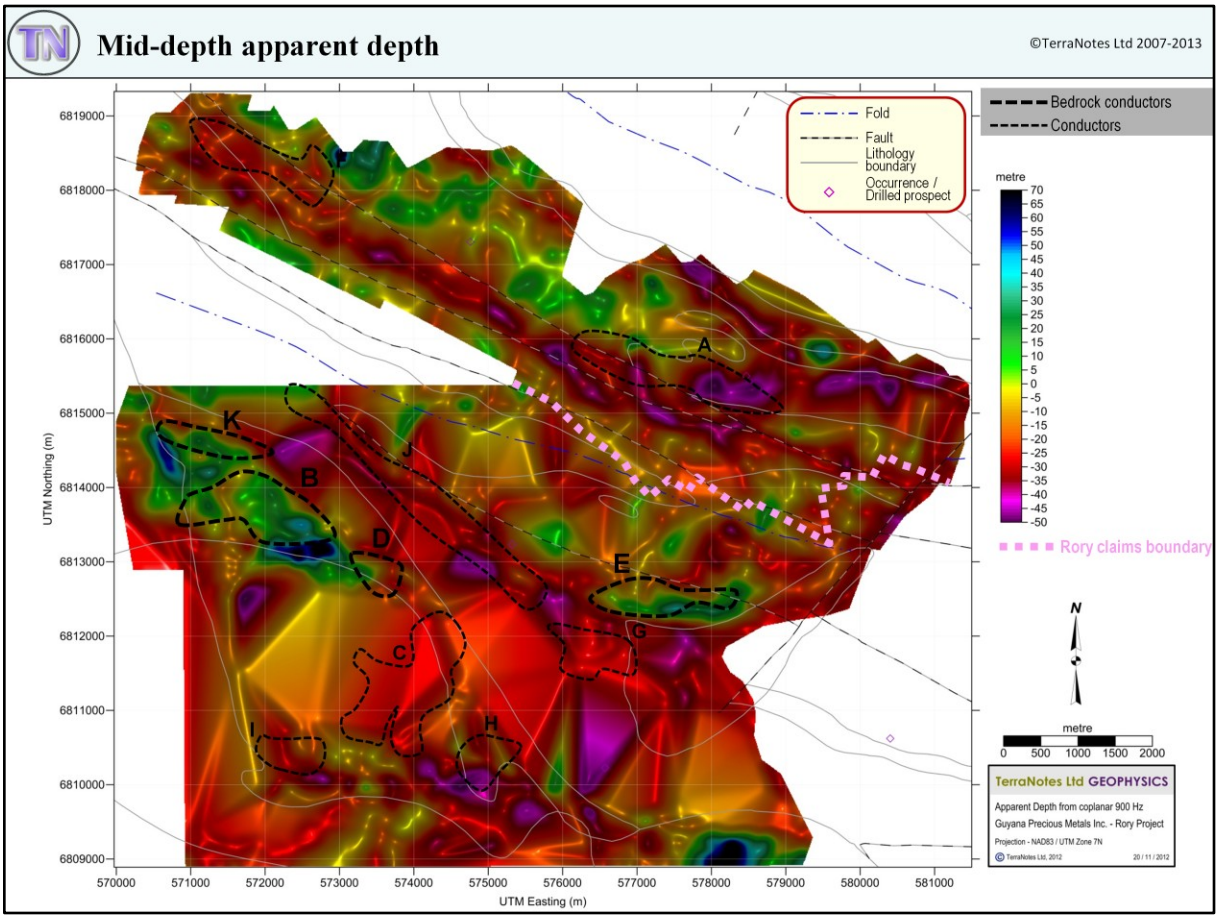


Figure 35. The calculated apparent depth using co-planar 900 Hz data, which arises from mid-depth sources. The dashed black polygons and letters mark the previously interpreted conductors. The pink diamonds indicate mineral occurrences of YGS. The gray polygons indicate the boundaries of the geological formations. The dashed black lines indicate the faults/shears and the dashed blue lines indicate fold axes. The pink dotted line approximately separates the Rory claims from the other claims.

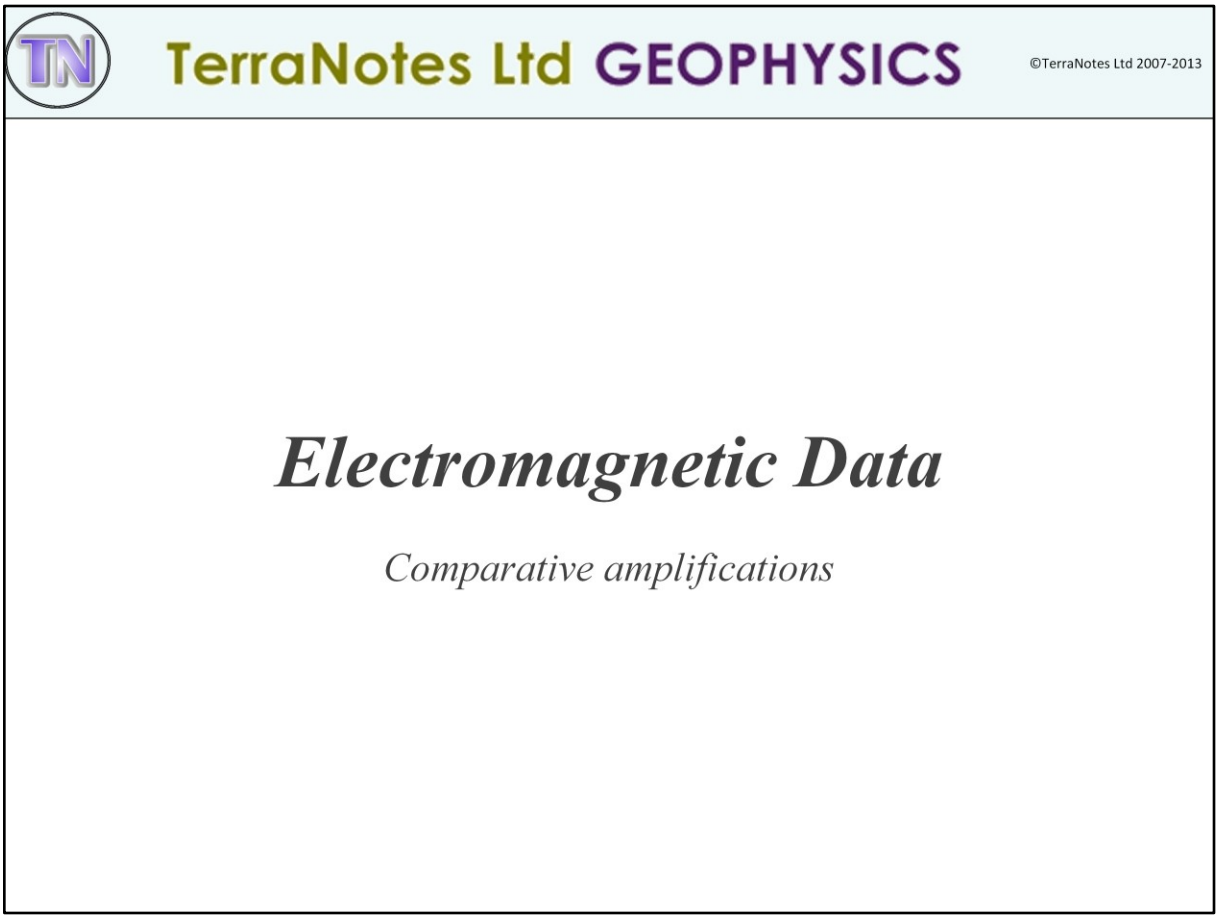
Special Note: Positive apparent depth indicates resistive top layer with conductive bottom layer, whereas the negative apparent depth indicates conductive top layer with resistive bottom layer.

Main Findings

Only Anomalies B, E, and K exhibit positive apparent depths which indicates a possibility of bedrock conductors.

The other anomalies, including D, exhibit negative apparent depth. Hence, the conductive zones at Anomalies D, G, and H could be thin and may not extend deeper.

The above interpretation cannot be applied to Anomalies A and F because they are affected by high susceptibilities. Those conductors might be very strong and may extend deep. A deeply penetrating ground EM survey could be conducted over these anomalies to obtain more details about these zones.


TerraNotes Ltd GEOPHYSICS
©TerraNotes Ltd 2007-2013
Electromagnetic Data
Comparative amplifications

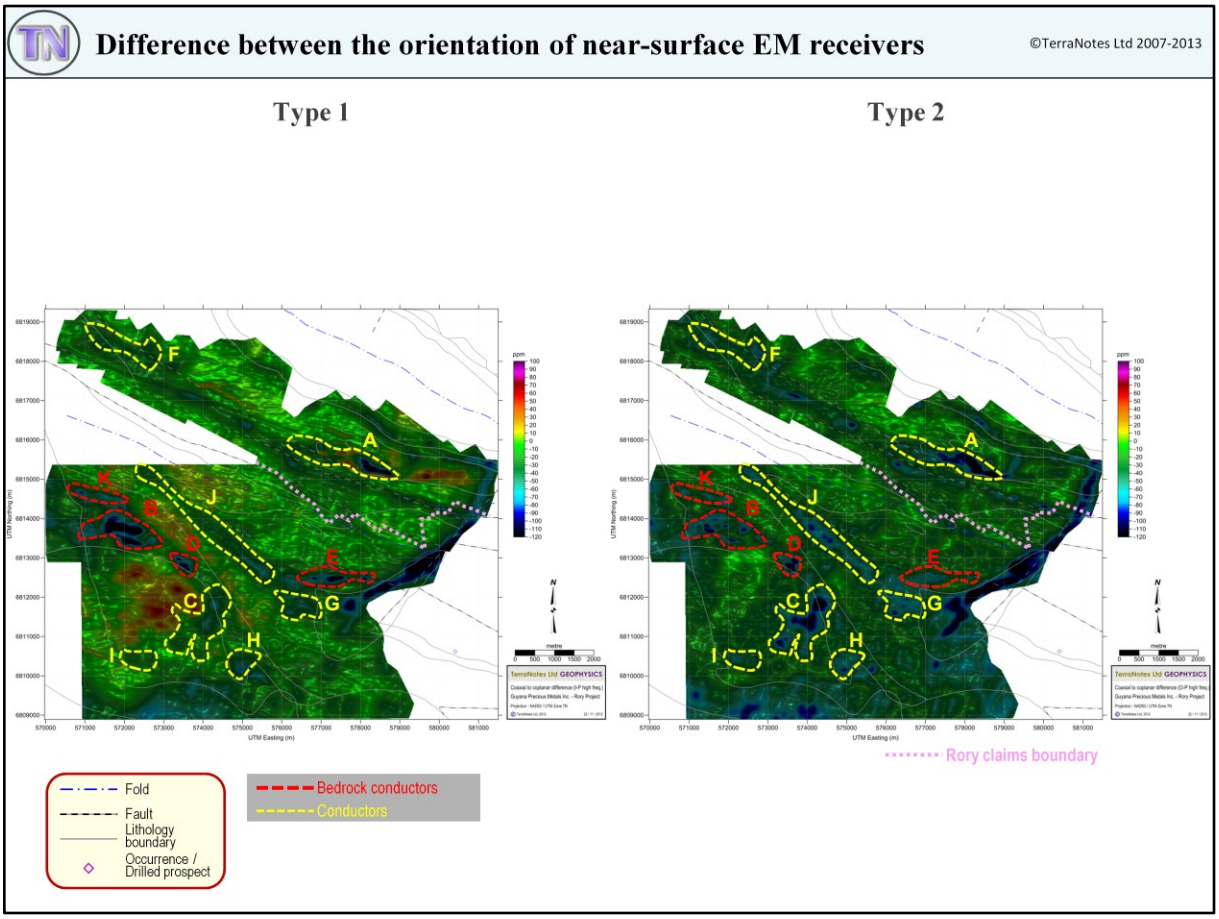


Figure 36. The left panel shows the in-phase component of the difference between the co-axial and co-planar data at high frequency and the right panel shows the quadrature component. The dashed yellow and red polygons and letters mark the previously interpreted conductors. The pink diamonds indicate mineral occurrences of YGS. The gray polygons indicate the boundaries of the geological formations. The dashed black lines indicate the faults/shears and the dashed blue lines indicate fold axes. The pink dotted line approximately separates the Rory claims from the other claims.

Special Notes: This procedure eliminates the responses from conductive ground, leaving the responses from bedrock conductors, cultural effects, and edge effects. The latter two effects can be evaluated by comparing these map with the apparent resistivity maps.

Thick vertical conductors (such as sulphide or graphite) exhibit negative anomalies whereas the thin, linear, and flat lying sheet conductors exhibit positive anomalies, particularly in the in-phase component.

Main Findings

The previously interpreted bedrock conductors (red dashed polygons) exhibit strong negative anomalies as expected.

The remaining conductors (yellow dashed polygons) are also negative in both components. This indicates that some type of conductors exist at these locations.

While inspecting the difference between the in-phase and quadrature components above, we can conclude that the Conductor C is a surficial one while Conductor B is mid-depth to deep.

The interpreted gabbro intrusion in the west of Anomaly C exhibits a positive anomaly, particularly in the in-phase component, indicating a resistive source.

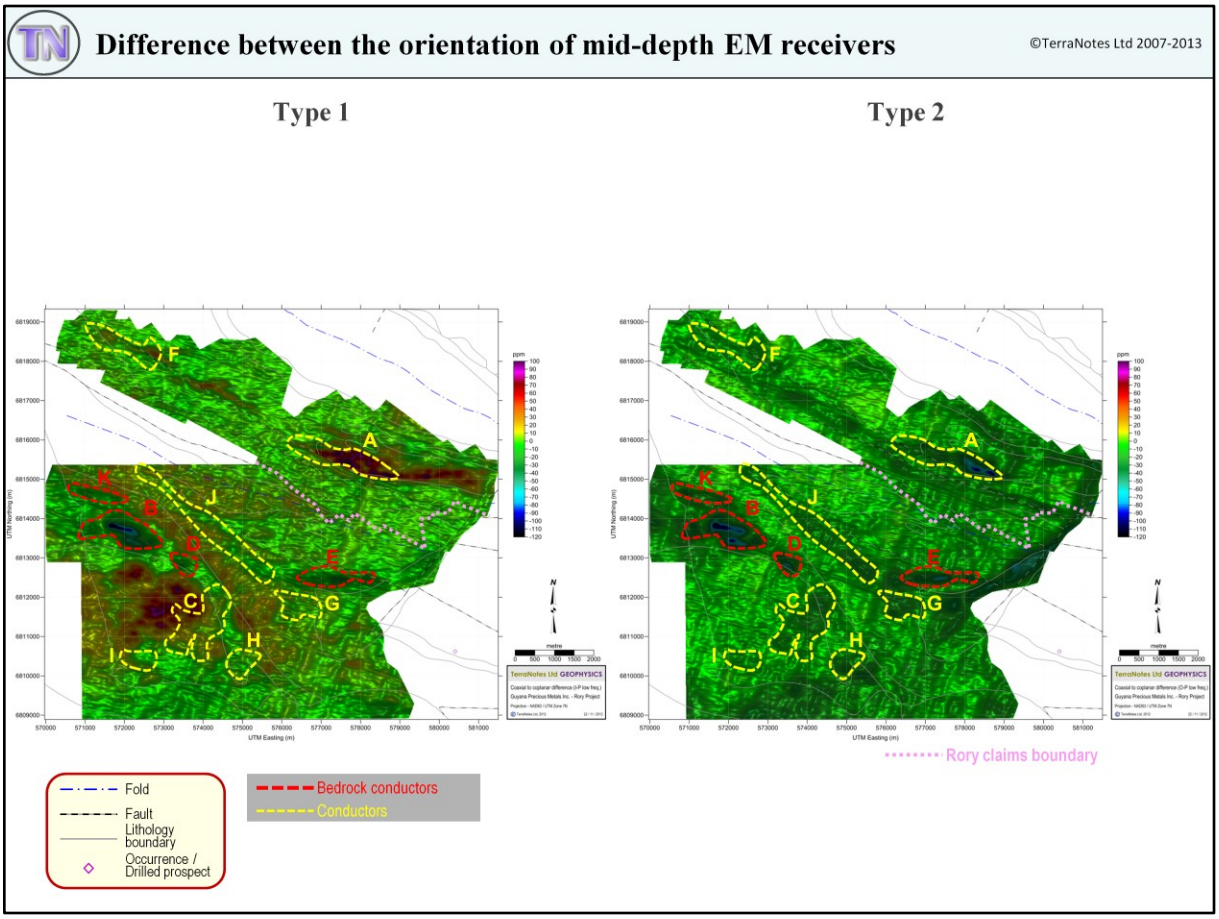


Figure 37. The left panel shows the in-phase component of the difference between the co-axial and co-planar data at low frequency and the right panel shows the quadrature component. The dashed yellow and red polygons and yellow and red letters mark the previously interpreted conductors. The pink diamonds indicate mineral occurrences of YGS. The gray polygons indicate the boundaries of the geological formations. The dashed black lines indicate the faults/shears and the dashed blue lines indicate fold axes. The pink dotted line approximately separates the Rory claims from the other claims.

Main Findings

According to these maps, only Anomalies A and B exhibits strong negative anomalies.

Although Anomaly A is positive in the in-phase component, this is due to the susceptibility effect and the quadrature component validates the conductive zone at this location.

The positive anomalies in the in-phase component illustrate the zones with high susceptibility. This interpretation is also validated by the quadrature component as they do not exceed zero. The details about the susceptibility effect can be found in Figure 38.

A weak negative anomaly can be observed at the location of Anomaly E possibly indicating another bedrock conductor.

The remaining conductors (yellow dashed polygons) are positive in the in-phase component and zero in the quadrature component. This indicates that these conductors are surficial or weak near-surface conductors due to alteration zones.

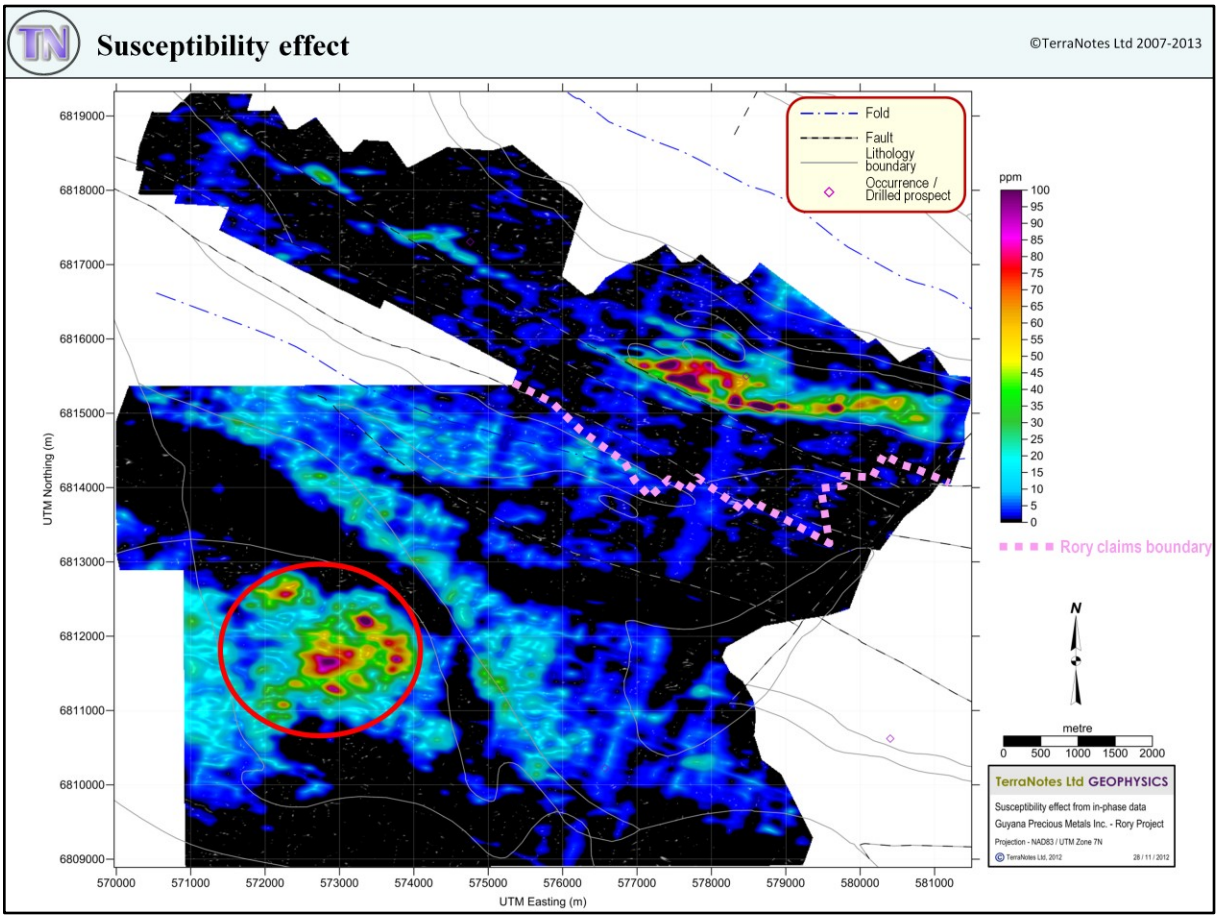


Figure 38. This map is same as the left panel of Figure 37 except that the colour palette has been changed to emphasize the susceptibility effect. The pink diamonds indicate mineral occurrences of YGS. The gray polygons indicate the boundaries of the geological formations. The dashed black lines indicate the faults/shears and the dashed blue lines indicate fold axes. The pink dotted line approximately separates the Rory claims from the other claims.

Main Findings

Taking the assumption below into consideration, the difference between the co-axial and co-planar data amplifies the susceptibility effect with positive anomalies

The positive anomalies indicate areas exhibiting the susceptibility effect. These areas are coincident with the Kluane Ultramafic Suite (PTrK), Kluane Ranges Plutonic Suite (EKK), and Nicolai formation (see Figure 4). The high susceptibility beneath the Quaternary (Q) in the west and beneath Kluane Ranges Plutonic Suite (EKK) may reflect a deeper source. Particularly, the high anomaly within the EKK formation (red circle) could indicate a gabbro intrusion. The source of the high magnetic intensity should be investigated for these two locations.

The black colour zones are coincident with the Skolai (CPS1) and, other Quaternary (Q) and Kluane Ranges Plutonic Suite (EKK) formations in the south.

Assumption

Frequency domain HEM data consists of conductive eddy currents and magnetic permeability. 1) The secondary field due to eddy currents is frequency dependent and consist of both in-phase and quadrature components which are always positive in sign. 2) the secondary field due to magnetic permeability is independent of frequency thus it consist of only in-phase data which is negative in sign.

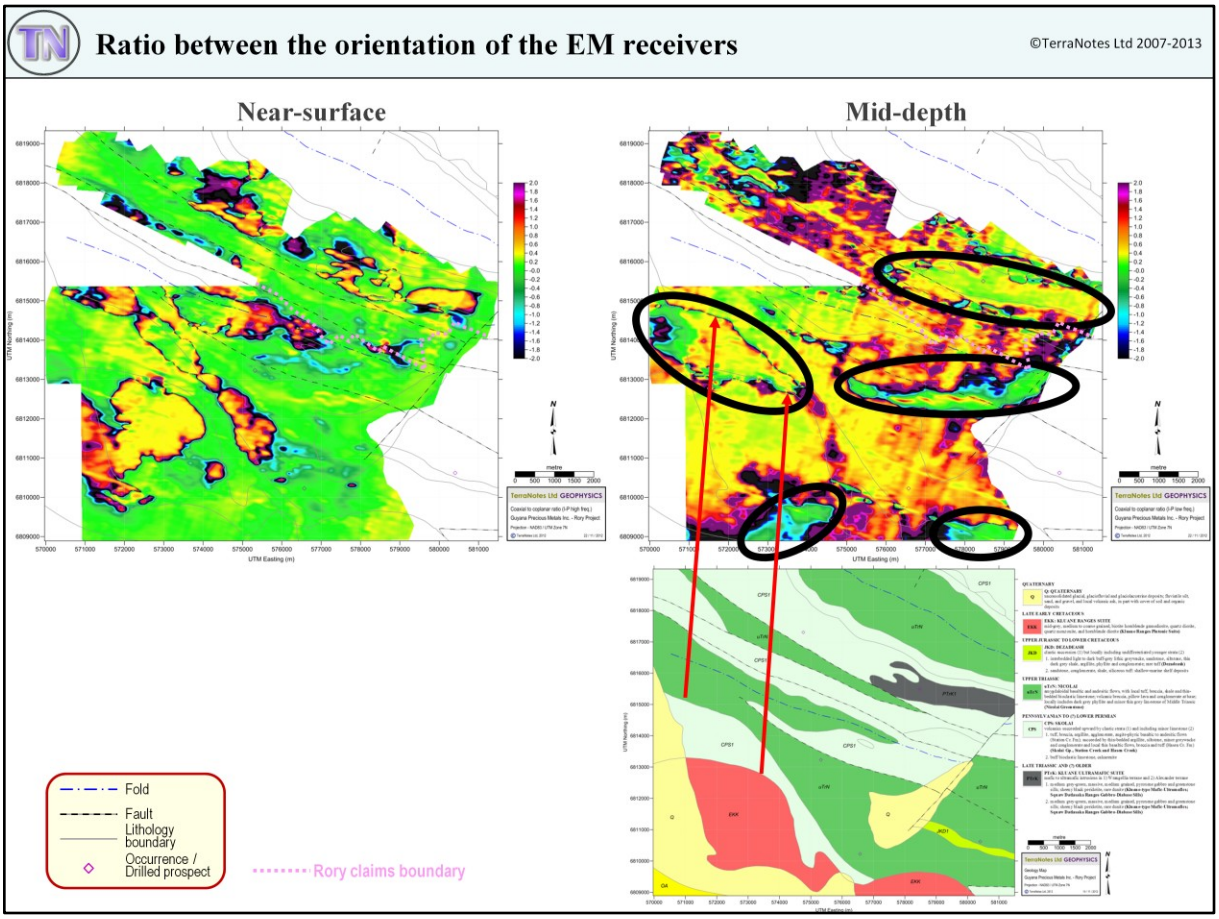
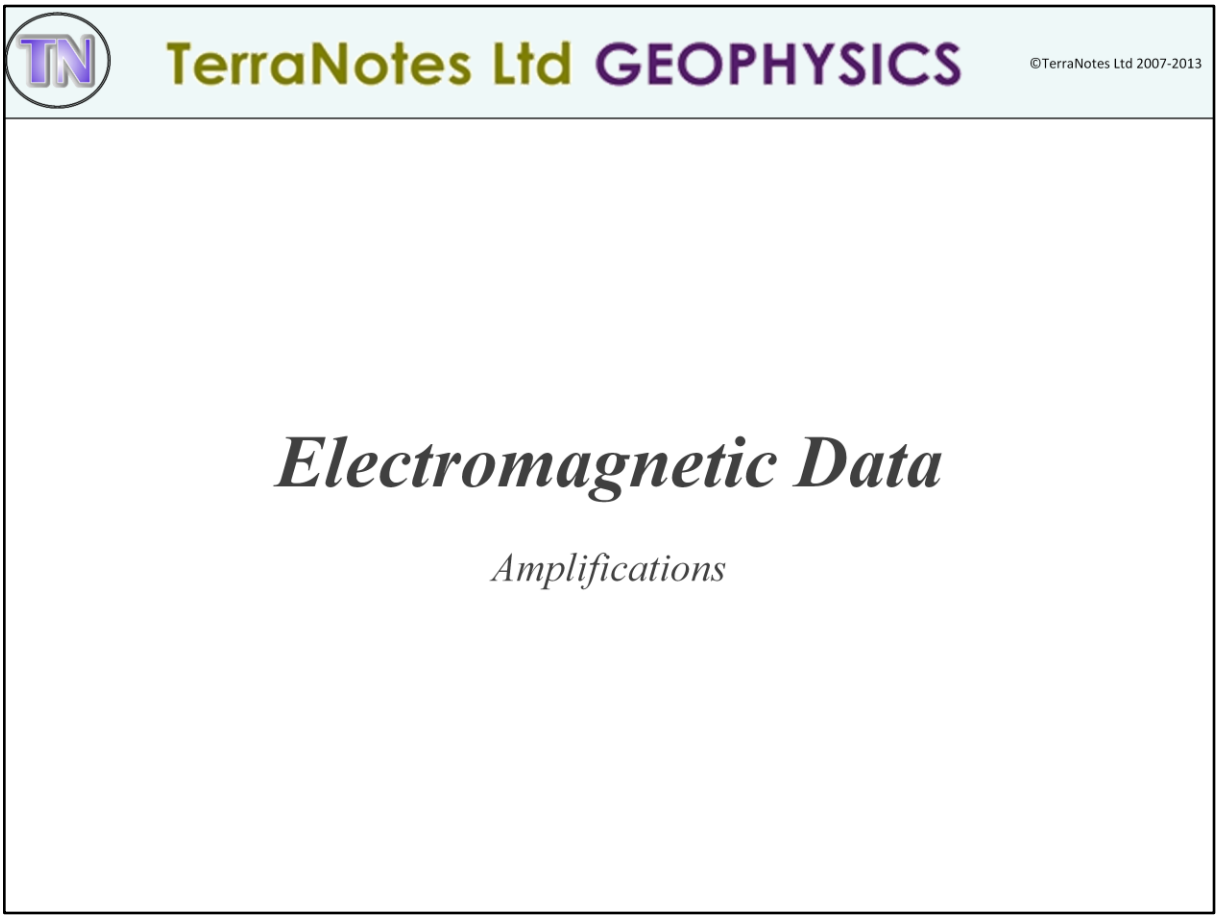


Figure 39. The left panel shows the in-phase component of the ratio between the co-axial and co-planar data in the near-surface. The right panel also shows the in-phase component of the ratio between the co-axial and co-planar data but at mid-depth as well as the geology map beneath it. The pink diamonds indicate mineral occurrences of YGS. The gray polygons indicate the boundaries of the geological formations. The dashed black lines indicate the faults/shears and the dashed blue lines indicate fold axes. The pink dotted line approximately separates the Rory claims from the other claims.

Main Findings

The near-surface map appears to be sensitive to magnetic bodies and it delineates the magnetic structures.

The mid-depth map in the right panel appears to be sensitive to conductive layers and it delineates the conductive geological formations at depth. The black ellipses mark these zones. Please note that there is a very strong correlation between the Skolai Formation boundaries in the geology map and the boundaries of the mid-depth map above it


TerraNotes Ltd GEOPHYSICS
©TerraNotes Ltd 2007-2013
Electromagnetic Data
Amplifications

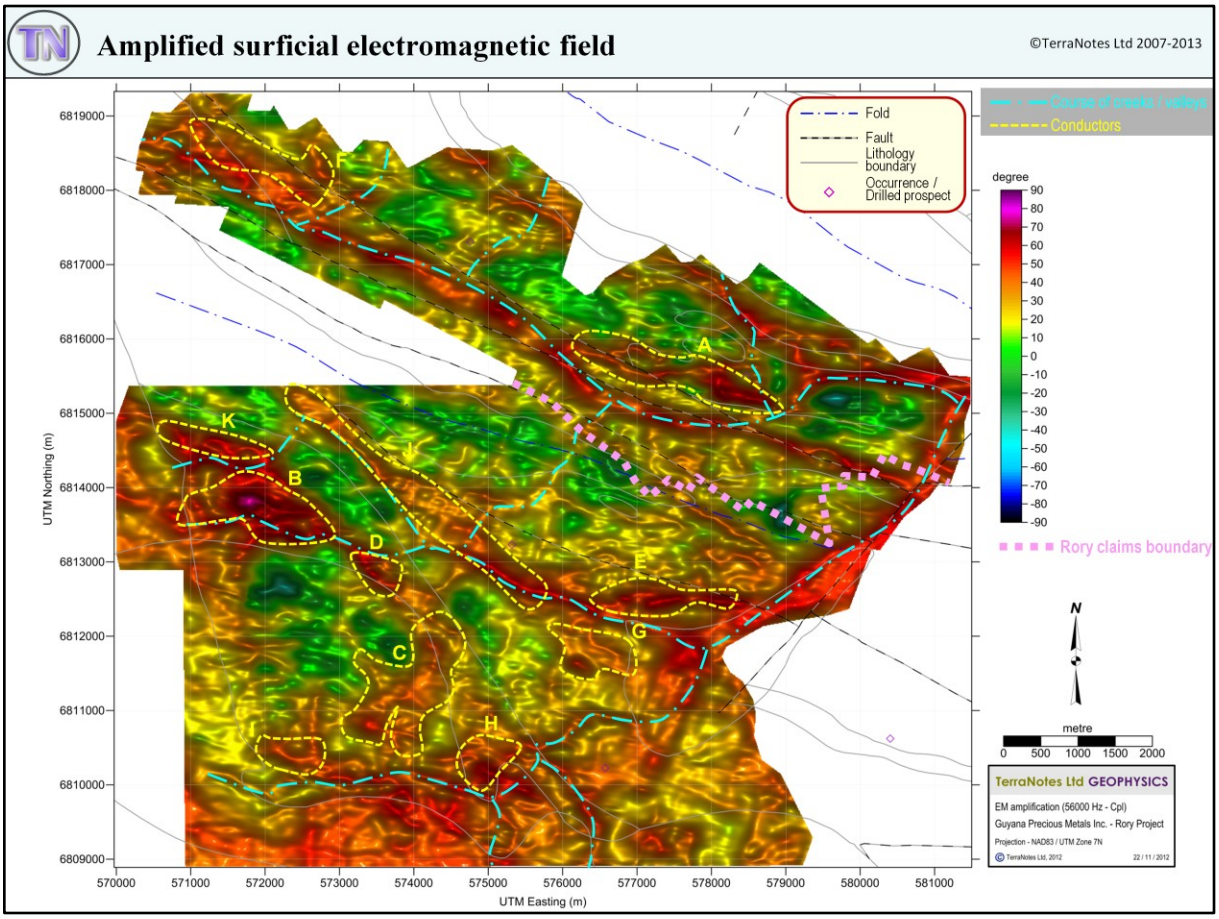


Figure 40. The amplified combination of the in-phase and quadrature components of 56000Hz co-planar data meant to image the surficial conductors. The dash-dotted cyan lines indicate the location of creeks and valleys. The dashed yellow polygons and letters mark the previously interpreted conductors. The pink diamonds indicate mineral occurrences of YGS. The gray polygons indicate the boundaries of the geological formations. The dashed black lines indicate the faults/shears and the dashed blue lines indicate fold axes. The pink dotted line approximately separates the Rory claims from the other claims.

Special Note: Theoretically, everything above 0° is conductive. A 45° anomaly shows a medium strength conductor while a 90° anomaly indicates a very strong conductor.

Main Findings

The only high angle (pink) anomaly is seen within Anomaly B, indicating the presence of a strong conductor at this location.

All the rest of the conductive zones (Anomalies A and C through K) seem to be medium strength conductive zones with an approximately 45° anomaly.

The other conductive trends are associated with the creeks (dash-dotted cyan lines), the Donjek River in the west, and the flat, low land in the south.

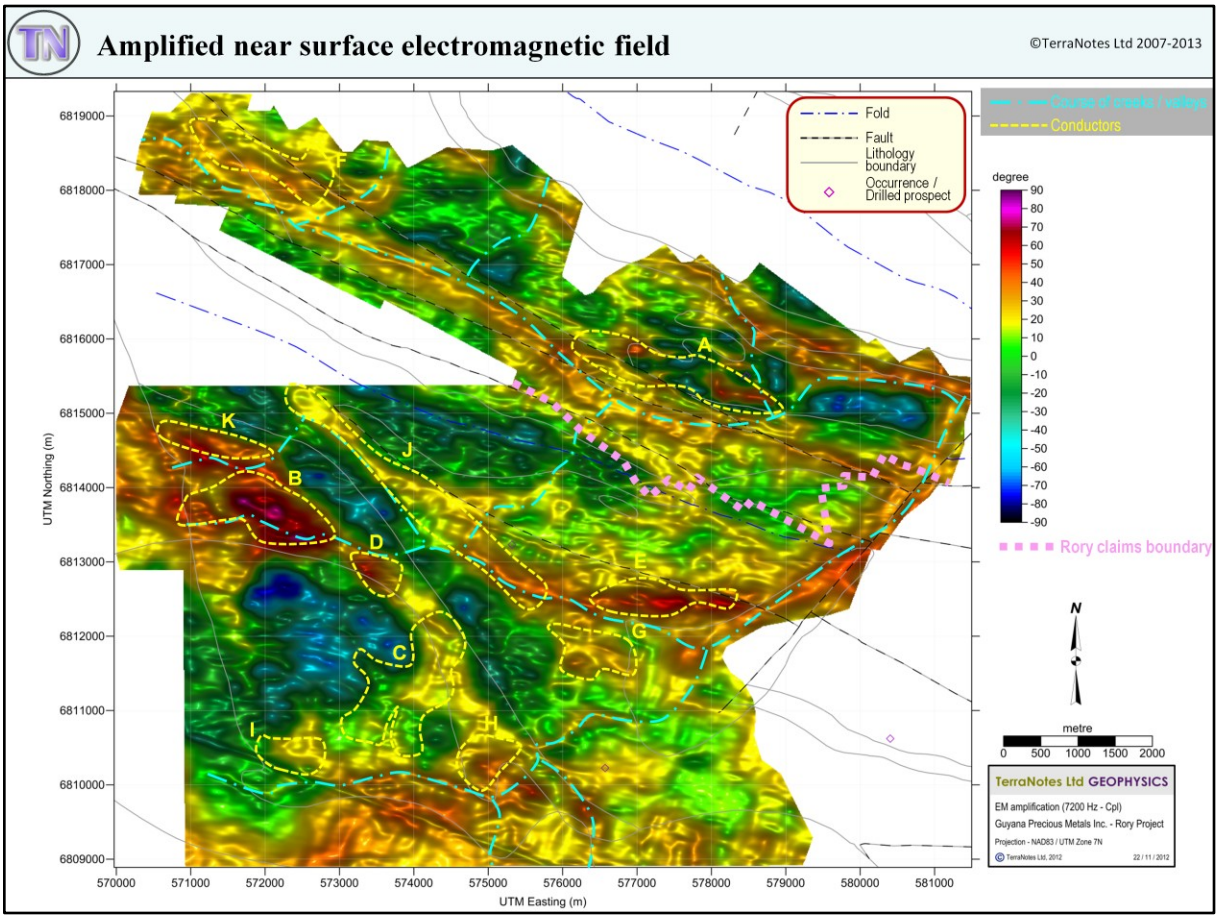


Figure 41. The amplified combination of the in-phase and quadrature components of 7200Hz co-planar data meant to image near-surface conductors. The dash-dotted cyan lines indicate the location of creeks and valleys. The yellow dashed polygons and letters mark the previously interpreted conductors. The pink diamonds indicate mineral occurrences of YGS. The gray polygons indicate the boundaries of the geological formations. The dashed black lines indicate the faults/shears and the dashed blue lines indicate fold axes. The pink dotted line approximately separates the Rory claims from the other claims.

Special Note: Theoretically, everything above 0° is conductive. A 45° anomaly shows a medium strength conductor while a 90° anomaly indicates a very strong conductor.

Main Findings

The overall conductivity decreased with depth (as compared to Figure 40), except Anomalies B and E, which remained strong with depth.

Anomalies D and K began to be distinguished from the background anomaly.

There appear to be individual electromagnetic anomalies on the east and west sides of Anomaly A.

Conductive trends can be observed that are associated with the creeks (dash-dotted cyan lines), the Donjek River in the west and flat, low land in the south.

The interpreted gabbro intrusion in the west and known Nikolai formations in the Rory claim group begins to appear resistive in the near-surface.

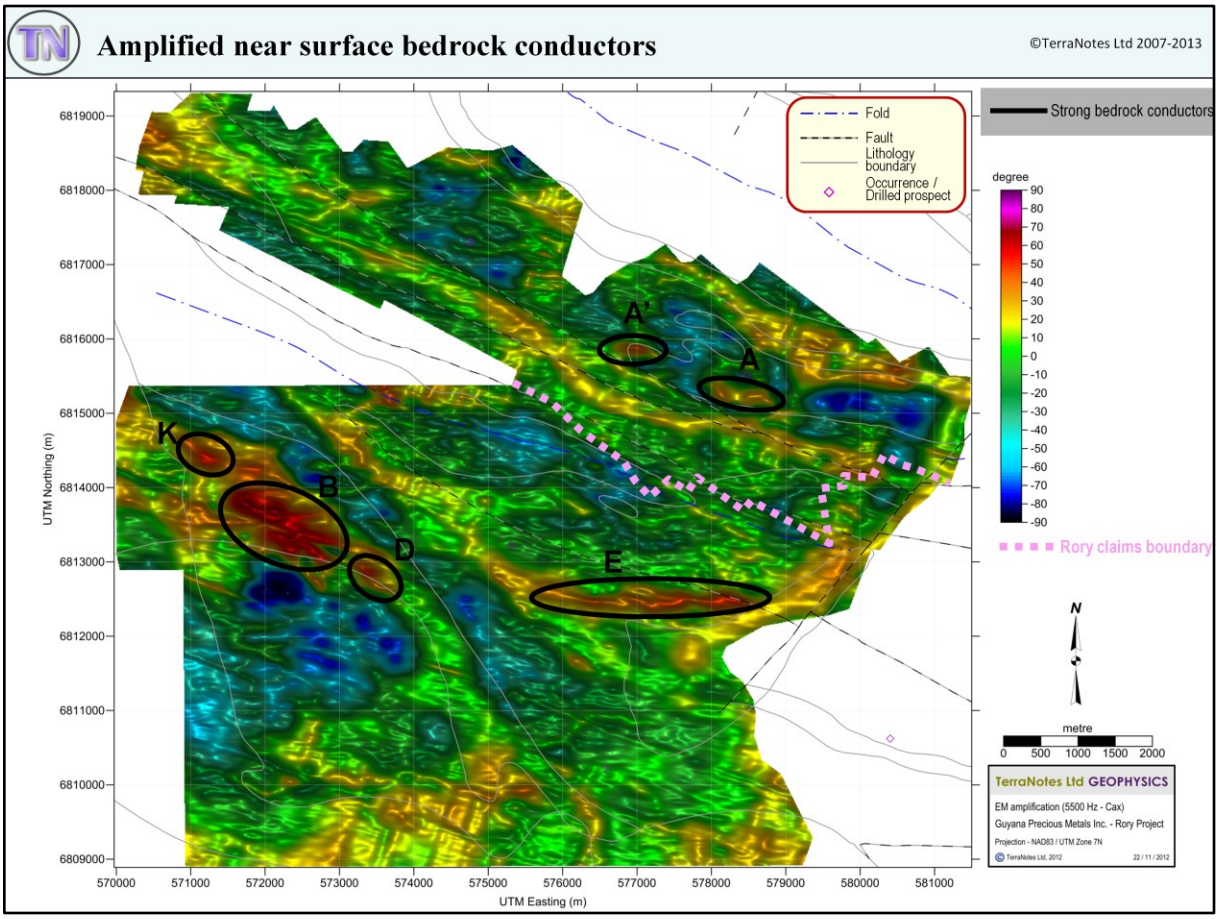


Figure 42. The amplified combination of in-phase and quadrature components of 5500Hz co-axial data meant to image near-surface bedrock conductors. The pink diamonds indicate mineral occurrences of YGS. The gray polygons indicate the boundaries of the geological formations. The dashed black lines indicate the faults/shears and the dashed blue lines indicate fold axes. The pink dotted line approximately separates the Rory claims from the other claims.

Special Note: Theoretically, everything above 0° is conductive. A 45° anomaly shows a medium strength conductor while a 90° anomaly indicates a very strong conductor.

Main Findings

It can be deduced from this figure that the topographic effects and overall conductivity decrease with depth (as compared to Figures 40 and 41). This figure focuses on the bedrock conductors instead of wide conductive zones due to the use of co-axial data rather than co-planar.

Anomaly B is still the strongest conductor, exhibiting ~70° strength anomaly.

Anomalies D and K are in the close proximity of Anomaly B and exhibit a 50° strength anomaly, indicating that they are medium to good conductors.

Anomaly E is just above a 45° strength anomaly, indicating a medium strength conductor.

Anomaly A is separated into two parts: A and A'. Anomaly A has a lower strength but it has been demonstrated that it is due to the susceptibility effect. Anomaly A' appears as a single 45° strength anomaly and may be classified as medium conductor at the western end of the ultramafic body.

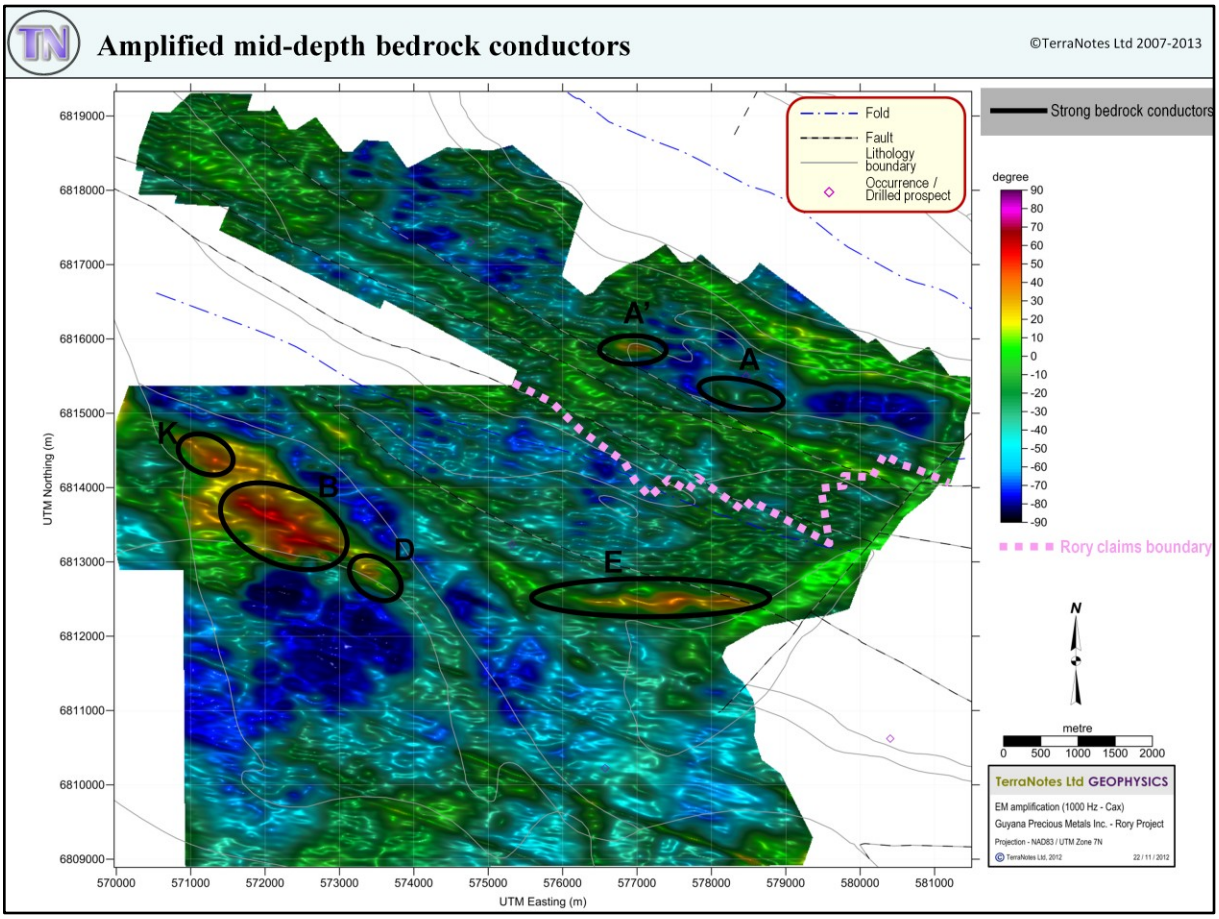


Figure 43. The amplified combination of in-phase and quadrature components of 1000Hz co-axial data meant to image mid-depth bedrock conductors. The pink diamonds indicate mineral occurrences of YGS. The gray polygons indicate the boundaries of the geological formations. The dashed black lines indicate the faults/shears and the dashed blue lines indicate fold axes. The pink dotted line approximately separates the Rory claims from the other claims.

Special Note: Theoretically, everything above 0° is conductive. A 45° anomaly shows a medium strength conductor while a 90° anomaly indicates a very strong conductor.

Main Findings

The topographical effects have almost disappeared at this depth and the overall conductivity is not very visible except in the western Skolai formation around Anomaly B.

Anomaly B is still the strongest conductor with a ~65° strength anomaly.

Anomaly K is just above 45°, indicating a medium conductor.

Anomalies A, A', D, and E are still visible, but have been reduced to weak to medium strength conductors at this depth.

Resistive zones due to interpreted gabbro intrusions in the west and the Nicolai formations become more prominent at mid-depth.

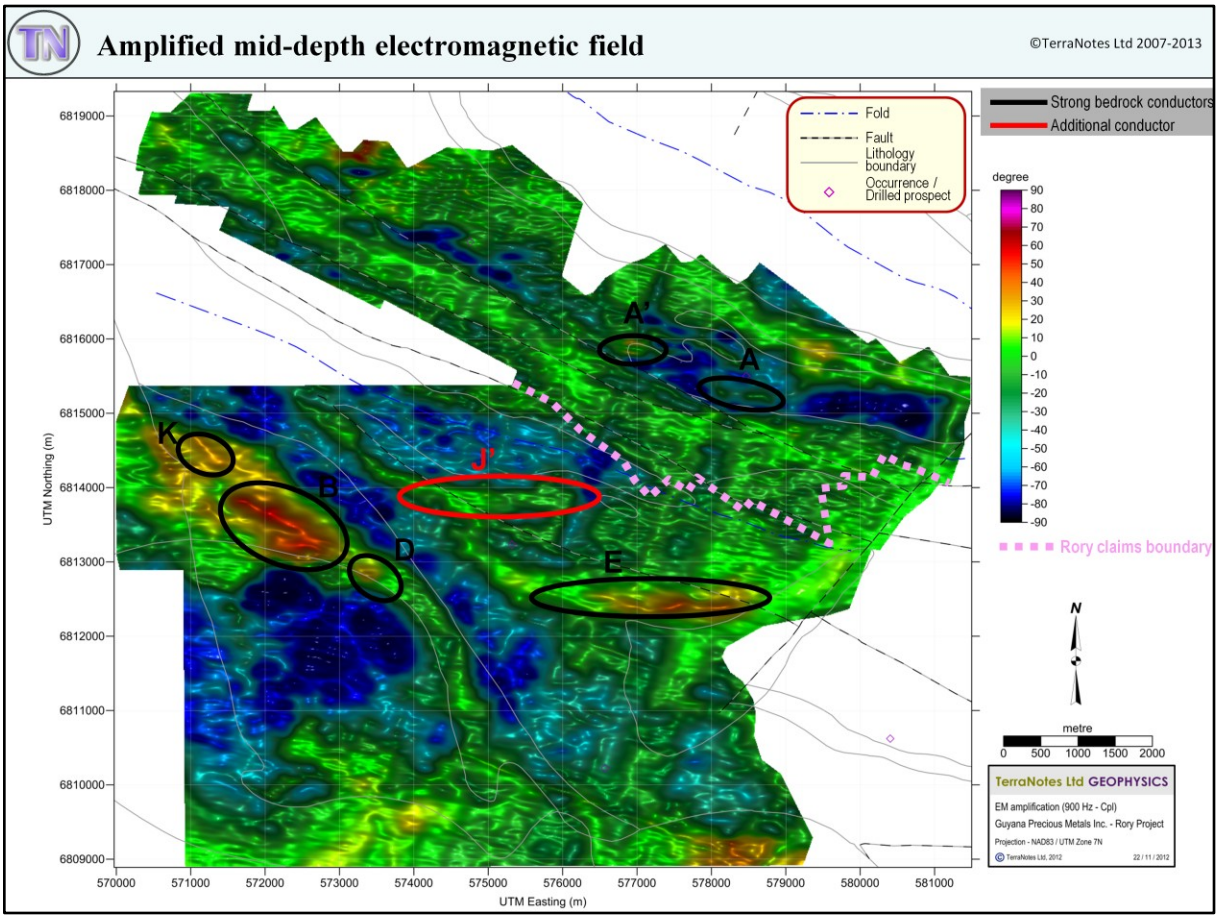


Figure 44. The amplified combination of in-phase and quadrature components of 900Hz co-planar data meant to image mid-depth conductors. The pink diamonds indicate mineral occurrences of YGS. The gray polygons indicate the boundaries of the geological formations. The dashed black lines indicate the faults/shears and the dashed blue lines indicate fold axes. The pink dotted line approximately separates the Rory claims from the other claims.

Special Note: Theoretically, everything above 0° is conductive. A 45° anomaly shows a medium strength conductor while a 90° anomaly indicates a very strong conductor.

Main Findings

The overall conductivity decreased with depth, but the large-scale geological formations are visible in this figure (and were not in Figures 42 and 43). For example, the green coloured background value with weak conductivity reflects the Skolai formation (CPS1 – Figure 4).

Anomalies B and E are the strongest anomalies in this figure. Anomaly B appears to consist of two independent conductive trends.

Anomalies A, A', D, and K are weaker in the co-planar channel than the co-axial channels (Figures 42 and 43). Also, A' had a single peak in the co-axial channels (Figures 42, 43) whereas it has double peaks in this map, which indicates a thin vertical conductor probably due to a sulphide mineralization.

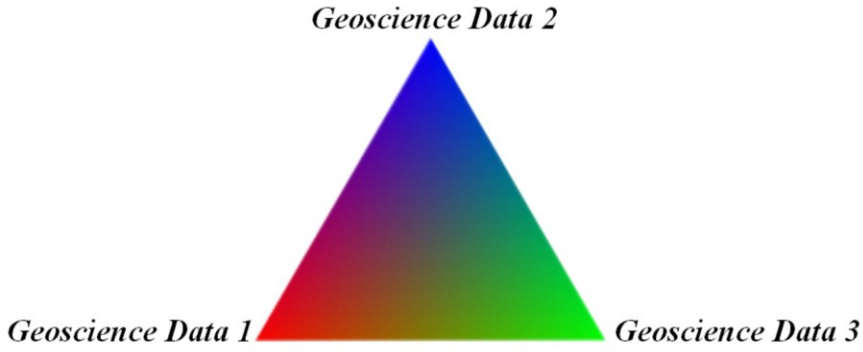
Anomaly A' appears stronger than A because it is visible in both the in-phase and quadrature components whereas Anomaly A is only visible in the quadrature component (see Figure 28).

The red ellipse marks an additional EM anomaly which shows similar characteristics to Anomaly E in terms of its shape. This anomaly is denoted J' since it appears to be located on a magnetic low, similar to Anomaly J, while Anomaly E is located on a weak magnetic high.

Resistive zones due to interpreted gabbro intrusions in the west and the Nicolai formations are also very prominent in this figure.

Example table for ternary imaging

©TerraNotes Ltd 2007-2013



Colour	*Geoscience Data 1*	*Geoscience Data 2*	*Geoscience Data 3*
Red	**100 %**	**-**	**-**
Green	**-**	**-**	**100 %**
Blue	**-**	**100 %**	**-**
Dark Yellow	**50 %**	**-**	**50 %**
Dark Magenta	**50 %**	**50 %**	**-**
Dark Cyan	**-**	**50 %**	**50 %**
Dark Gray	**33 %**	**33 %**	**33 %**

Table 1. Example table for ternary imaging.

Description

The ternary technique uses three different datasets to produce one map. In the example above, three different data sets data are utilized to produce a composite image. This process is more effective than traditional contour imaging, especially for viewing faint anomalies.

In the example above, red is assigned to Geoscience Data 1, blue is assigned to Geoscience Data 2, and green is assigned to Geoscience Data 3. The table shows examples of colours for specific percentages of each component. Maps produced using the above table would be used to locate enrichments of the specific radioelements and associated lithologies and alterations.

This process requires the data to be interpolated onto a regular grid. Many of the standard gridding algorithms are unsuited to the Airborne data because of the inherent statistical variations. A data-specific gridding technique is utilized for our purposes.

To produce the following maps, we assigned red-green-blue (RGB) colours for each specific gridded dataset and mathematically combined them into one image using statistical methods and rescaling.

As a result, these maps are useful in distinguishing anomalies due to mineralization and/or alterations from anomalies due to different rock types.

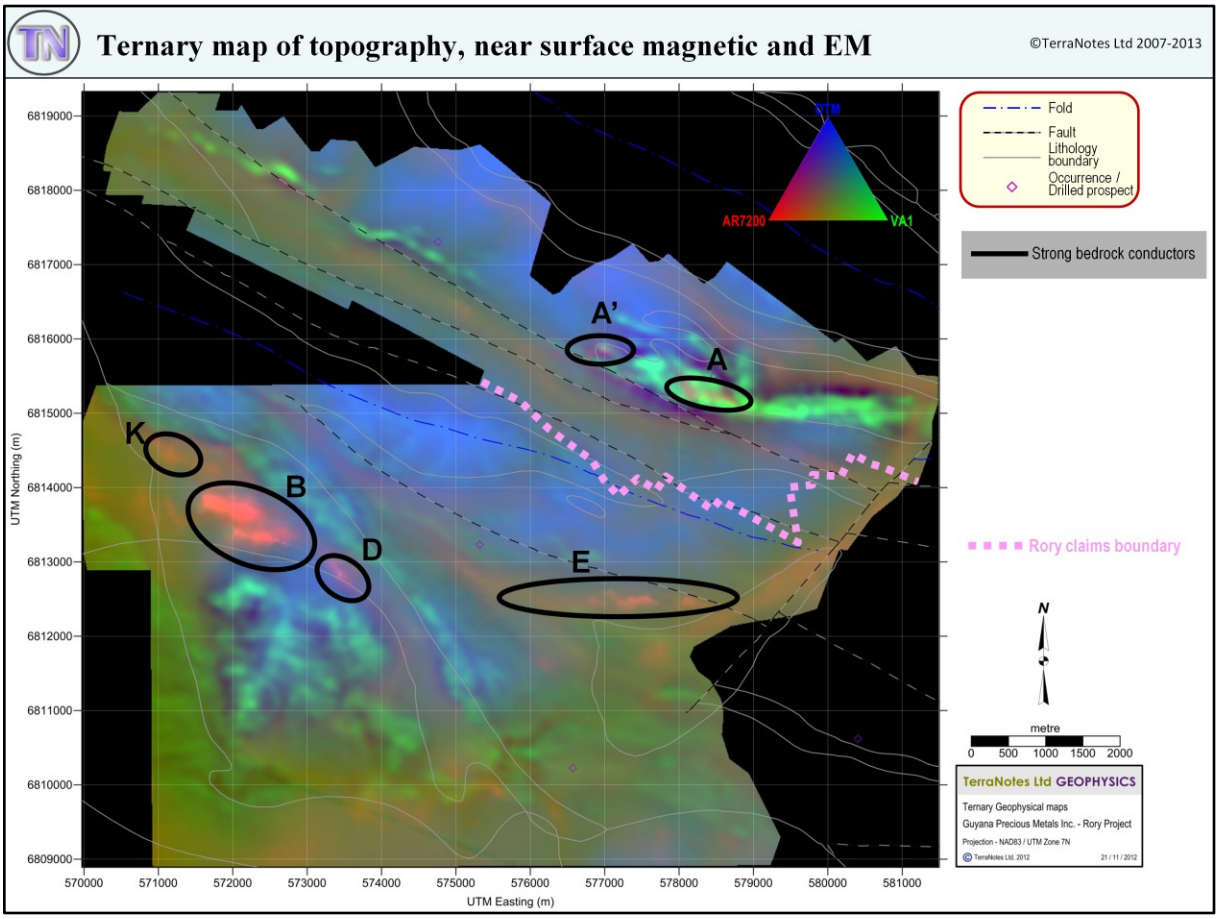


Figure 45. The ternary map of topography, near surface magnetic, and EM in RGB (red-green-blue) colours. Blue represents the topography, green represents the near-surface magnetic anomalies, and red represents the near surface EM anomalies. This is an Intensity-Hue-Saturation (IHS) ternary map where brighter colours indicate the most anomalous zones. The pink diamonds indicate mineral occurrences of YGS. The gray polygons indicate the boundaries of the geological formations. The dashed black lines indicate the faults/shears and the dashed blue lines indicate fold axes. The pink dotted line approximately separates the Rory claims from the other claims. The black ellipses indicate the previously identified bedrock-type conductive anomalies.

Main Findings

The strongest anomaly is seen within the previously identified Anomaly B.

Anomalies D, E, and K appear to be weak in the near-surface.

Anomaly A occurs between the magnetic highs at the breaks on the ultramafic zone. The original Wellgreen deposit was also found in this kind of embayment, so this type of structure could be important for further exploration.

Anomaly A' occurs at the western tip of the ultramafic rocks.

The most important colour for Cu-Ni-PGE exploration in this figure is bright yellow. However, even the Wellgreen deposit did not produce this colour of anomaly.

The bright green anomalies indicate ultramafic rocks in the north, interpreted gabbro in the southwest, and mafic rocks of the Nicolai formation (compare with Figure 4).

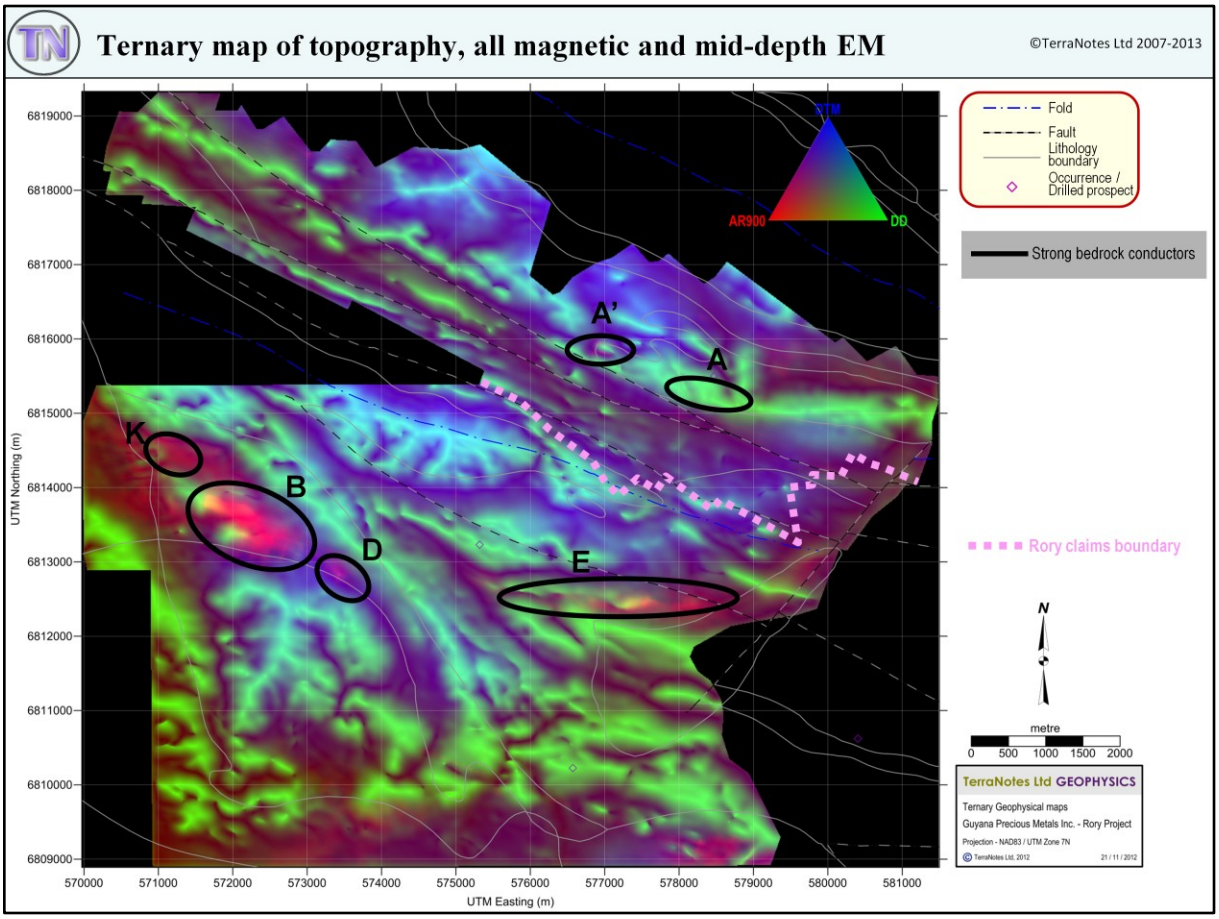


Figure 46. The ternary map of topography, all magnetic structures, and mid-depth EM in RGB colours. Blue represents the topography, green represents the magnetic anomalies, and red represents the mid-depth EM anomalies. This is an IHS ternary map where brighter colours indicate the most anomalous zones. The pink diamonds indicate mineral occurrences of YGS. The gray polygons indicate the boundaries of the geological formations. The dashed black lines indicate the faults/shears and the dashed blue lines indicate fold axes. The pink dotted line approximately separates the Rory claims from the other claims. The black ellipses indicate the previously identified bedrock-type conductive anomalies.

Main Findings

When investigating more deeply both the magnetic and EM data, conductive Anomaly A vanishes while conductive Anomaly E become stronger.

All of the previously identified bedrock-type conductors (black ellipses), except Anomaly D, appear to be associated with magnetic structures. At A and A', the magnetic anomalies are very strong due to ultramafic rocks. At the other zones, magnetic structures are very weak.

Yellow-coloured anomalies, which are the most important for Cu-Ni-PGE exploration, can be observed in the western portions of Anomalies B and E. Consequently, Anomalies B and E form the highest priority targets in the Rory claims.

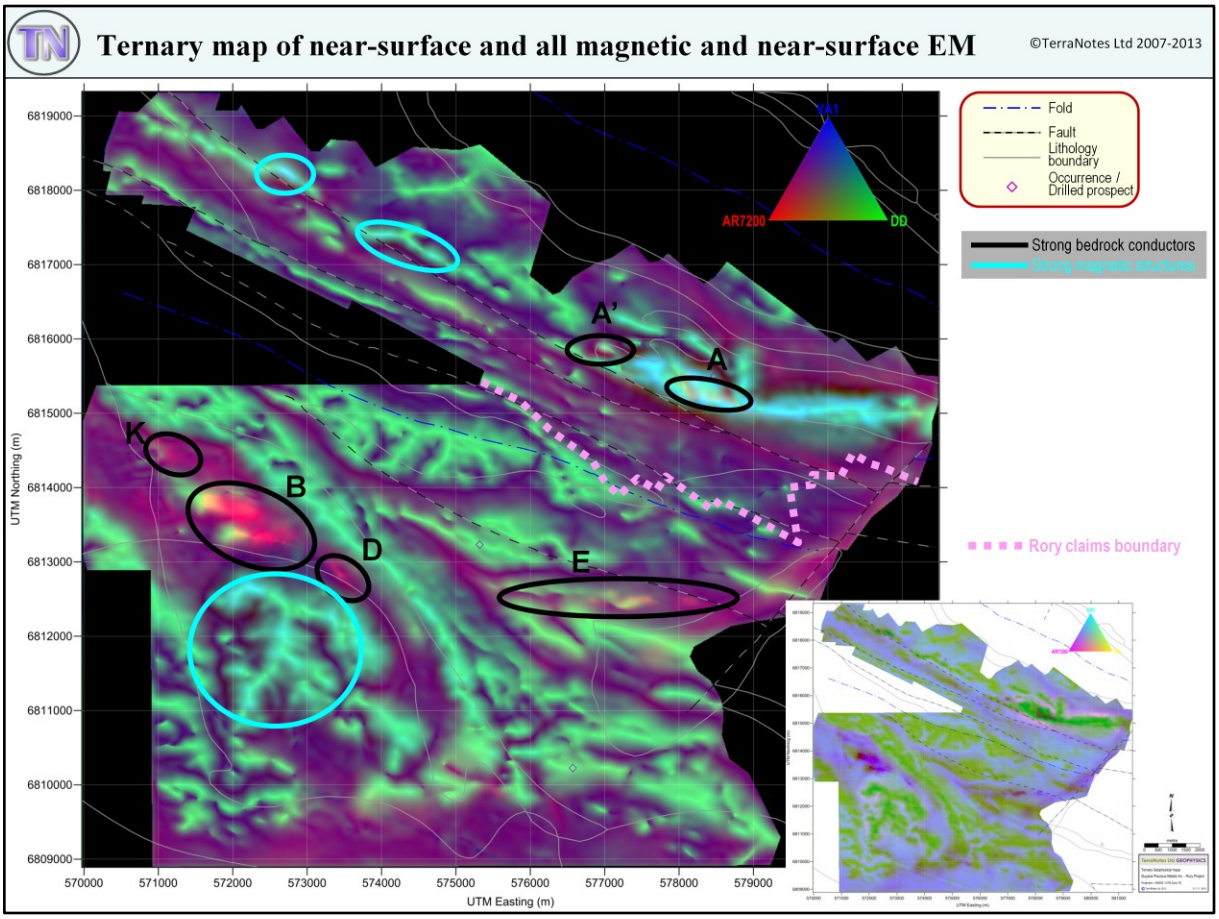


Figure 47. The main map is the ternary map of near-surface magnetic, all magnetic structures, and near-surface EM in RGB colours. The inset map on the bottom right uses CMY (cyan-magenta-yellow) colours, which are the reciprocals of RGB. Blue/cyan represents the near-surface magnetic anomalies, green/yellow represents the all depth and strength magnetic anomalies, and red/magenta represents the near-surface EM anomalies. The main map is an IHS ternary map where brighter colours indicate the most anomalous zones. Darker colours indicate the most anomalous zones in the CMY map. The pink diamonds indicate mineral occurrences of YGS. The gray polygons indicate the boundaries of the geological formations. The dashed black lines indicate the faults/shears and the dashed blue lines indicate fold axes. The pink dotted line approximately separates the Rory claims from the other claims. The black ellipses indicate the previously identified bedrock-type conductive anomalies.

Main Findings

This map provides the same details and interpretation as the previous figure for the Rory claims (Anomalies B, D, E and K).

The difference between this map and Figure 46 is observed in the Wellgreen area (Anomalies A and A'). The magnetic structure is very strong (as the cyan colour suggests) and a conductor is observed beneath this structure in the near-surface.

Strong conductors may be seen better in the CMY map (inset) as black anomalies. Particularly A, A', and two anomalies in B and E are clearer in the inset map.

The cyan ellipses mark the other cyan-coloured anomalies which may indicate ultramafic intrusions in the north (in the Arch claims) and the interpreted gabbro intrusion in the southwest.

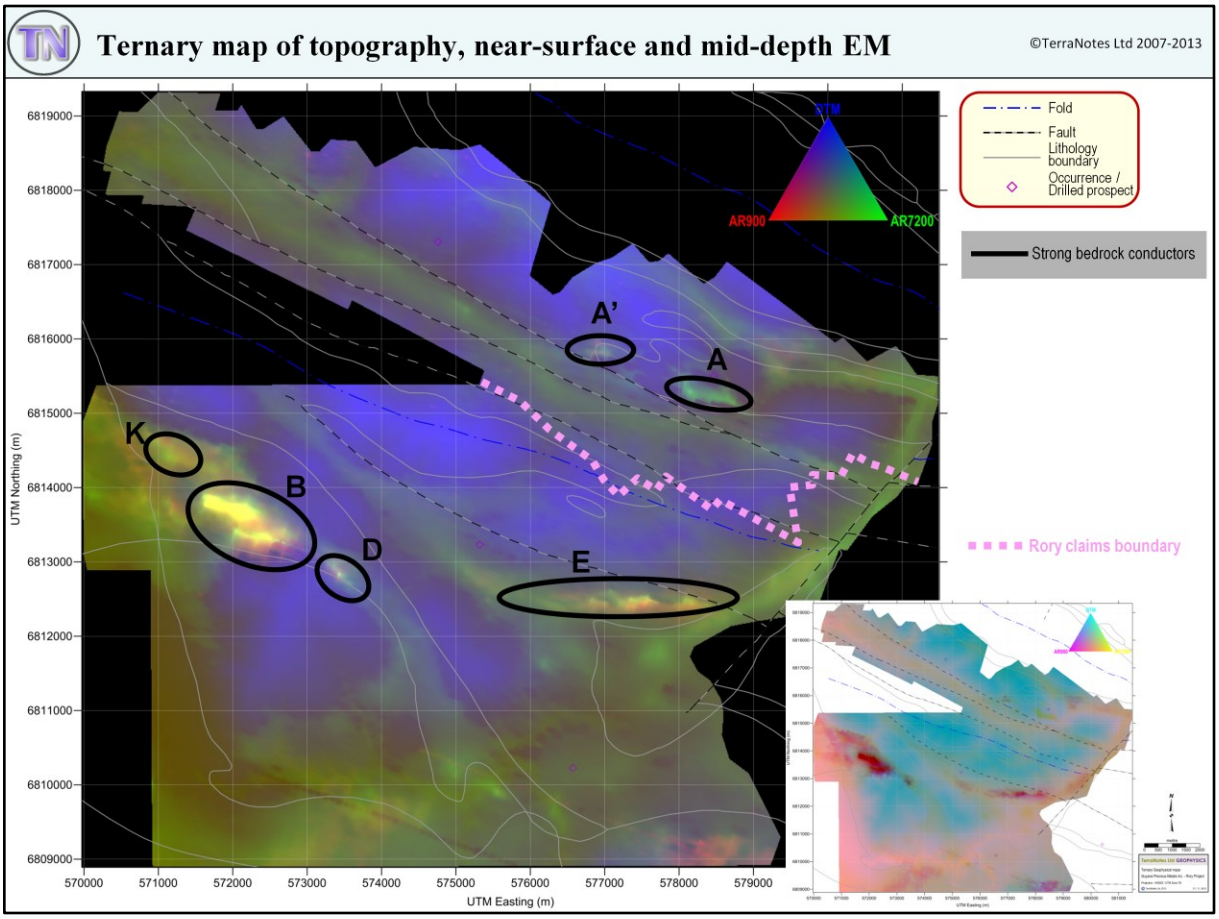


Figure 48. The main map is a ternary map of topography, near-surface EM, and mid-depth EM in RGB colours. The inset map on the bottom right uses CMY colours, which are the reciprocals of RGB. Blue/cyan represents the topography, green/yellow represents the near-surface EM anomalies, and red/magenta represents the mid-depth EM anomalies. The main map is an IHS ternary map where brighter colours indicate the most anomalous zones. Darker colours indicate the most anomalous zones in the CMY map. The pink diamonds indicate mineral occurrences of YGS. The gray polygons indicate the boundaries of the geological formations. The dashed black lines indicate the faults/shears and the dashed blue lines indicate fold axes. The pink dotted line approximately separates the Rory claims from the other claims. The black ellipses indicate the previously identified bedrock-type conductive anomalies.

Main Findings

The yellow in the main map indicates the coincident near-surface and mid-depth conductors. This is observed at Anomalies B and E. Anomaly B is completely yellow, suggesting a thick conductor that begins in the near-surface and extends to mid-depth (and is open at depth). Anomaly E is yellow and red, indicating a deeper source than the other anomalies.

Anomalies A, A' D, and K are mainly green indicating near-surface sources. But Anomaly A may be masked by a susceptibility effect. Anomaly A' has a faint orange to red colour indicating a deeper EM source at this location.

All the EM anomalies are located at the edges of a topographic high (blue in the main map).

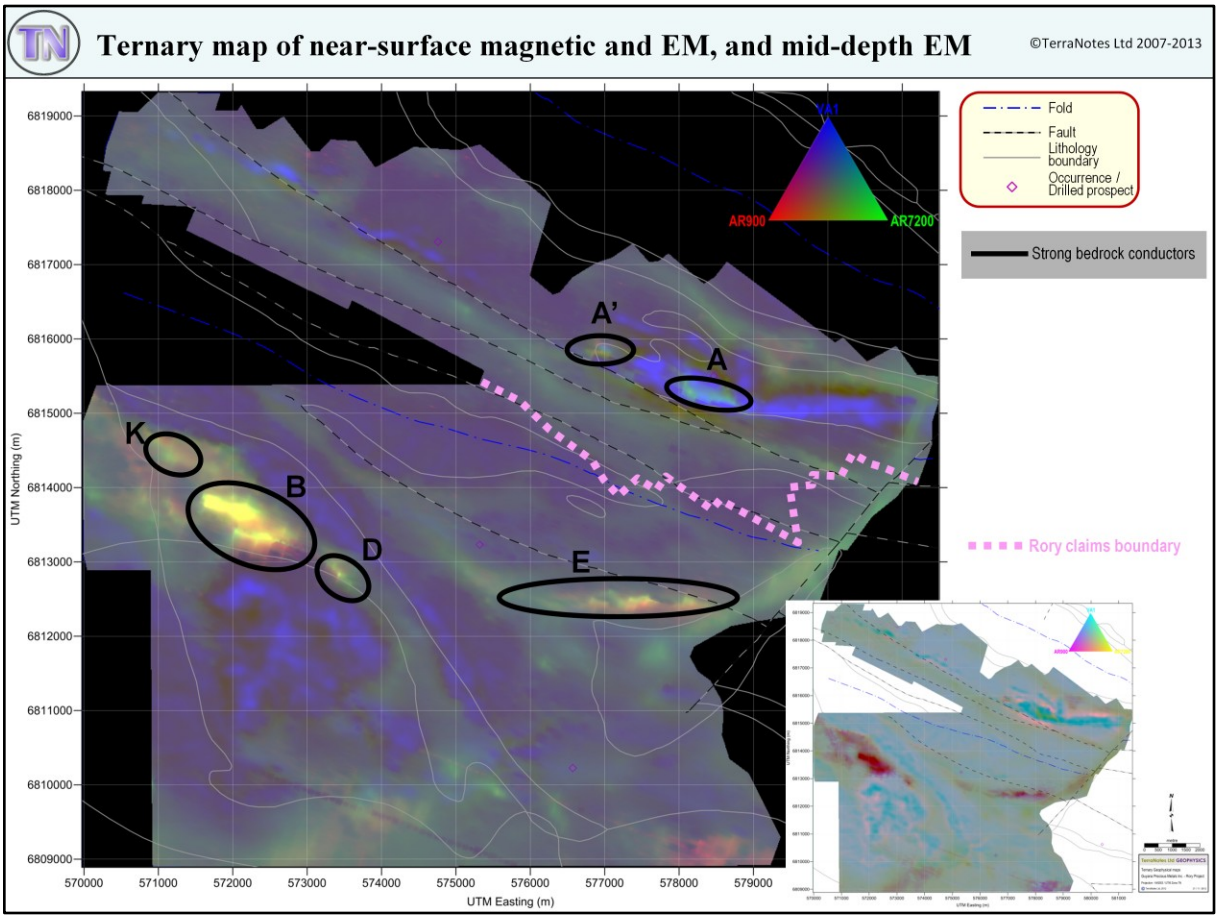


Figure 49. The main map is the ternary map of near-surface magnetic, near-surface EM, and mid-depth EM in RGB colours. The inset map on the bottom right uses CMY colours, which are the reciprocals of RGB. Blue/cyan represents the near-surface magnetic, green/yellow represents the near-surface EM anomalies, and red/magenta represents the mid-depth EM anomalies. The main map is an IHS ternary map where brighter colours indicate the most anomalous zones. Darker colours indicate the most anomalous zones in the CMY map. The pink diamonds indicate mineral occurrences of YGS. The gray polygons indicate the boundaries of the geological formations. The dashed black lines indicate the faults/shears and the dashed blue lines indicate fold axes. The pink dotted line approximately separates the Rory claims from the other claims. The black ellipses indicate the previously identified bedrock-type conductive anomalies.

Main Findings

This map validates the EM interpretation of Figure 48.

Anomalies A and A' are located on a strong magnetic zone (blue colour) while the other EM anomalies are occurred on weak to low magnetic zones.

The background green colour (in both maps above) represents the Skolai Formation (CPS1 – see Figure 4).

The bright blue colours indicate ultramafic or gabbro intrusions while the faded blue colours indicate the mafic rocks of the Nicolai formation.

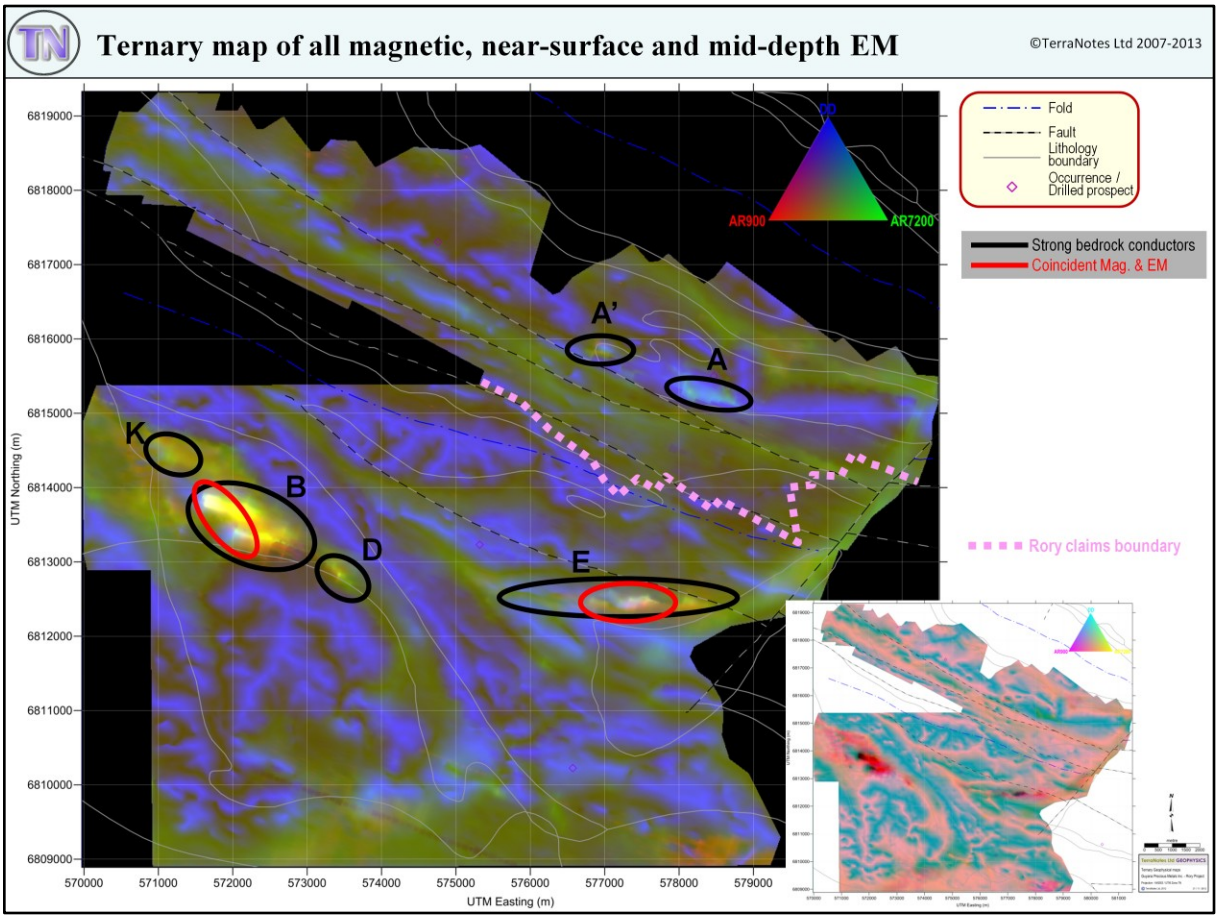


Figure 50. The main map is the ternary map of all magnetic structures, near-surface EM, and mid-depth EM in RGB colours. The inset map on the bottom right uses CMY colours, which are the reciprocals of RGB. Blue/cyan represents the all depth and strength magnetic anomalies, green/yellow represents the near-surface EM anomalies, red/magenta represents the mid-depth EM anomalies. The main map is an IHS ternary map where brighter colours indicate the most anomalous zones. Darker colours indicate the most anomalous zones in the CMY map. The pink diamonds indicate mineral occurrences of YGS. The gray polygons indicate the boundaries of the geological formations. The dashed black lines indicate the faults/shears and the dashed blue lines indicate fold axes. The pink dotted line approximately separates the Rory claims from the other claims. The black ellipses indicate the previously identified bedrock-type conductive anomalies.

Main Findings

The red ellipses indicate the most important parts of Anomalies B and E as is suggested by the white zones in the main map (and black in the inset map). These indicate coincident weak magnetic and strong EM anomalies.

The remainder of the figure validates the previous interpretations.

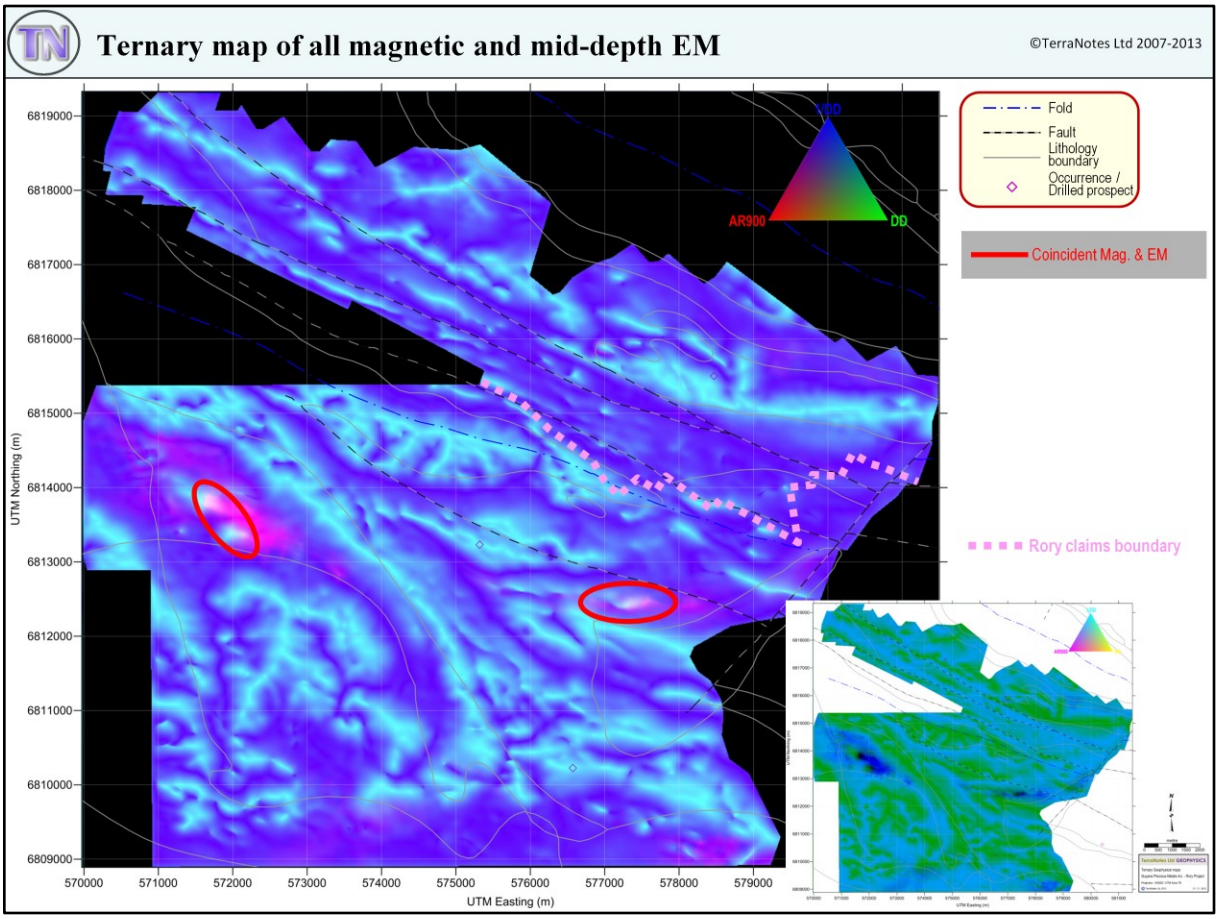


Figure 51. The main map is the ternary map of the reciprocal of reciprocal of all magnetic structures, all magnetic structures, and mid-depth EM in RGB colours. The inset map on the bottom right uses CMY colours, which are the reciprocals of RGB. Blue/cyan represents low strength magnetic anomalies, green/yellow represents high strength magnetic anomalies, and red/magenta represents mid-depth EM anomalies. *Please note that cyan in the RGB map indicates high magnetic strength whereas it indicates low magnetic strength in the CMY map.* The main map is an IHS ternary map where brighter colours indicate the most anomalous zones. Darker colours indicate the most anomalous zones in the CMY map. The pink diamonds indicate mineral occurrences of YGS. The gray polygons indicate the boundaries of the geological formations. The dashed black lines indicate the faults/shears and the dashed blue lines indicate fold axes. The pink dotted line approximately separates the Rory claims from the other claims.

Main Findings

This figure emphasizes the high and low magnetic strength structures with blue and cyan (in the main and inset maps, respectively). Therefore, yellow indicates coincident high magnetic strength and high conductivity anomalies and magenta denotes coincident low magnetic strength and high conductivity anomalies in the main map.

Both Anomalies B and E contain yellow and magenta. These anomalies are magenta in the east and light yellow to white in their western extents (see red ellipses), indicating that they denote the most important zones. The black anomalies in the inset map confirm this interpretation.

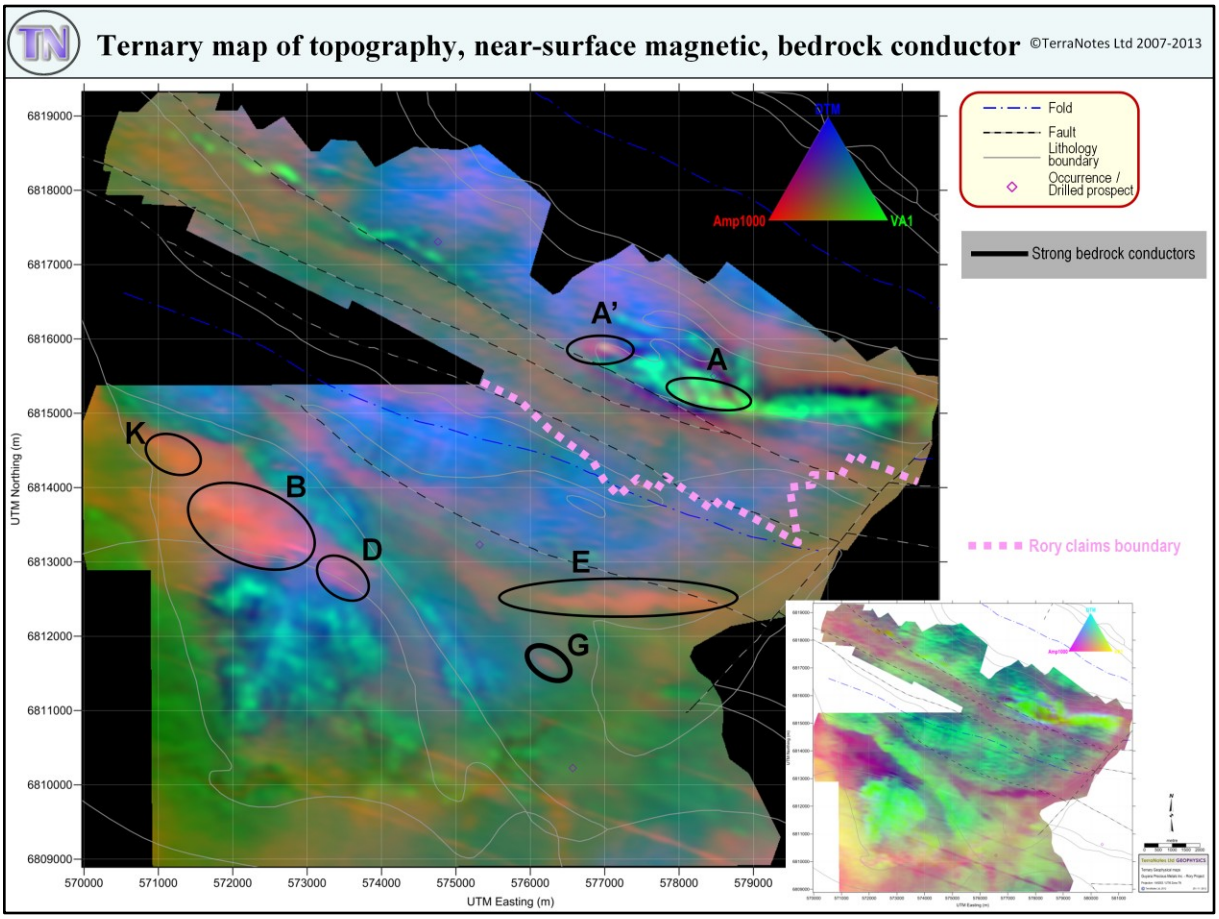


Figure 52. The main map is the ternary map of topography, near-surface magnetic, and mid-depth bedrock conductors in RGB colours. The inset map on the bottom right uses CMY colours, which are the reciprocals of RGB. Blue/cyan represents the topography, green/yellow represents the near-surface magnetic, and red/magenta represents the mid-depth bedrock conductors. The main map is an IHS ternary map where brighter colours indicate the most anomalous zones. Darker colours indicate the most anomalous zones in the CMY map. The pink diamonds indicate mineral occurrences of YGS. The gray polygons indicate the boundaries of the geological formations. The dashed black lines indicate the faults/shears and the dashed blue lines indicate fold axes. The pink dotted line approximately separates the Rory claims from the other claims.

Main Findings

This figure is similar to Figure 45, but uses the co-axial component of the EM amplification instead of the co-planar component apparent resistivity. It should be more sensitive than Figure 45 to bedrock conductors.

Anomalies A and A' are much more prominent in the map above, particularly A'.

Although this figure is meant to be more sensitive to bedrock conductors, the overall background conductivity in the vicinity of the Anomalies B and E is higher. Because of the high background conductivity, it becomes hard to distinguish Anomalies D and K.

Anomaly G is visible in this map, but it is located on a low magnetic trend.

Deep penetrating EM methods are recommended for the areas exhibiting bright green anomalies to investigate the possibility of bedrock conductors beneath the ultramafic and gabbro intrusions.

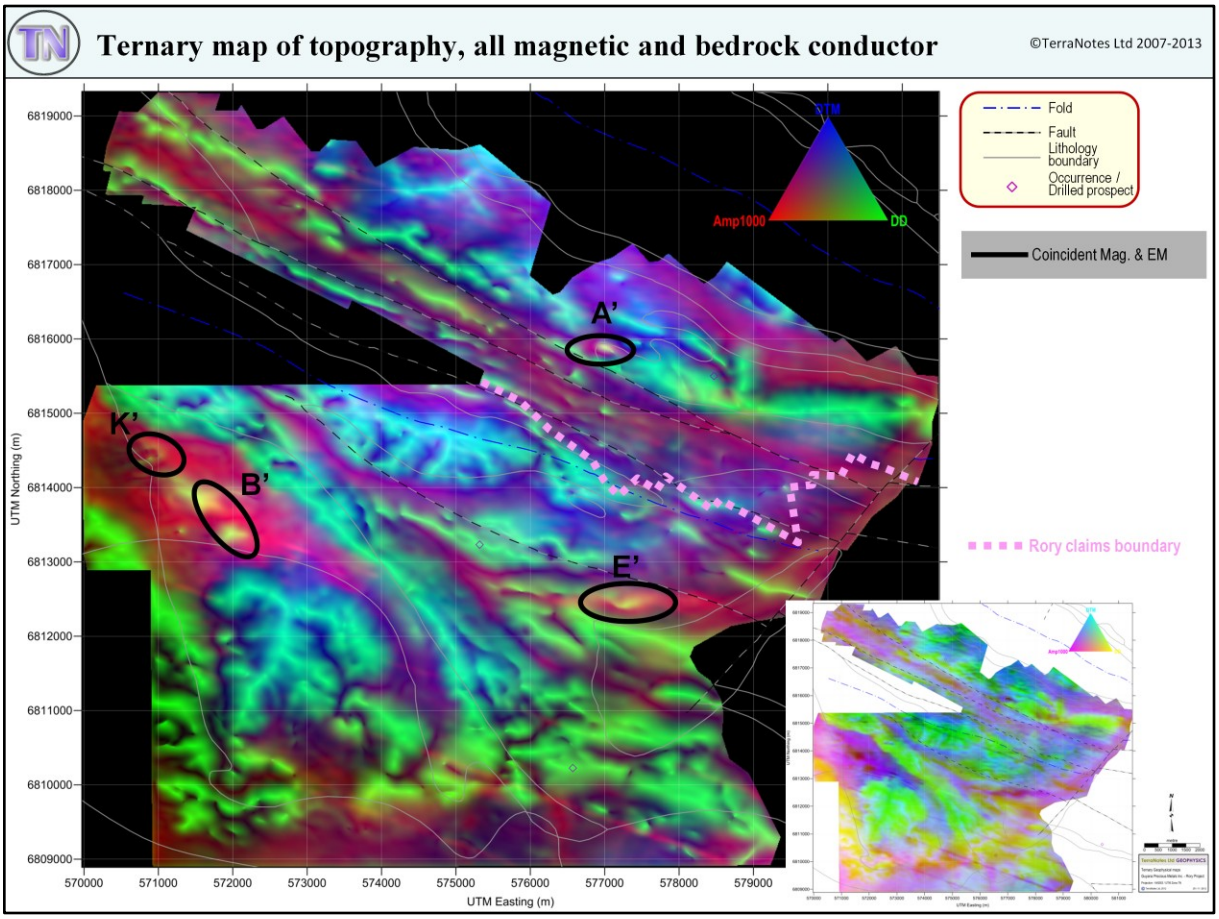


Figure 53. The main map is the ternary map of topography, all magnetic structures, and mid-depth bedrock conductors in RGB colours. The inset map on the bottom right uses CMY colours, which are the reciprocal of RGB. Blue/cyan represents the topography, green/yellow represents all magnetic structures, and red/magenta represents the mid-depth bedrock conductors. The main map is an IHS ternary map where brighter colours indicate the most anomalous zones. Darker colours indicate the most anomalous zones in the CMY map. The pink diamonds indicate mineral occurrences of YGS. The gray polygons indicate the boundaries of the geological formations. The dashed black lines indicate the faults/shears and the dashed blue lines indicate fold axes. The pink dotted line approximately separates the Rory claims from the other claims.

Main Findings

This figure is similar to Figure 46, but uses the co-axial component of the EM amplification instead of the co-planar component apparent resistivity. It should be more sensitive than Figure 46 to bedrock conductors.

Yellow is very prominent in this figure, particularly in the western portions of the conductive zones. These partial anomalies have been labelled A', B', E', and K', which constitute the high priority targets. The black anomalies in the inset map confirm this interpretation.

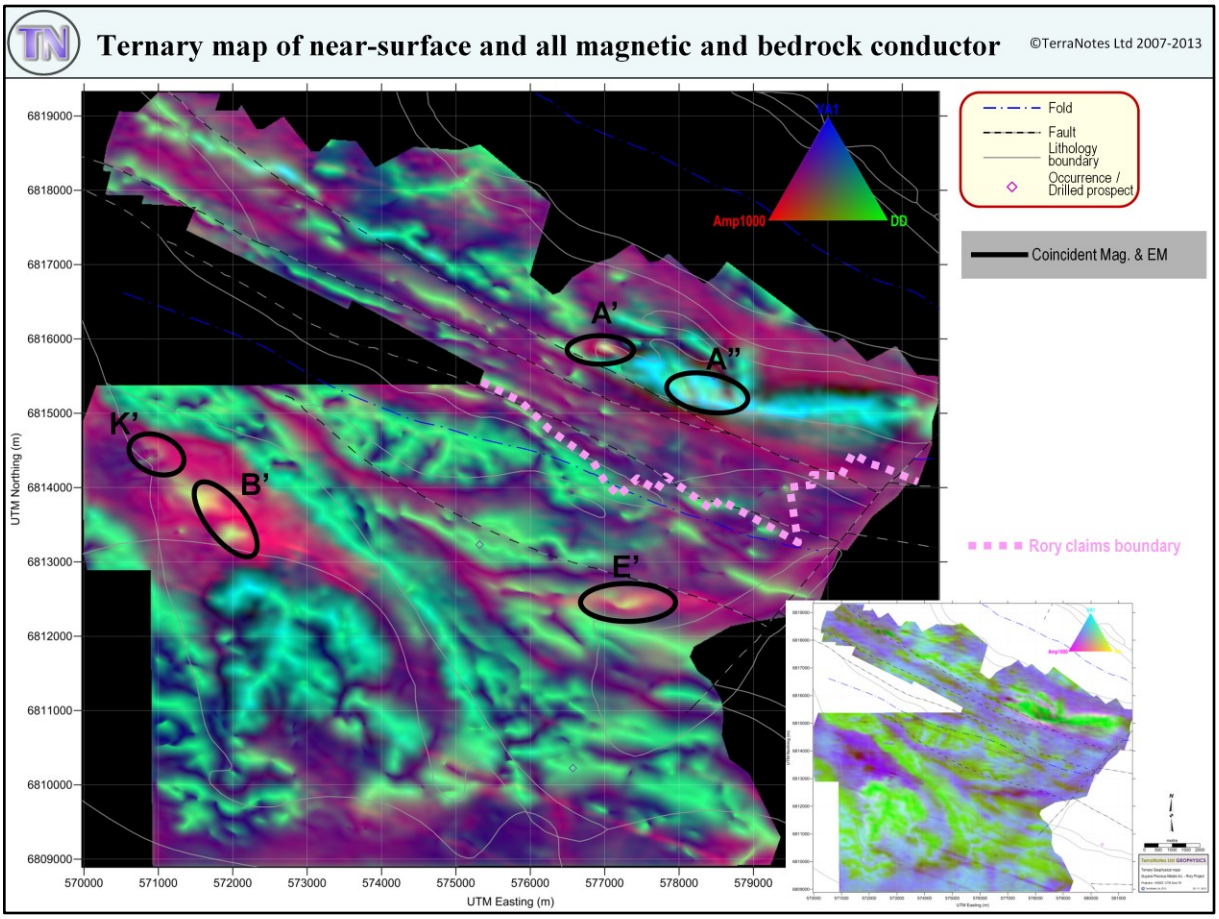


Figure 54. The main map is the ternary map of near-surface magnetic, all magnetic structures, and mid-depth bedrock conductors in RGB colours. The inset map on the bottom right uses CMY colours, which are the reciprocals of RGB. Blue/cyan represents the near-surface magnetic anomalies, green/yellow represents all magnetic structures, and red/magenta represents the mid-depth bedrock conductors. The main map is an IHS ternary map where brighter colours indicate the most anomalous zones. Darker colours indicate the most anomalous zones in the CMY map. The pink diamonds indicate mineral occurrences of YGS. The gray polygons indicate the boundaries of the geological formations. The dashed black lines indicate the faults/shears and the dashed blue lines indicate fold axes. The pink dotted line approximately separates the Rory claims from the other claims. The black ellipses indicate the previously identified bedrock-type conductive anomalies.

Main Findings

This figure is similar to Figure 47 but uses the co-axial component of the EM amplification instead of the co-planar component apparent resistivity. It should be more sensitive than Figure 47 to bedrock conductors.

This figure validates the interpretation of Figure 53.

A very weak EM conductor is visible in the centre of Anomaly A where the magnetic structure is strongest. This partial anomaly is labelled Anomaly A".

Deep penetrating EM methods are recommended for the areas exhibiting cyan anomalies to investigate the possibility of bedrock conductors beneath the ultramafic and gabbro intrusions.

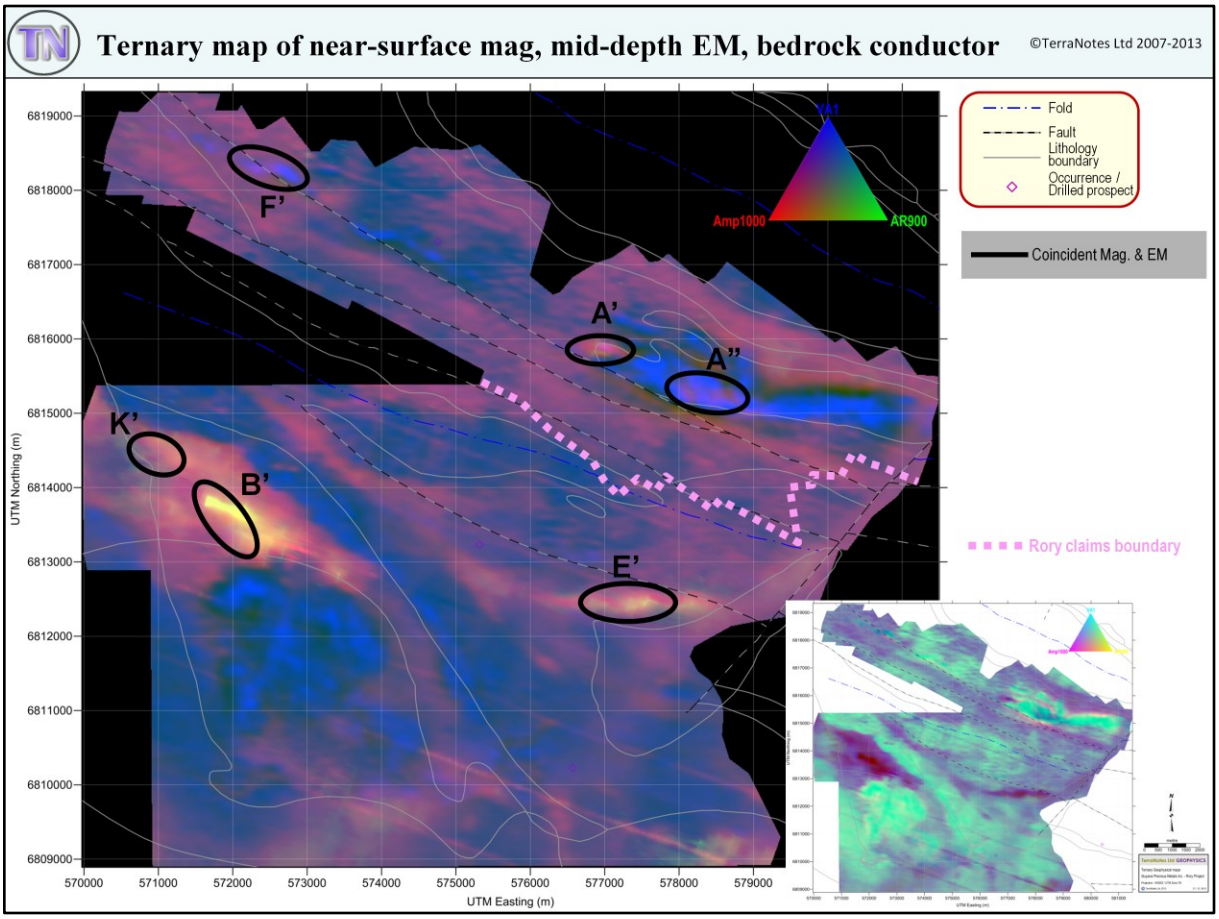


Figure 55. The main map is the ternary map of near-surface magnetic, mid-depth EM, and mid-depth conductors in RGB colours. The inset map on the bottom right uses CMY colours, which are the reciprocals of RGB. Blue represents the near-surface magnetic anomalies, green represents the mid-depth EM anomalies, and red represents the mid-depth bedrock conductors. The main map is an IHS ternary map where brighter colours indicate the most anomalous zones. Darker colours indicate the most anomalous zones in the CMY map. The pink diamonds indicate mineral occurrences of YGS. The gray polygons indicate the boundaries of the geological formations. The dashed black lines indicate the faults/shears and the dashed blue lines indicate fold axes. The pink dotted line approximately separates the Rory claims from the other claims.

Main Findings

This figure integrates the apparent resistivity calculation from the co-planar component and the EM amplification calculation from the co-axial component with near-surface and strong magnetic structures. It is sensitive to both broad conductive zones and narrow bedrock conductors.

Bright yellow anomalies are the most important features, and they are observed at B' and E'. Anomaly K' is yellowish orange, which suggests a weaker conductor.

Bright magenta anomalies are also important as they indicate coincident strong magnetic and conductive zones. Such anomalies are observed at A', A'' and F'.

Bright blue anomalies indicate the ultramafic and gabbro intrusions which could be associated with Ni-Cu-PGE mineralization. Further EM data acquisition is recommended for these zones.

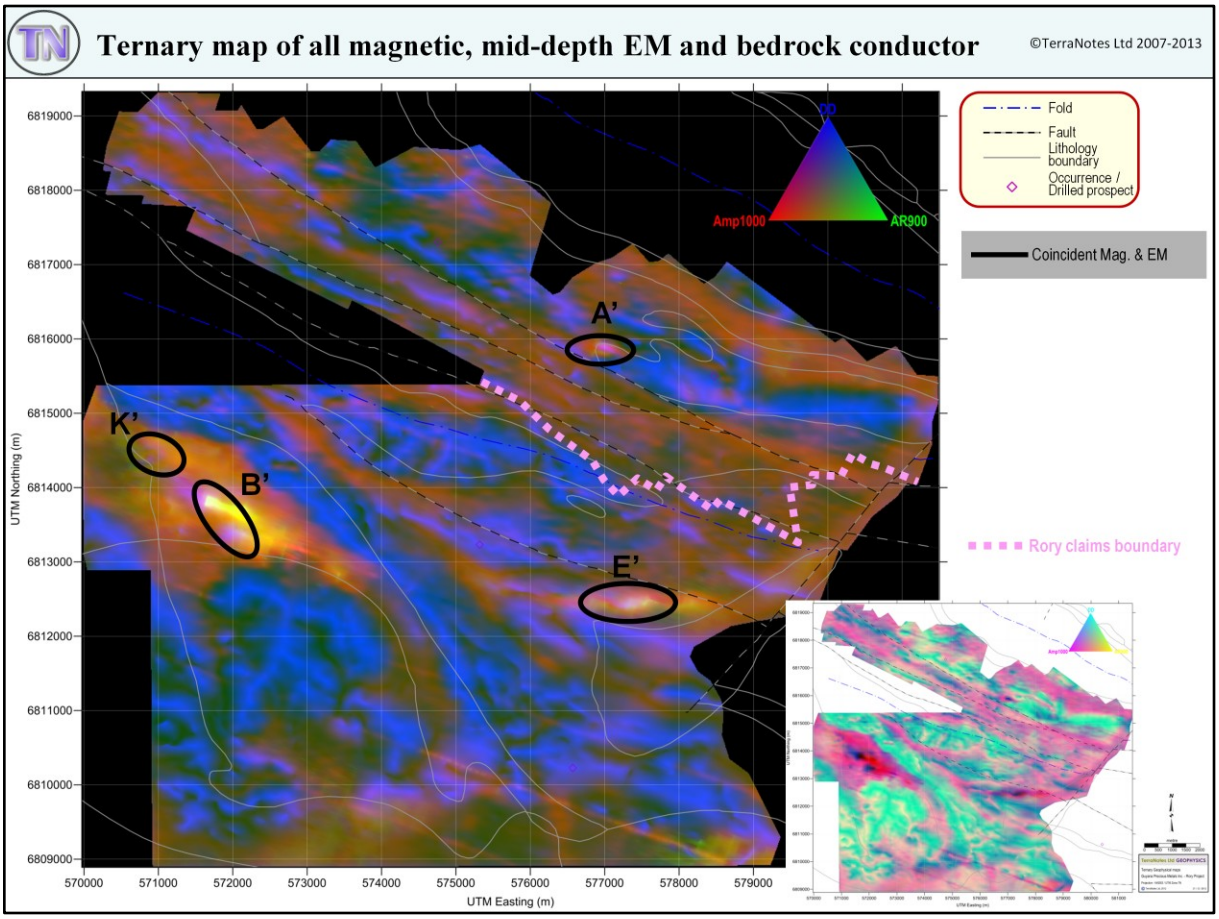
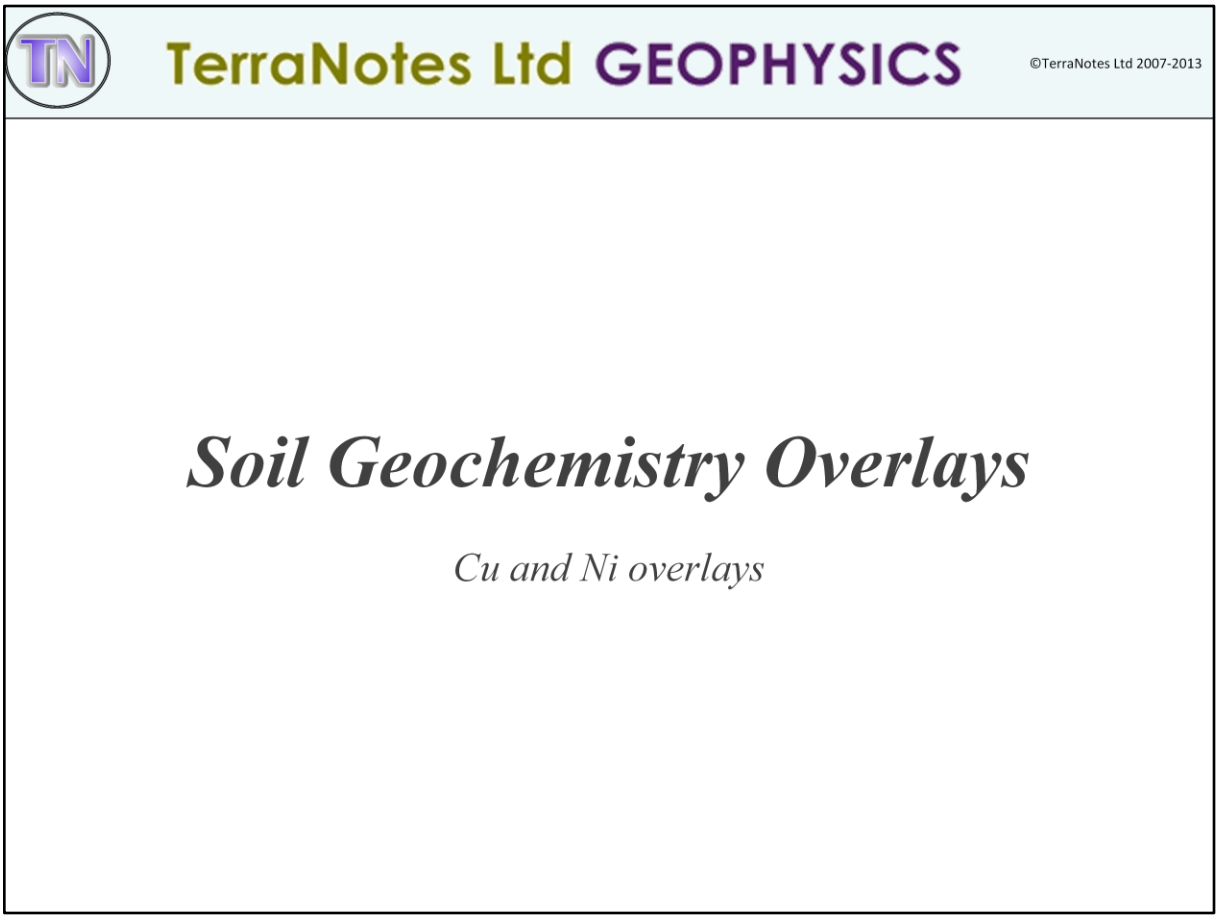


Figure 56. The main map is the ternary map of all magnetic structures, mid-depth EM, and mid-depth conductors in RGB colours. The inset map on the bottom right uses CMY colours, which are the reciprocals of RGB. Blue represents all magnetic structures, green represents the mid-depth EM anomalies, and red represents the mid-depth bedrock conductors. The main map is an IHS ternary map where brighter colours indicate the most anomalous zones. Darker colours indicate the most anomalous zones in the CMY map. The pink diamonds indicate mineral occurrences of YGS. The gray polygons indicate the boundaries of the geological formations. The dashed black lines indicate the faults/shears and the dashed blue lines indicate fold axes. The pink dotted line approximately separates the Rory claims from the other claims.

Main Findings

This figure integrates the apparent resistivity calculation from the co-planar component and the EM amplification calculation from the co-axial component with all magnetic structures. It is sensitive to both broad conductive zones and narrow bedrock conductors.

This figure, like Figure 55, indicates that the most important anomalies are A', B', E', and K'. Anomalies B' and E' exhibit white colours next to bright magenta. These white colour zones are the most important zones as the conductors intersect the magnetic structures, and they are the indicator of possible sulphide mineralization.


TerraNotes Ltd GEOPHYSICS
©TerraNotes Ltd 2007-2013
Soil Geochemistry Overlays
Cu and Ni overlays

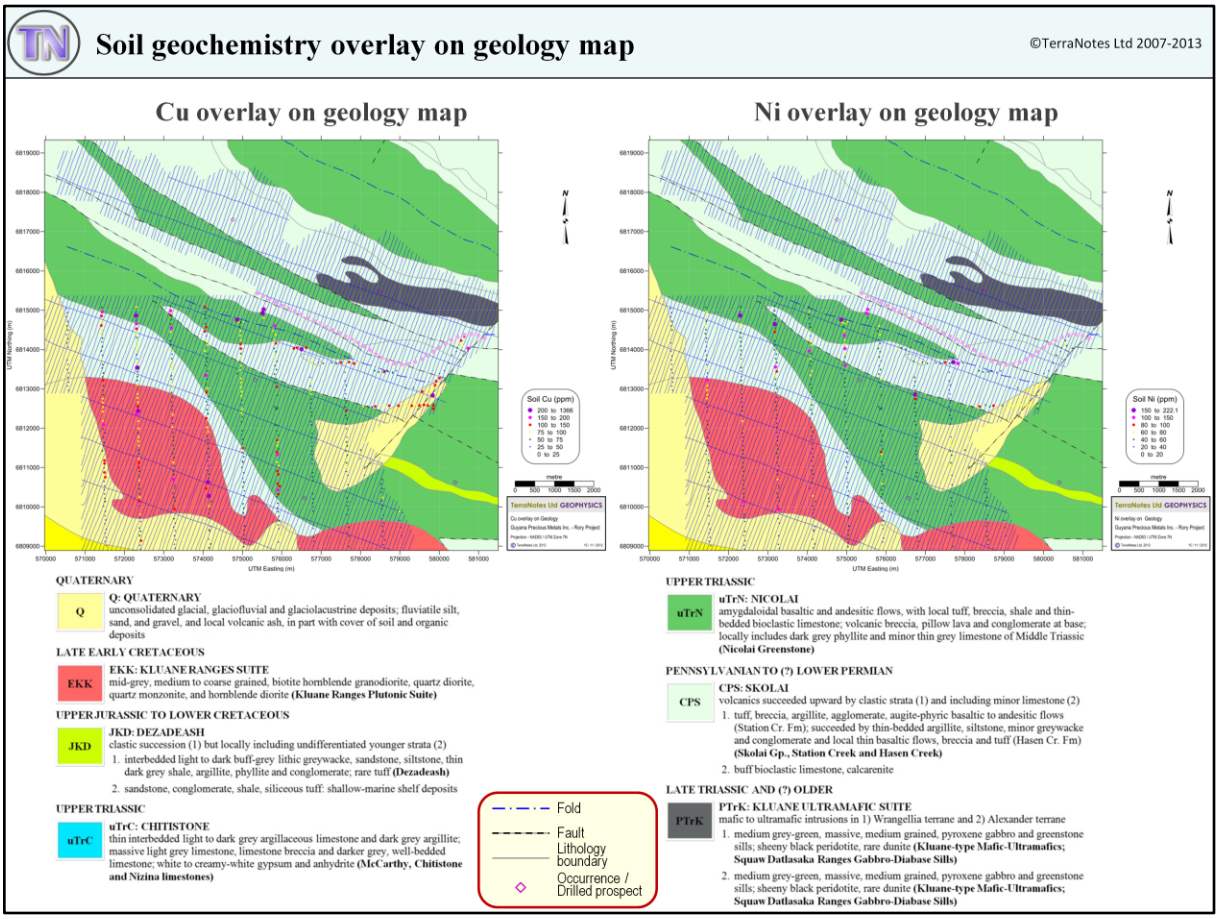


Figure 57. The left panel is the Cu overlays and the right panel is the Ni overlays, both on the geology map. Please see the legend for Cu and Ni concentrations in parts per million (ppm). The pink diamonds indicate mineral occurrences of YGS. The gray polygons indicate the boundaries of the geological formations. The dashed black lines indicate the faults/shears and the dashed blue lines indicate fold axes. The pink dotted line approximately separates the Rory claims from the other claims.

Main Findings

The soil Cu anomalies mainly occur at the contact between the Skolai (light green – CPS1) and Nicolai (dark green – uTrN) formations. A good amount of copper is also found in the plutonic suite (EKK) in the southwest. Cu is distributed everywhere in the Rory claim group. The highest occurrences exist at the geological contacts, which is in accordance with the findings of the Wellgreen deposit.

The soil Ni anomalies mainly occur on the northern portion of the claim group around the Nicolai formation and its contact. The Skolai formation appears to host less Ni than the Nicolai formation, or the Ni occurrences in the Skolai formation are rather deep. Since it is known that the Wellgreen deposit occurs at the contact between the Skolai formation and ultramafic rocks (PTrK), Ni mineralization in the Skolai formation within the Rory claims cannot be dismissed.

Magnetic maps will play a crucial role in determining where Cu mineralization occurs in the Plutonic Suite (EKK). If the Cu mineralization is within the magnetic highs or their contacts, it may indicate a similar mineralization to Wellgreen beneath the EKK formation.

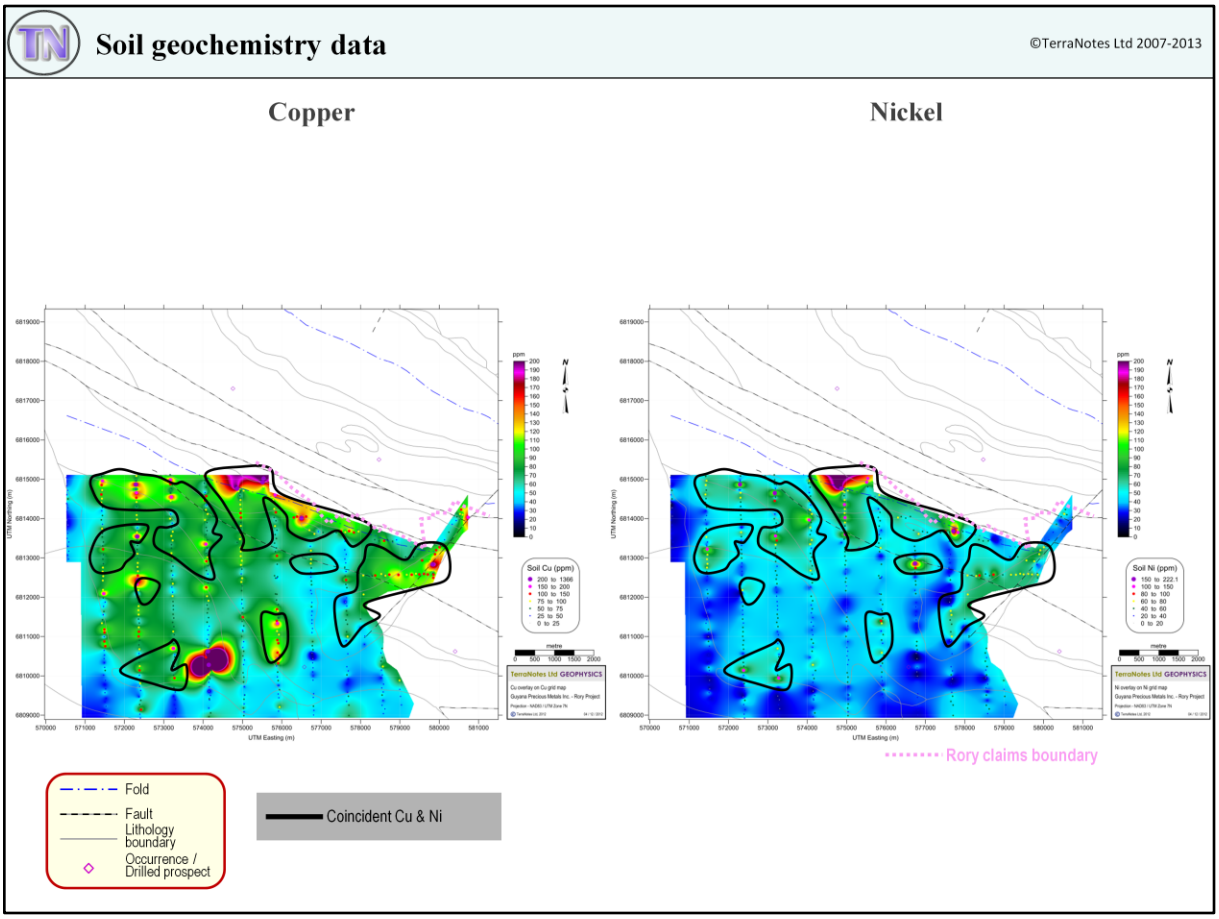


Figure 58. The left panel is the Cu overlays on the Cu grid map and the right panel is the Ni overlays on the Ni grid map. Please see the legends and colour bars for Cu and Ni concentrations in ppm. The pink diamonds indicate mineral occurrences of YGS. The gray polygons indicate the boundaries of the geological formations. The dashed black lines indicate the faults/shears and the dashed blue lines indicate fold axes. The pink dotted line approximately separates the Rory claims from the other claims.

Main Findings

The black polygons indicate areas with higher than 60 ppm Ni in soil. The anomalous Ni values in soil appear to coincide with the anomalous Cu values. This can be observed by comparing the black polygons on both maps.

Cu seems to be more widespread than the Ni, especially in the south and southwest areas. These Cu anomalies are not coincident with Ni anomalies.

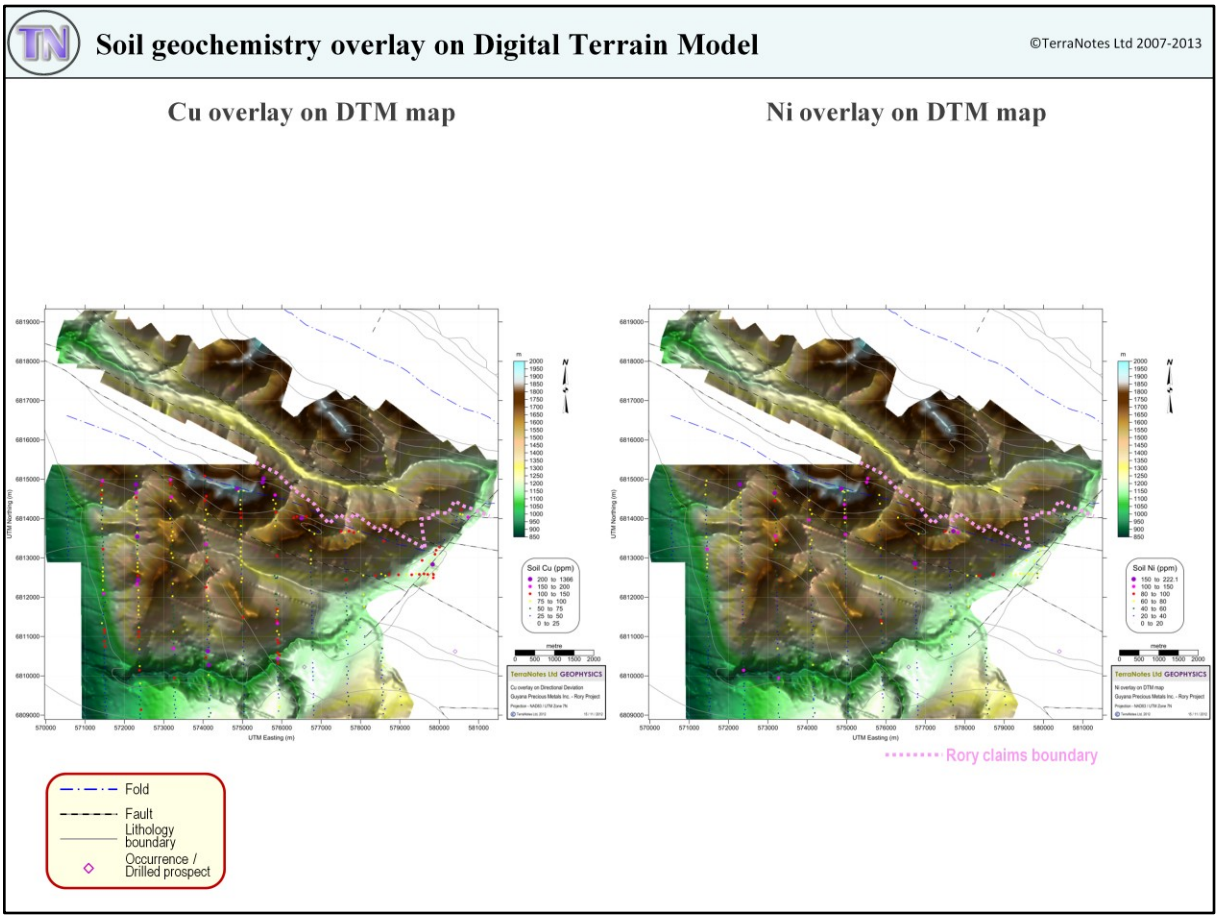


Figure 59. The left panel is the Cu overlays and the right panel is Ni overlays, both on the DTM map. Please see the legend for Cu and Ni concentrations in ppm. The pink diamonds indicate mineral occurrences of YGS. The gray polygons indicate the boundaries of the geological formations. The dashed black lines indicate the faults/shears and the dashed blue lines indicate fold axes. The pink dotted line approximately separates the Rory claims from the other claims.

Main Findings

Both the Cu and Ni soil geochemistry data were collected on the high topographic features. They should not have been transported from long distances and should reflect the anomalies at the locations at which they were collected.

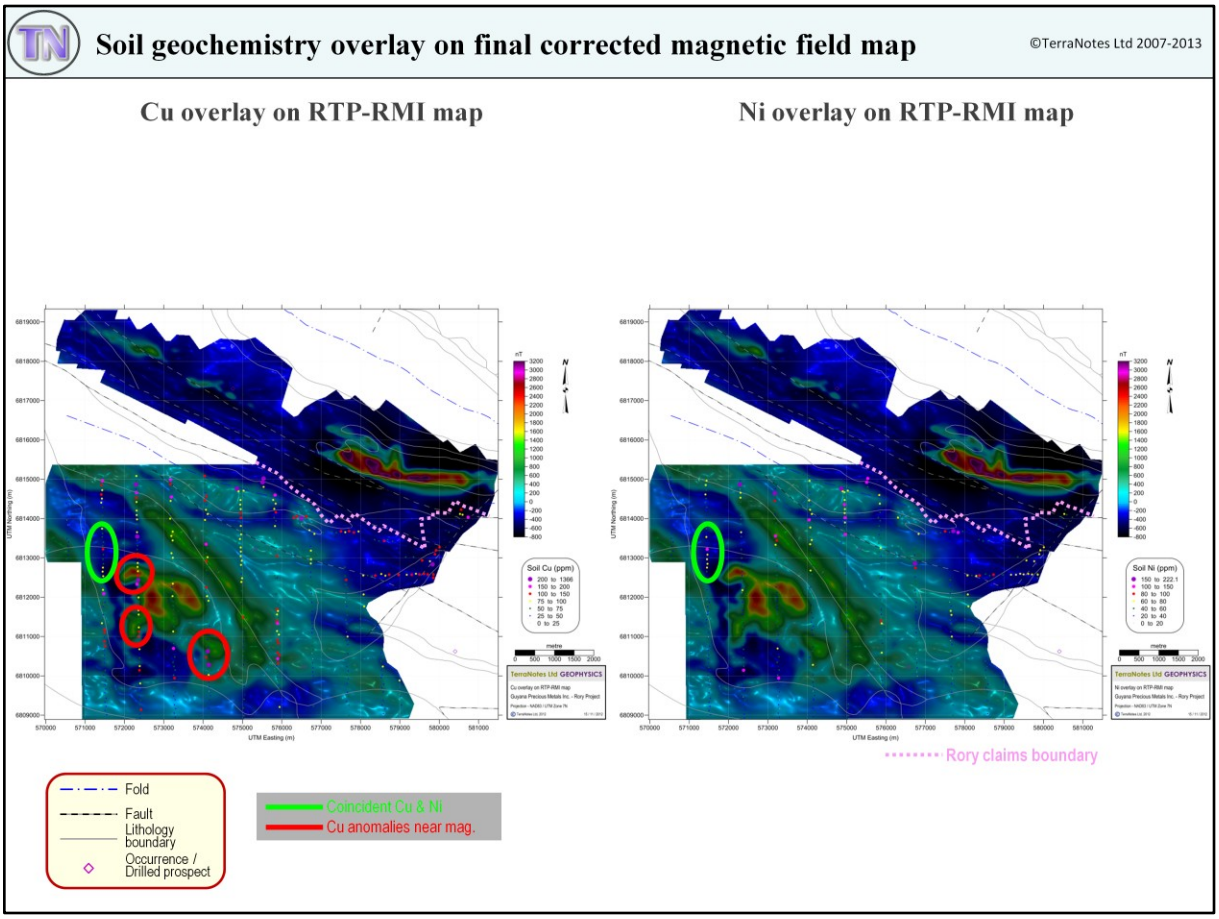


Figure 60. The left panel is the Cu overlays and the right panel shows Ni overlays, both on the RTP-RMI map. Please see the legend for Cu and Ni concentrations in ppm. The pink diamonds indicate mineral occurrences of YGS. The gray polygons indicate the boundaries of the geological formations. The dashed black lines indicate the faults/shears and the dashed blue lines indicate fold axes. The pink dotted line approximately separates the Rory claims from the other claims.

Main Findings

All the Cu anomalies occur at the contacts of high magnetic anomalies, except those located in the east. Even the south and southwest Cu anomalies occur at the contact zones of high magnetic anomalies (see red ellipses).

Few Ni anomalies occur in the south and southwest and those that do are mostly sporadic with one high concentration occurrence. The only anomalous trend occurs in the west (green ellipse) with a coincident Cu anomaly. This anomaly occurs in a low magnetic zone, similar to other high Ni occurrences in the south and southwest.

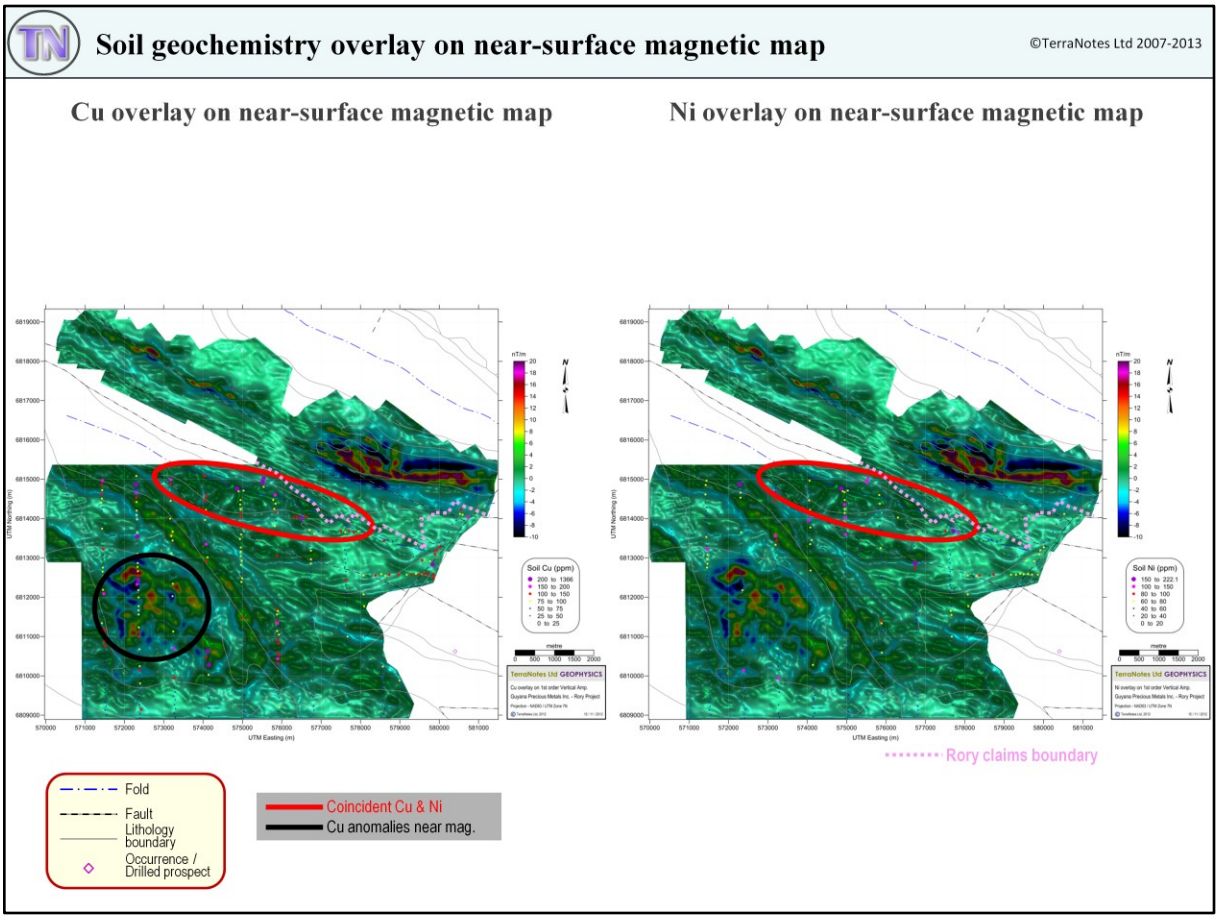


Figure 61. The left panel is the Cu overlays and the right panel is Ni overlays, both on the near-surface magnetic map. Please see the legend for Cu and Ni concentrations in ppm. The pink diamonds indicate mineral occurrences of YGS. The gray polygons indicate the boundaries of the geological formations. The dashed black lines indicate the faults/shears and the dashed blue lines indicate fold axes. The pink dotted line approximately separates the Rory claims from the other claims.

Main Findings

The black ellipse indicates the Cu anomalies in the Plutonic Suite (EKK). The Cu anomalies at this location occur at the contacts and/or embayments of the high magnetic anomalies. This magnetic behaviour is similar to the Wellgreen deposit.

The red ellipse shows the coincident Cu and Ni anomalies in the northern portion of Rory claims. The Cu and Ni mineralization at this location also occurs at the embayments of the high magnetic anomaly, again similar to the Wellgreen deposit. Figure 62 depicts this phenomenon clearly.

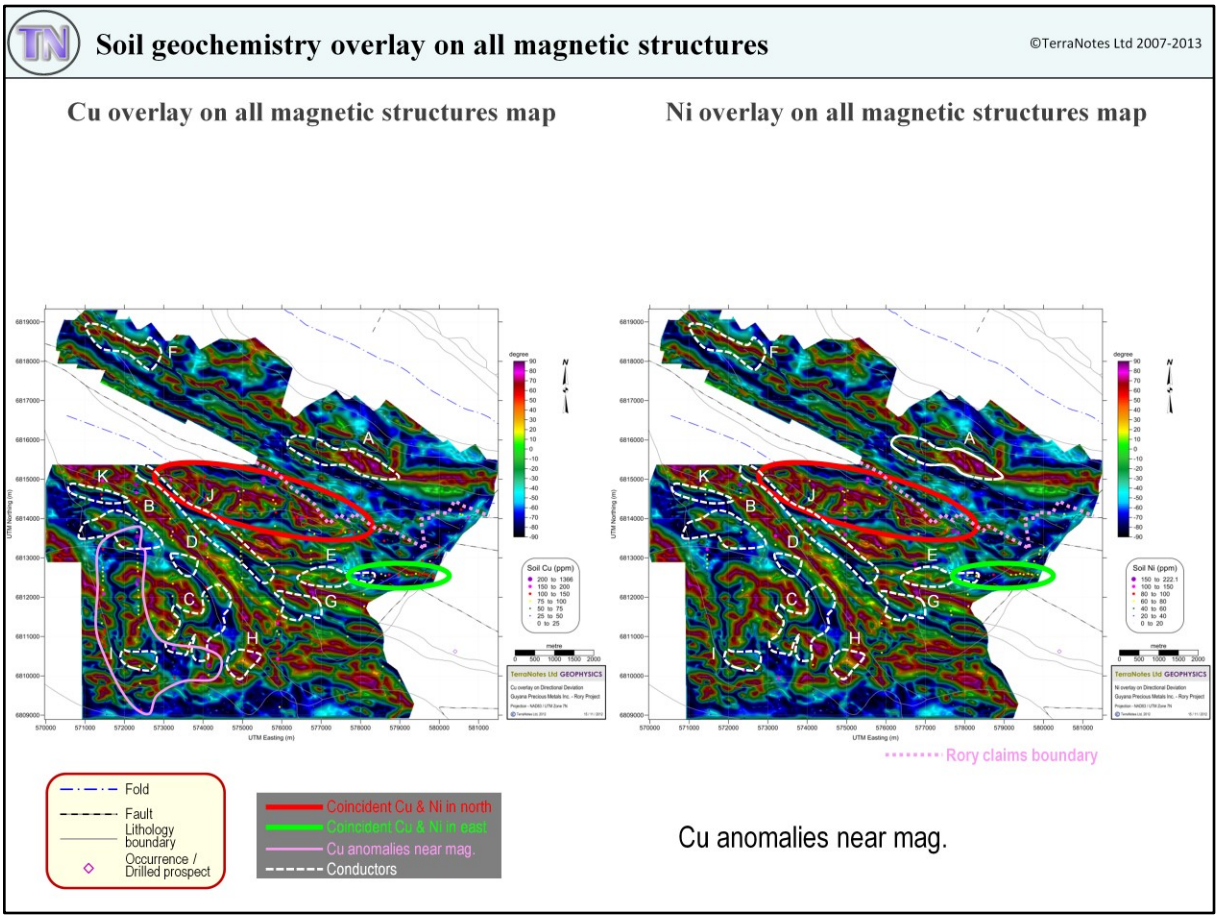


Figure 62. The left panel is the Cu overlays and the right panel shows Ni overlays, both on the all magnetic structures map. Please see the legend for Cu and Ni concentrations in ppm. The pink diamonds indicate mineral occurrences of YGS. The gray polygons indicate the boundaries of the geological formations. The dashed black lines indicate the faults/shears and the dashed blue lines indicate fold axes. The pink dotted line approximately separates the Rory claims from the other claims. The white dashed polygons and letters indicate the previously identified EM anomalies.

Main Findings

Although there is no EM anomaly within the red ellipse, the soil Cu and Ni anomalies occur at the embayments of the high magnetic anomalies (most probably in the Nicolai formation). This indicates that there may be Ni-Cu-PGE mineralization beneath the Nicolai formation at greater depths. A deeper EM method could be employed to look for deeper conductors at this location.

In analysis performed in previous sections, Anomalies B, E, K, and D were selected as the most important. Anomalies B, D, and K show sporadic Cu and Ni anomalies in close relationship with weak magnetic anomalies.

The green ellipses show the E-W oriented Cu and Ni trend in the eastern portion of the Rory claims. The high conductivity and weak magnetic Anomaly E appears to be the continuation of this Cu and Ni trend.

All the anomalous Cu values within the pink polygon coincide with the contacts of magnetic structures.

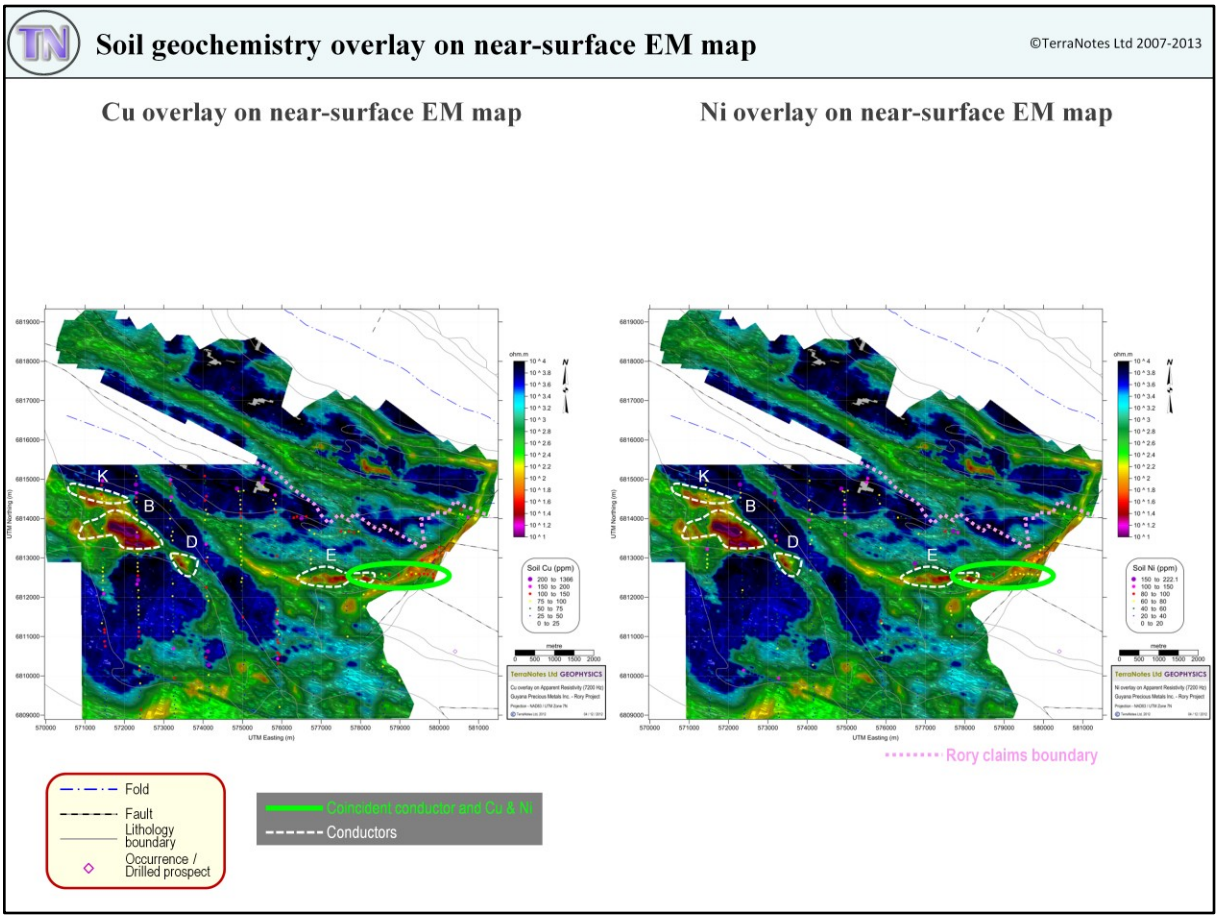


Figure 63. The left panel is the Cu overlays and the right panel is Ni overlays, both on the near-surface EM map. Please see the legend for Cu and Ni concentrations in ppm. The pink diamonds indicate mineral occurrences of YGS. The gray polygons indicate the boundaries of the geological formations. The dashed black lines indicate the faults/shears and the dashed blue lines indicate fold axes. The pink dotted line approximately separates the Rory claims from the other claims.

Main Findings

Cu mineralization in soil occurs on both conductive and resistive anomalies in the near-surface. However, the most anomalous Cu mineralization occurs on the resistive ground, which is mainly coincident with Nicolai (uTrN) and Kluane Plutonic Suite (EKK) formations. This indicates that economic mineralizations may be located beneath these formations at their basal contacts. For example, at the contact between the overlying gabbro and underlying Skolai formations. Deep penetrating EM methods should be employed to image the basement conductors beneath these resistive formations.

The conductive zones (white dashed polygons) that have been located in the west (Anomalies B, D, and K) and in the east (Anomaly E) could also be associated with Cu mineralization.

The anomalous Ni mineralization in soil occurs only on resistive zones in the near-surface. It occurs on the contacts between the Nicolai and Skolai formations. The economic Ni mineralization may be located at the basal contact of the Nicolai formation. Deep penetrating EM methods may be useful to image the bedrock conductors due to sulphide mineralization at this contact.

The green ellipse in the east indicates coincident Cu and Ni mineralizations on a conductive zone. The western continuation of this anomalous trend exhibits a strong bedrock conductor. Therefore, economic Cu-Ni-PGE mineralization may be found in the near-surface to mid-depths within Anomaly E.

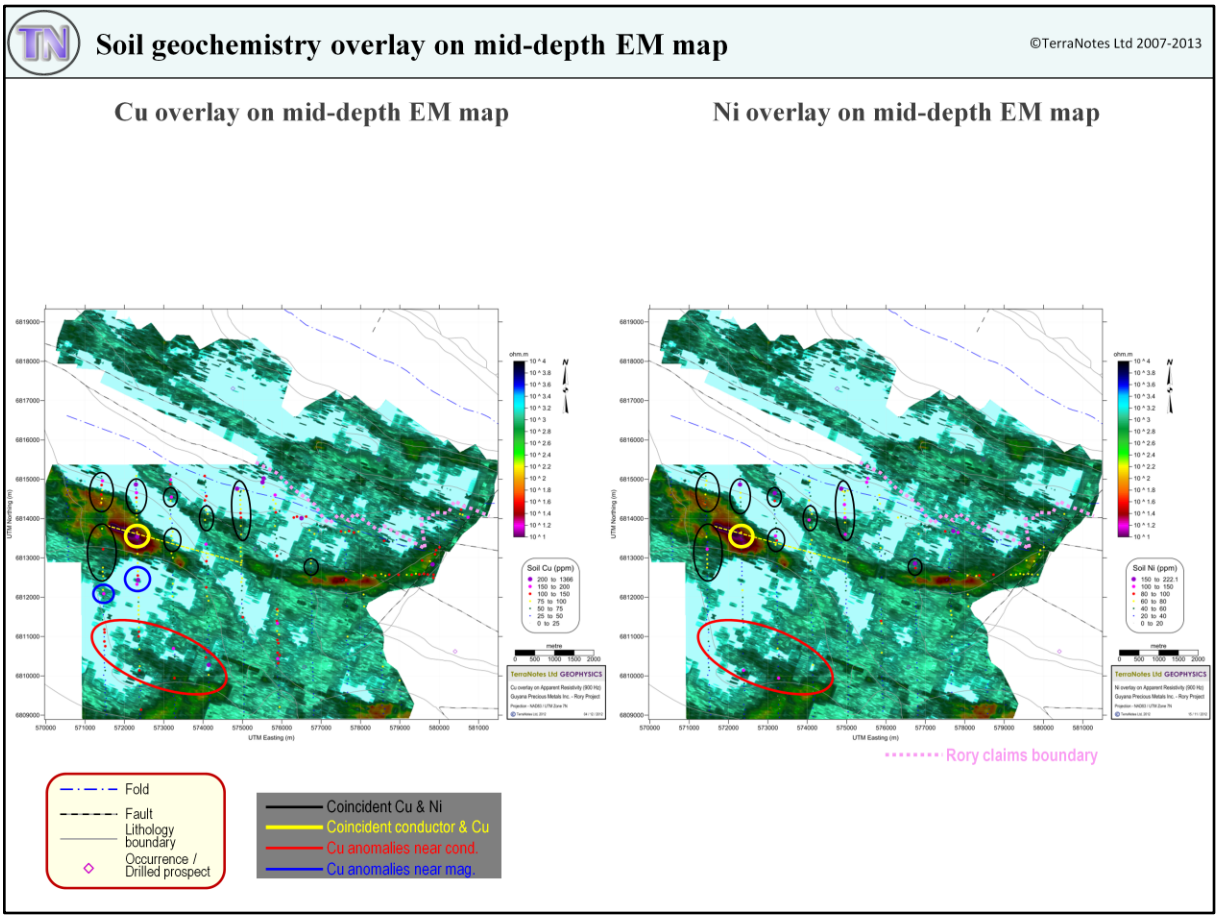


Figure 64. The left panel is the Cu overlays and the right panel is Ni overlays, both on the mid-depth EM map. Please see the legend for Cu and Ni concentrations in ppm. The pink diamonds indicate mineral occurrences of YGS. The gray polygons indicate the boundaries of the geological formations. The dashed black lines indicate the faults/shears and the dashed blue lines indicate fold axes.

Main Findings

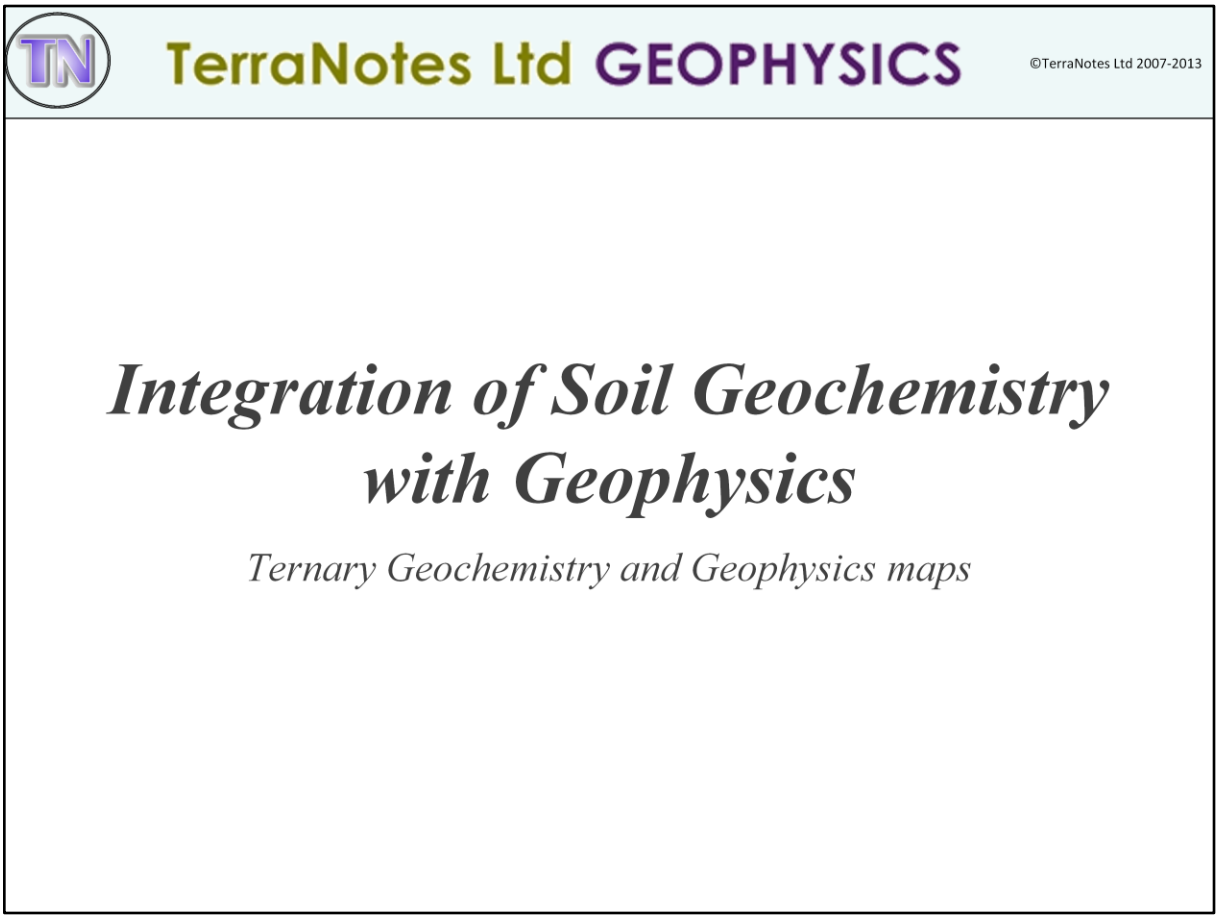
There is no soil geochemistry data collection line that crosses the most conductive anomaly (B). However, the eastern part of that anomaly exhibits very high Cu and moderate Ni concentrations (see yellow circle). Assuming the yellow dashed line represents the axis for the bedrock conductor at Anomaly B, then the anomalous Cu and Ni values coincide with this conductor axis.

The black ellipses show the coincident Ni and Cu mineralizations in soil in the vicinity and at the contact of the conductive Skolai formation.

The red ellipse in the south shows another weak conductor (Anomaly I) that is related to the Cu mineralization in soil. It also exhibits sporadic anomalous Ni values. It was shown in Figure 62 that the anomalous values in this zone are located at the contacts of magnetic structures.

The blue ellipses show the anomalous Cu values within the Kluane Plutonic Suite (EKK) coincident with very weak conductivity anomalies, as the flat zone was disturbed with some resistivity anomalies (see greenish resistivity anomalies inside the blue ellipses).

Deep EM methods may reveal the conductors beneath the gabbro.


TerraNotes Ltd GEOPHYSICS
©TerraNotes Ltd 2007-2013
Integration of Soil Geochemistry with Geophysics
Ternary Geochemistry and Geophysics maps

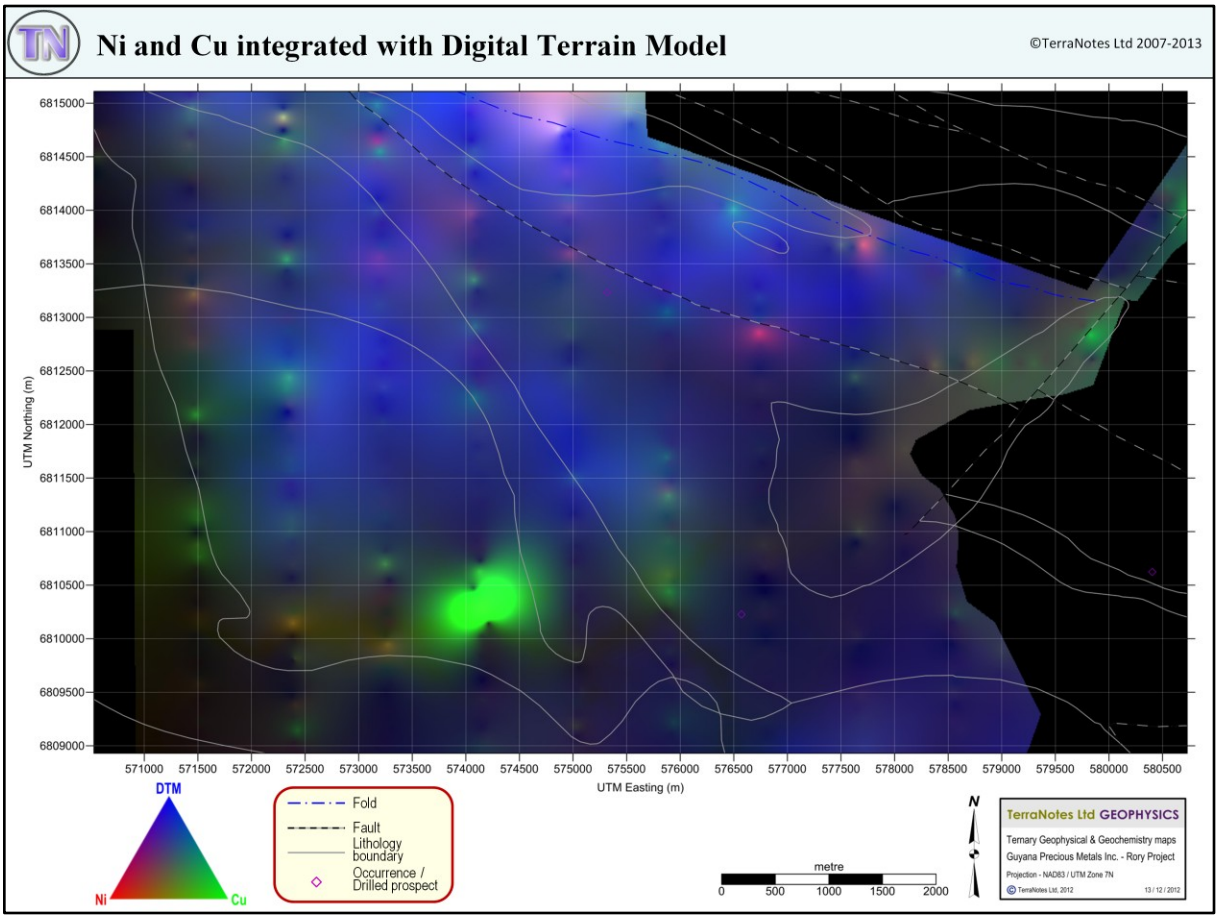


Figure 65. Ternary map of Ni and Cu integrated with the DTM. Blue represents the DTM, green represents Cu concentrations in the soil, and red represents Ni concentrations in the soil. This map is an IHS ternary map where brighter colours indicate the most anomalous zones. The pink diamonds indicate mineral occurrences of YGS. The gray polygons indicate the boundaries of the geological formations. The dashed black lines indicate the faults/shears and the dashed blue lines indicate fold axes.

Main Findings

Cu mineralization (green) seems to be more abundant than Ni in the south.

Ni and Cu concentrations in soil increase in the vicinity of higher elevations (bright blue) in the northern area. This observation confirms the interpretation of Figures 58 and 59.

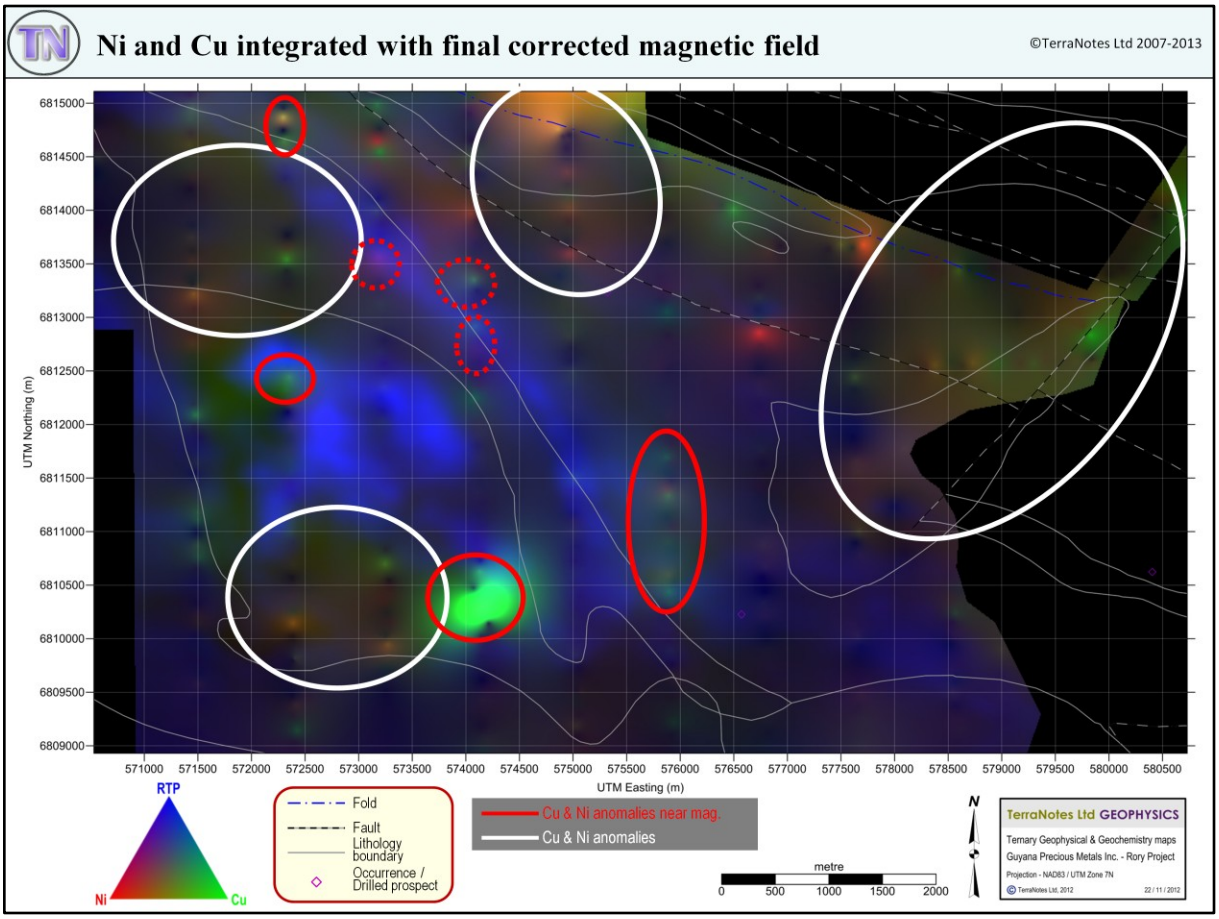


Figure 66. Ternary map of Ni and Cu integrated with the RTP-RMI. Blue represents the RTP-RMI, green represents Cu concentrations in the soil, and red represents the Ni concentrations in the soil. This map is an IHS ternary map where brighter colours indicate the most anomalous zones. The pink diamonds indicate mineral occurrences of YGS. The gray polygons indicate the boundaries of the geological formations. The dashed black lines indicate the faults/shears and the dashed blue lines indicate fold axes.

Main Findings

White to yellow anomalies are the most important anomalies to show the desired mineralization. There are no bright yellow anomalies in the figure above but the white ellipses indicate faint yellow anomalies with coincident regional Ni and Cu anomalies.

The yellow, red, and green anomalies in the vicinity of bright blue anomalies may be of interest for further exploration. Red ellipses show these kinds of Ni and Cu anomalies at the contacts of magnetic structures. The solid red ellipses mark strong soil geochemistry anomalies while the dotted red ellipses mark the very weak ones.

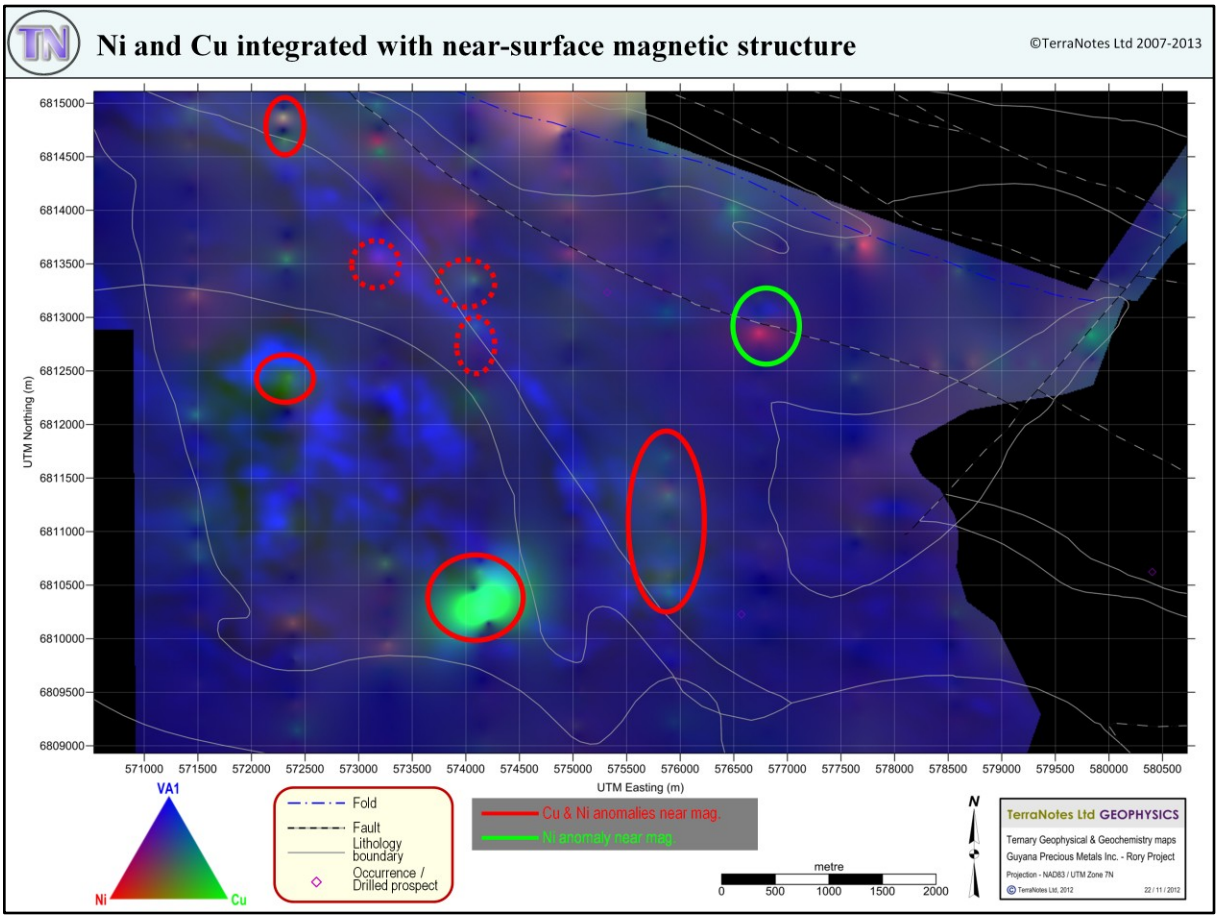


Figure 67. Ternary map of Ni and Cu integrated with near-surface magnetic structure. Blue represents the first order vertical amplification (which enhances near-surface magnetic structure), green represents Cu concentrations in the soil, and red represents Ni concentrations in the soil. This map is an IHS ternary map where brighter colours indicate the most anomalous zones. The pink diamonds indicate mineral occurrences of YGS. The gray polygons indicate the boundaries of the geological formations. The dashed black lines indicate the faults/shears and the dashed blue lines indicate fold axes.

Main Findings

This figure confirms the interpretation done in Figure 66. The red ellipses mark the Ni and Cu anomalies at the contact zones of magnetic structures.

The green ellipse shows an additional Ni anomaly at the southern contact of a weaker near-surface magnetic structure.

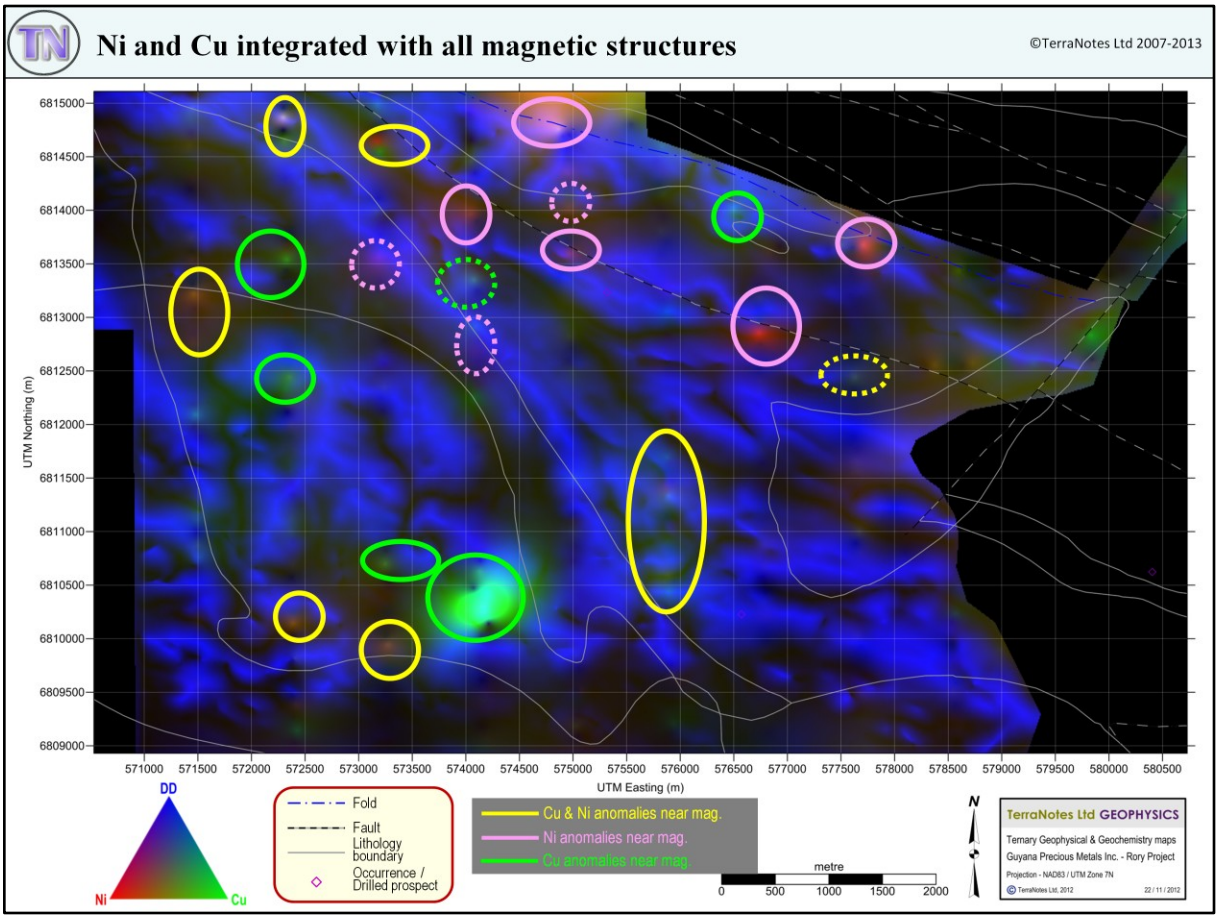


Figure 68. Ternary map of Ni and Cu integrated with all magnetic structures. Blue represents the magnetic data, green represents Cu concentrations in the soil, and red represents Ni concentrations in the soil. This map is an IHS ternary map where brighter colours indicate the most anomalous zones. The pink diamonds indicate mineral occurrences of YGS. The gray polygons indicate the boundaries of the geological formations. The dashed black lines indicate the faults/shears and the dashed blue lines indicate fold axes.

Main Findings

The ellipses in this figure shows the coincident soil Cu and Ni anomalies and magnetic anomalies. They have been placed into three categories.

1. YELLOW GROUP is composed of coincident Ni and Cu anomalies with magnetic structures (denoted by yellow ellipses)
2. PINK GROUP is composed of coincident Ni anomalies with magnetic structures (denoted by pink ellipses)
3. GREEN GROUP is composed of coincident Cu anomalies with magnetic structures (denoted by green ellipses)

Please note that dotted ellipses indicate very weak soil geochemistry anomalies.

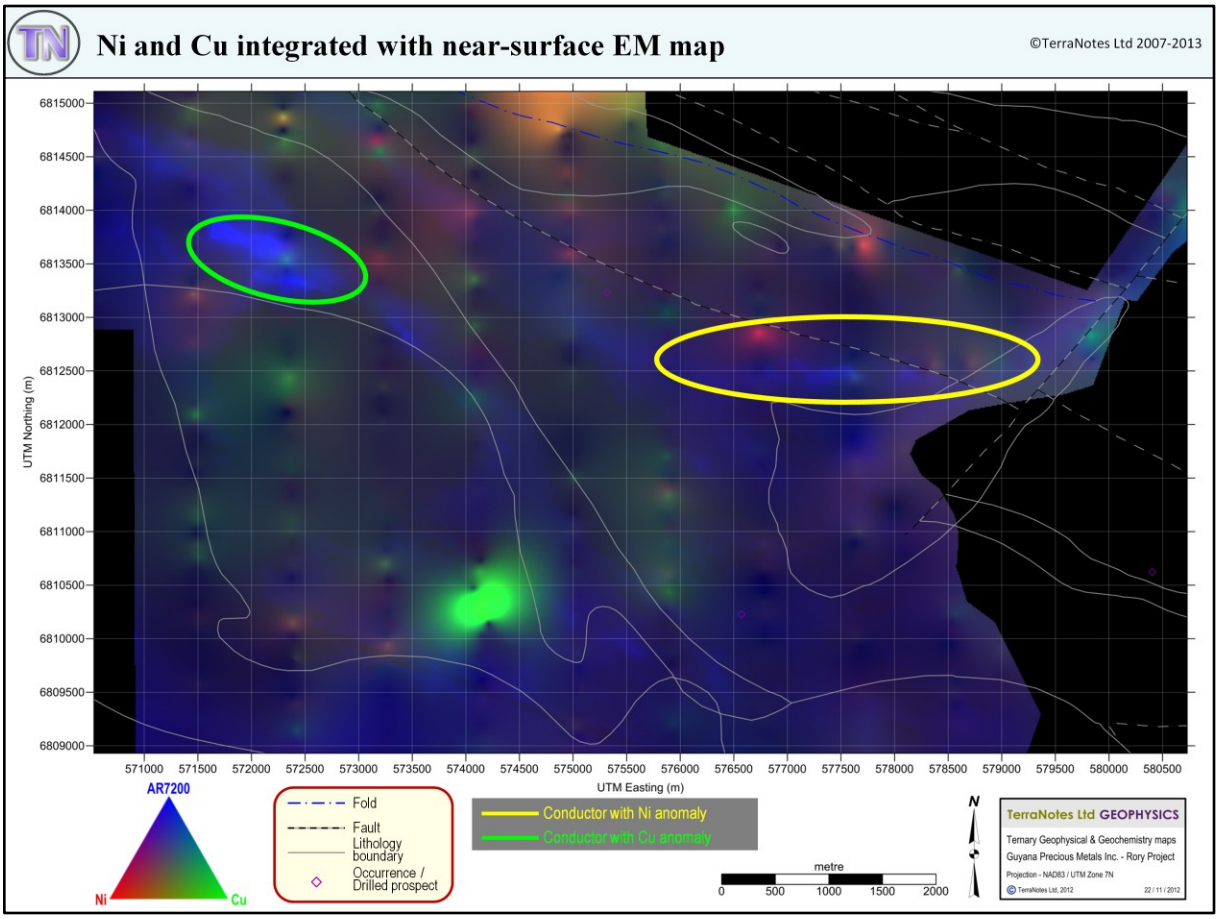


Figure 69. Ternary map of Ni and Cu integrated with near-surface EM. Blue represents the apparent resistivity in the near-surface, green represents Cu concentrations in the soil, and red represents Ni concentrations in the soil. This map is an IHS ternary map where brighter colours indicate the most anomalous zones. The pink diamonds indicate mineral occurrences of YGS. The gray polygons indicate the boundaries of the geological formations. The dashed black lines indicate the faults/shears and the dashed blue lines indicate fold axes.

Main Findings

The eastern tip of the previously identified Anomaly B (green ellipse) exhibits an anomalous Cu concentration in soil. Ni anomalies are observed to the east and southwest of the conductor.

Anomaly E is coincident with a very faint yellow anomaly indicating weaker Cu and Ni anomalies at the surface. Anomalous Ni is observed in the vicinity, to the north of the conductor.

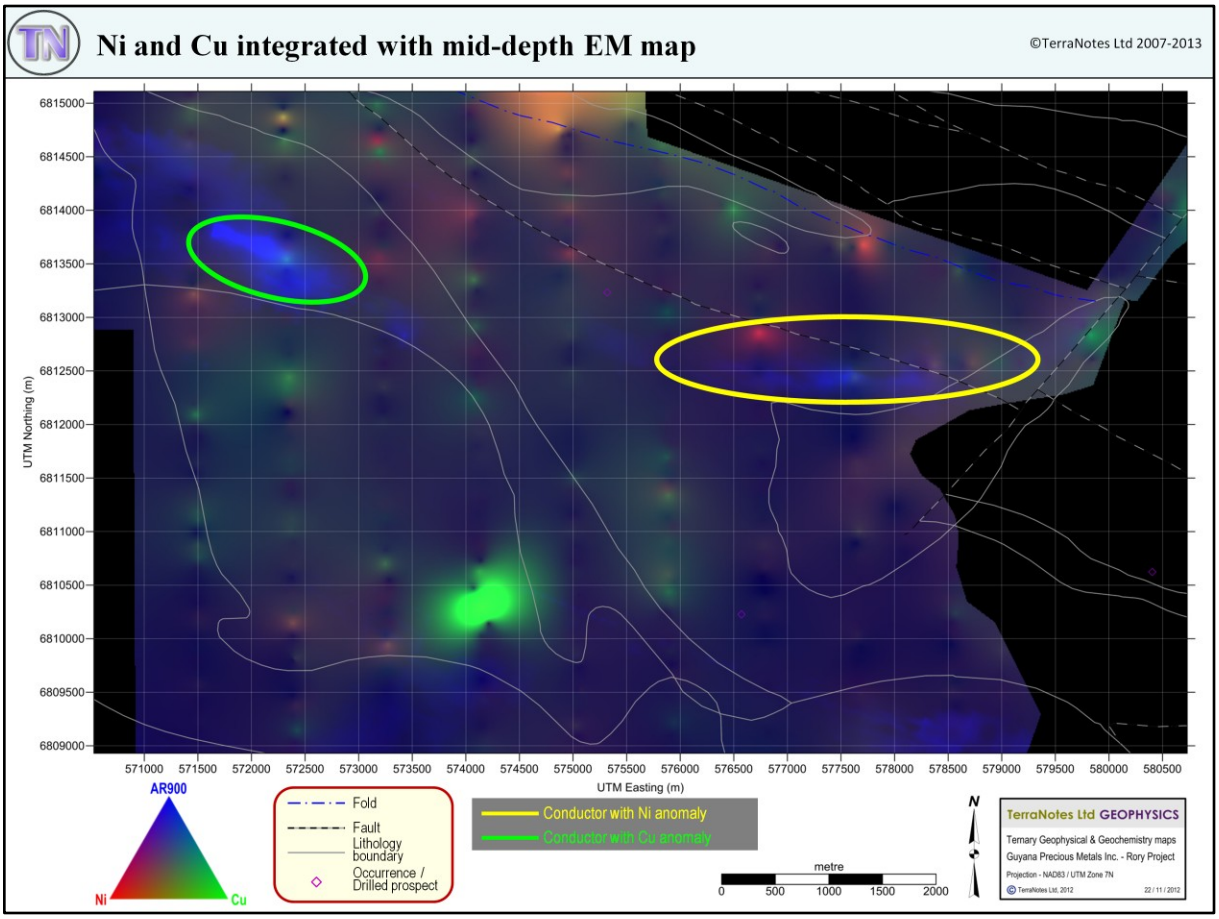


Figure 70. Ternary map of Ni and Cu integrated with mid-depth EM. Blue represents the apparent resistivity at mid-depth, green represents Cu concentrations in the soil, and red represents Ni concentrations in the soil. This map is an IHS ternary map where brighter colours indicate the most anomalous zones. The pink diamonds indicate mineral occurrences of YGS. The gray polygons indicate the boundaries of the geological formations. The dashed black lines indicate the faults/shears and the dashed blue lines indicate fold axes.

Main Findings

This figure confirms the interpretation of Figure 69.

The green ellipse indicates coincident Cu and mid-depth EM anomalies and the yellow ellipse indicates coincident Cu-Ni anomalies in the soil.

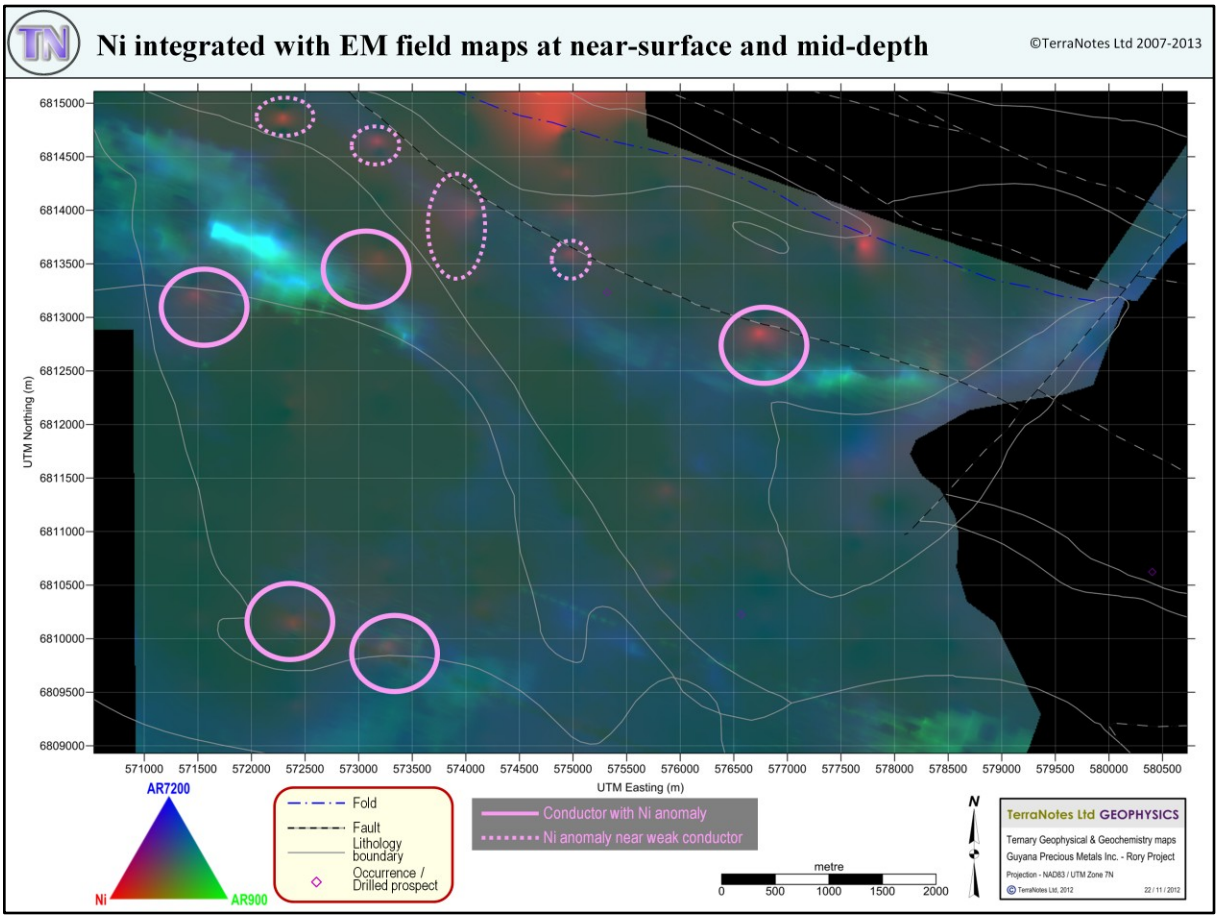


Figure 71. Ternary map of Ni concentrations in soil integrated with near-surface and mid-depth EM. Blue represents the apparent resistivity in the near-surface, green represents the apparent resistivity at mid-depth, and red represents Ni concentrations in the soil. This map is an IHS ternary map where brighter colours indicate the most anomalous zones. The pink diamonds indicate mineral occurrences of YGS. The gray polygons indicate the boundaries of the geological formations. The dashed black lines indicate the faults/shears and the dashed blue lines indicate fold axes.

Main Findings

Bright and faint cyan indicate strong and moderate conductors, respectively. Solid pink ellipses indicate high Ni concentrations in soil in the vicinity of those cyan anomalies which could be crucial for further Ni-Cu-PGE exploration.

Dotted pink ellipses indicate high Ni concentration in the soil coincident with weak or surficial conductors.

The red anomalies are situated in resistive zones. Possible conductors at these locations could be deep, at the basal contact of the Skolai or Nicolai formations.

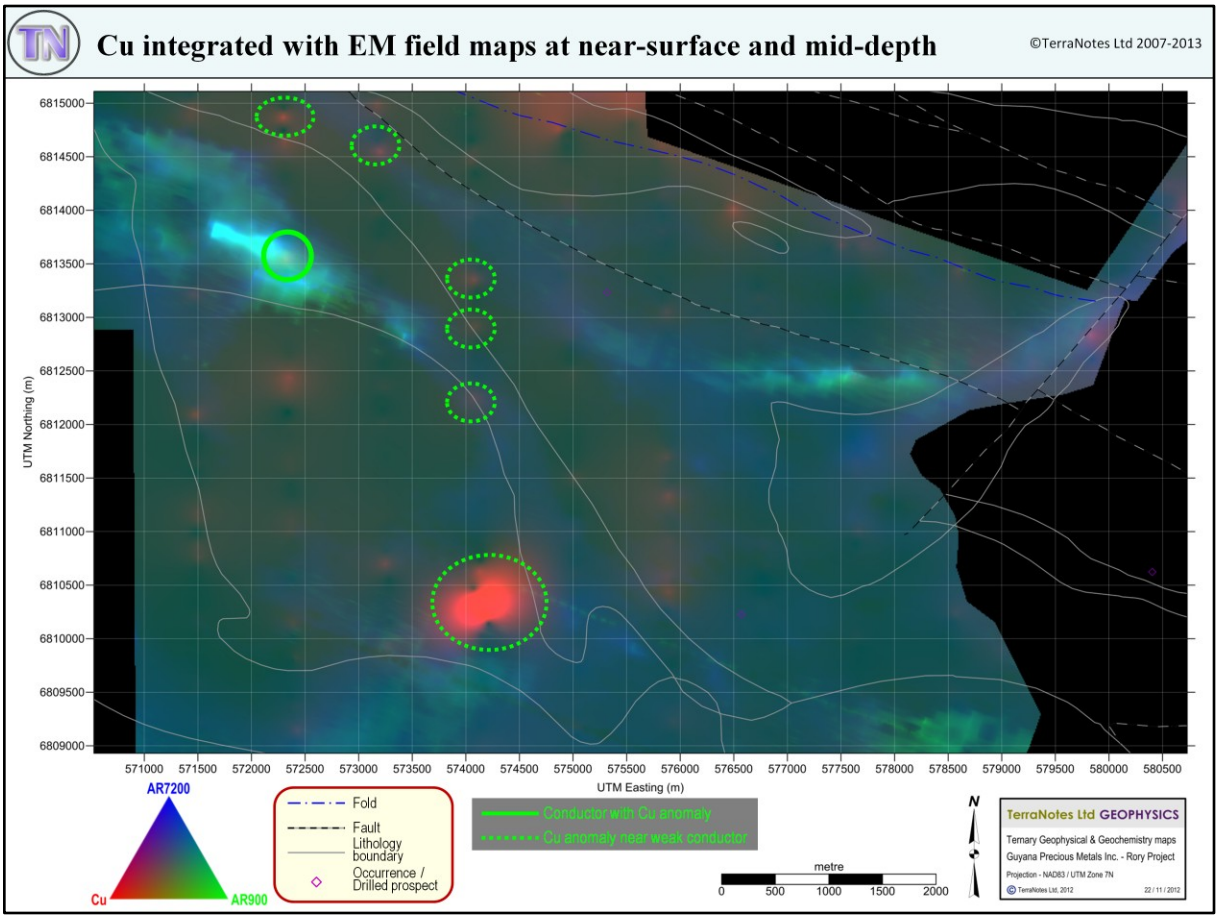


Figure 72. Ternary map of Cu concentrations in soil integrated with near-surface and mid-depth EM. Blue represents the apparent resistivity in the near-surface, green represents the apparent resistivity at mid-depth, and red represents Cu concentrations in the soil. This map is an IHS ternary map where brighter colours indicate the most anomalous zones. The pink diamonds indicate mineral occurrences of YGS. The gray polygons indicate the boundaries of the geological formations. The dashed black lines indicate the faults/shears and the dashed blue lines indicate fold axes.

Main Findings

High Ni concentrations display a stronger relation to conductors than high Cu concentrations. The only significant Cu anomaly occurred within Anomaly B (solid green ellipse).

The dotted green ellipses indicate high Cu concentrations in soil coincident with weak or surficial conductors.

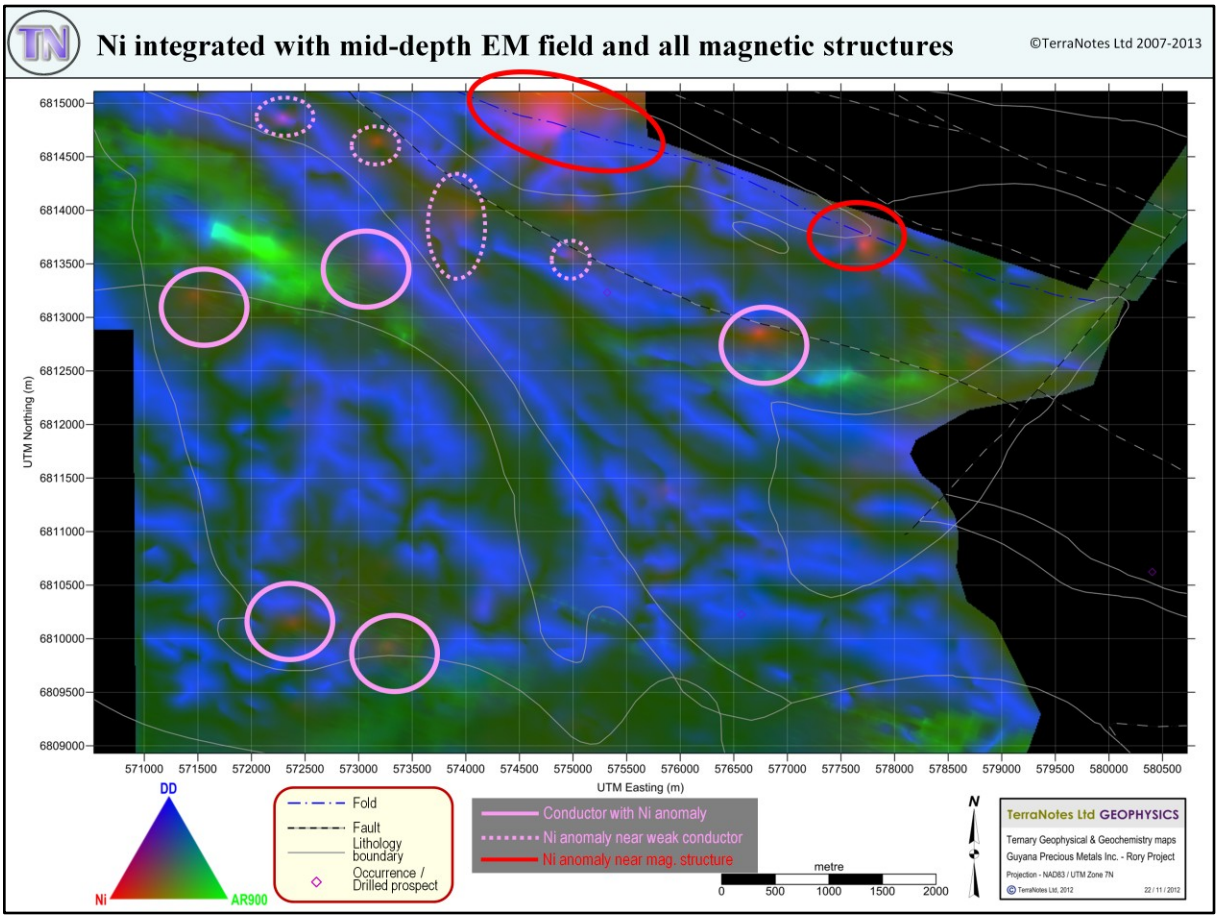


Figure 73. Ternary map of Ni concentrations in soil integrated with mid-depth EM and all magnetic structures. Blue represents all magnetic structures, green represents the apparent resistivity at mid-depth, and red represents Ni concentrations in the soil. This map is an IHS ternary map where brighter colours indicate the most anomalous zones. The pink diamonds indicate mineral occurrences of YGS. The gray polygons indicate the boundaries of the geological formations. The dashed black lines indicate the faults/shears and the dashed blue lines indicate fold axes.

Main Findings

The interpretation of Figure 71 is confirmed in this figure. Anomalies not found in Figure 71 are marked with red ellipses. These occur where there are high Ni concentrations in soil coincident with magnetic structures.

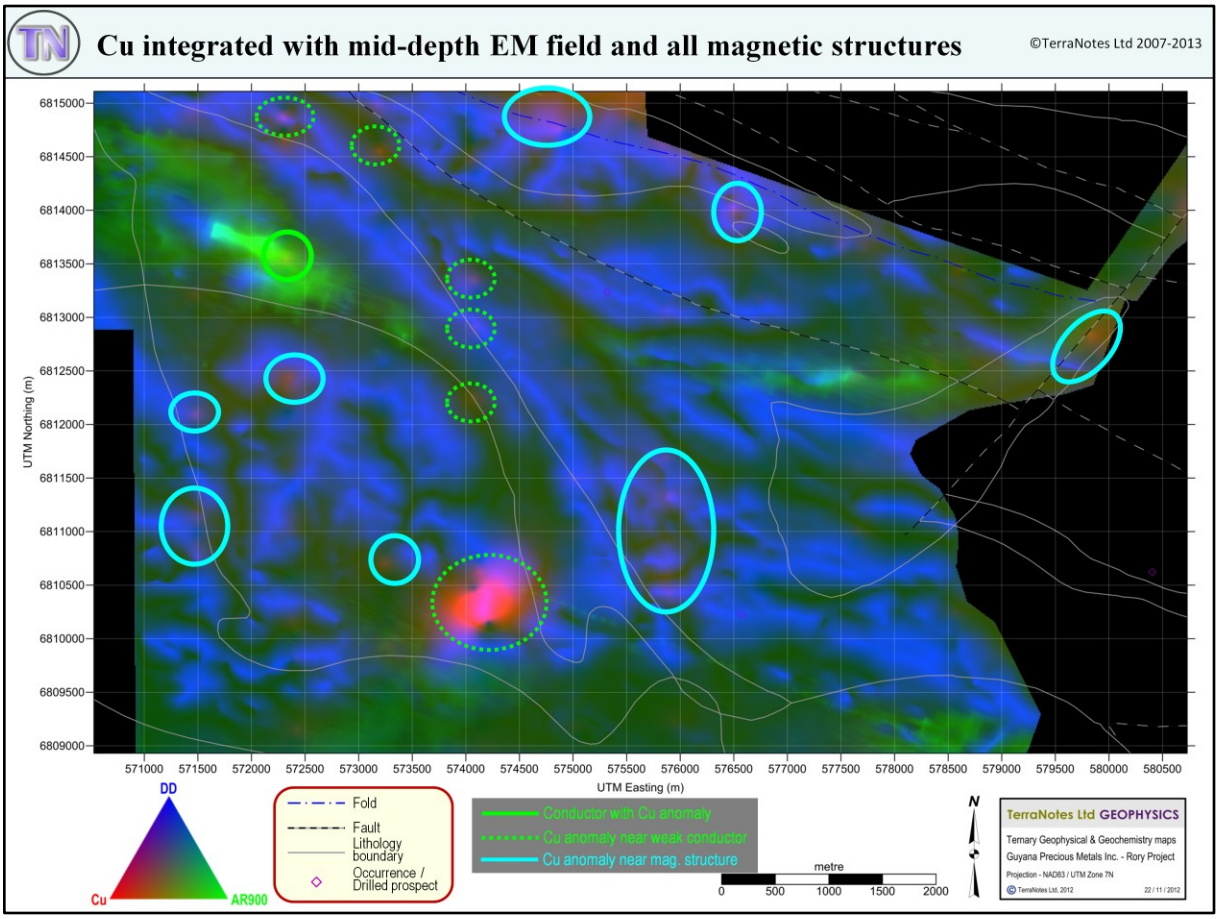
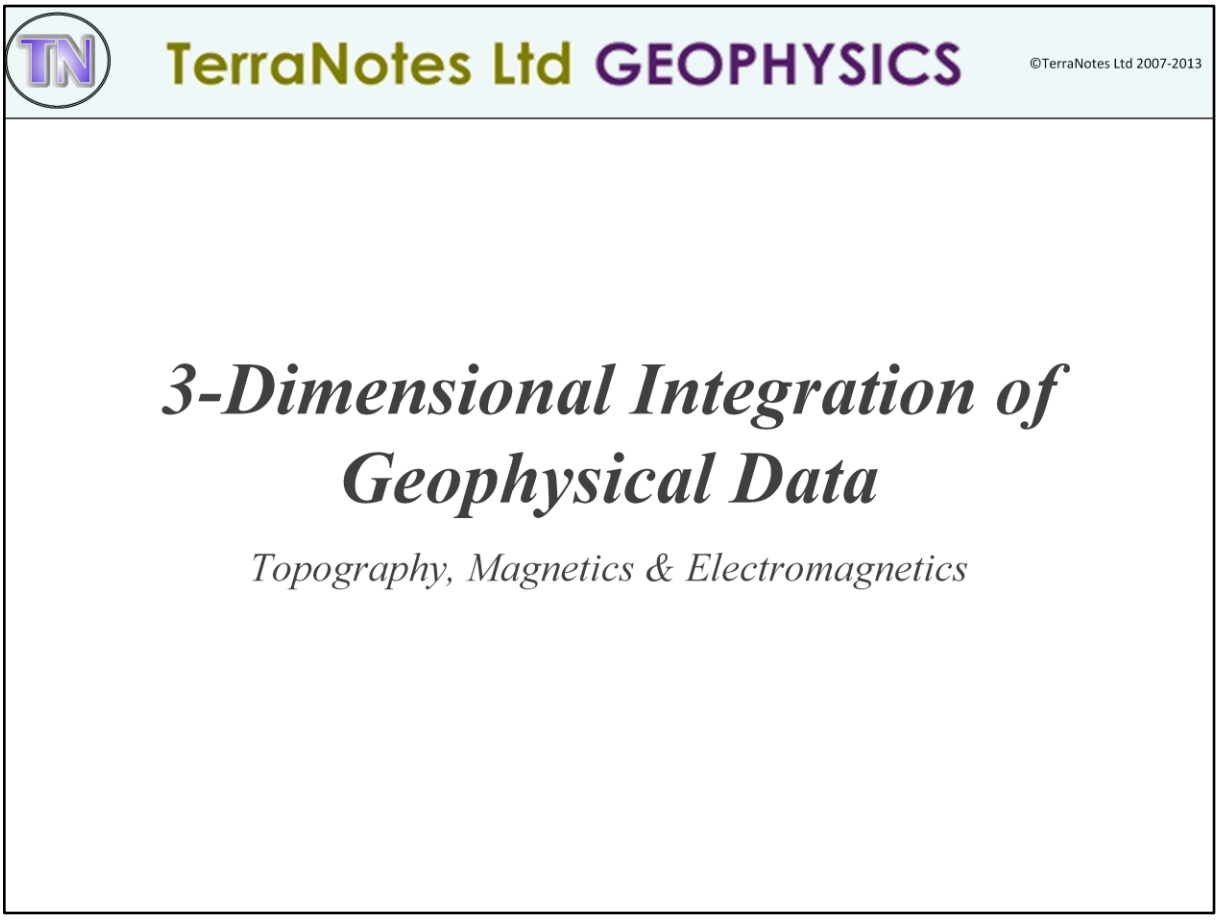


Figure 74. Ternary map of Cu concentrations in soil integrated with mid-depth EM and all magnetic structures. Blue represents all magnetic structures, green represents the apparent resistivity at mid-depth, and red represents Cu concentrations in the soil. This map is an IHS ternary map where brighter colours indicate the most anomalous zones. The pink diamonds indicate mineral occurrences of YGS. The gray polygons indicate the boundaries of the geological formations. The dashed black lines indicate the faults/shears and the dashed blue lines indicate fold axes.

Main Findings

This figure confirms the importance of the green ellipse anomalies that were marked in Figure 72. Cyan ellipses mark the additional high Cu concentrations in soil coincident with magnetic structures.


TerraNotes Ltd GEOPHYSICS
©TerraNotes Ltd 2007-2013
3-Dimensional Integration of Geophysical Data
Topography, Magnetics & Electromagnetics

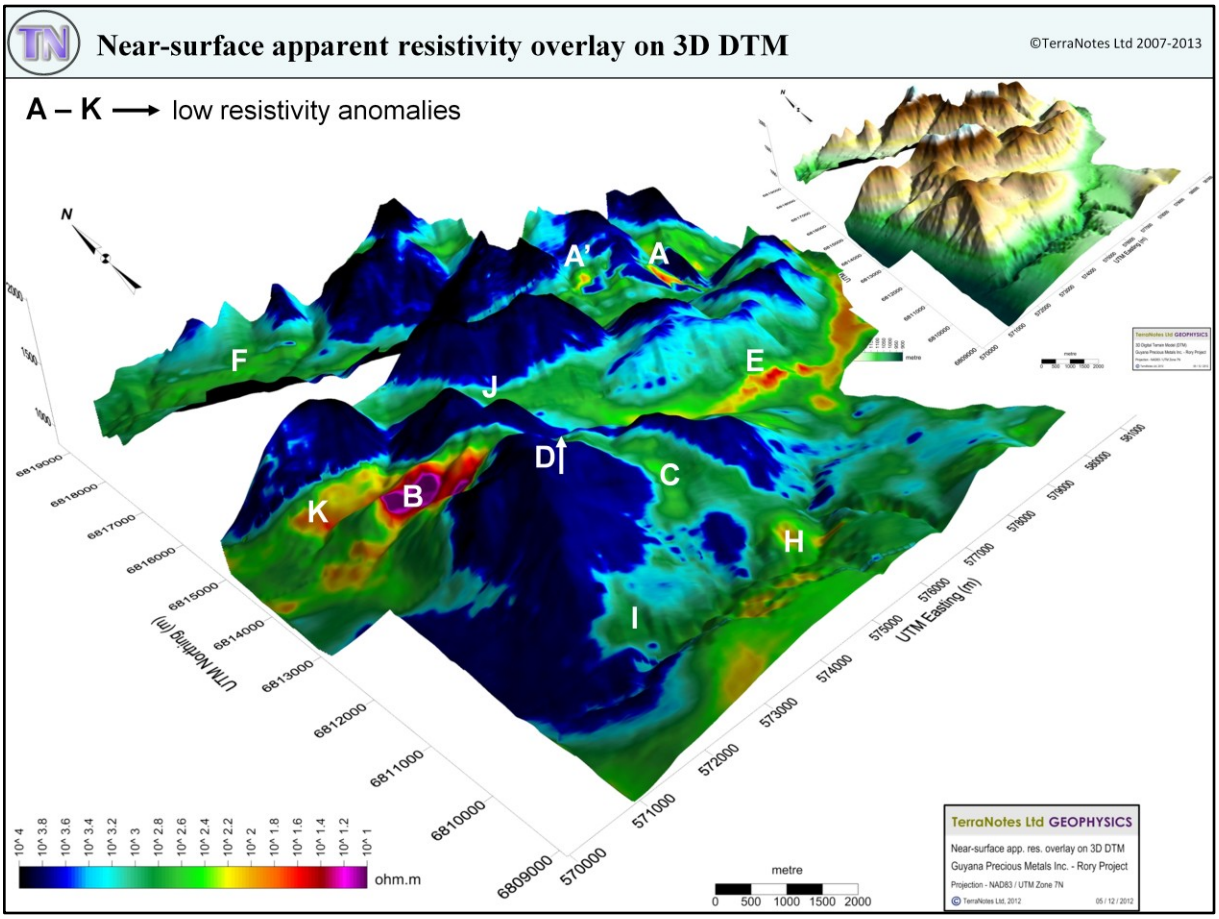


Figure 75. Overlay of near-surface apparent resistivity on the DTM. Warm colours indicate conductive zones, cool colours indicate resistive zones, and the shape is the topographic relief. The original 3D DTM map is shown in the inset map on the top right.

Main Findings

The most conductive zones are located on high topographic features or on their flanks and should not be due to the erosions by rivers, creeks, etc.

The letters indicate the locations of the previously identified conductive anomalies. Please note that Anomaly D is not visible since it is located behind the hill.

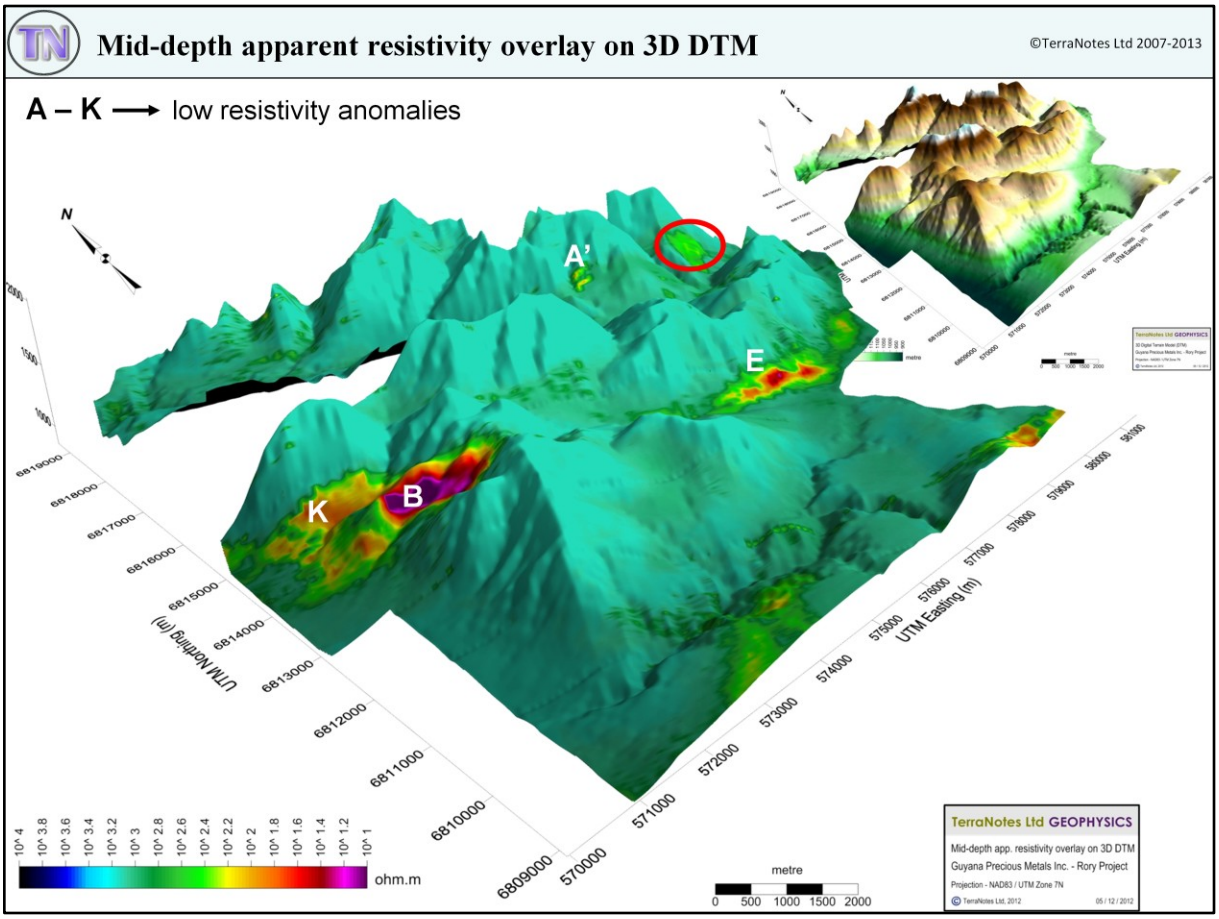


Figure 76. Overlay of mid-depth apparent resistivity on the 3D DTM. Warm colours indicate conductive zones, cool colours indicate resistive zones, and the shape is the topographic relief. The original 3D DTM map is shown in the inset map on the top right.

Main Finding

This map confirms that the most important conductive anomalies (A', B, E, and K) are located on the top or flanks of high topographic features. This indicates that their conductivity source is independent of the superficial effects.

The red ellipse indicates an additional conductive zone outside of the Rory claims to the north of the Wellgreen deposit. The approximate distance from the Wellgreen deposit is 1 km.

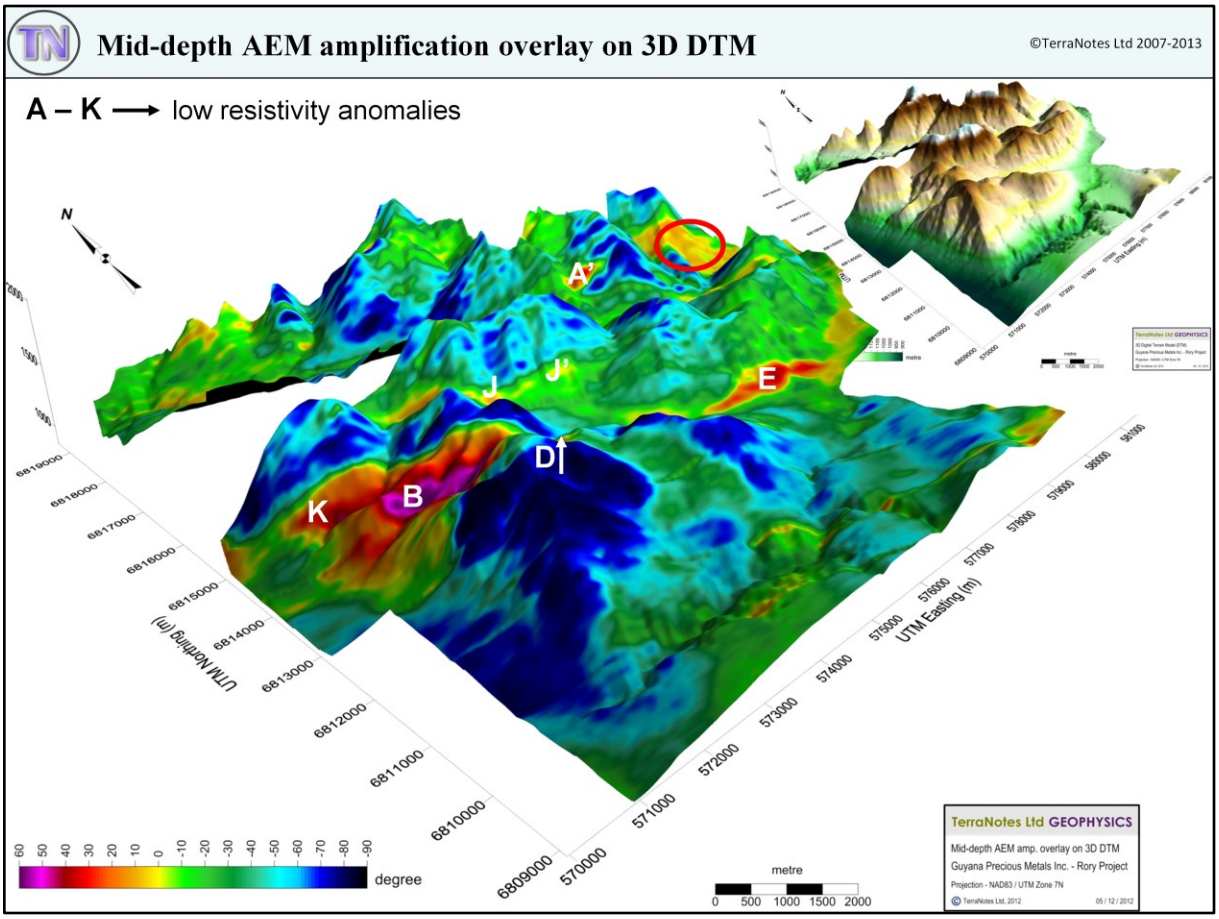


Figure 77. Overlay of mid-depth EM amplification on the 3D DTM. Warm colours indicate conductive zones, cool colours indicate resistive zones, and the shape is the topographic relief. The original 3D DTM map is shown in the inset map on the top right.

Main Findings

This figure is more sensitive to vertical bedrock conductors and it confirms that the strongest bedrock conductors, Anomalies A', B, E, and K are located on the top or flanks of high topographic features.

In addition to the anomalies mentioned above, Anomaly J and the tip of Anomaly D are stronger in the map above. They are also located on the flanks of the high topographic features.

The anomaly marked by the red ellipse still exists.

Anomaly J' is more visible in the map above, and it is also located at the flank of the high topography.

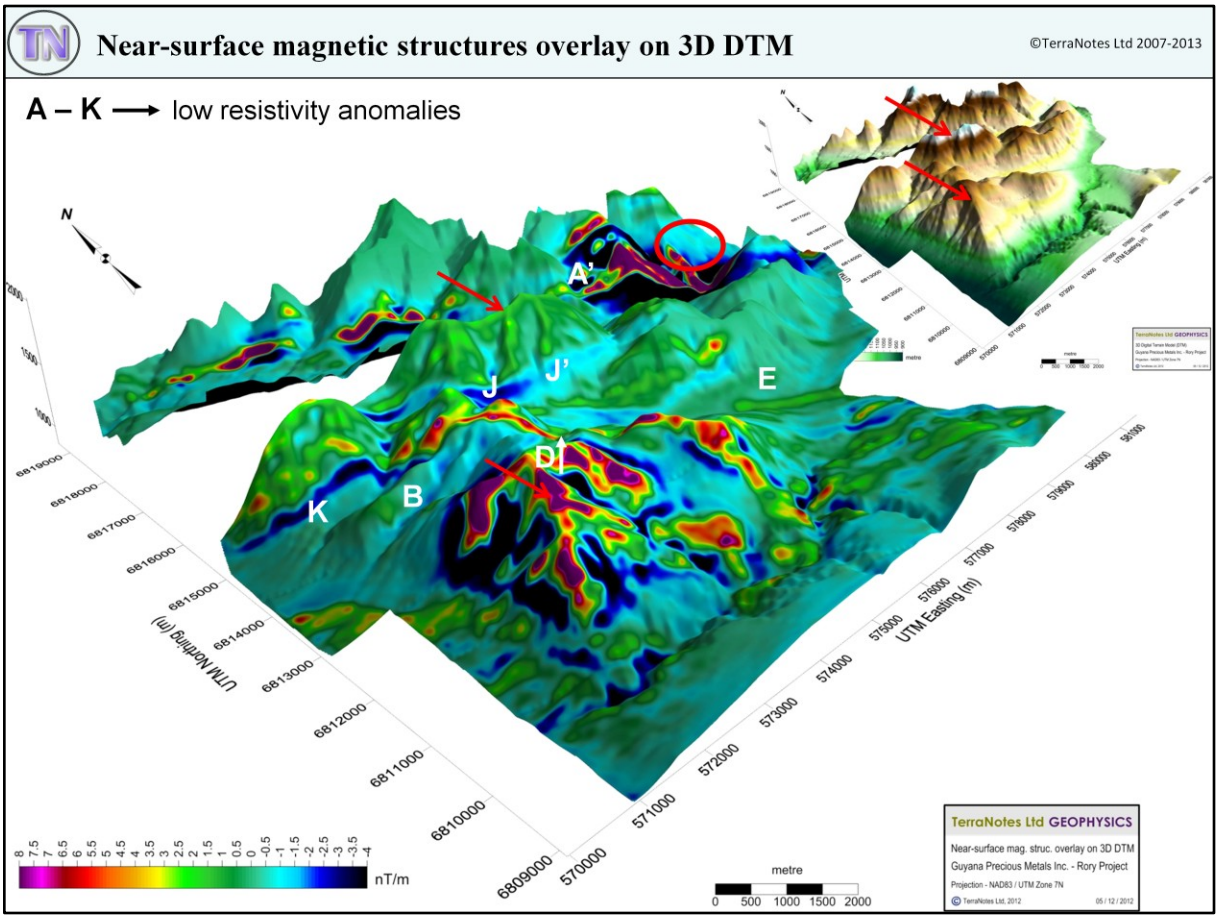


Figure 78. Overlay of near-surface magnetic structures on the 3D DTM. Warm colours indicate high magnetic intensity zones, cool colours indicate low magnetic intensity zones, and the shape is the topographic relief. The original 3D DTM map is shown in the inset map on the top right.

Main Findings

There is a linear relationship between the strongest magnetic structures and high topographic features.

The conductive anomalies are marked on the magnetic structures overlay map. All of the conductive anomalies are associated with either strongly or weakly high magnetic anomalies, except for Anomalies J and J', which are located on a low magnetic trend.

The interpreted gabbro intrusions and the mafic rocks of the Nicolai formation are located on the tops of hills (marked by red arrows).

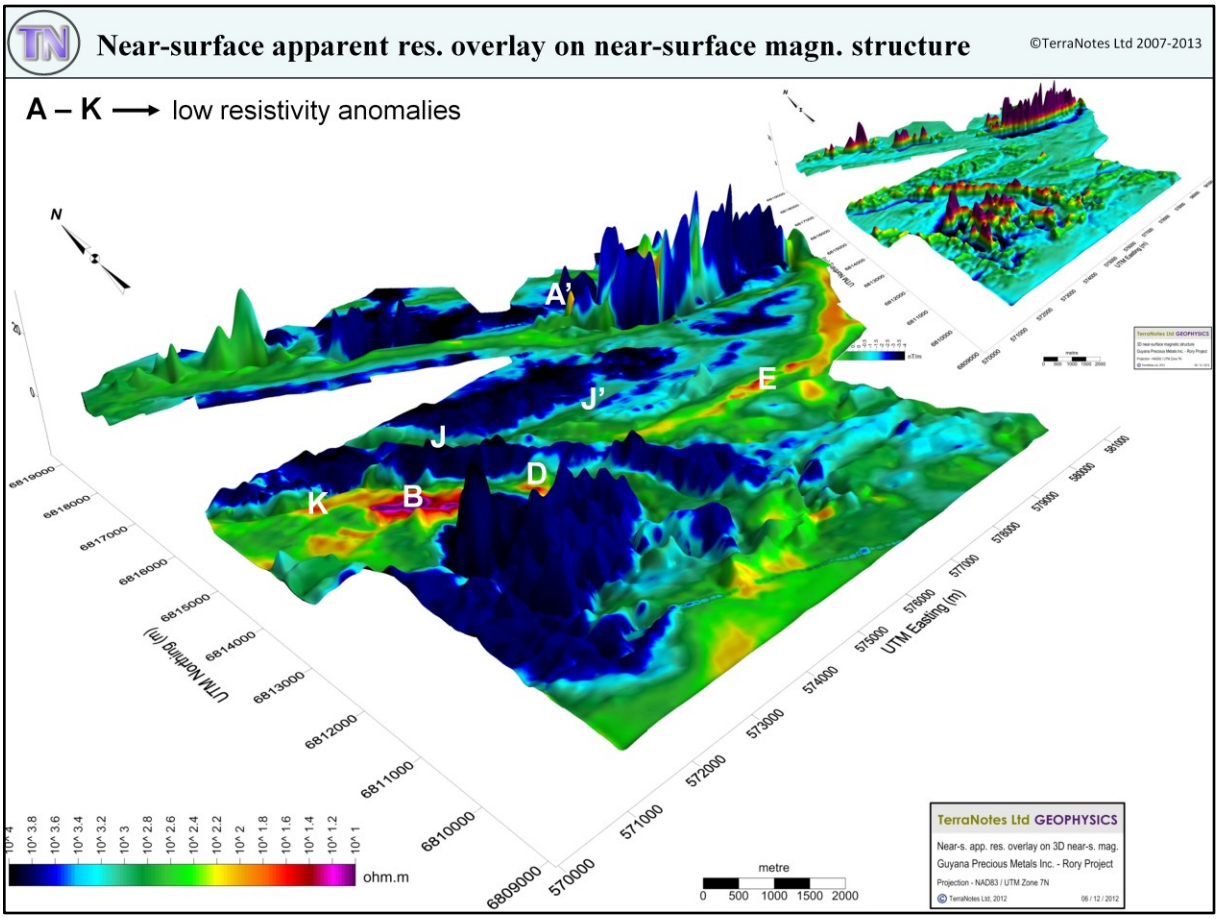


Figure 79. Overlay of the near-surface apparent resistivity on the 3D near-surface magnetic structures. Warm colours indicate conductive zones, cool colours indicate the resistive zones, and the shape represents the relief of the near-surface magnetic structures. The original 3D near-surface magnetic structures map is shown in the inset map on the top right.

Main Findings

This figure is meant to assist in understanding and evaluating the relationship between EM anomalies and near-surface magnetic structures.

Letters mark the previously identified conductive zones. It should be noted that, except Anomaly A', all of the conductive anomalies are located either on the weakly high magnetic zones (B, E, and K) or low magnetic zones (D, J and J').

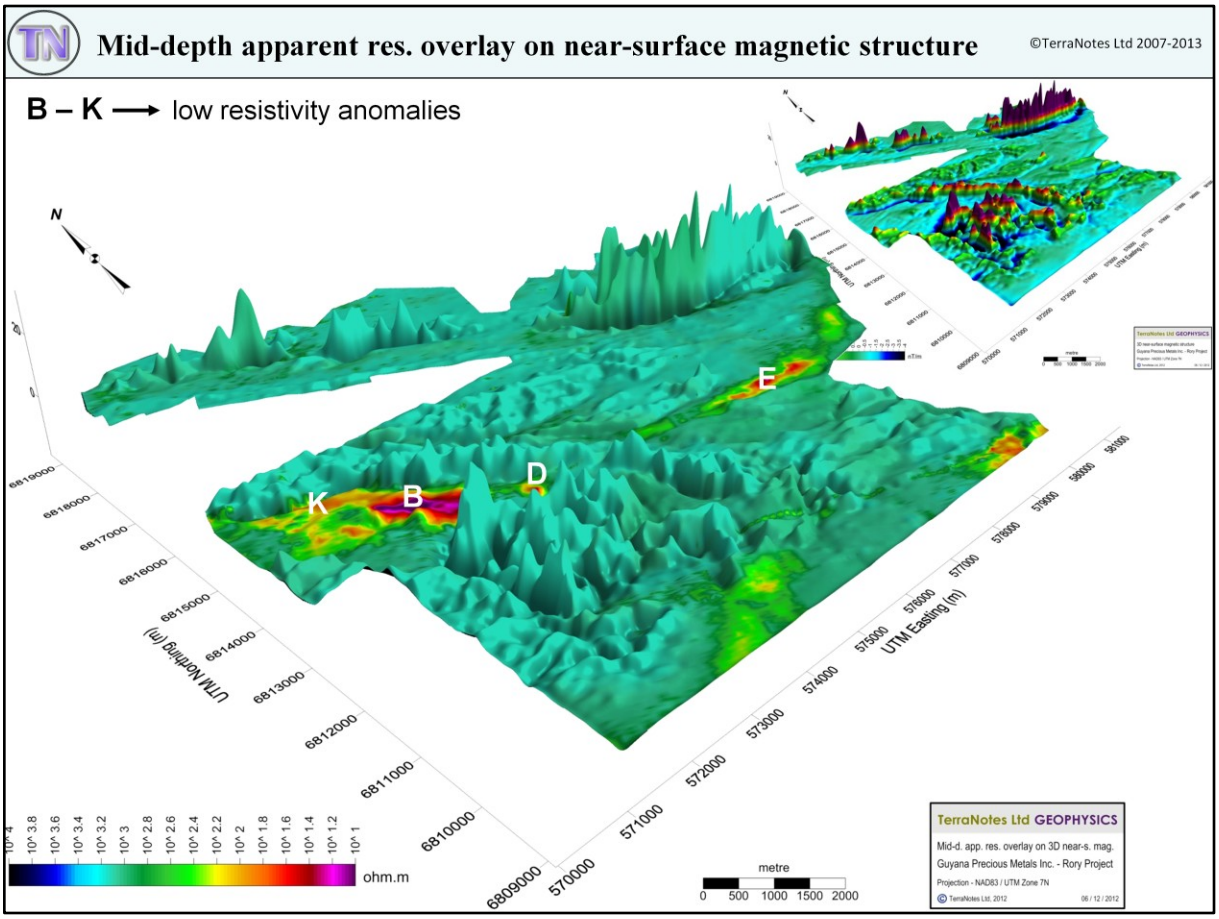


Figure 80. Overlay of mid-depth apparent resistivity on the 3D near-surface magnetic structures. Warm colours indicate conductive zones, cool colours indicate the resistive zones, and the shape represents the relief of the near-surface magnetic structures. The original 3D near-surface magnetic structures map is shown in the inset map on the top right.

Main Findings

The strongest conductive anomalies (B, D, E, and K) are located on weak magnetic structures, the sources of which may occur at greater depths.

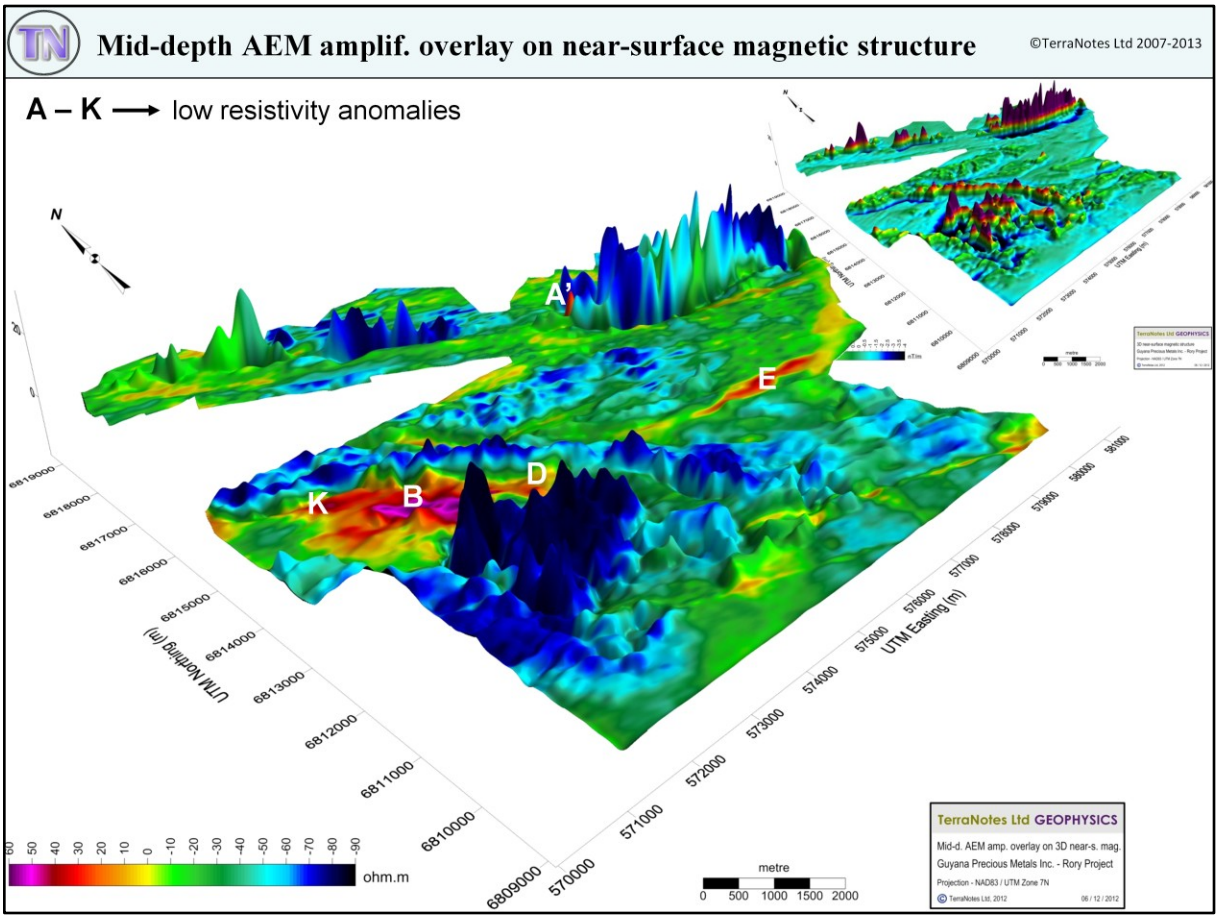


Figure 81. Overlay of mid-depth EM amplification map on the 3D near-surface magnetic structures. Warm colours indicate conductive zones, cool colours indicate resistive zones, and the 3D shape is the relief of the near-surface magnetic structures. The original 3D near-surface magnetic structures map is shown in the inset map on the top right.

Main Findings

This figure confirms the interpretation of the previous figure. Anomaly A' is more visible at the tip of the very strong near-surface magnetic structure.

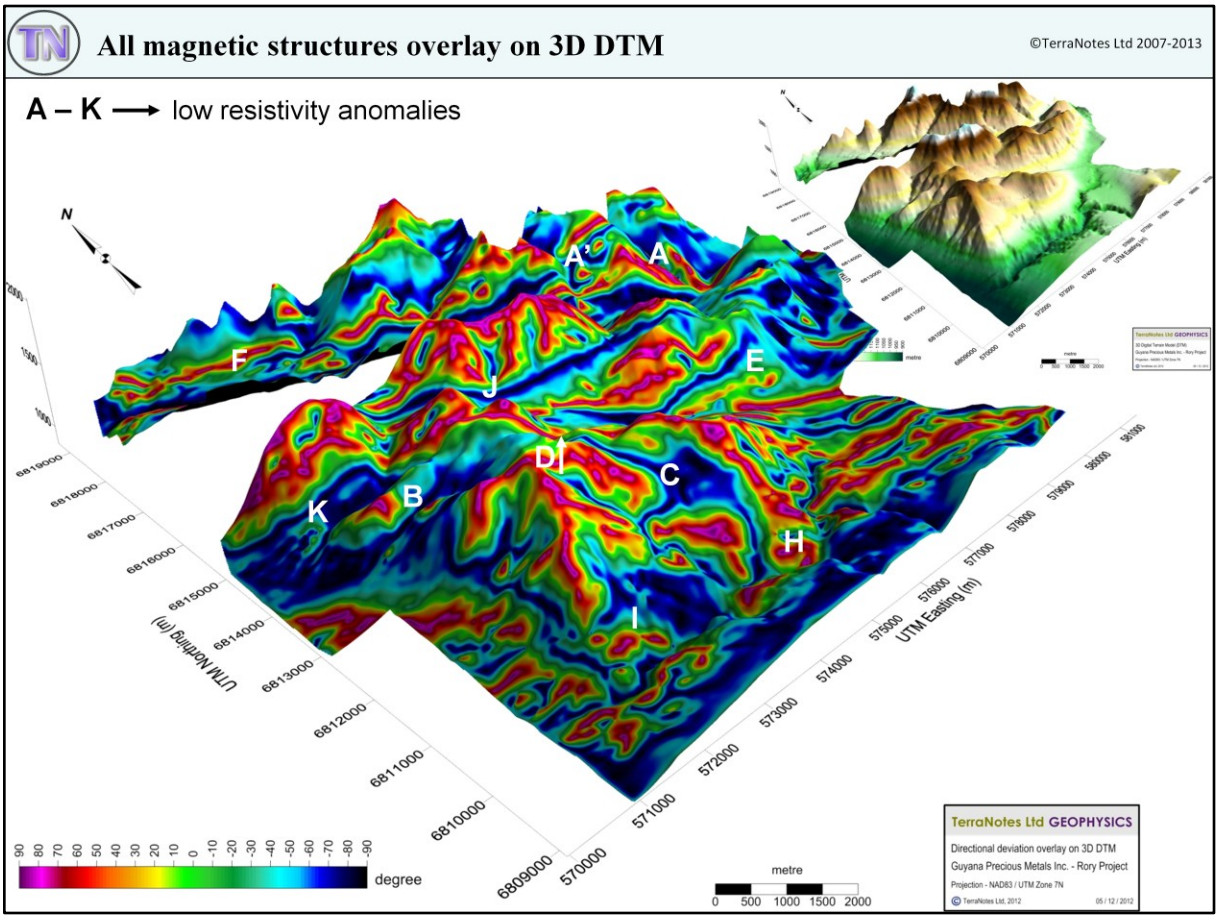


Figure 82. Overlay of all magnetic structures on the 3D DTM map. Warm colours represent conductive zones, cool colours represent resistive zones, and the 3D shape is the topographic relief. The original 3D DTM map is shown in the inset map on the top right of the figure.

Main Findings

Letters mark the conductive anomalies on the all magnetic structures overlay.

Anomalies C, D, and, to some degree, F are located on the low magnetic trends while the remaining anomalies are located on strong magnetic structures. Anomaly K is located on a very weak magnetic structure.

The relationship between EM and magnetic anomalies is explored in the following three figures (83-85).

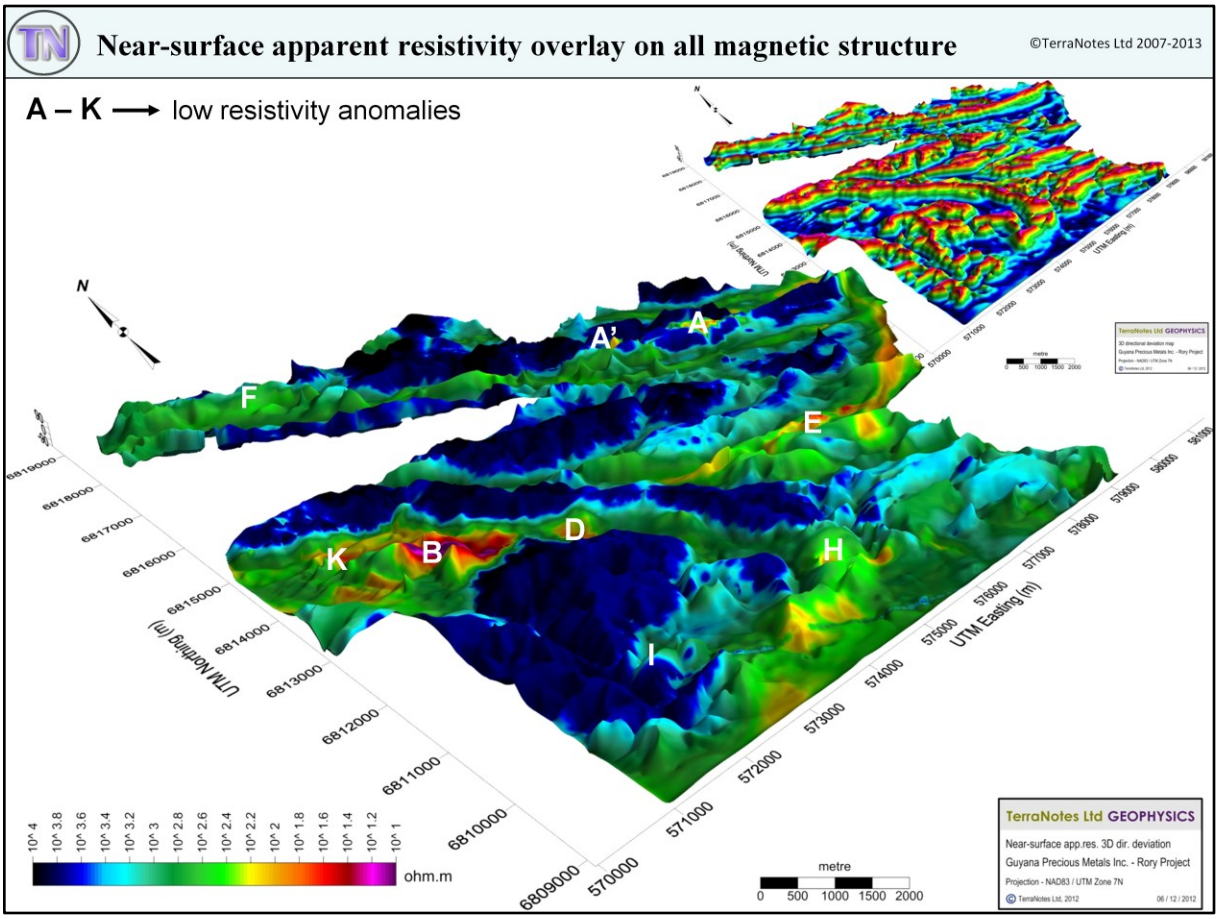


Figure 83. Overlay of near-surface apparent resistivity on the 3D all magnetic structures. Warm colours represent conductive zones, cool colours represent resistive zones, and the 3D shape is the amplified relief of all magnetic structures. The original 3D all magnetic structures map is shown in the inset map on the top right of the figure.

Main Findings

This figure suggests that the strong conductive Anomalies A, A', B, and E are located on strong magnetic structures.

The weaker conductive Anomalies F, H, and I are also located on high magnetic structures.

Anomalies D and K are located on very weak magnetic structures. Anomaly D may even be located on a low magnetic zone.

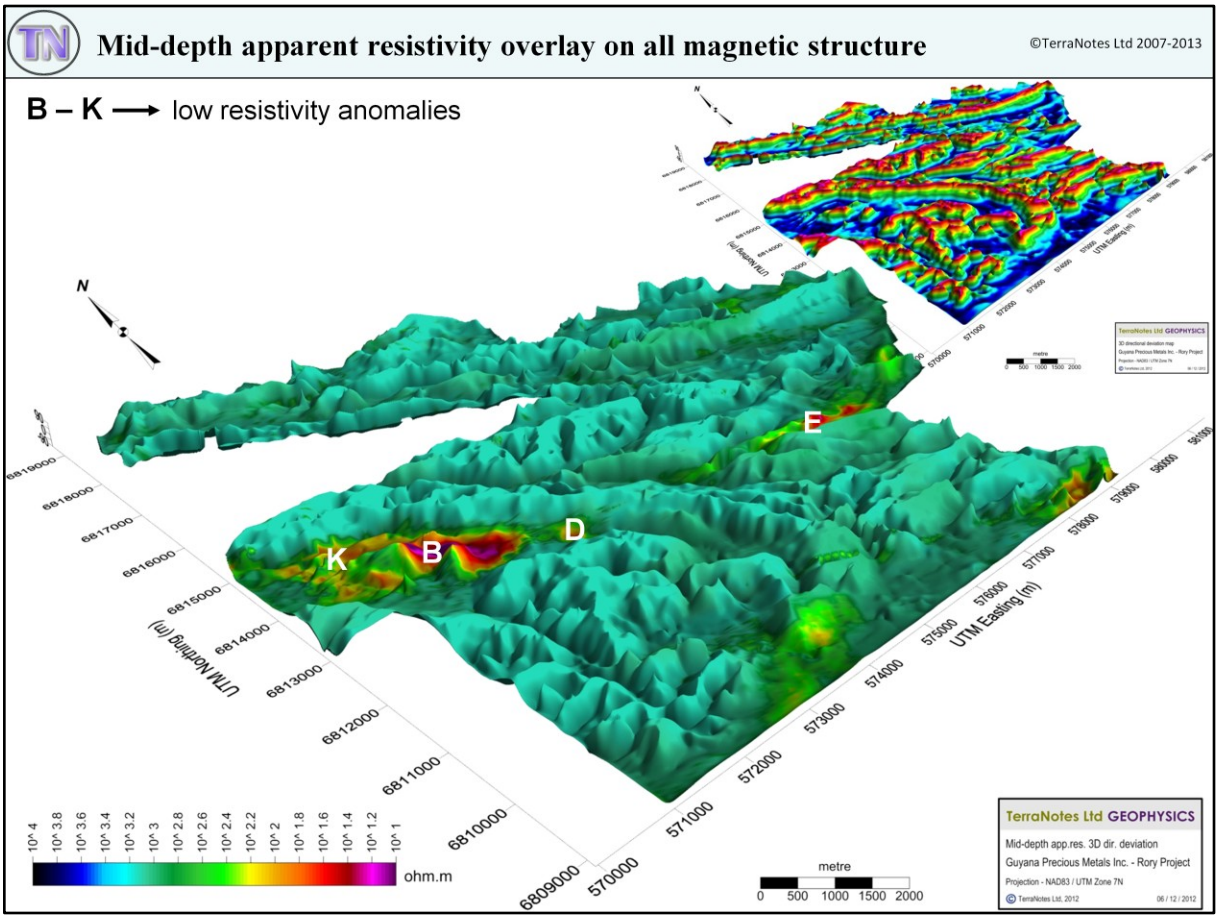


Figure 84. Overlay of mid-depth apparent resistivity on the 3D all magnetic structures. Warm colours represent conductive zones, cool colours represent resistive zones, and the 3D shape represents the amplified relief of all magnetic structures. The original 3D all magnetic structures map is shown in the inset map on the top right of the figure.

Main Findings

The strongest conductors (Anomalies B, D, E ,and K) are located on weak magnetic structures.

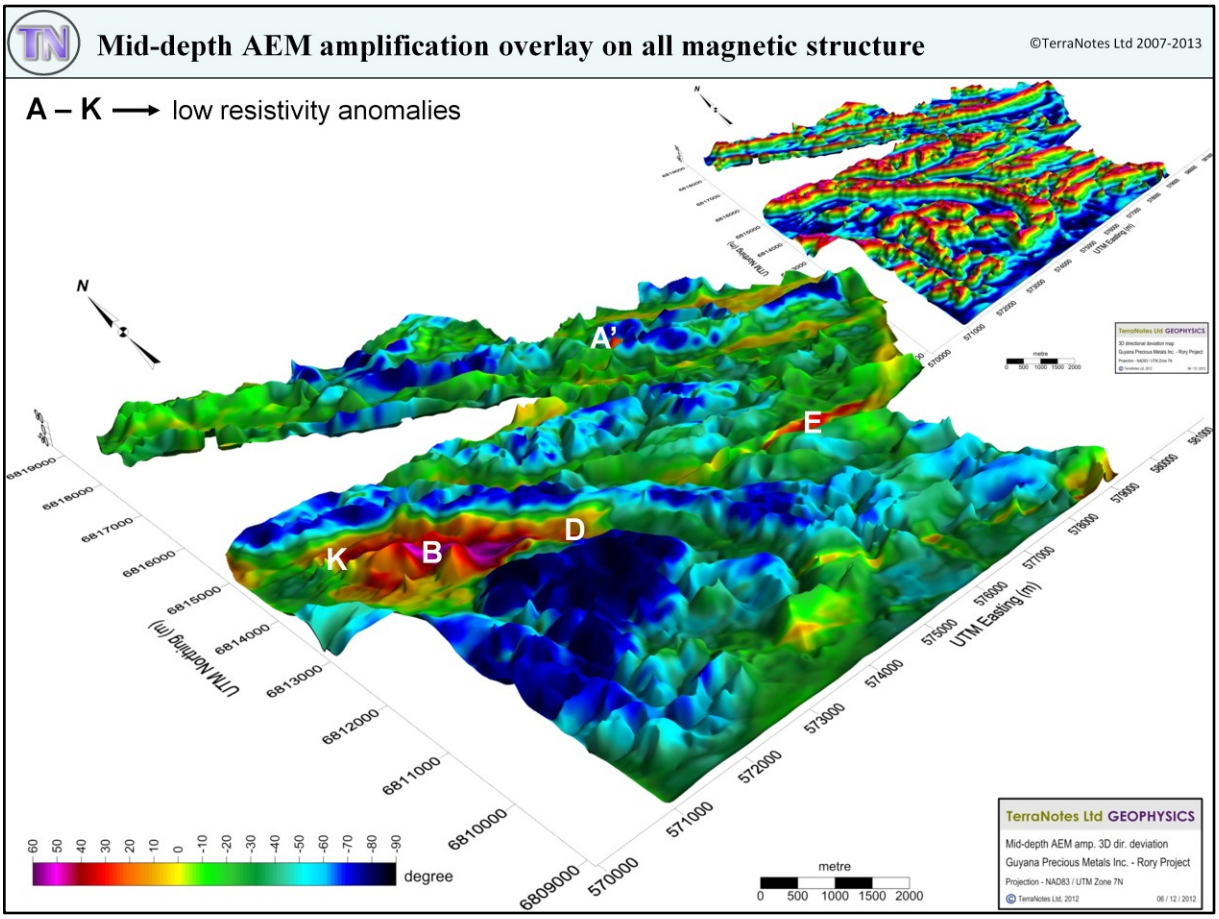


Figure 85. Overlay of mid-depth EM amplification on the 3D all magnetic structures. Warm colours represent conductive zones, cool colours represent resistive zones, and the 3D shape is the amplified relief of the all magnetic structures. The original 3D all magnetic structures map is shown in the inset map on the top right of the figure.

Main Findings

This figure confirms the interpretation of the previous figure. The strongest conductors (B, D, E and K) are located on the weak magnetic structures.

Anomaly A' is more visible at the tip of the high magnetic structure.



TerraNotes Ltd GEOPHYSICS

©TerraNotes Ltd 2007-2013

Analysis and Interpretation of selected profiles

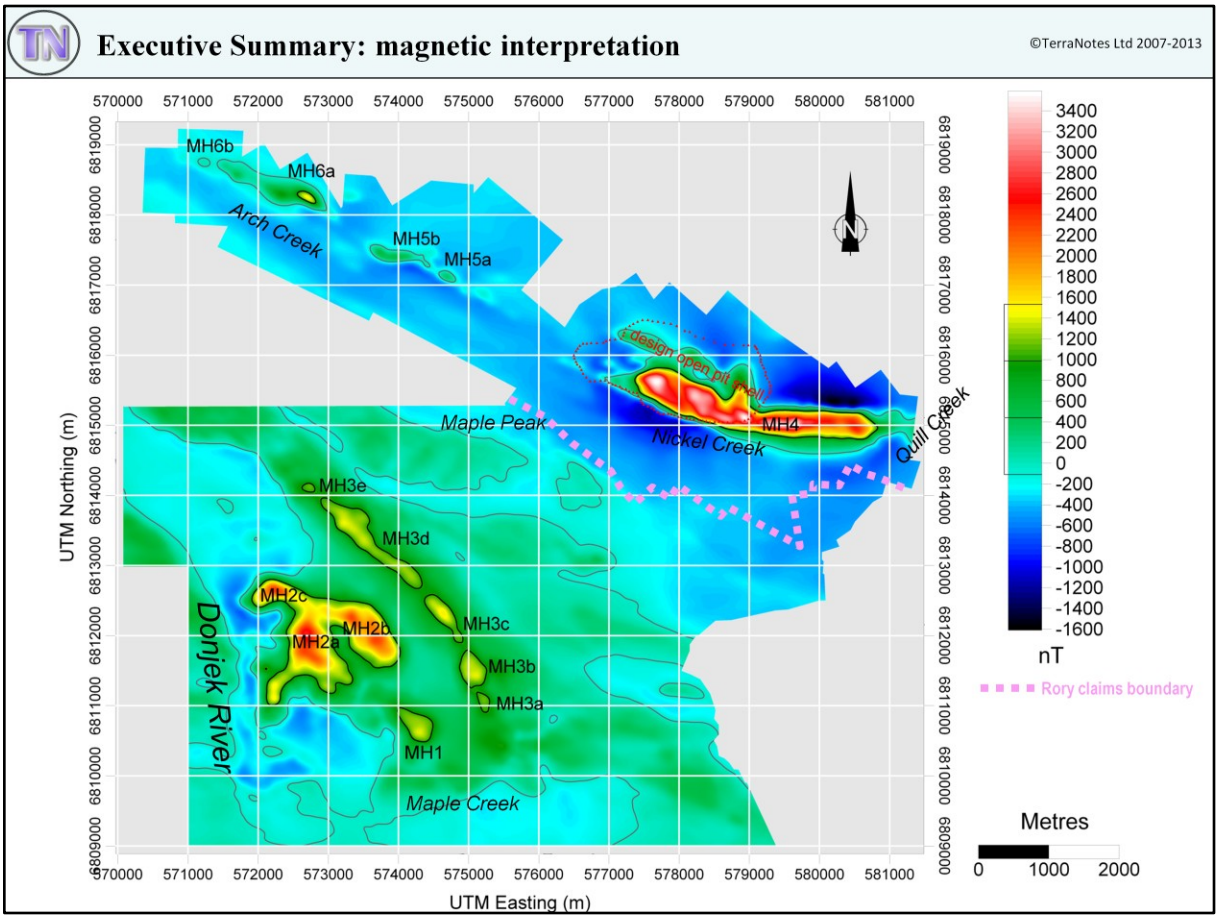


Figure 86. Identification of magnetic highs on the RTP-RMI map.

As most Cu-Ni sulphide mineralization/deposits in southwest Yukon are related to basalt and gabbro intrusion, which are physically characterized by high magnetic anomalies, identification and delineation of meaningful magnetic highs is crucial in targeting potential zones of interest in geophysical interpretation. In Rory and Wellgreen, the magnetic highs are identified mostly based on the RTP-RMI values equal to or higher than 1000 nT. Three (3) magnetic highs are outlined in Rory and another three (3) in Wellgreen.

The identities and centre coordinates of the magnetic highs and their sub-regions are as follows:

MH-1:	(574298E, 6810654N)	
MH-2a:	(572724E, 6811922N)	
MH-2b:	(573603E, 6812065N)	
MH-2c:	(572233E, 6812637N)	
MH-3a:	(575219E, 6811042N)	
MH-3b:	(575076E, 6811513N)	
MH-3c:	(574626E, 6812331N)	
MH-3d:	(573358E, 6813599N)	
MH-3e:	(572703E, 6814110N)	
MH-4:	(578941E, 6815112N)	(in Wellgreen)
MH-5a:	(574687E, 6817137N)	(in Wellgreen)
MH-5b:	(573951E, 6817423N)	(in Wellgreen)
MH-6a:	(572662E, 6818303N)	(in Wellgreen)
MH-6b:	(571640E, 6818650N)	(in Wellgreen)

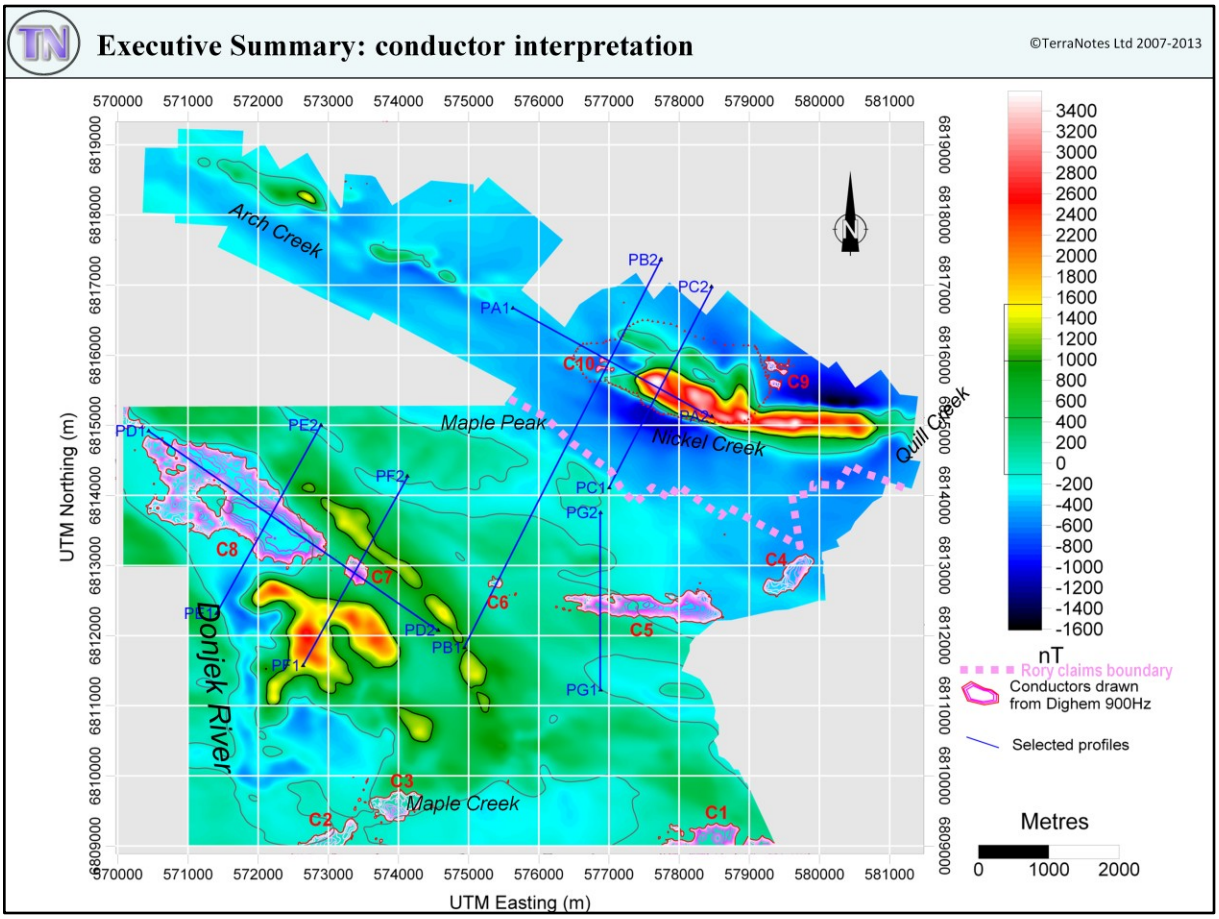


Figure 87. Identification of DIGHEM conductors on the low frequency apparent resistivity map.

The conductive anomalies in Rory and Wellgreen are almost in agreement with the magnetic trends. This observation may suggest that the conductors are related to bedrock rather than conductive overburden. The bedrock conductors are mainly caused by sulphidization, which makes them targets in Cu-Ni-PGE exploration. However, there are some areas where high-frequency apparent resistivity calculations appear to be strongly influenced by conductive materials that follow the local terrain aspects. Thus, deep conductors are mainly identified and outlined using DIGHEM low-frequency apparent resistivity values equal to or less than 300 Ω·m. Eight (8) conductors are identified and outlined in Rory and two (2) in Wellgreen.

The identities and centre coordinates of the identified conductors are as follows:

C1: (578511E, 6809120N)

C2: (573030E, 6809099N)

C3: (573971E, 6809570N)

C4: (579575E, 6812801N)

C5: (577530E, 6812413N)

C6: (575382E, 6812740N)

C7: (573378E, 6812903N)

C8: (572110E, 6813599N)

C9: (579370E, 6815746N) (in Wellgreen)

C10: (576916E, 6815848N) (in Wellgreen)

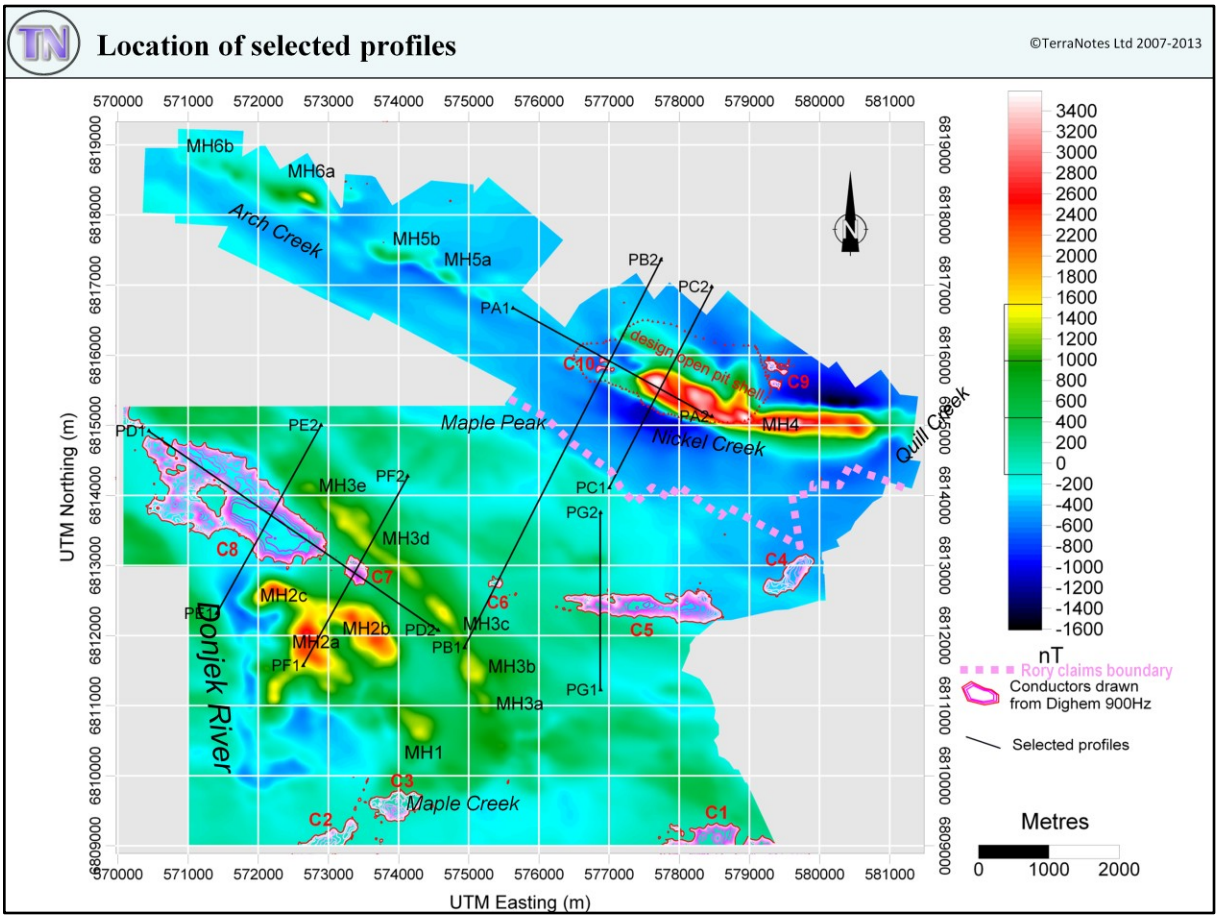


Figure 88. Location of selected profiles. Black lines indicate the selected profiles overlaid on the RTP-RMI map for further analyses. Pink to purple contours indicate the conductive zones that have less than 300 Ω·m apparent resistivity at the lowest frequency.

Main Findings

Profiling analysis aims to examine local magnetic and resistivity features as well as terrain situations which may relate to underlying Ni-Cu PGE mineralization/deposits. Seven (7) profiles are selected for this purpose: Profiles A, B, and C are located in Wellgreen and Profiles B, D, E, F, and G are located in Rory. All the profiles cross zones which are meaningful geophysically and are potential zones of Cu-Ni-PGE mineralization/deposits. Please note that Profile B crosses both Wellgreen and Rory allowing correlative analysis of local geophysical features between a known Wellgreen conductive zone (Conductor-10) and Rory's Conductor-6.

The seven profile' identities and their start/end coordinates are as follows:

Profile A (A1-A2): (575631E, 6816672N) – (578466E, 6815127N)
Profile B (B1-B2): (574940E, 6811830N) – (577739E, 6817361N)
Profile C (C1-C2): (577005E, 6814110N) – (578461E, 6816977N)
Profile D (D1-D2): (570440E, 6814920N) – (574565E, 6812077N)
Profile E (E1-E2): (571407E, 6812316N) – (572895E, 6815003N)
Profile F (F1-F2): (572639E, 6811573N) – (574127E, 6814275N)
Profile G (G1-G2): (576879E, 6811226N) – (576879E, 6813755N)

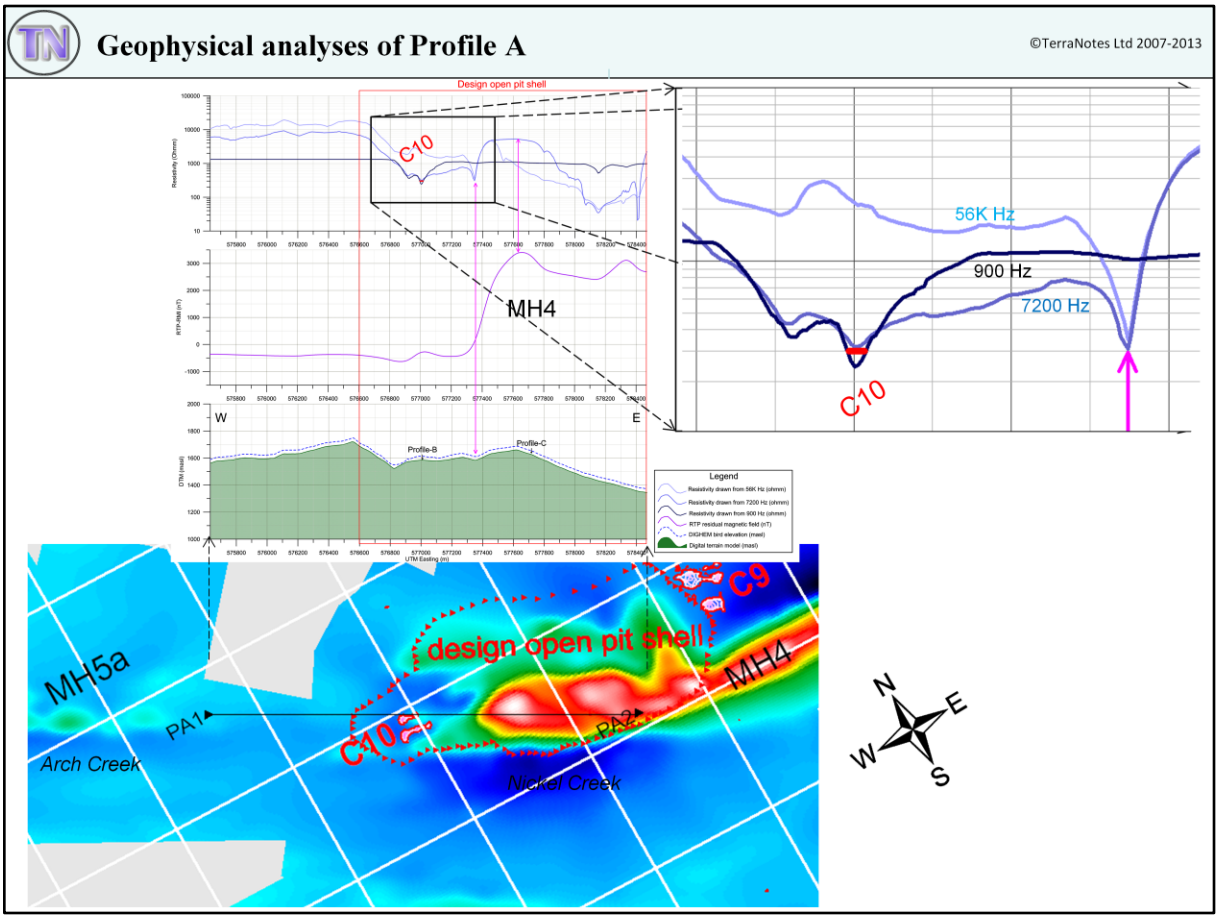


Figure 89. The main image is the DTM, RTP-RMI, and apparent resistivity values along Profile A. The bottom image is the RTP RMI map rotated in agreement with Profile A. The inset image on right panel is the zoomed DIGHEM resistivity curves in the vicinity of C10, which was also shown as Anomaly A'.

Main Findings

The deposit in the Wellgreen zone is associated with a magnetite-rich ultramafic intrusion (MH4) which occurs in its basal contact with sedimentary Skolai Formation.

Magnetic simulation along the profile reveals that MH4 appears outcropped in the zone and slightly dipping south and southwest.

It is inferred that the main deposit occurs on the northern flank of MH4.

Areas of the Wellgreen mineralization/deposit feature high magnetic intensity.

The bottom panel shows two bedrock conductors (C9 and C10) in the northeast and west of the ultramafic zone, both trending in the WSW-ENE direction.

The lengths of both C9 and C10 are less than 450m (see bottom panel).

In the west, the apparent resistivity decreases with frequency and, therefore, depth. In the east (on MH4), 900Hz apparent resistivity is higher than 7200 Hz, which indicates a resistive bedrock at depth as is expected for an ultramafic intrusions.

Areas of mineralization/deposit may or may not be conductive in terms of 900Hz resistivity, because the susceptibility effect of ultramafic rocks may artificially increase the resistivity (as previously discussed).

The lower resistivity of the high frequency channels immediately to the east of C10 (see pink arrow) is coincident with the local terrain low (possibly a valley), indicating that it is a surficial conductor.

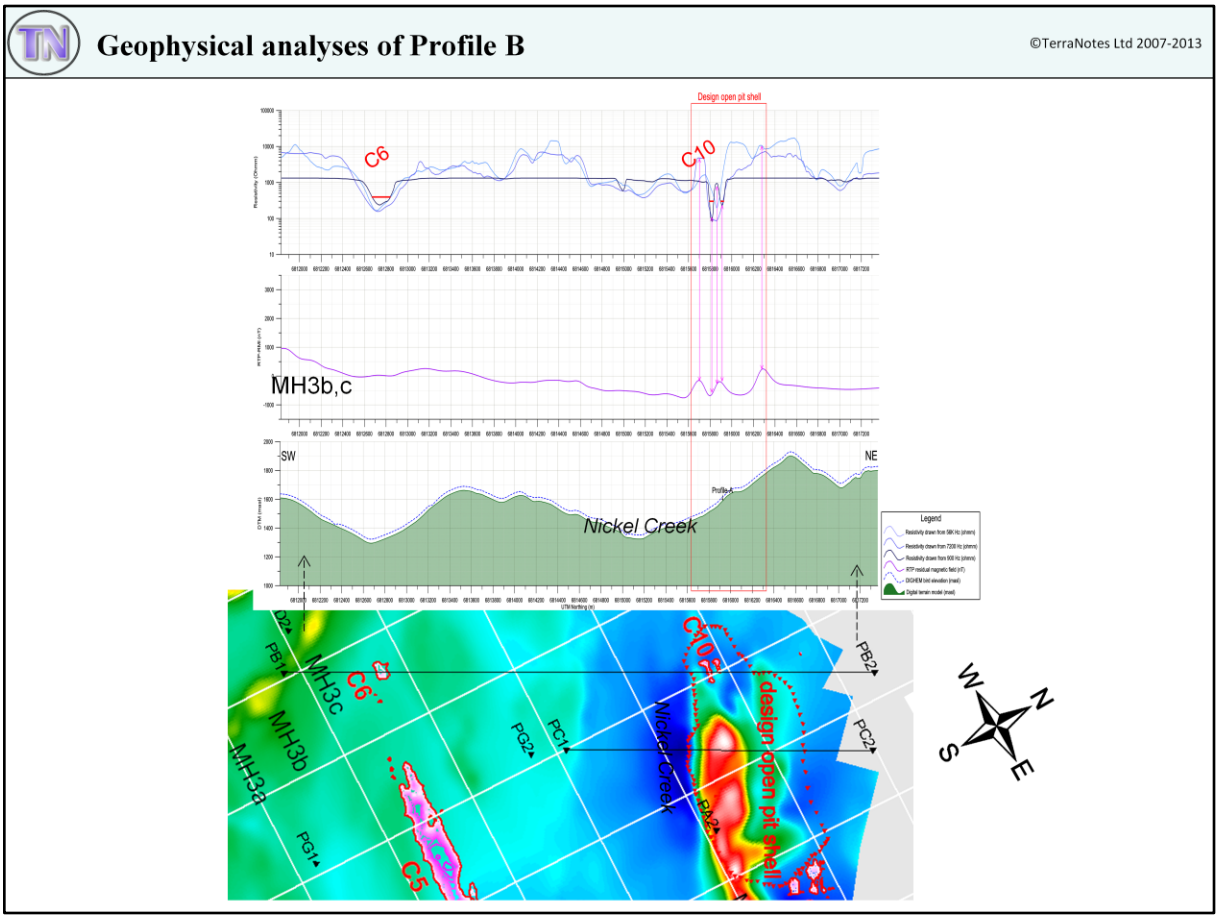


Figure 90. The main image is the DTM, RTP-RMI, and apparent resistivity values along Profile B. The inset image is the RTP-RMI map rotated in agreement with the profile.

Main Findings

C10 is situated in the middle of the slope of a high topographic feature and is, due to this, probably not surficial.

C10 is located in an area which features two weak magnetic peaks. These are the western extensions of MH4 (ultramafic rock).

C6 in Rory is situated close to the bottom of an anonymous creek.

C6 is located in a flat magnetic background; the magnitude of which is approximately the same as the magnetic peaks of C10.

C10 and C6 are located in two different magnetic units.

(continued in the following figure)

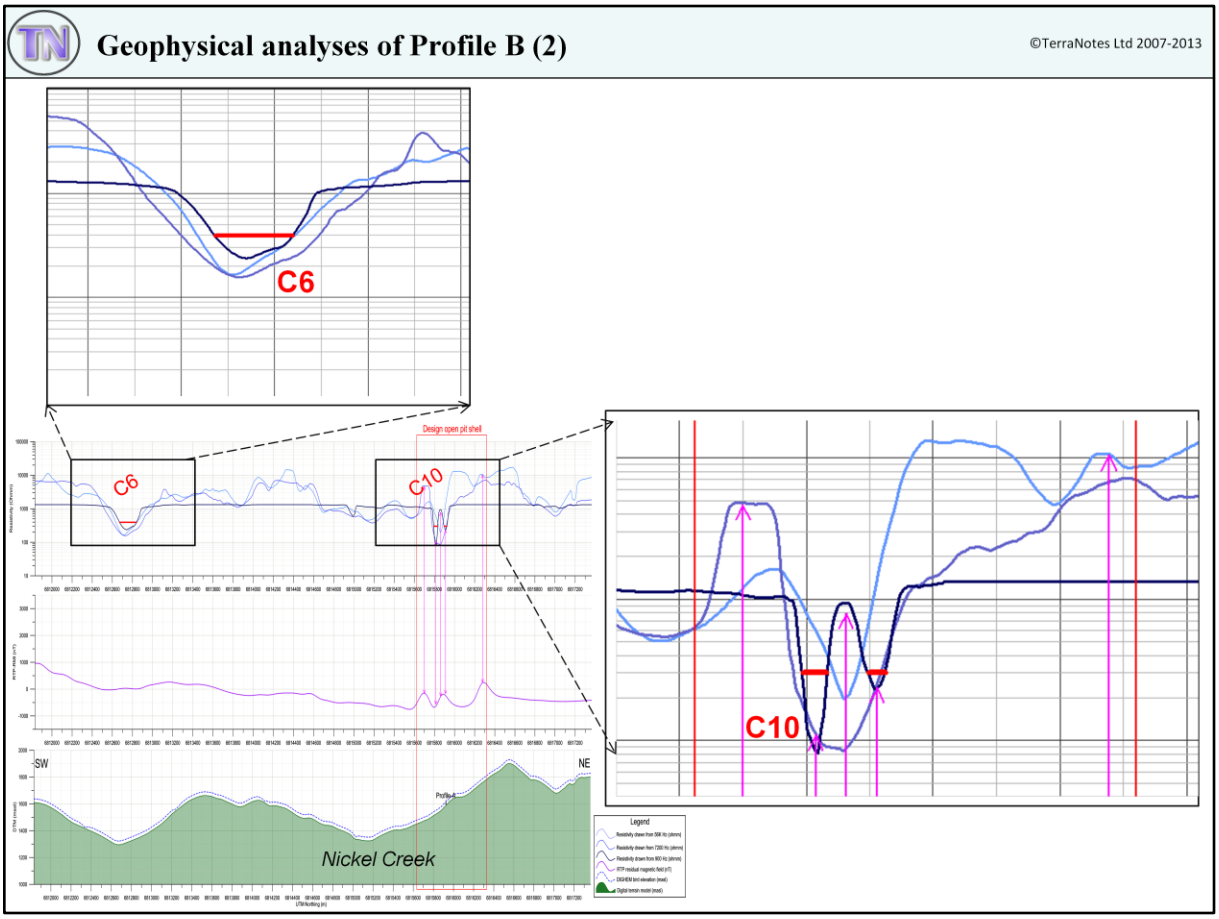


Figure 91. The main image is the DTM, RTP-RMI, and apparent resistivity values along Profile B (as seen in figure 90). The inset image on top is the zoomed resistivity curves of C6. The inset image on right panel is the zoomed resistivity curves of C10;

Main Findings (Cont'd)

The irregular shapes of all three resistivity curves at C10 suggest geo-electrical complexity, particularly at greater depth.

Along the profile, 56K/7200/900Hz resistivity values show no consistency, which suggests C10 is probably a vertical bedrock conductor and not a stratified conductor.

There appears to be a correlation between the local magnetic peaks and resistivity valleys. Since DIGHEM resistivity may be strongly influenced by high magnetization in magnetite-rich area, the cause of the correlation remains unknown.

For C6, apparent resistivity is greatest in the 900Hz channel and lowest in the 7200Hz channel. This suggests a conductance-stratified model and a surficial conductor.

The first, fourth, and fifth pink arrows on the right panel indicate the local magnetic highs. The fourth pink arrow is associated with the low resistivity, indicating a sulphide mineralization.

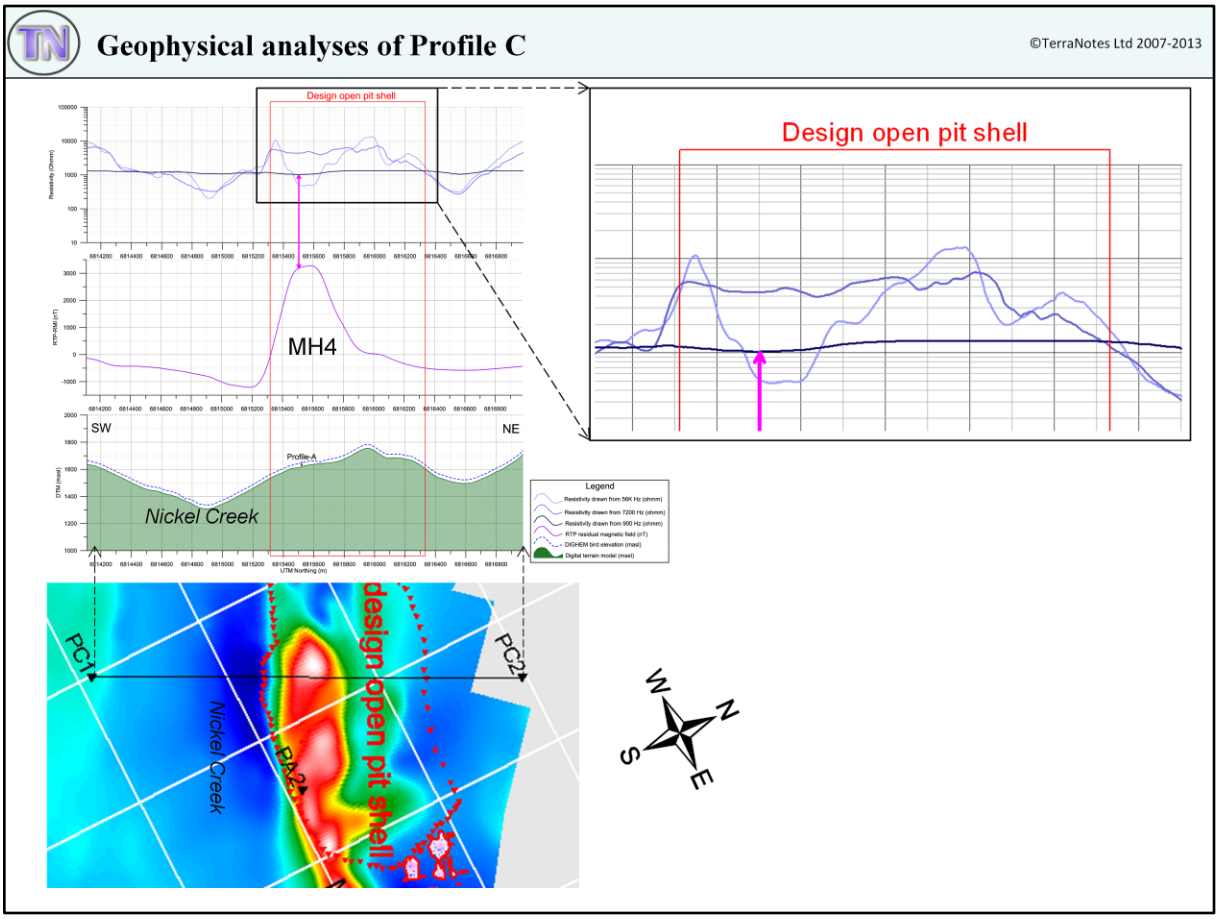


Figure 92. The main image is the DTM, RTP-RMI, and apparent resistivity values along Profile C. The image at bottom is the RTP-RMI map rotated in agreement with Profile C. The inset image on right panel is the zoomed DIGHEM resistivity curves in the range of Wellgreen "design open pit shell" (see Prophecy Platinum Corp's website).

Main Findings

Profile C is selected perpendicular to the trend of the MH4 to present its full sectional shape. The shape of MH4 suggests that it is slightly dipping to the south. Magnetic simulation indicates that it is largely outcropped.

The 900Hz resistivity features a very weak low in the range of the MH4 peak, whereas the 56KHz resistivity yields a conductive anomaly, suggesting that surficial materials may be enriched with conductive materials such as clay.

No bedrock conductor can be identified along the profile. This indicates that the sulphide mineralization/deposits may not always be bedrock conductors. This can be understood and interpreted, for example, in the case that the mineralization/deposit appears disseminated in the rocks.

Alternatively, high susceptibility in this ultramafic zone may also cause an increase in the calculated resistivity of the frequency domain EM data, which masks the underlying bedrock conductors. This phenomenon (susceptibility effect) was observed approximately 1 km east of Profile C, in the vicinity of PA2 (see bottom panel). Hence, deep penetrating time-domain EM data should be used to image these possible hidden bedrock conductors.

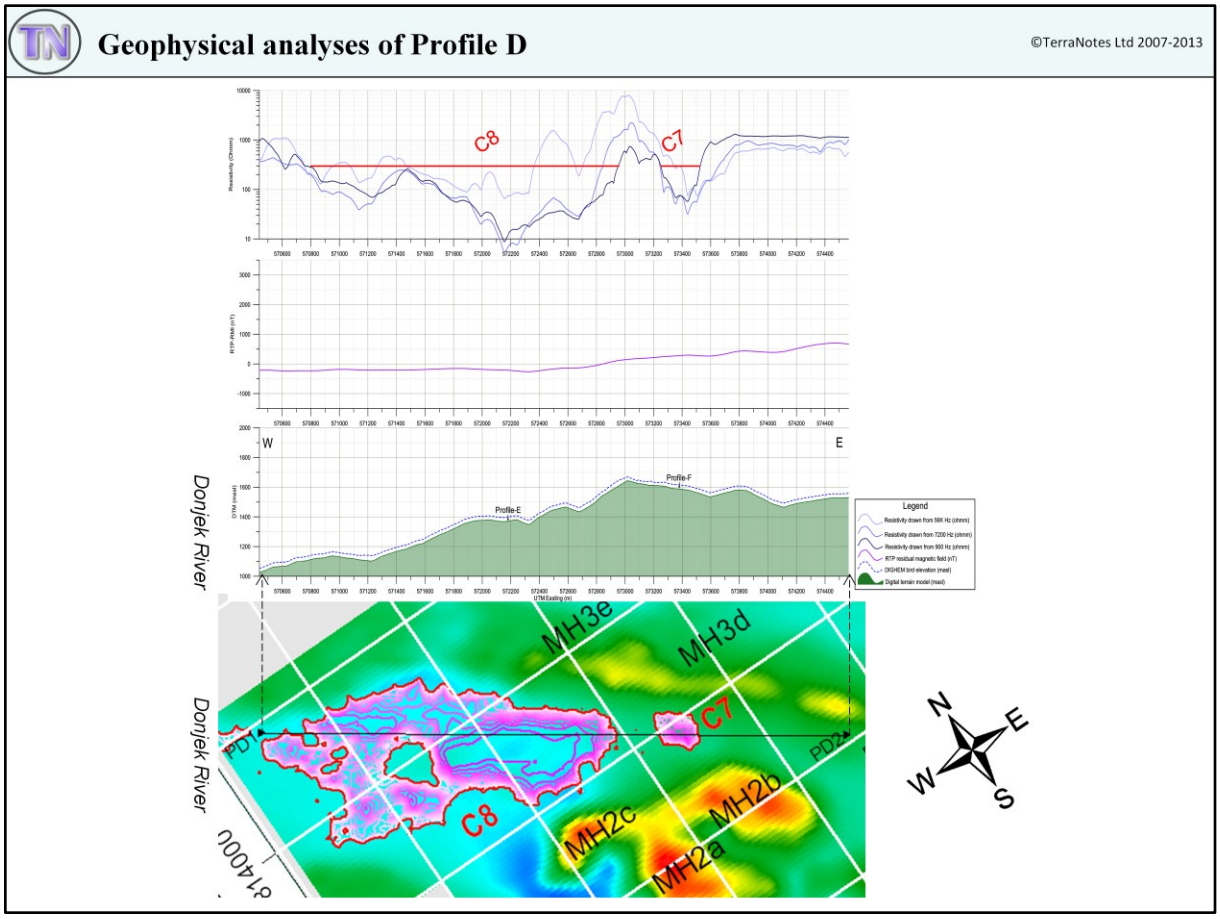


Figure 93. The main image is the DTM, RTP-RMI, and apparent resistivity values along Profile D. The image at the bottom is the RTP-RMI map rotated in agreement with Profile D.

Main Findings

To examine the largest conductor (C8) in Rory, Profile D was selected to follow the C8 trend. C8 is situated in a relatively silent magnetic area between MH3 and MH2. This silent magnetic background could correspond to local lithologies (e.g., siltstone and volcaniclastic sandstones).

In its southeast portion where the terrain is relatively high, C8 features the lowest resistivity values (see 900Hz & 7200Hz curves) in the entire claim group. For this, three following hypotheses are presented (and require further investigation):

(a) the rocks are clay-enriched;

(b) the rocks underwent sulphidization by fluids from around intrusions (MH2 and/or MH3);

(c) Both (a) and (b);

Conductor-7 (C7) is located in between MH2b and MH3d. Such magnetic situation suggests that this bedrock conductor possesses a high potential to be a mineralization/deposit of interest.

(continued in the following figure)

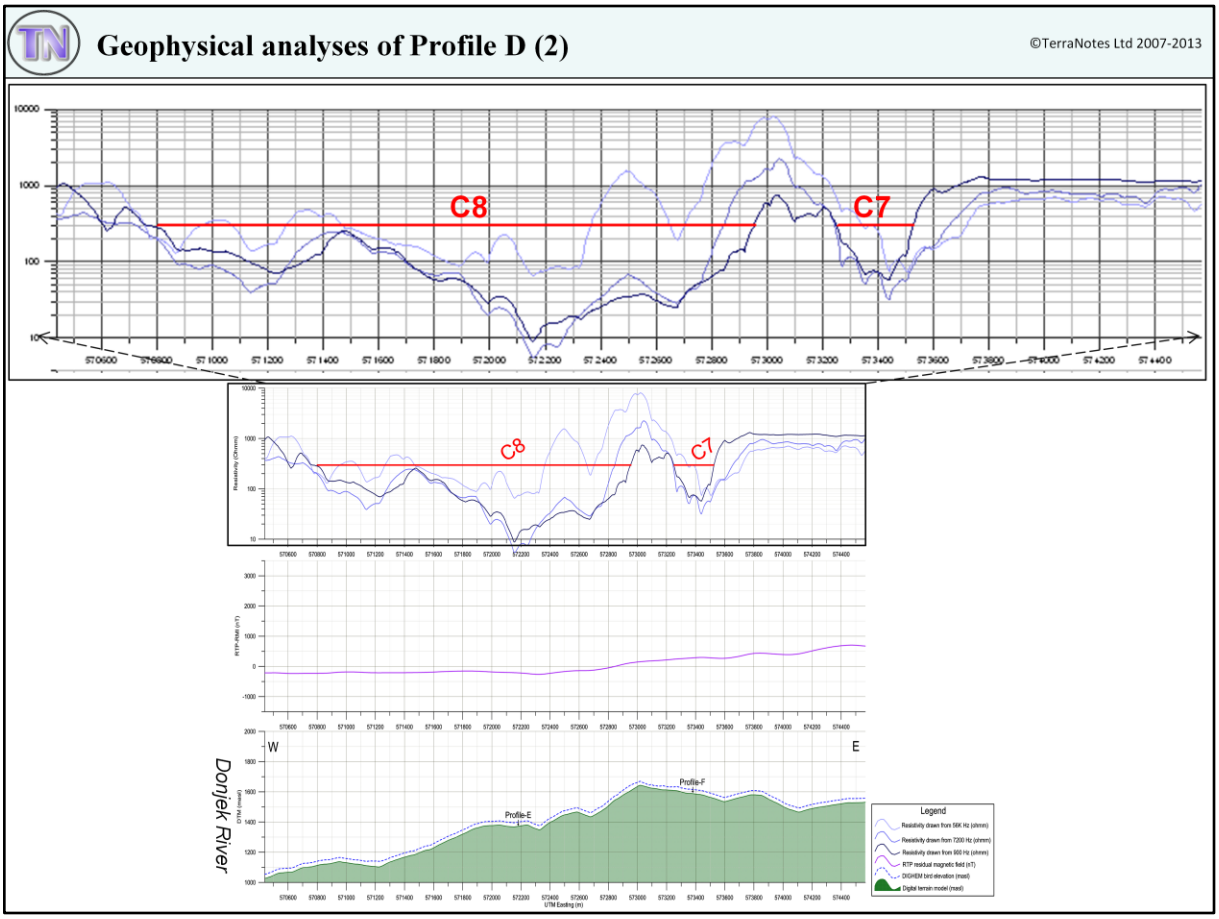


Figure 94. The main image is the DTM, RTP-RMI, and apparent resistivity values along Profile D. The image on top is the zoomed DIGHEM resistivity curves in the range of C7 and C8.

Main Findings (Cont'd)

The shapes of the C8 resistivity curves do not reflect a simple conductance-stratified layer model. It is probably a vertical bedrock conductor extending more than 2 km (as the profile is parallel to the conductor axis) with two local lows.

The southeast portion of C8 appears deeper and more conductive than the northwest portion.

C7 is located southeast of C8 with a magnetic background slightly higher than C8.

No geophysical observation indicates that C7 and C8 are connected, even though in regional geology they are in the same lithological unit.

C7 and its vicinity should receive additional attention in future exploration.

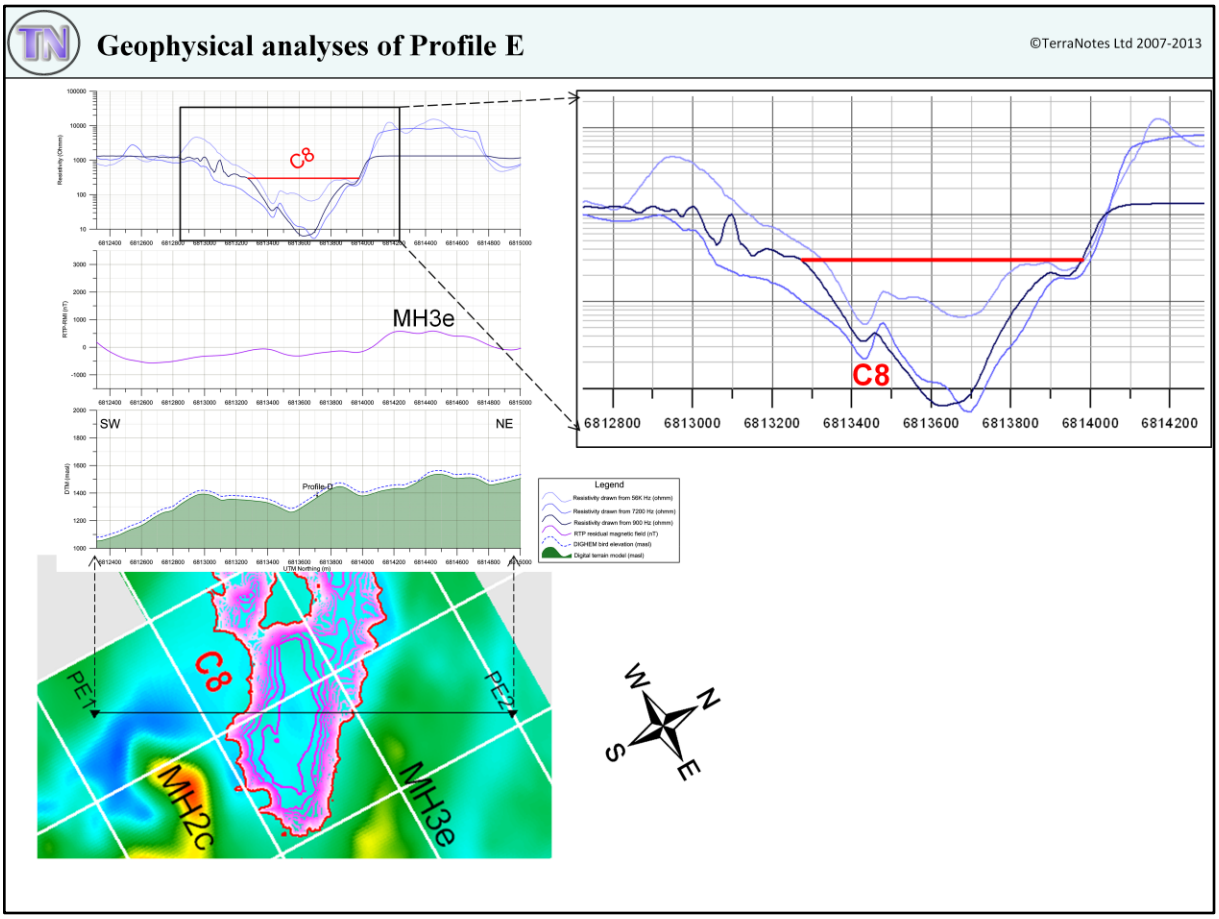


Figure 95. The main image is the DTM, RTP-RMI, and apparent resistivity values along Profile E. The image at the bottom is the RTP-RMI map rotated in agreement with Profile E. The inset image on the right is the zoomed DIGHEM resistivity curves in the range of C8.

Main Findings

C8 appears to be a V-shaped conductor with roughly symmetrical sides.

The faint asymmetry at local minima may suggest a very steep, almost vertical S-SW dipping conductor.

Both 7200Hz and 900Hz data show less than 10 Ω·m apparent resistivity for C8, which indicates that the real resistivity is much lower than 10 Ω·m. Since clay lithologies does not generally show this level of low resistivity, the C8 anomaly most probably indicates a sulphide mineralization.

On the southwest side, the 7200Hz channel apparent resistivity is greater than that of the 900Hz channel. On the northeast side, the relative values are reversed. This reversal is similar to what is observed in C10 on Profiles A1 and A2.

The southeast portion of C8, near MH2c and MH3e, also requires further geological attention.

The immediate northwest of Profile E (within C8), where there is an abrupt change in resistivity (see bottom image), is geophysically very interesting and warrants further investigation.

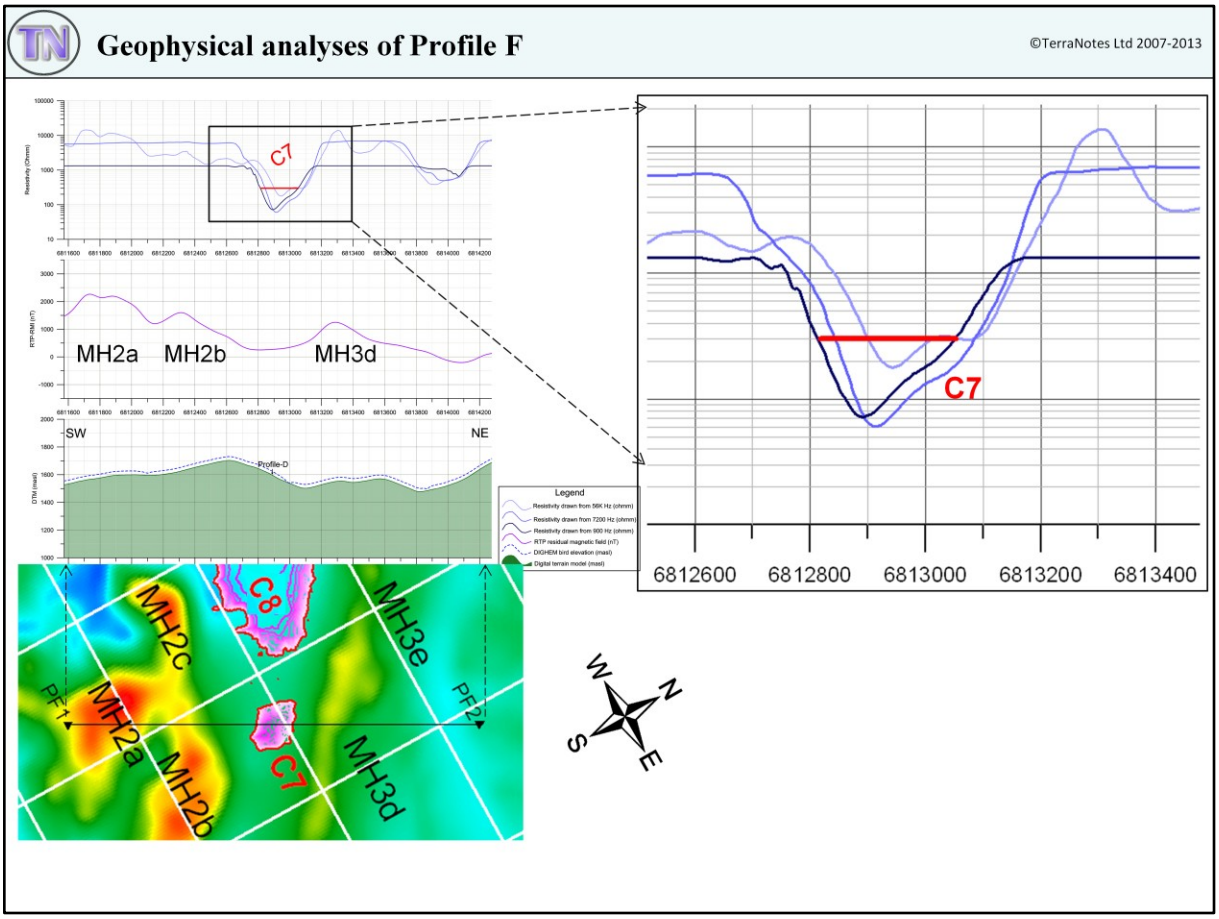


Figure 96. The main image is the DTM, RTP-RMI, and apparent resistivity values along Profile F. The image at bottom is the RTP-RMI map rotated in agreement with Profile F. The inset image on right panel is the zoomed DIGHEM resistivity curves in the range of C7.

Main Findings

C7 is situated in the middle of the topographical slope – favourite terrain situation since the conductor is not situated at the bottom of a valley.

C7 has a preferable magnetic background, close to magnetic highs MH2b and MH3d.

The resistivity curves behave similar to C8 in that there is a resistivity value reversal on both sides of the conductor.

Both conductors' sides are apparently asymmetrical and are consistent with local magnetic trends.

In fact, C7 and C8 are located in the low part of the large, regional magnetic high consisting of MH1, MH2, and MH3. In comparison, deeper Wellgreen conductors (C9 and C10) are only associated with MH4 with clear boundaries.

Magnetic simulation shows that the buried depth of MH1, MH2, and MH3 ranges from 20m to 85m while MH4 ranges from 5m to 15m. So, the deeper depths for western conductors (C7 and C8) and magnetic sources may make the resistivity and magnetic curves smoother, not appearing rugged like what was found in Profiles A and B in Wellgreen.

The location of the local minima in the resistivity curves (top right) suggest a S-SW dip.

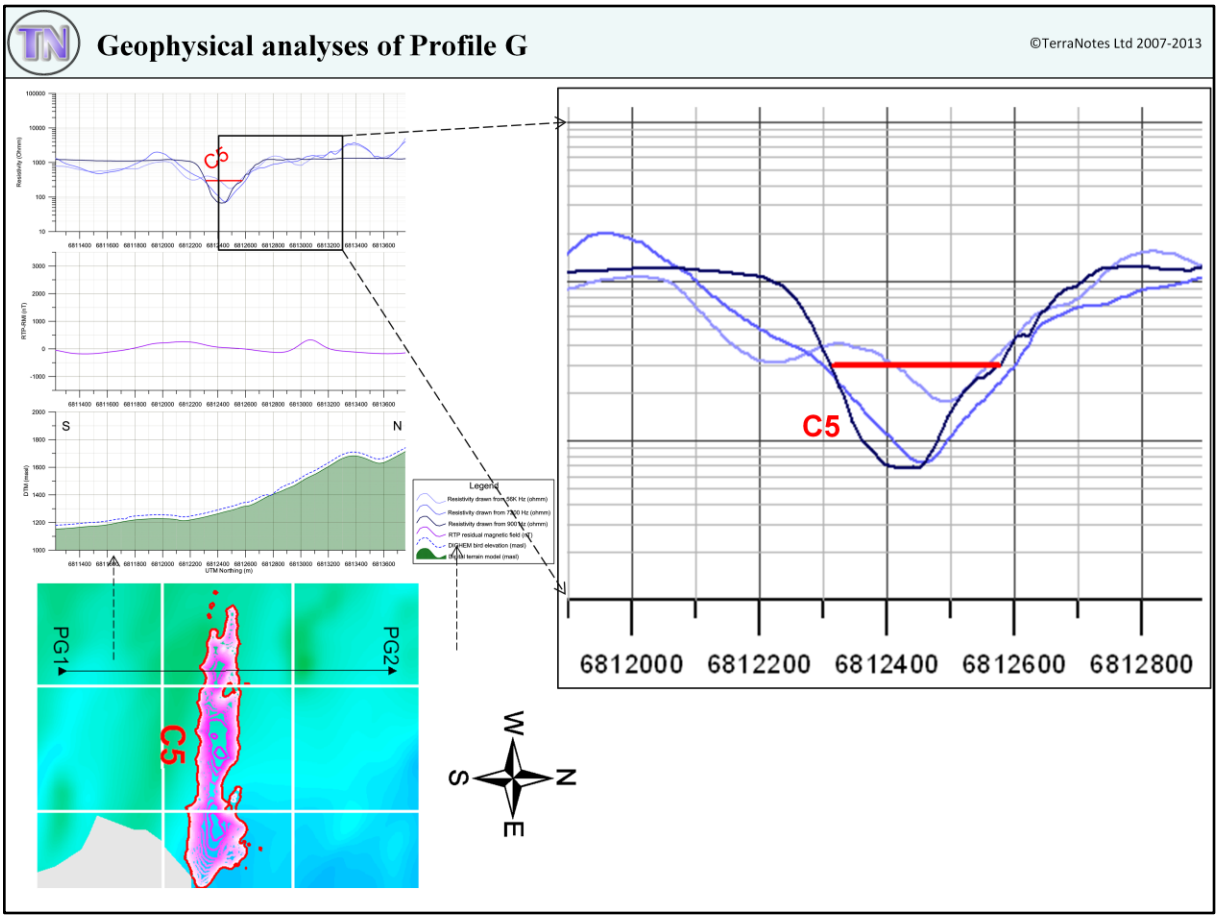


Figure 97. The main image is the DTM, RTP-RMI, and apparent resistivity values along Profile F. The inset image at bottom is the RTP RMI map rotated in agreement with Profile G. The inset image on right panel is the zoomed DIGHEM resistivity curves in the range of C5.

Main Findings

C5 is located on the lower flank of a high topographic feature.

This profile is selected at the location where the E-W trending conductor intersects the WNW-ESE trending magnetic structure.

In the south, the magnetic field appears slightly stronger than in the north. This observation suggests that the C5 anomaly is located on a litho-structure.

The relatively weak magnetic background of C5 indicates that it is situated in a sedimentary formation. Hence, an intrusion within this sedimentary formation could be of interest for further Cu-Ni-PGE exploration. The centre of the C5 anomaly exhibits the lowest resistivity and a weak magnetic anomaly, which may indicate a intrusion in the sedimentary formation. This anomaly was previously denoted as Anomaly E.

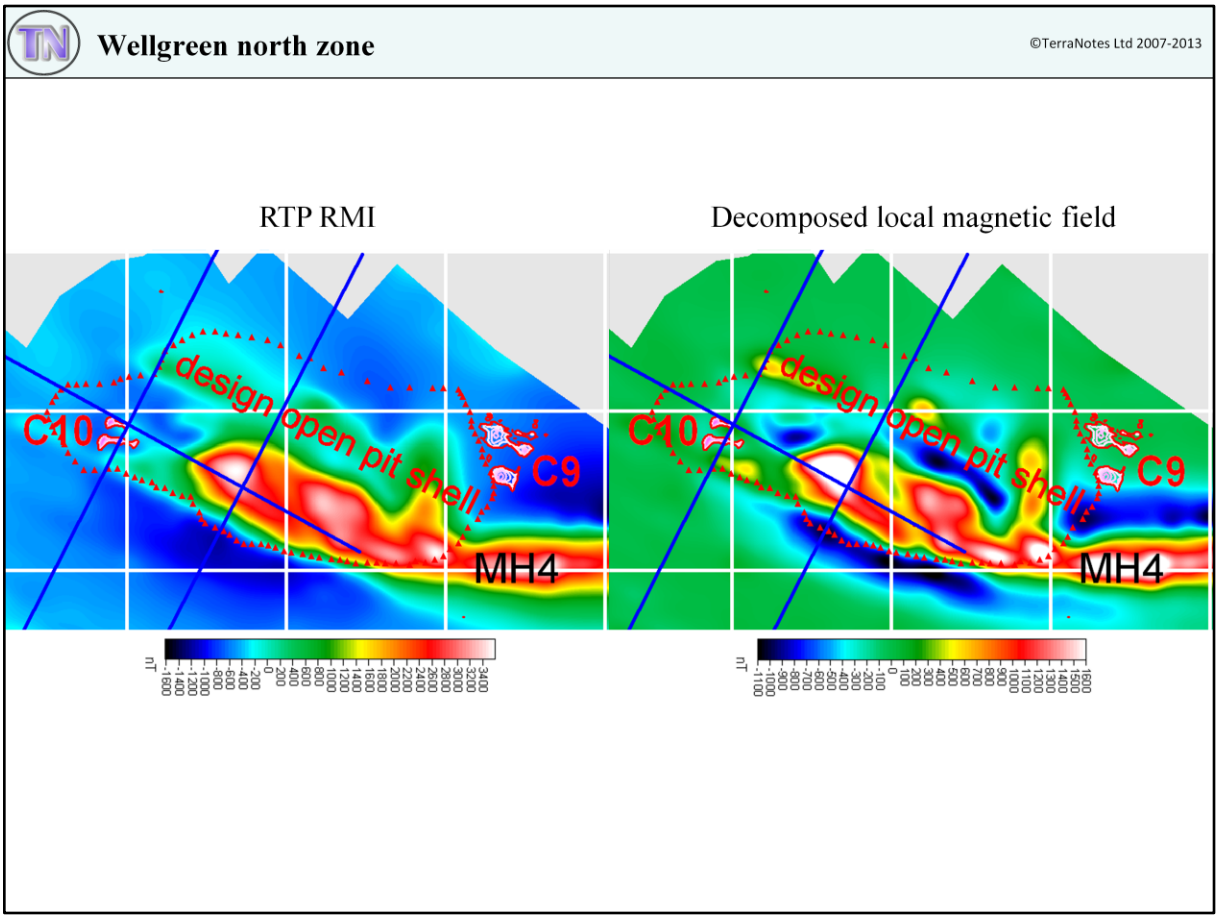


Figure 98. The image in the left panel is the zoomed RTP RMI of the Wellgreen north zone. The image in right panel is the zoomed local magnetic field of the same area. Red triangles delineate the boundary of the "design open pit shell" of Prophecy Platinum Corp.

Main Findings

From the decomposed local magnetic map (right panel), MH4 can be divided into nine (9) local anomalies.

Both the total magnetic anomaly (MH4) and the local magnetic anomalies suggest shallow magnetic sources with clear boundaries.

Negative magnetic intensity around MH4 indicates that the depth extent of the magnetic sources are limited.

The decomposed local magnetic field provides the possibility of correlating local, detailed magnetic features with the known deposit once drilling results are available.

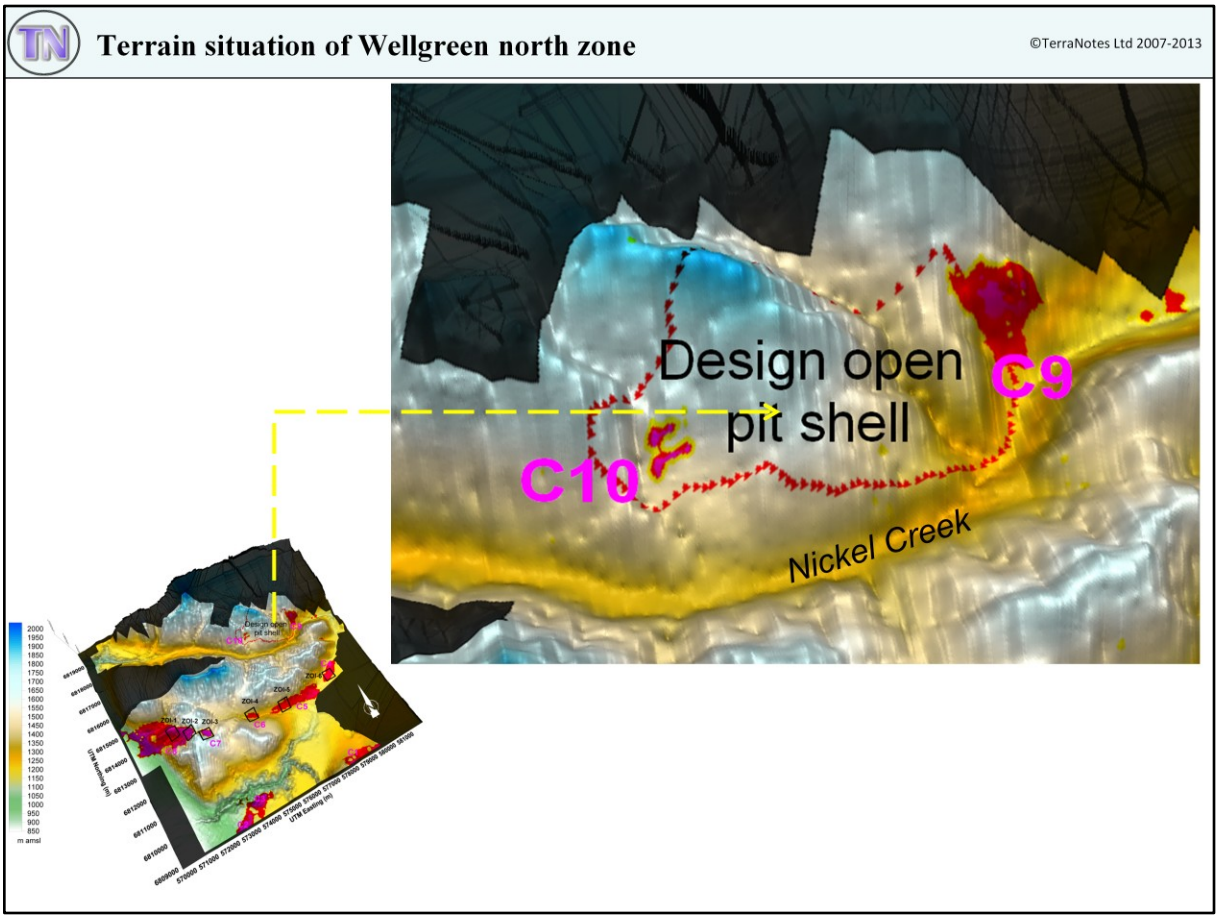


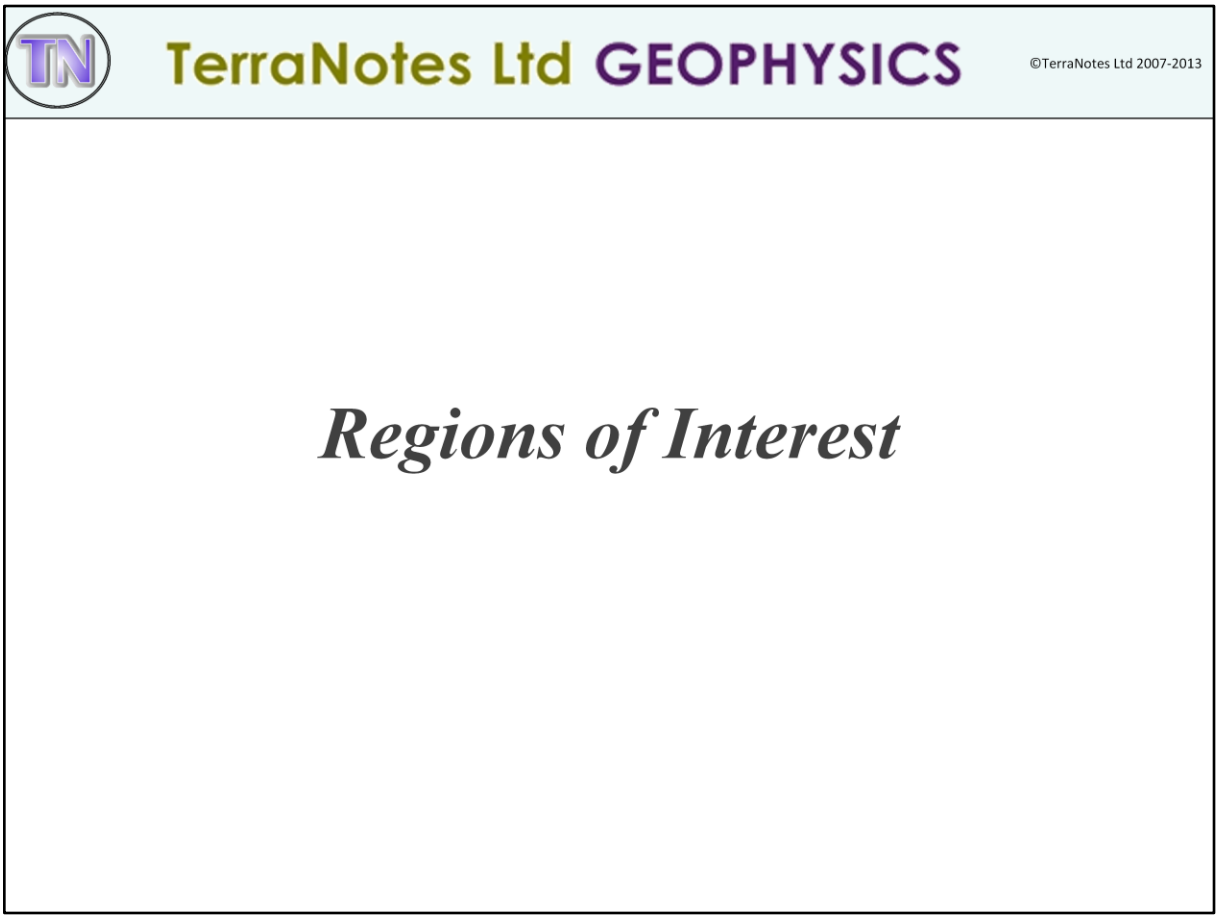
Figure 99. The zoomed 3D view of the topography of the Wellgreen north zone. The red triangles delineate the boundary of the "design open pit shell" of Prophecy Platinum Corp. The inset map on the bottom left is the topography of the entire survey area.

Main Findings

The Wellgreen north zone is situated on the slope of a high topographic feature (see "design open pit shell" denoted by red triangles).

C9 and C10 are located on the south and southwest flanks of this high terrain, respectively.

The conductors are oriented perpendicular to the slope of the terrain, indicating bedrock conductors at these locations.


TerraNotes Ltd GEOPHYSICS
©TerraNotes Ltd 2007-2013
Regions of Interest

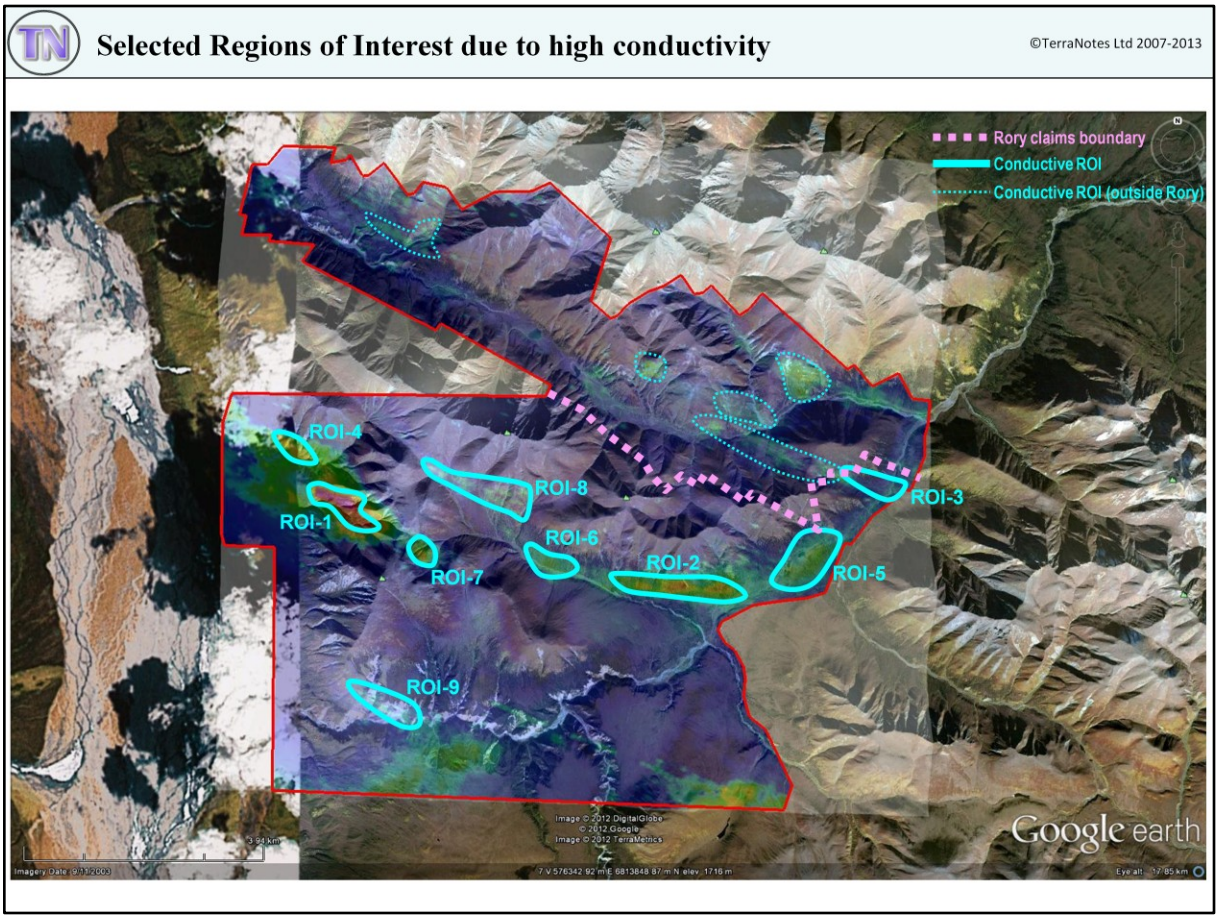


Figure 100. The mid-depth apparent resistivity map overlaid on the Google Earth map of the survey area. The pink dotted line approximately separates the Rory claims from the other claims.

Main Findings

The cyan polygons indicate the regions of interest (ROI) selected due to their higher conductivity. The numbers indicate their priority, ROI-1 being the most important and ROI-9 being the least important.

ROI-1 is the strongest conductor within the Rory claims and exhibits characteristics of a bedrock conductor. It is also coincident with a weak magnetic anomaly, so it could be a favourable location for Ni-Cu-PGE mineralization. On the other hand, the fault intersecting this location may produce a graphite deposit and the conductor may be due to the existence of graphite.

ROI-2 is another strong bedrock conductor which is also coincident with the weak magnetic structure. Hence, it could also be a favourable location for Ni-Cu-PGE mineralization.

ROI-3 is a very weak conductor that seems to be connected to the Wellgreen deposit in the NW-SE direction. Thus, similar Ni-Cu-PGE mineralization may be found in this ROI. However, it is also coincident with a valley and the conductive structure may have a superficial source.

ROI-4 shows similar characteristics to ROI-1 but both EM and magnetic anomalies are very weak. If assays from ROI-1 are found to be positive, ROI-4 could be considered a new ROI.

ROI-5 is an intermediate conductor coincident with a weak magnetic anomaly. The orientations of the EM and magnetic anomalies, however, are perpendicular to each other.

ROI-6, -7, -8, and -9 are weak to intermediate conductors, but they exist on the low magnetic zones and have, therefore, low priority in terms of further exploration.

The dotted cyan polygons show the other ROI that are situated outside the Rory claims.

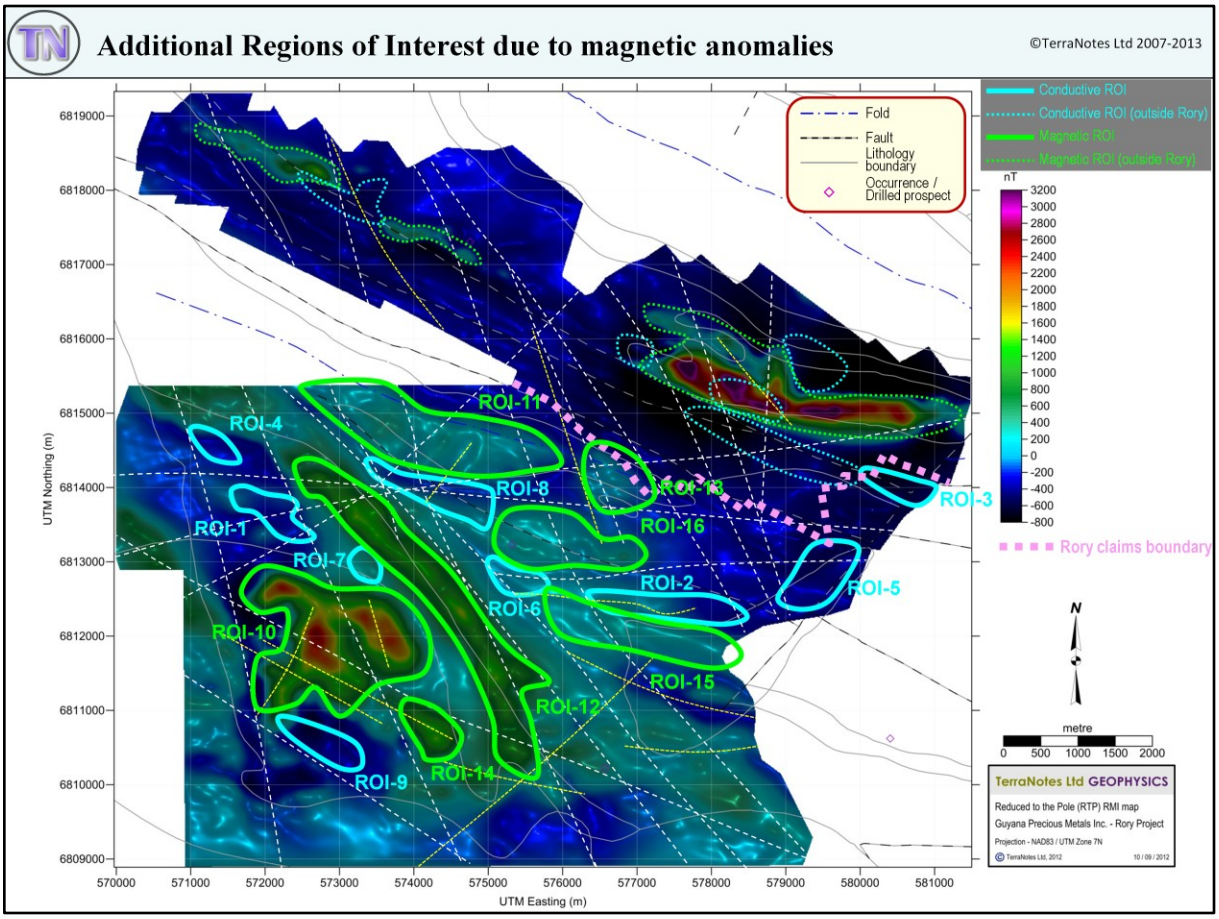


Figure 101. Regions of interest on the final corrected magnetic field map. The pink diamonds indicate mineral occurrences of YGS. The gray polygons indicate the boundaries of the geological formations. The dashed black lines indicate the faults/shears and the dashed blue lines indicate fold axes. The pink dotted line approximately separates the Rory claims from the other claims. The previously identified faults are marked with thin white dashed lines and the local breaks are marked with thin yellow dashed lines.

Main Findings

The green polygons indicate the ROI selected due to their higher magnetic intensity. The numbers again indicate their priority, ROI-1 being the most important and ROI-16 being the least.

ROI-10 is a very high magnetic anomaly which is not expected for Kluane Range Plutonic Suites according to the Geology map (see Figure 4). Hence, there may be ultramafic rocks within this anomaly similar to the Wellgreen area in the northeast and its basal contact may exhibit Ni-Cu-PGE mineralization. Gabbro is observed within the Kluane Range Plutonic Suites in the east of Rory around Duke River and same phenomenon may occur at this location.

The other high magnetic ROI (11-16) may exhibit similar characteristics. Therefore, deep penetrating ground electromagnetic methods are recommended for exploring possible basal conductors beneath these high magnetic structures.

Among these ROI, ROI-10 and ROI-11 form embayment structures similar to the type of structure where the Wellgreen mineralization was found.

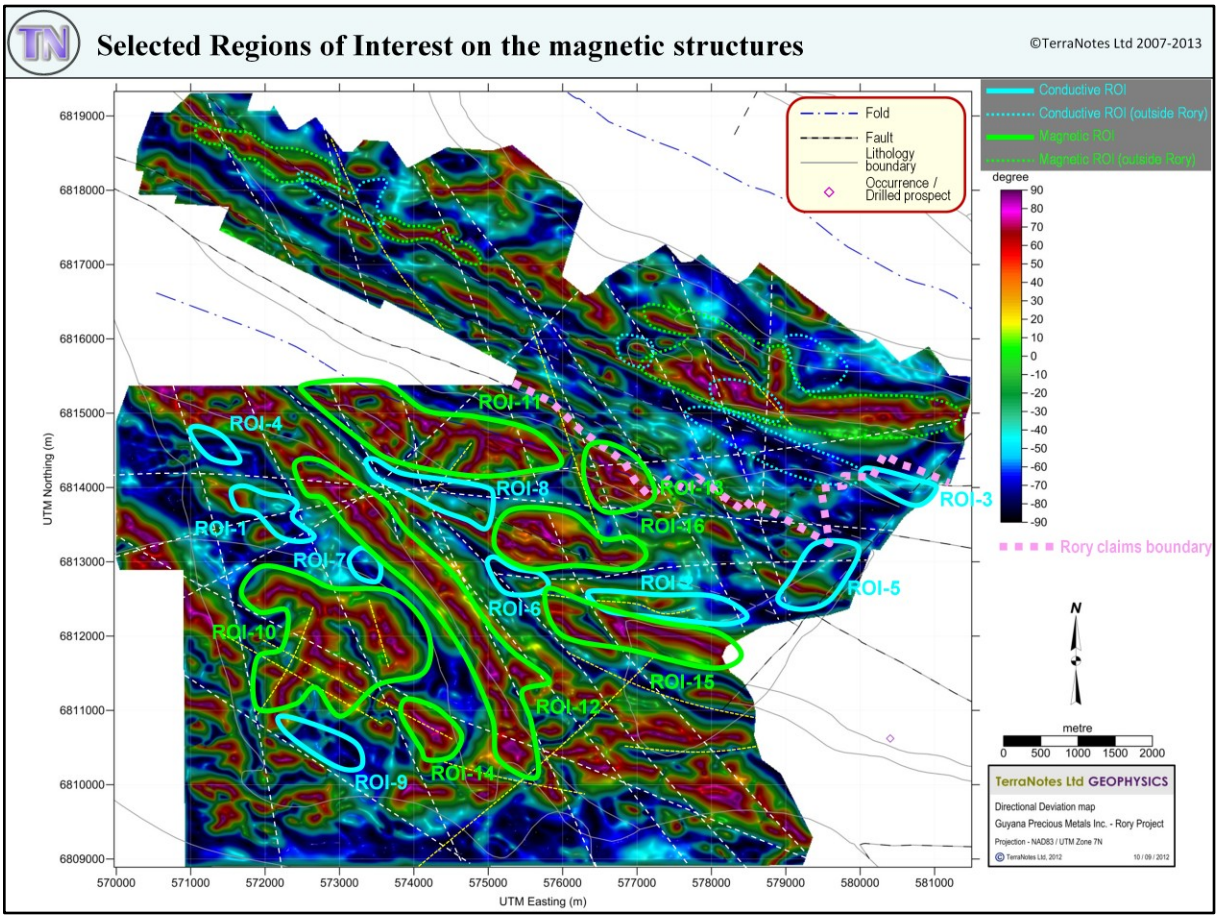


Figure 102. Regions of interest on the magnetic structures. The pink diamonds indicate mineral occurrences of YGS. The gray polygons indicate the boundaries of the geological formations. The dashed black lines indicate the faults/shears and the dashed blue lines indicate fold axes. The pink dotted line approximately separates the Rory claims from the other claims. The previously identified faults are marked with thin white dashed lines and the local breaks are marked with thin yellow dashed lines.

Main Findings

This map confirms the interpretation of the selected ROI (see Figure 101).

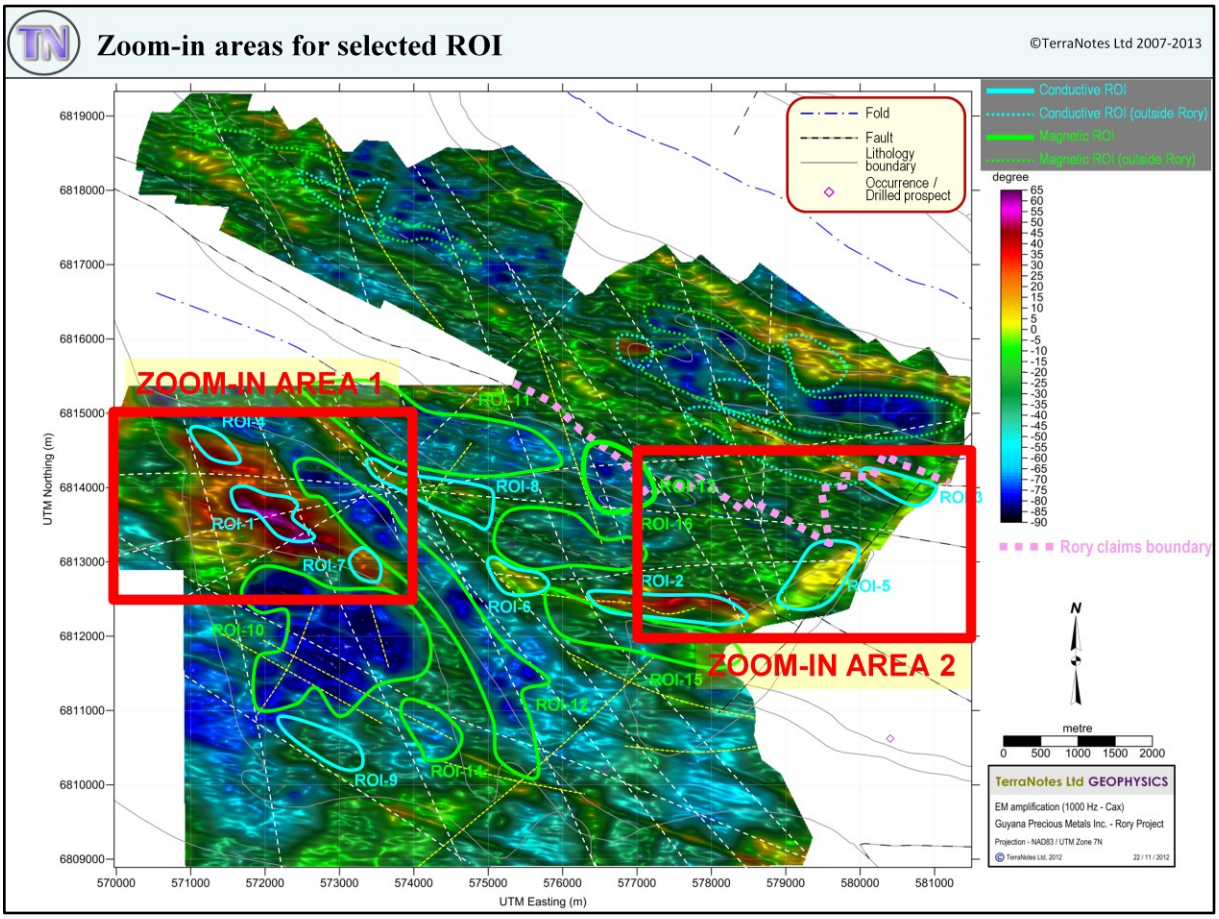


Figure 103. The map above amplifies the combination of in-phase and quadrature data of the 1000Hz co-axial channel to image the mid-depth bedrock conductors. The pink diamonds indicate mineral occurrences of YGS. The gray polygons indicate the boundaries of the geological formations. The dashed black lines indicate the faults/shears and the dashed blue lines indicate fold axes. The pink dotted line approximately separates the Rory claims from the other claims.

Main Findings

Theoretically, everything above 0° is conductive. A 45° anomaly indicates a medium strength conductor and a 90° anomaly indicates a very good conductor.

As seen above, ROI-1 and -2 are the strongest EM anomalies.

All the cyan anomalies show some degree of high conductivity.

The green ROI are low in conductivity and high in susceptibility. Deep penetrating EM methods are recommended to assess what exists beneath the green ROI.

The red boxes mark two crucial areas for possible Cu-Ni-PGE mineralization. The following section contains an examination of these areas.

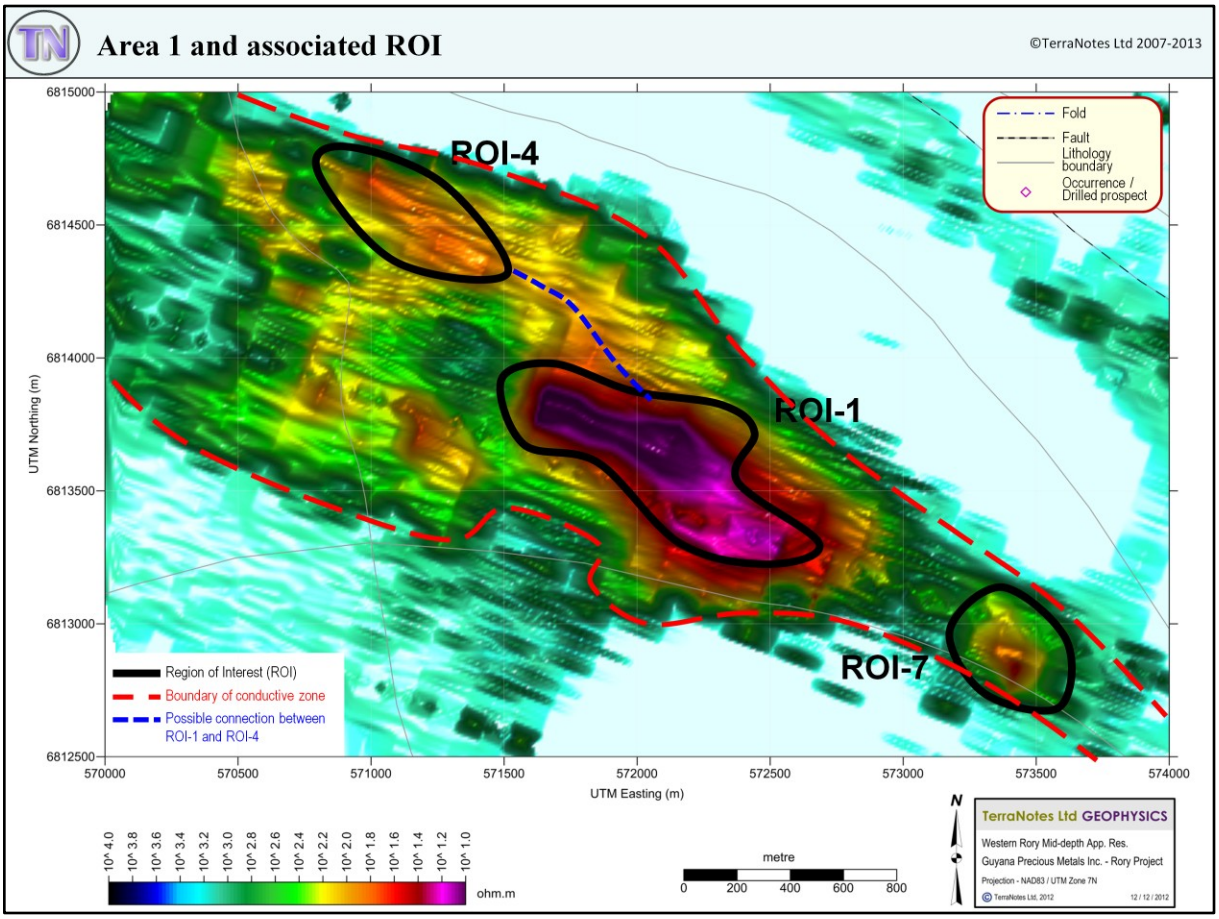


Figure 104. The map above shows the calculated apparent resistivity using co-planar 900 Hz data of Area 1. The gray polygons indicate the boundaries of the geological formations. The black polygons indicate ROI-1, -4 and -7 within Area 1 (defined in Figure 103).

Main Findings

The red dashed lines delineate the boundaries of the high conductivity background. This conductive zone coincides with the Skolai formation (see this gray lines). Thin-bedded argillite within the Skolai formation could be the reason for weak conductivity but the high conductivity zones (such as ROI-1) should be due to a strong bedrock conductor such as sulphide mineralization or graphite.

This figure clearly shows the three ROI within the Skolai formation, and they are the stronger anomalies within the whole conductive background (delineated with red dashed lines).

The dashed blue line indicates the possible connection between ROI-1 and -4. ROI-1 could also be connected to ROI-7 in the southeast.

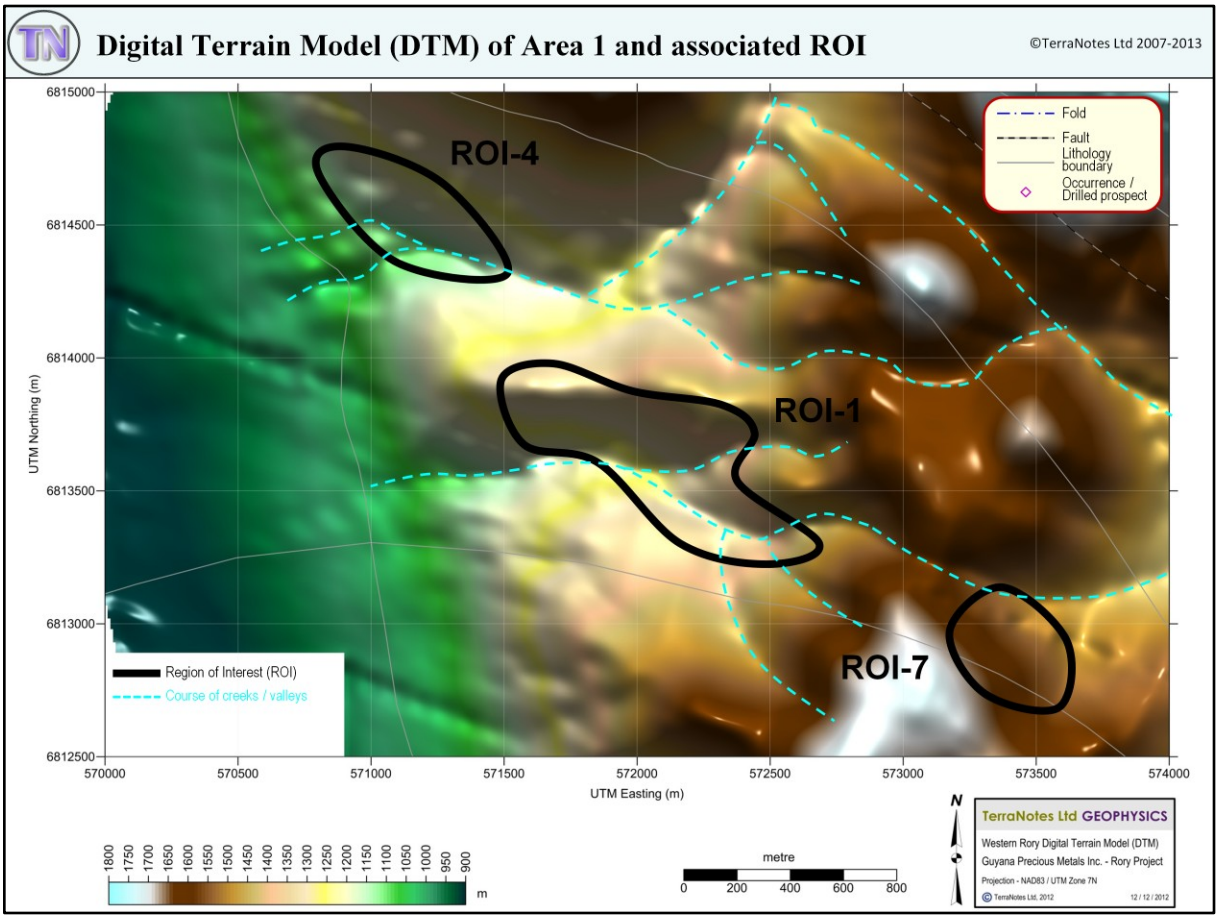


Figure 105. The topography of Area 1. The thin gray polygons indicate the boundaries of the geological formations. The dashed cyan lines mark significant valleys that are deduced from the DTM map. The thick black polygons indicate ROI-1, -4, and -7 within Area 1.

Main Findings

This map shows that ROI-7 and the northern part of ROI-1 are entirely independent from the topographical features.

The valleys (dashed cyan lines) are used to observe any possible relationship between them and the conductors.

ROI-4 and the southern extension of ROI-1 are coincident with the small valleys that connect to the Donjek River in the west. The conductivity at this location might be associated with sediments deposited by erosion in these rather steep valleys. However, since the other valleys in Area 1 do not exhibit higher conductivity and the conductive zones in ROI-4 and southern part of ROI-1 are not oriented in the same direction as valleys, high conductivity due to sedimentary deposition appears to be a less likely possibility.

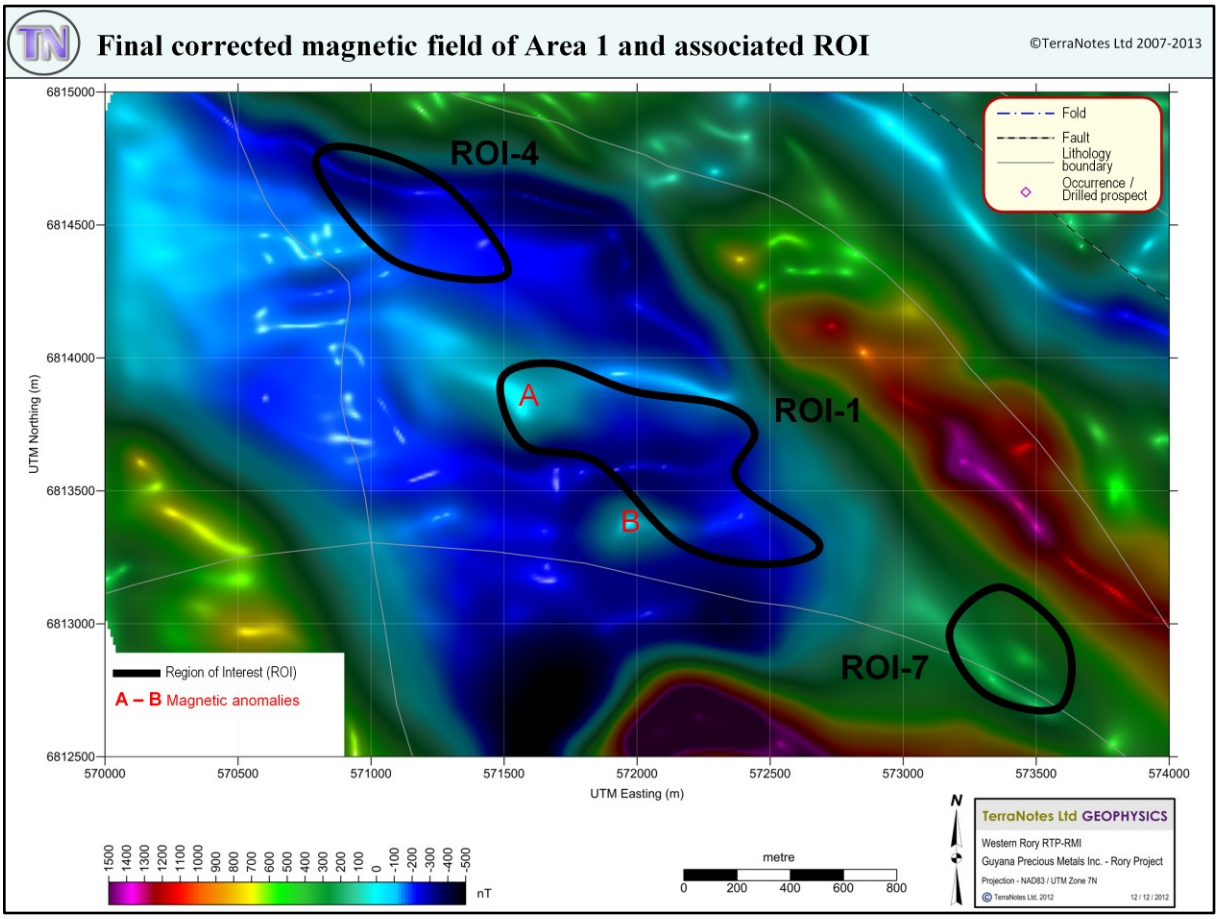


Figure 106. RTP-RMI map of Area 1. The thin gray polygons indicate the boundaries of the geological formations. The thick black polygons indicate ROI-1, -4, and -7 within Area 1.

Main Findings

ROI-1 and ROI-4 are situated on a weak magnetic high within a low magnetic zone.

In contrast, ROI-7 is situated on the lower magnetic intensity zone of a high magnetic area.

ROI-1 exhibits two separate weak magnetic highs marked with red letters (A and B). This zone has been interpreted as being divided by an ENE-WSW trending fault. However, there is a tie-line between these two anomalies. In order to be sure this is not due to a tie-line effect, we have removed it from the raw magnetic data, re-gridded, and imaged the result in the following figure (107).

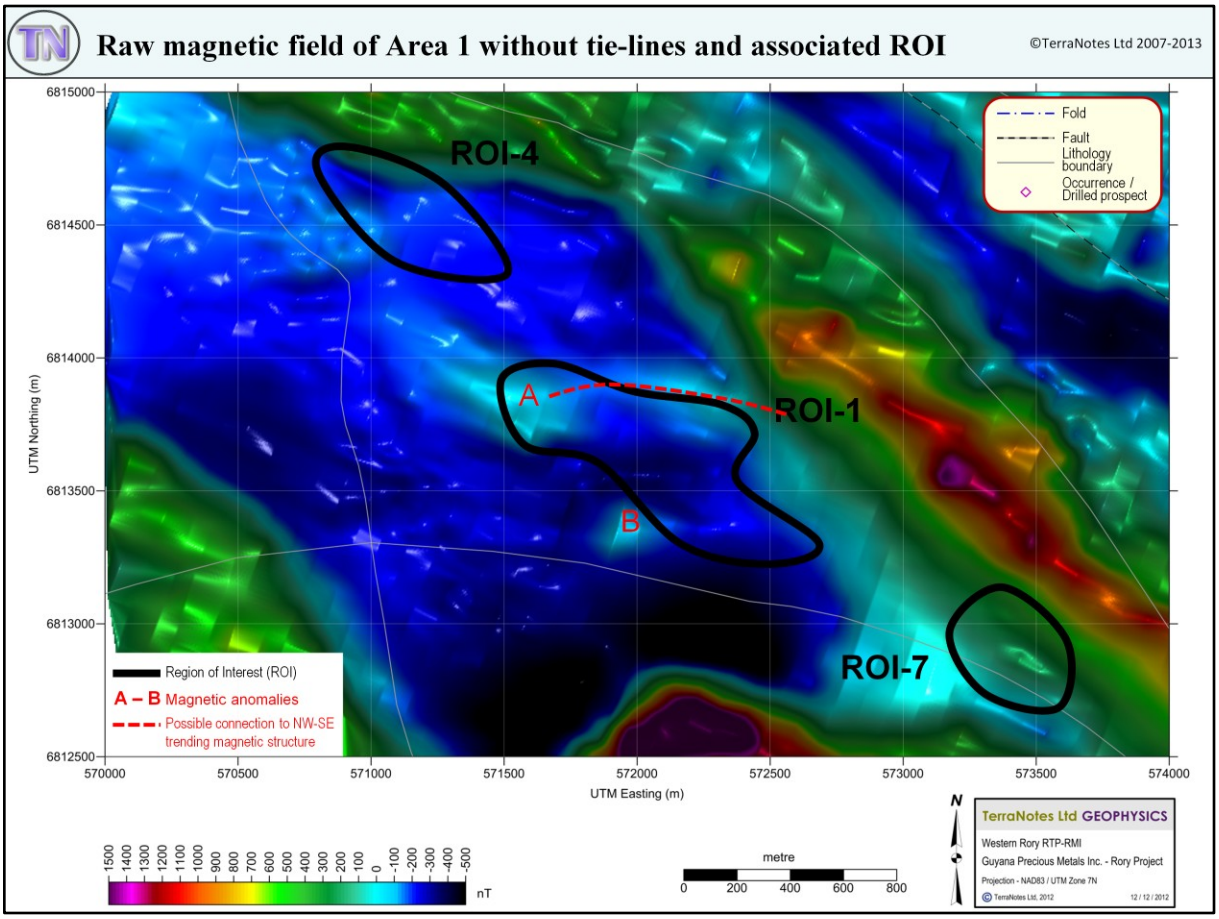


Figure 107. RMI map of Area 1 without tie-lines. The thin gray polygons indicate the boundaries of the geological formations. The thick black polygons indicate ROI-1, -4, and -7 within Area 1.

Main Findings

Following the removal of the tie-line, there are still two separate magnetic anomalies (A and B). Hence, this separation is not due to a tie-line effect.

The red dashed line shows a possible connection between the Anomaly A and the high magnetic NW-SE trending Nicolai formation. This observation may indicate a conduit structure from the Nicolai formation (see next map for further examination of this possibility).

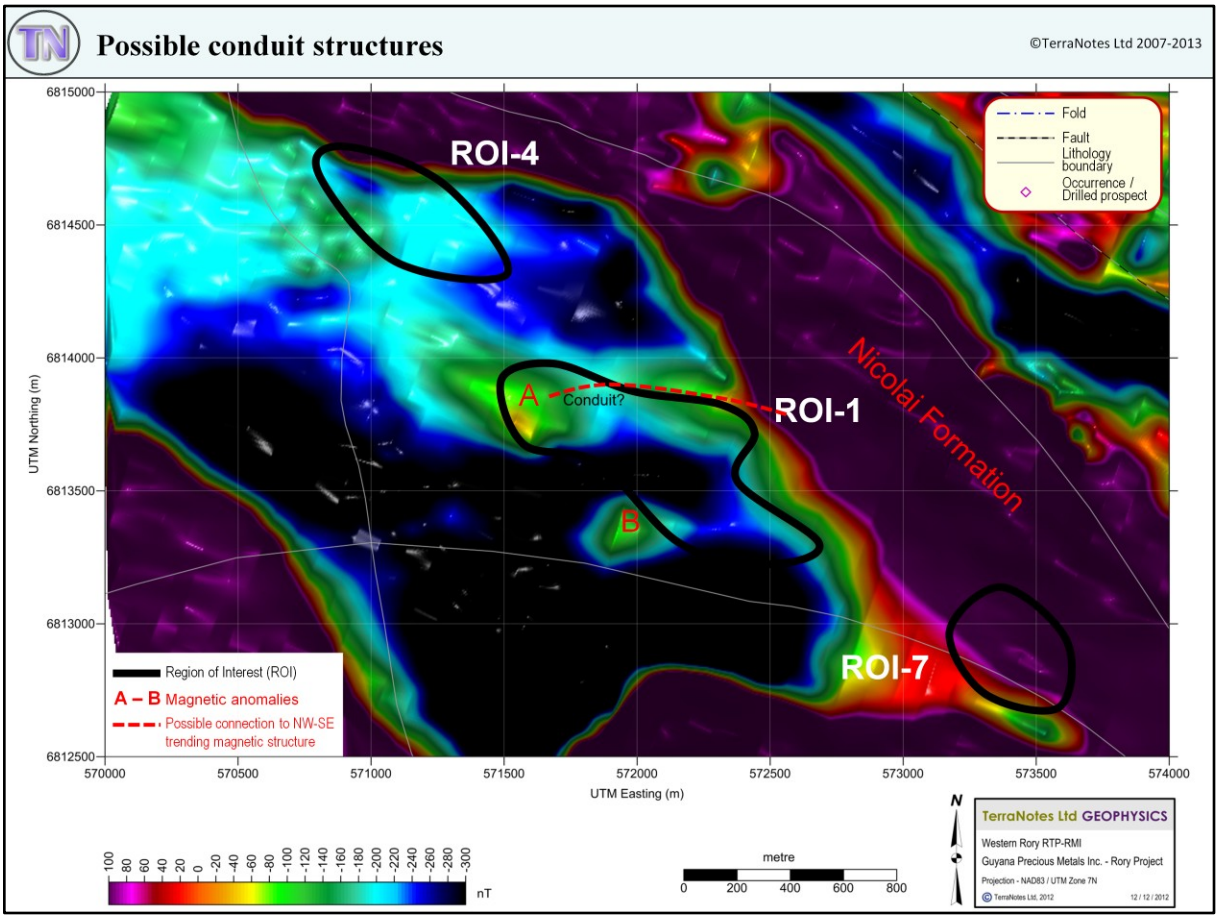


Figure 108. This figure is same as the previous figure with a different colour scheme to enhance the possible conduit structures in the low magnetic zone. The thin gray polygons indicate the boundaries of the geological formations. The thick black polygons indicate ROI-1, -4, and -7 within Area 1.

Main Findings

This map clearly shows the connection between the Anomaly A and high magnetic anomaly due to the Nicolai formation. It also appears that Anomaly B could be connected to the Nicolai formation in a similar fashion. Therefore, these weak magnetic anomalies could be conduit structures, which are favourable for Ni mineralization.

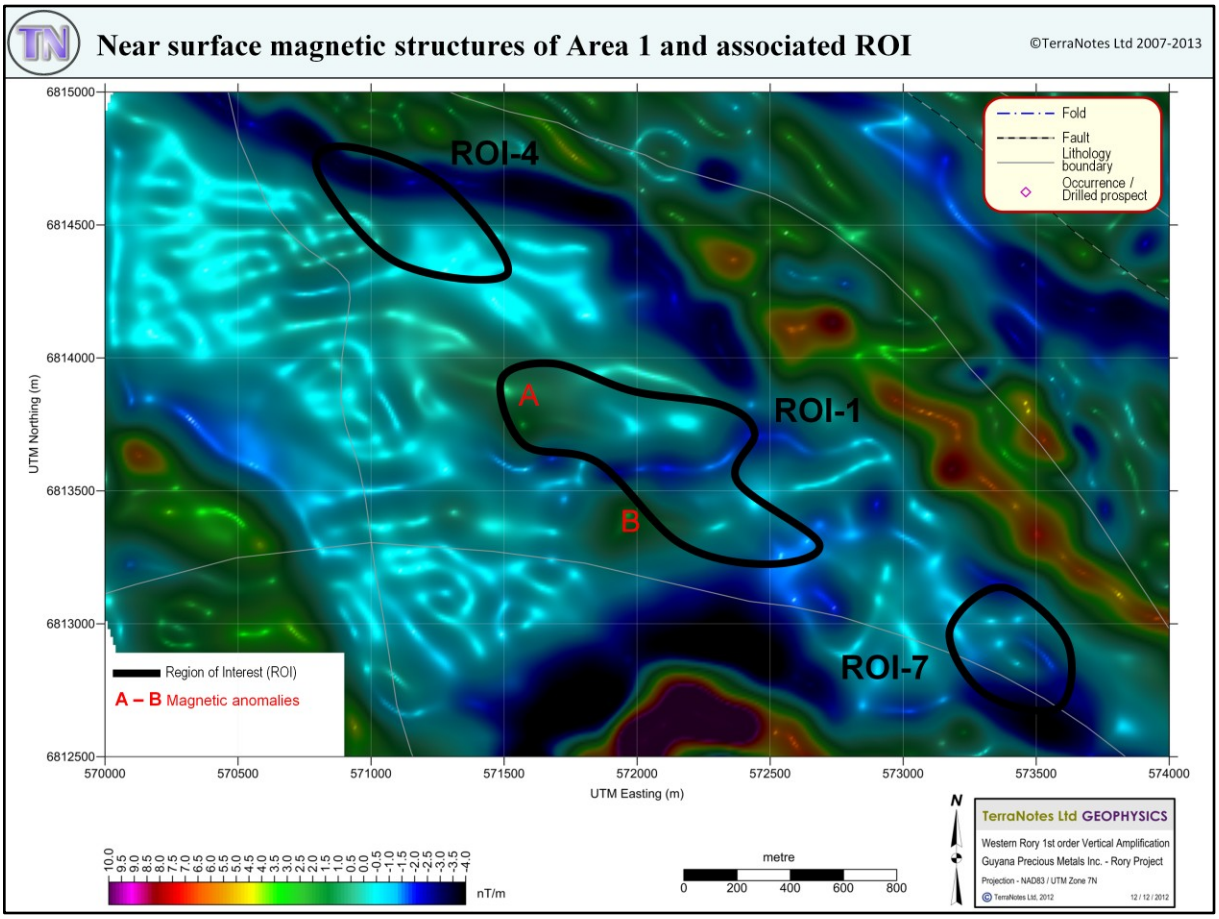


Figure 109. The strong, near-surface magnetic anomalies of Area 1. The purpose of this map is to amplify the strong, near-surface magnetic anomalies in order to see their structures in detail. The thin gray polygons indicate the boundaries of the geological formations. The thick black polygons indicate ROI-1, -4, and -7 within Area 1.

Main Findings

Anomalies A and B remain the strongest among the near-surface anomalies.

The background is weakly magnetic, which is consistent with the Skolai formation. Very low magnetic trends are observed at the contacts between Skolai and Nicolai, as well as between the Skolai and Kluane Ranges Plutonic Suite

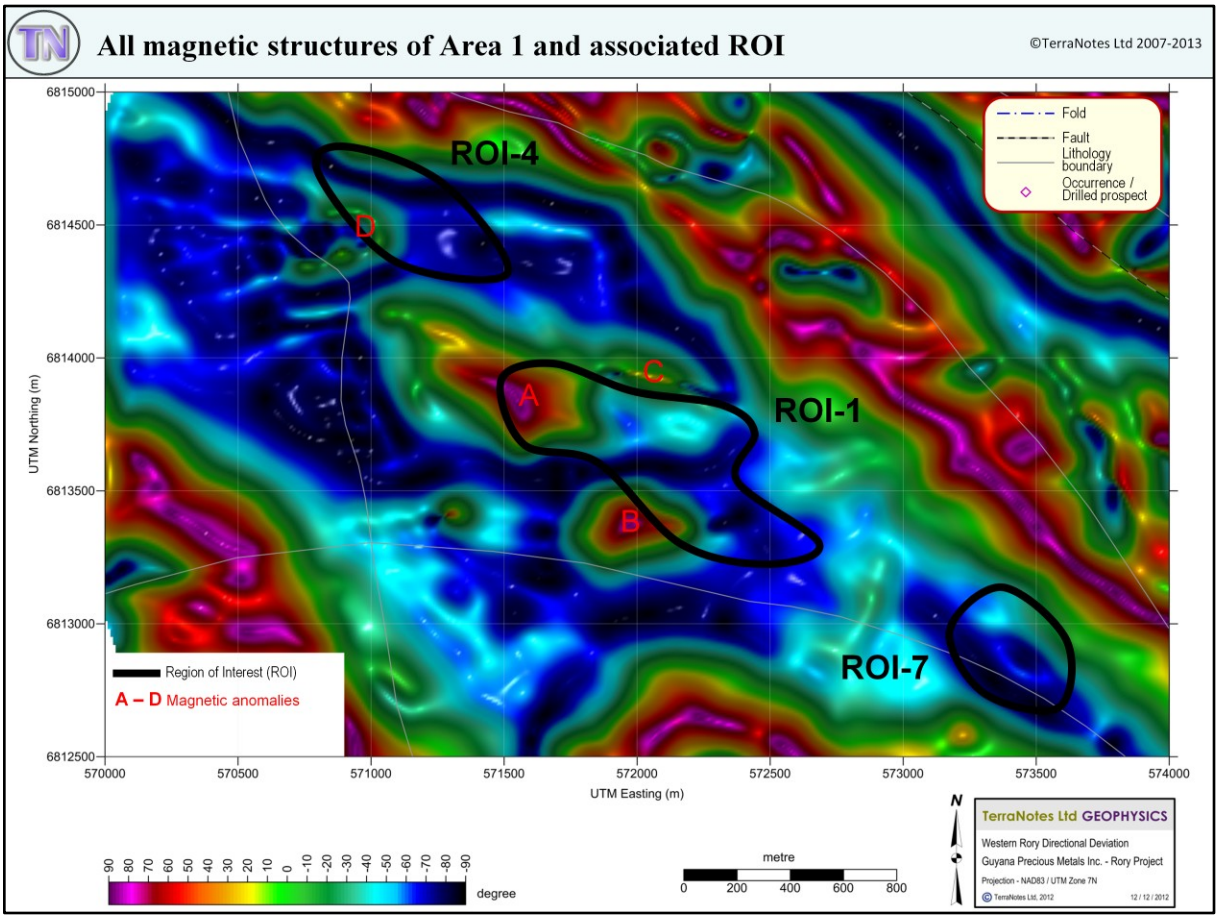


Figure 110. The all magnetic structures map of Area 1. The thin gray polygons indicate the boundaries of the geological formations. The thick black polygons indicate ROI-1, -4 and -7 within Area 1.

Main Findings

Anomalies A and B are now shown clearly in this figure.

In addition to Anomalies A and B, a very weak magnetic extension is visible and labelled Anomaly C.

There is also a very weak magnetic anomaly (D) that is associated with ROI-4.

The Skolai formation is coincident with the low magnetic background, as can be seen above. Anomalies A, B, C, and D are structures that are intruded into the Skolai formation as conduits. Therefore, these anomalies may be favorable for Ni-Cu-PGE mineralization.

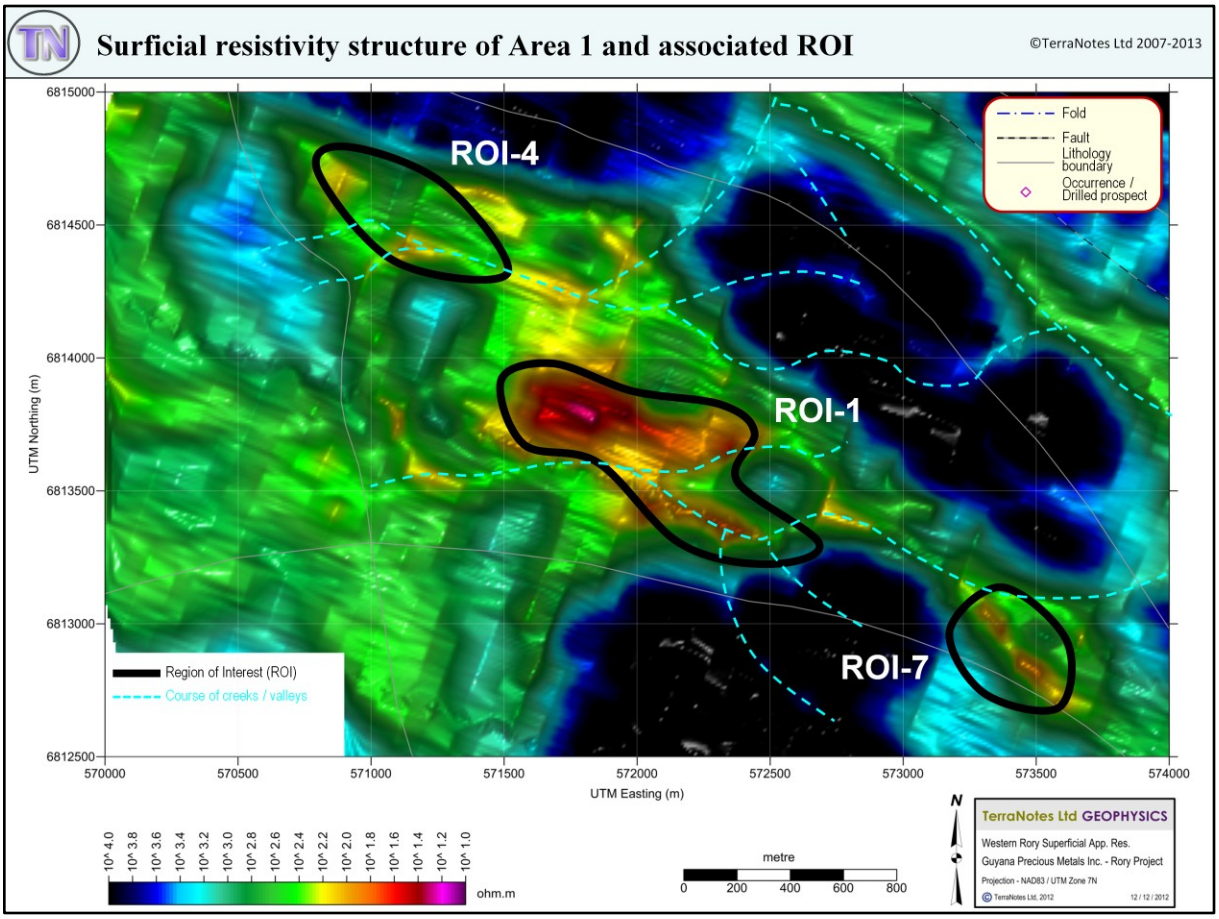


Figure 111. The surficial apparent resistivity map of Area 1. The thin gray polygons indicate the boundaries of the geological formations. The dashed cyan lines mark significant valleys that are deduced from the DTM map. The thick black polygons indicate ROI-1, -4, and -7 within Area 1.

Main Findings

ROI-1 and ROI-7 are observed in the surficial apparent resistivity map, hence they start at or near the surface.

The defined valleys (dashed cyan lines) are used to help determine any relationship between them and the surficial conductors. Some weak conductive trends coincide with the valleys, but the main anomalies (ROI-1 and -7) are independent from the topographic features.

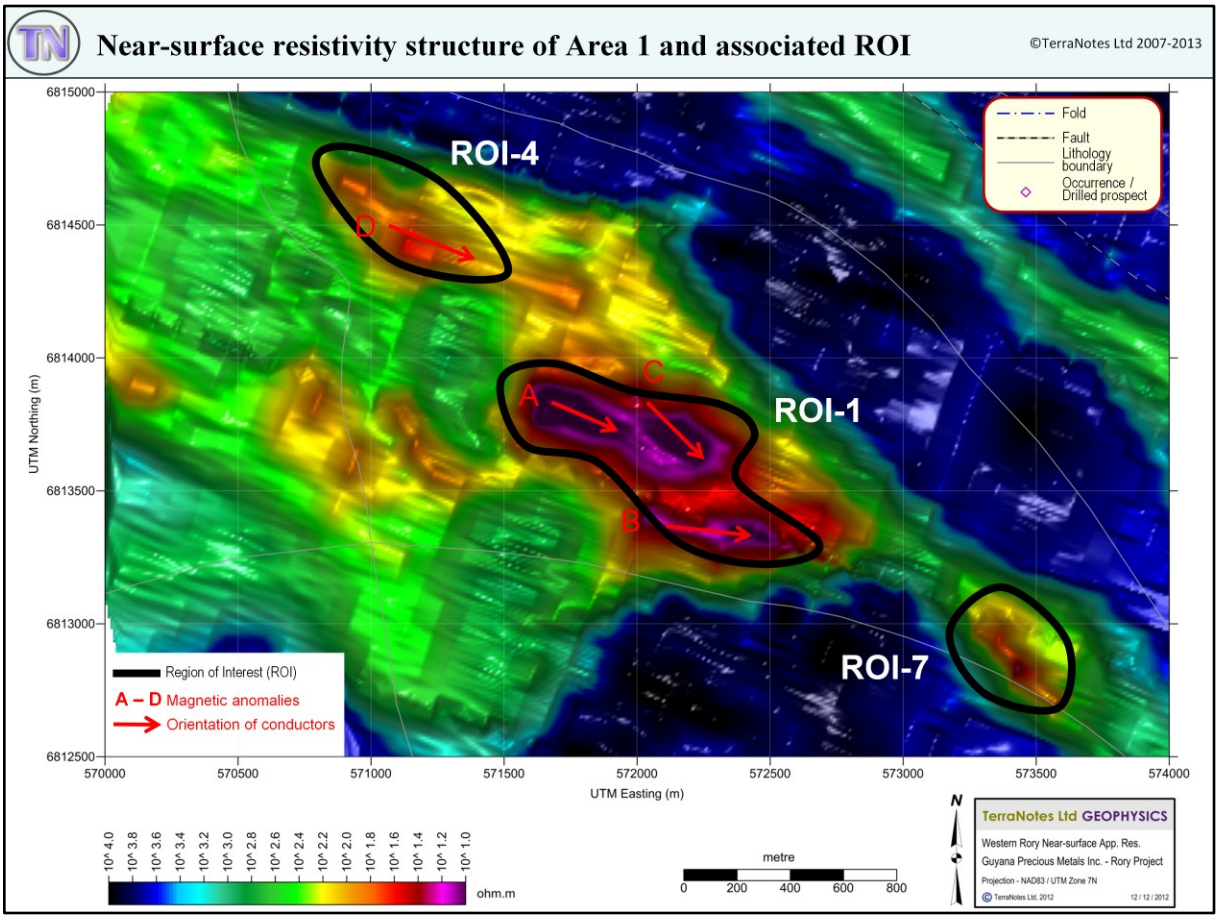


Figure 112. The near-surface apparent resistivity map of Area 1. The thin gray polygons indicate the boundaries of the geological formations. The thick black polygons indicate ROI-1, -4, and -7 within Area 1.

Main Findings

ROI-1 exhibits three different conductive trends immediately below the surface. The red arrows show the orientation of these trends and the red letters mark the locations of the weak magnetic highs deduced in the previous maps. Since each arrow appears to be associated with a weak magnetic anomaly, these conductive trends may represent sulphide mineralization at the contact of the interpreted conduits.

ROI-4 exhibits a similar characteristic to ROI-1 since it also contains a conductive trend immediately below the surface coming from a weak magnetic high.

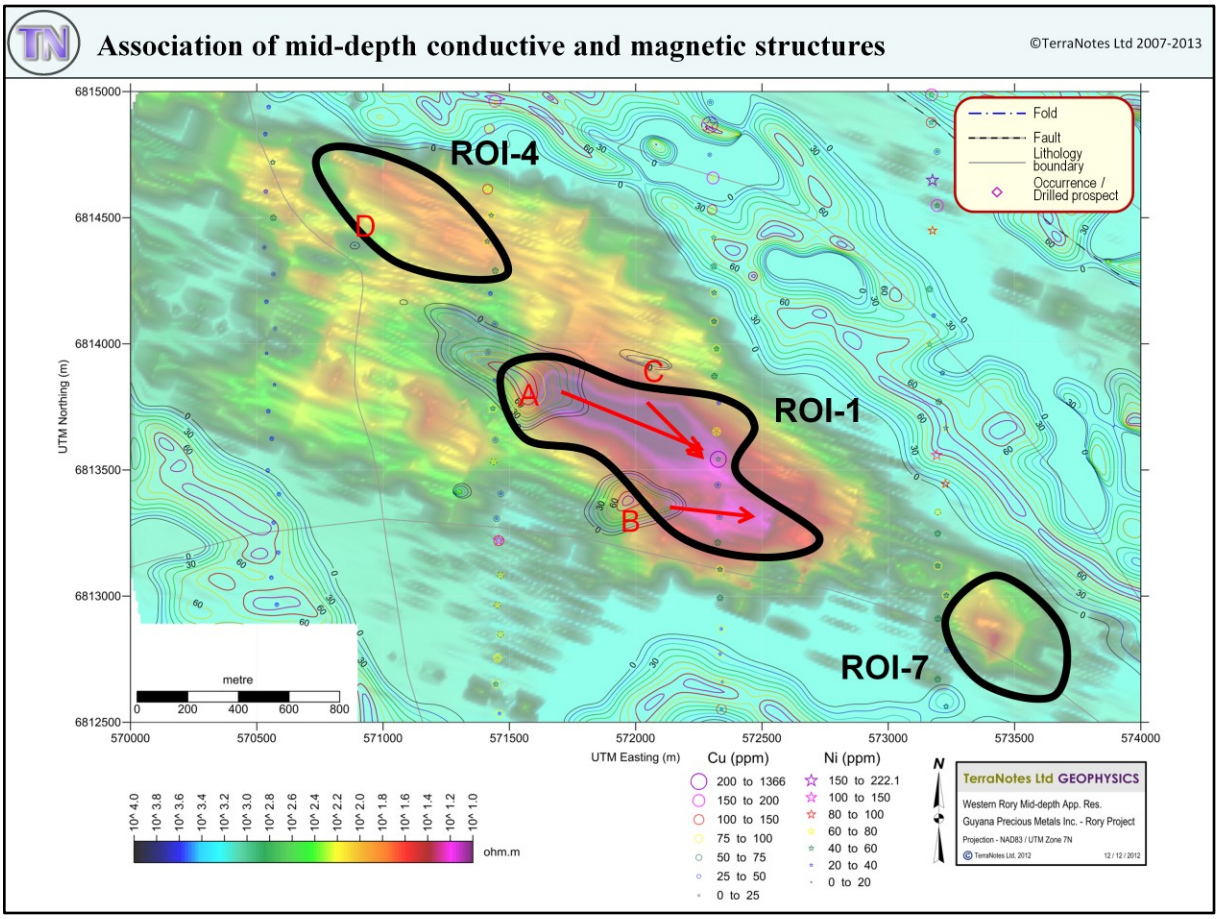


Figure 113. The mid-depth apparent resistivity map of Area 1. The Ni and Cu anomalies in soil are overlaid on the map as stars and circles, respectively (please refer to the legend at the bottom of the figure). The contours indicate the high magnetic anomalies of the all magnetic structures map. The thin gray polygons indicate the boundaries of the geological formations. The thick black polygons indicate ROI-1, -4, and -7 within Area 1.

Main Findings

The conductive trends that seem to be coming from magnetic anomalies A and C appear to be merged at mid-depth. Hence, the conductive zone, particularly from magnetic anomaly A, extends deeper.

The Cu value in soil is very anomalous (> 200 ppm) where the two red arrows from magnetic Anomalies A and C merge (see purple circle). The Ni value in soil at the same location is between 40 and 60 ppm (the green star within the purple circle). Immediately north of that point both Cu and Ni exhibit a yellow mark, indicating 75-100 ppm Cu and 60-80 ppm Ni.

On the other hand, more anomalous Cu and Ni in soil is found on the more resistive zones in the north. Hence, deep penetrating geophysical EM methods should be used in the north to thoroughly evaluate its potential.

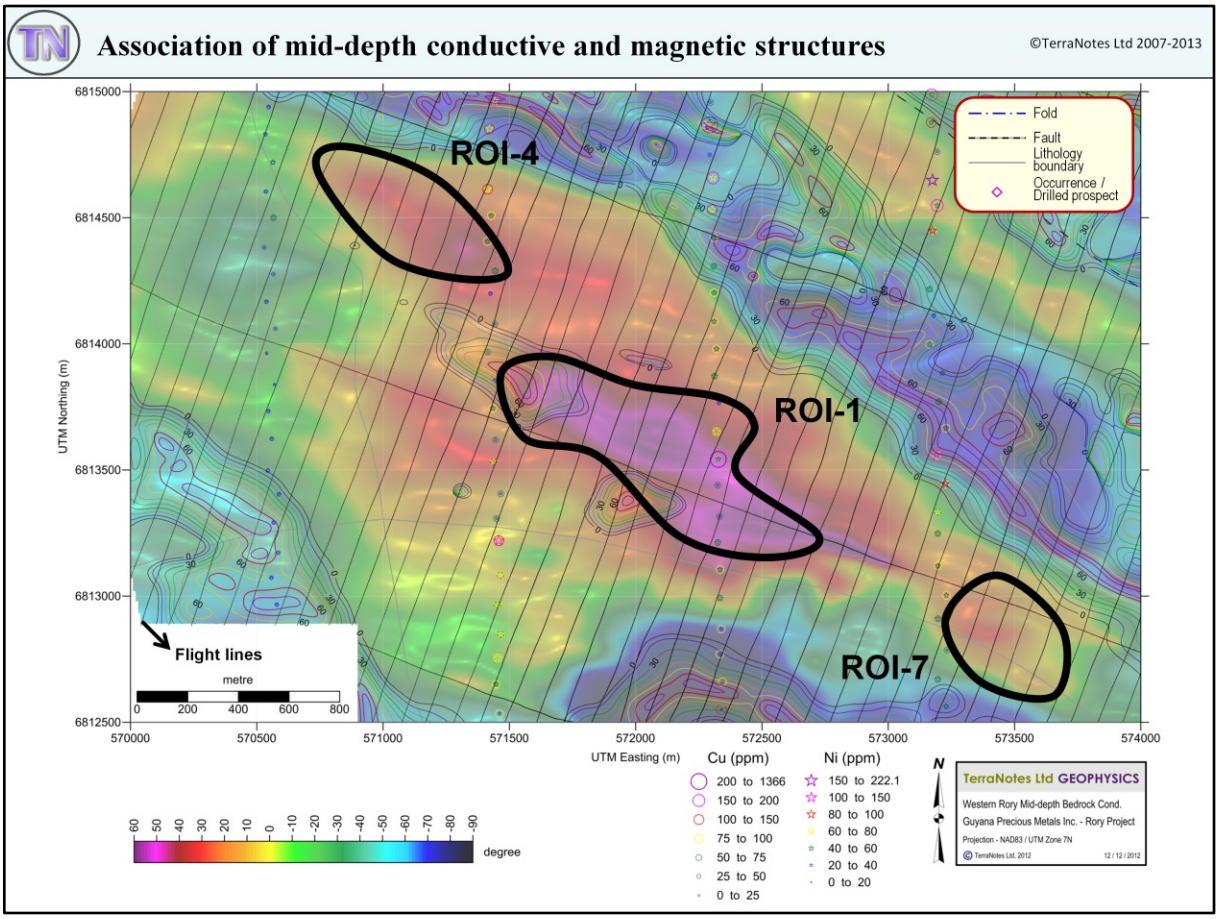


Figure 114. The mid-depth EM amplification map of Area 1. The Ni and Cu anomalies in soil are overlaid on the map as stars and circles respectively (please refer to the legend at the bottom of the figure). The contours indicate the high magnetic anomalies of the all magnetic structures. The thin gray polygons indicate the boundaries of the geological formations. The thick black polygons indicate ROI-1, -4, and -7 within the Area 1.

In the map above, everything above 0° is conductive. A 45° anomaly shows a medium strength conductor and a 90° anomaly indicates a very good conductor.

Main Findings

The mid-depth EM amplification map confirms the interpretation of the previous figure. Traverse and tie-lines of the airborne survey are overlaid to observe if flight-line effects exist. This map indicates few flight line effects outside the ROI.

The conductive background and the non-magnetic zone match well, except for Anomalies A, B, and C. Please see the zero (0) contour of the all magnetic structures in the map above as it approximately contours the conductive zone, particularly in the north.

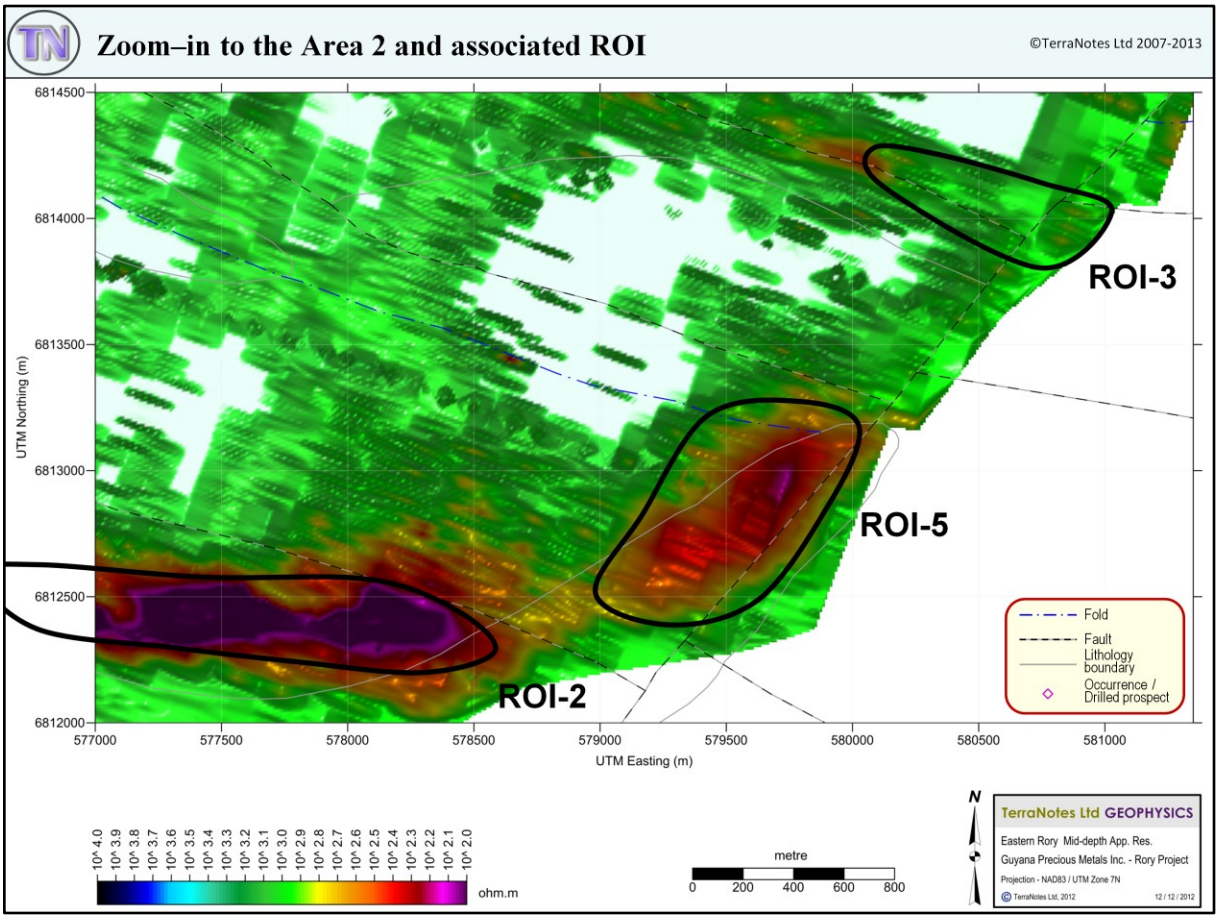


Figure 115. The calculated mid-depth apparent resistivity using co-planar 900 Hz data in Area 2. The gray polygons indicate the boundaries of the geological formations. The dashed black lines indicate the faults/shears and the dashed blue lines indicate fold axes. The black polygons indicate ROI-2, -3, and -5 within Area 2.

Main Findings

ROI-2 is the strongest E-W trending conductor and its resistivity is less than 100 Ω·m at greater depths. Hence, it could be a bedrock conductor.

ROI-3 seems to be extending from the Wellgreen area. Although it seems resistive at mid-depths, it shows some elevated Ni and Cu values in soil. On the other hand, it is located on a small valley and the elevated conductivity at the surface could be due to the erosion (see DTM).

ROI-5 is less resistive than ROI-3 at just above 100 Ω·m. However, it is coincident with the course of Quill Creek and the high conductivity could be due to transported sediments (see next map). Hence, groundtruthing is required before further exploration.

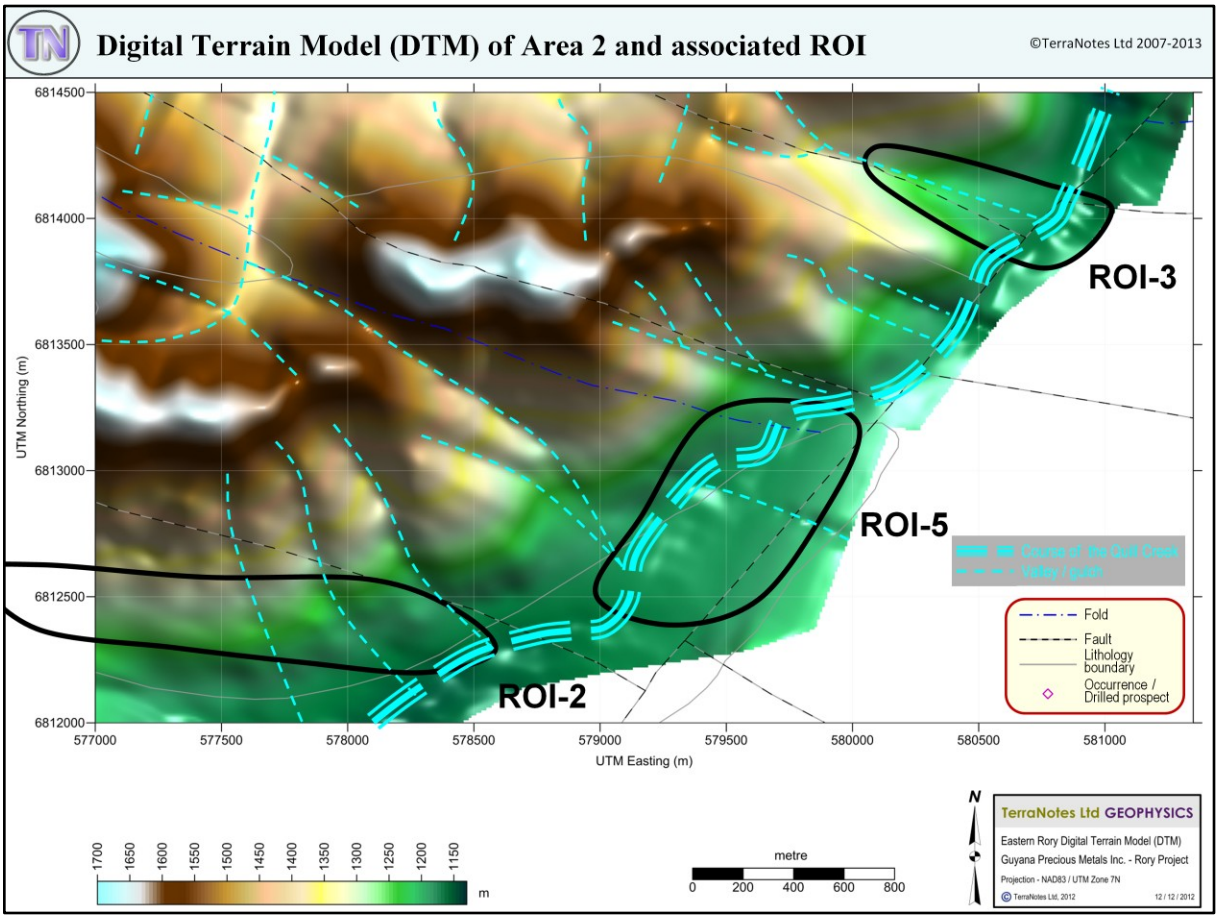


Figure 116. The topography (DTM map) of Area 2. The thin gray polygons indicate the boundaries of the geological formations. The dashed black lines indicate the faults/shears and the dashed blue lines indicate fold axes. The thick black polygons indicate ROI-2, -3, and -5 within Area 2.

Main Findings

The thick cyan line indicate the course of Quill Creek whereas the thin dashed cyan lines mark significant valleys that we have observed on the DTM map.

ROI-5 is coincident with the course of Quill Creek and it runs parallel to the creek.

ROI-3 is perpendicular to Quill Creek, but it is coincident with a small valley. Hence, further work is recommended to validate this anomaly.

ROI-2 is neither parallel to Quill Creek nor the valleys. It is totally independent from topographic effects. It also exhibits the highest conductivity at mid-depth. Therefore we can conclude that ROI-2 is a bedrock conductor at this location.

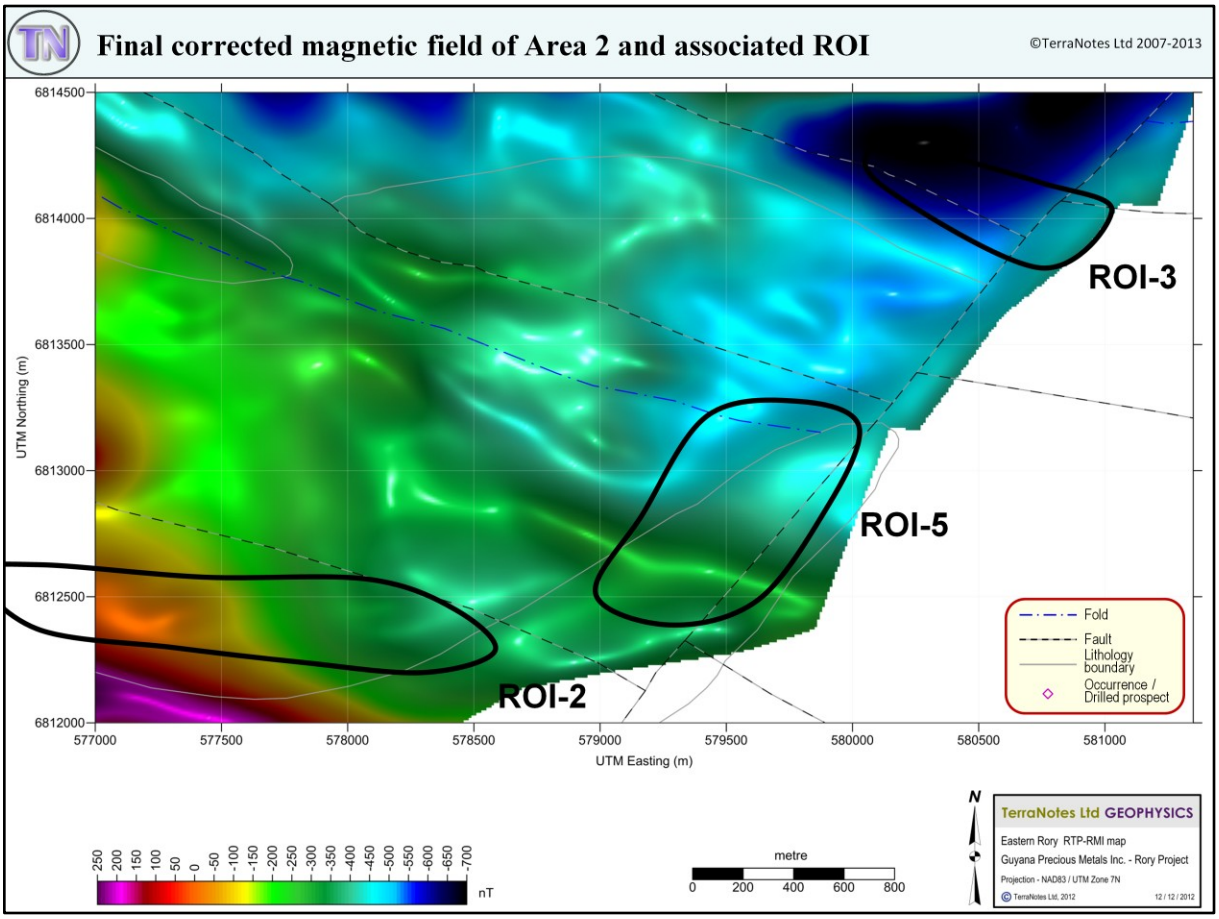


Figure 117. The RTP-RMI map of Area 2. The thin gray polygons indicate the boundaries of the geological formations. The dashed black lines indicate the faults/shears and the dashed blue lines indicate fold axes. The thick black polygons indicate ROI-2, -3, and -5 within Area 1.

Main Findings

There are no significant magnetic anomalies associated with any of the ROI. These ROI is located on a weak magnetic zones because the magnetic intensity values even within ROI-2 are negative.

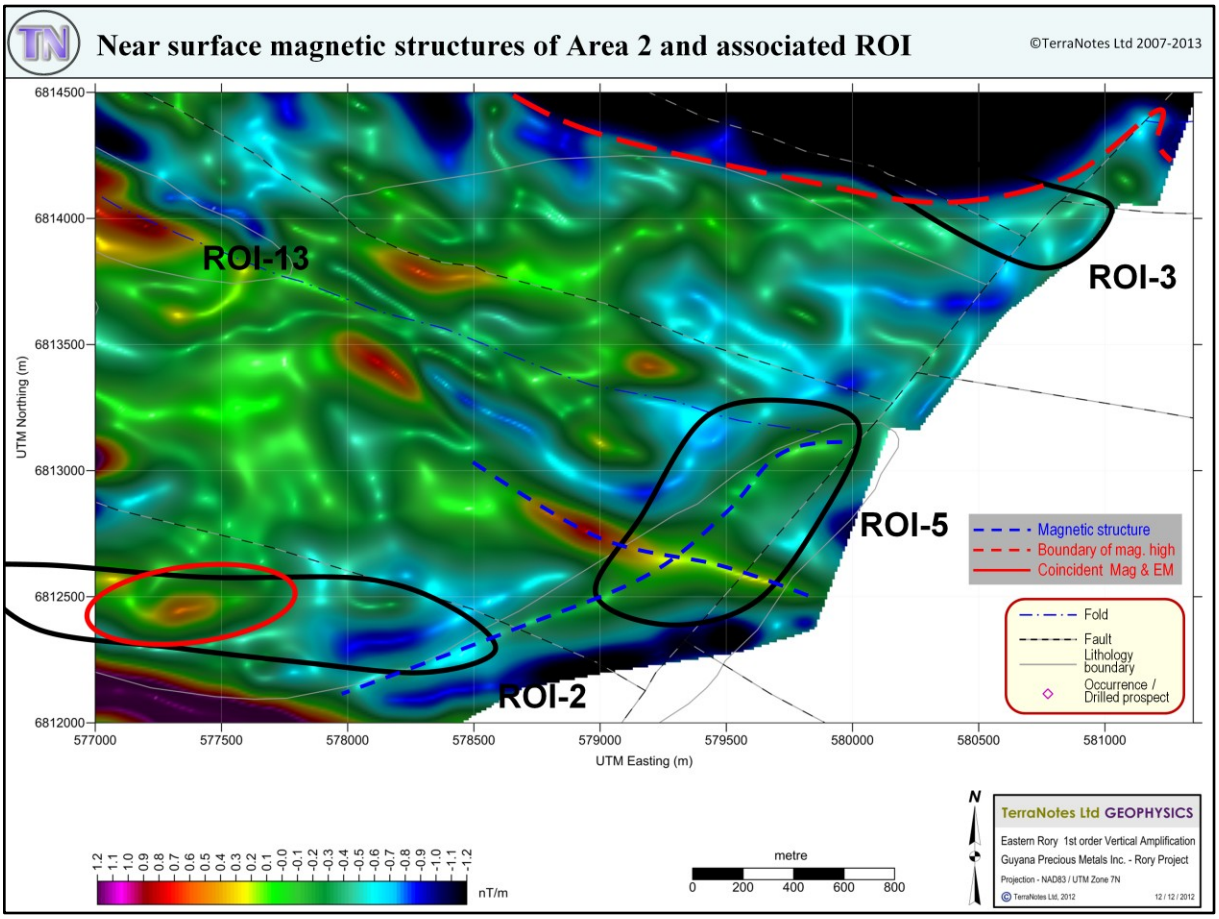


Figure 118. Amplification of the strong, near-surface magnetic anomalies and their structures in detail. The thin gray polygons indicate the boundaries of the geological formations. The dashed black lines indicate the faults/shears and the dashed blue lines indicate fold axes. The thick black polygons indicate ROI-2, -3, and -5 within Area 2.

Main Findings

The red ellipse in the south indicates a local magnetic anomaly which could be a feeder or conduit from a high magnetic trend. It could, therefore, be related to Ni-Cu mineralization.

The red dashed line in the north delineates what appears to be a geological boundary along which ROI-3 is situated.

The dashed blue lines indicate the weak magnetic trends in different directions. They intersect each other within ROI-5.

The eastern tip of ROI-13 is also visible in the near-surface map.

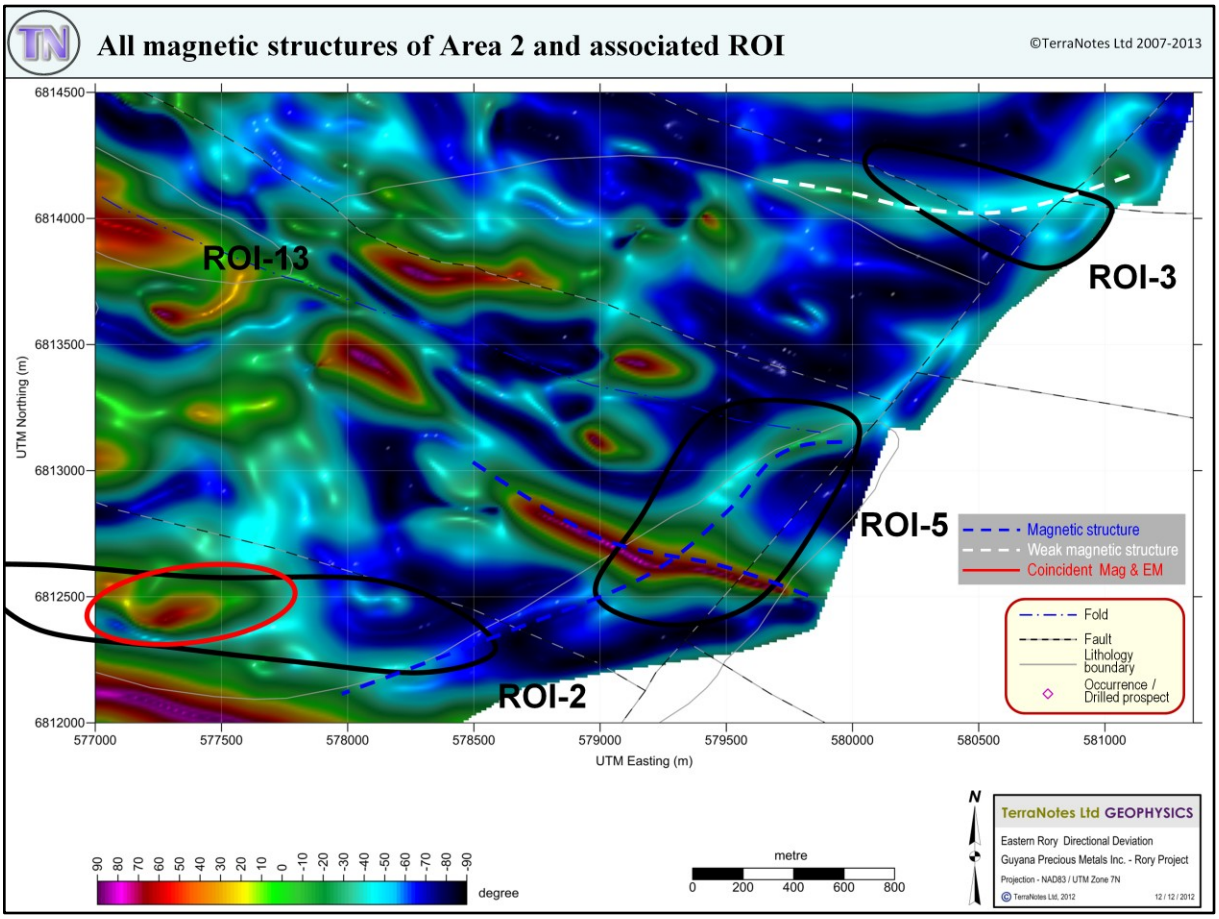


Figure 119. The all magnetic structures map of Area 2. The thin gray polygons indicate the boundaries of the geological formations. The dashed black lines indicate the faults/shears and the dashed blue lines indicate fold axes. The thick black polygons indicate ROI-2, -3, and -5 within Area 2.

Main Findings

The red ellipse anomaly within ROI-2 is still present (first observed in Figure 118) and it is a very weak magnetic anomaly since it is much less than 90^{o} in its strength.

The NW-SE trending dashed blue line is stronger than the SW-NE trending one. Hence, the magnetic anomaly trending parallel to Quill Creek is very weak.

The white dashed line could also indicate a very weak magnetic trend within ROI-3.

Please note that the pink anomalies are more accurate where as the other colours, particularly cyan and green, could be an effect of noise in the magnetic data.

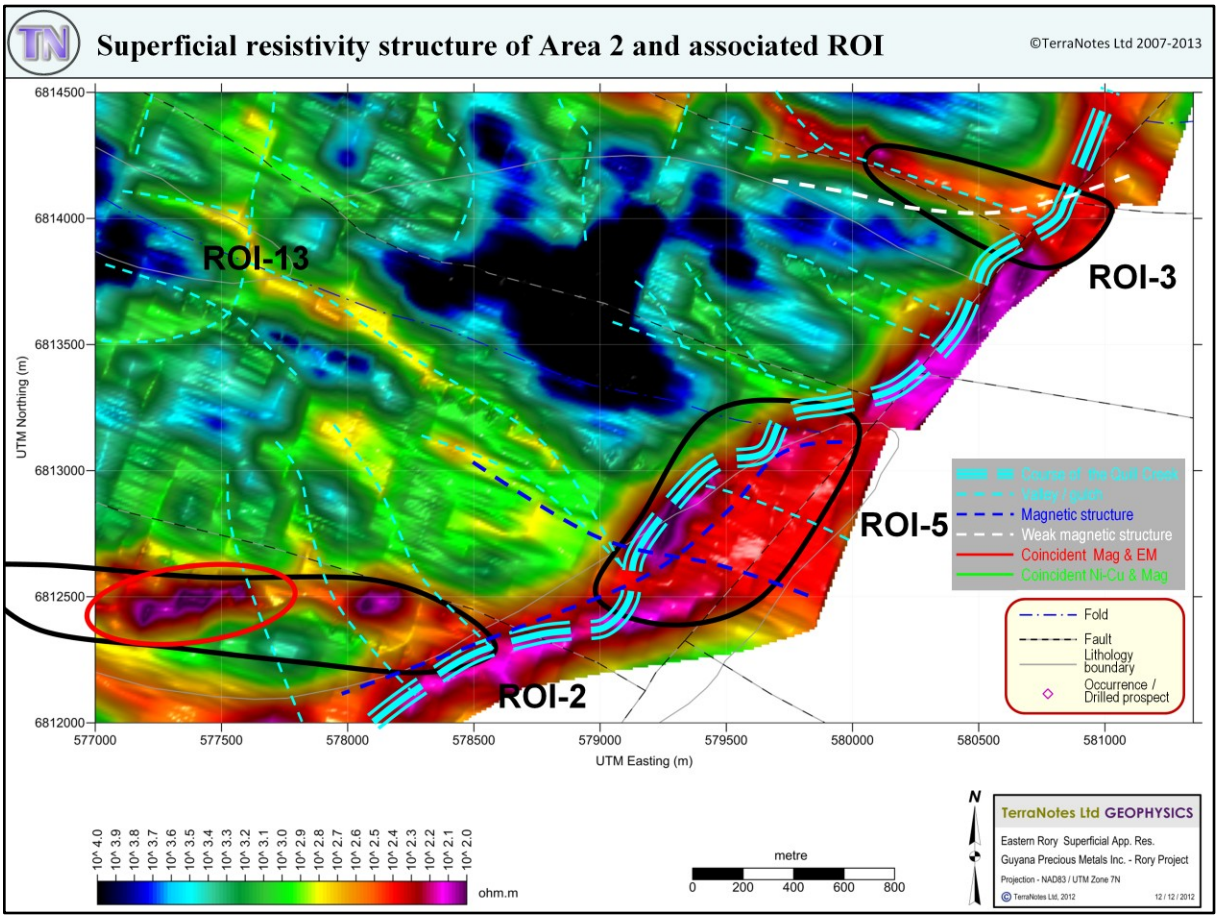


Figure 120. The surficial apparent resistivity map of Area 2. The thin gray polygons indicate the boundaries of the geological formations. The dashed black lines indicate the faults/shears and the dashed blue lines indicate fold axes. The thick black polygons indicate ROI-2, -3, and -5 within Area 2. The thick cyan line indicates the course of Quill Creek and the thin dashed cyan lines mark significant valleys that have been observed on the DTM map. The red ellipse indicates the weak magnetic anomaly within ROI-2. The dashed white line indicates a very weak magnetic trend within ROI-3 and the dashed blue lines indicate weak magnetic trends in ROI-5.

Main Findings

All the ROI are conductive in the surficial apparent resistivity map.

The conductive anomaly at ROI-2 is exactly coincident with the weak magnetic anomaly (red ellipse), forming an interesting structure in terms of further Ni-Cu exploration.

The conductive trend in ROI-3 follows a valley (dashed cyan line) instead of the magnetic trend (dashed white line). Thus, it becomes an secondary target.

The most conductive anomaly at ROI-5 also follows the course of Quill Creek at the surface.

The ROI-13 appears resistive at surface.

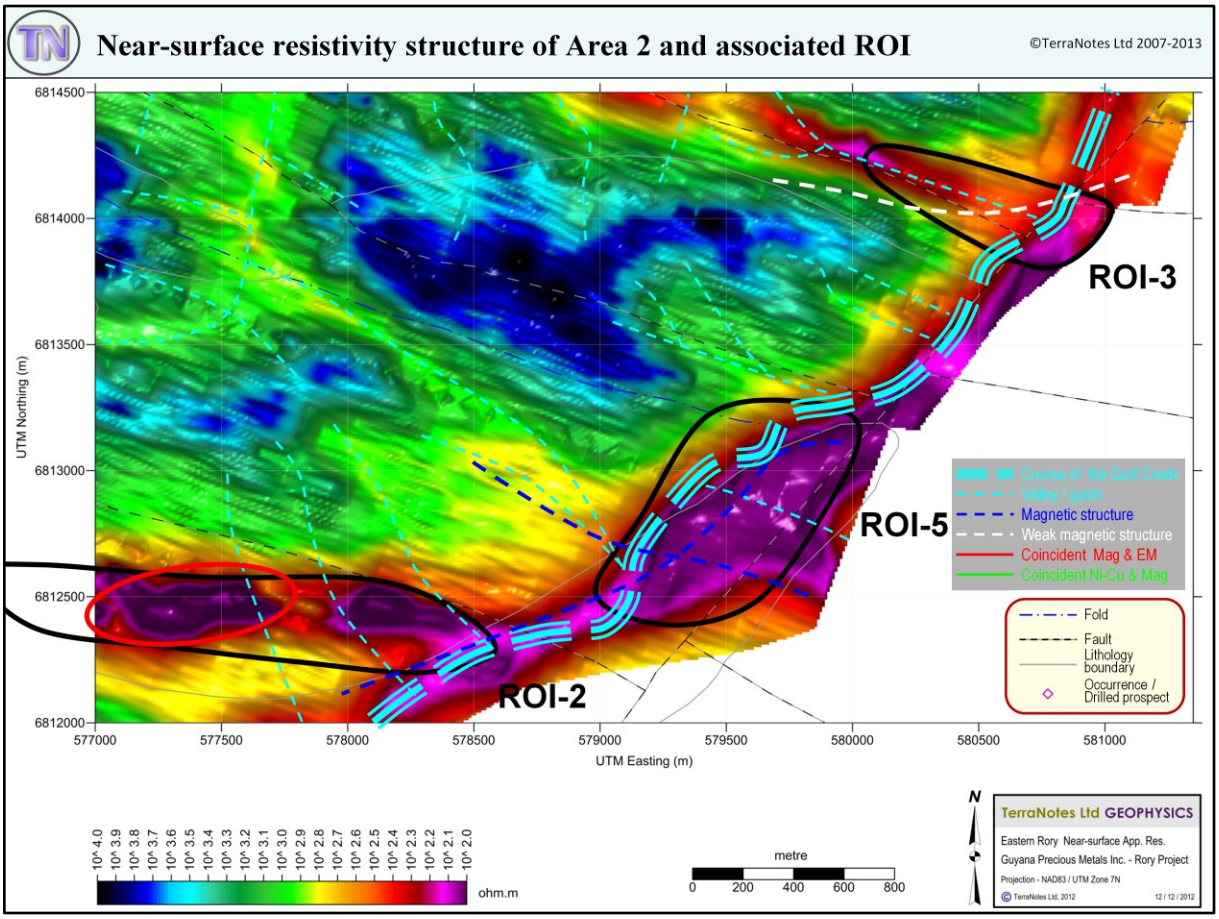


Figure 121. The near-surface apparent resistivity map of Area 2. The thin gray polygons indicate the boundaries of the geological formations. The dashed black lines indicate the faults/shears and the dashed blue lines indicate fold axes. The thick black polygons indicate ROI-2, -3, and -5 within Area 2. The thick cyan line indicates the course of Quill Creek whereas the thin dashed cyan lines mark significant valleys observed on the DTM map. The red ellipse indicates the weak magnetic anomaly within ROI-2. The dashed white line indicates a very weak magnetic trend within ROI-3 and the dashed blue lines indicate weak magnetic trends in ROI-5.

Main Findings

All the ROI are also conductive in the near-surface apparent resistivity map.

The conductive anomalies within ROI-2 become even stronger and thicker below the surface. It still coincides with the weak magnetic anomaly.

The strength of the conductive zone at ROI-3 remains the same and it still follows a valley.

The conductive zone at ROI-5 becomes stronger immediately below the surface and is shifted further east. Now, instead of the course of Quill Creek (thick cyan line), it coincides with a weak magnetic trend (dashed blue line). Hence, it may be associated with mineralization.

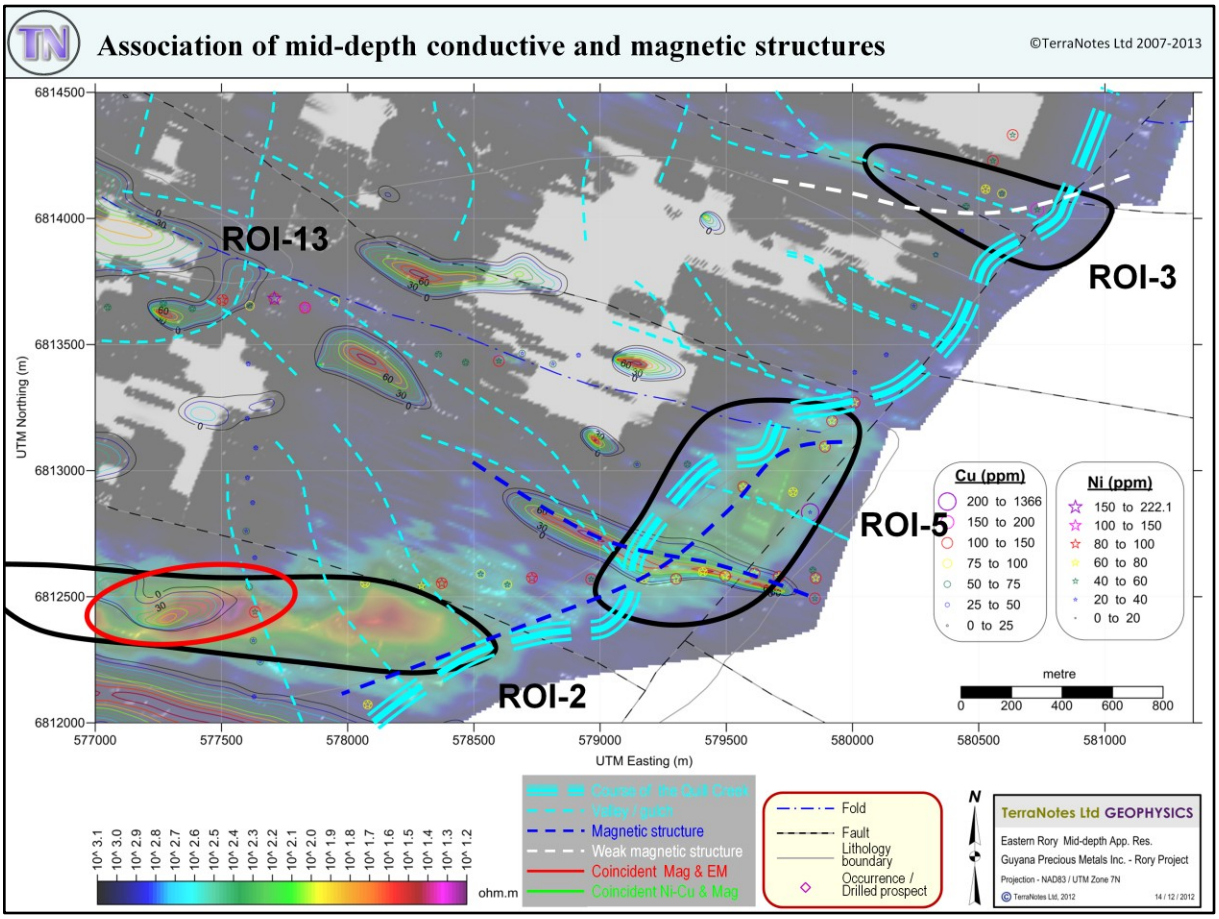


Figure 122. The mid-depth apparent resistivity map of Area 2. The Ni and Cu anomalies in soil are overlaid on the map as stars and circles, respectively (please refer to the legend at the bottom of the figure). The contours indicate the high magnetic anomalies of the all magnetic structures map. The thin gray polygons indicate the boundaries of the geological formations. The dashed black lines indicate the faults/shears and the dashed blue lines indicate fold axes. The thick black polygons indicate ROI-2, -3, and -5 within Area 2. The thick cyan line indicates the course of Quill Creek and the thin dashed cyan lines mark significant valleys that have been observed on the DTM map. The red ellipse indicates a weak magnetic anomaly within ROI-2. The dashed white line indicates a very weak magnetic trend within ROI-3 and the dashed blue lines indicate weak magnetic trends in ROI-5. Please note that different colour limits have been used in this figure to see the full strength of the anomalies and to better differentiate them.

Main Findings

The red ellipse shows the coincident weak magnetic anomaly and the strong mid-depth conductor. The resistivity value is approximately 15 Ω·m (~10^1.2), which is low enough to say it could be a sulphide mineralization. Hence, the red ellipse area is a high priority target for Ni-Cu mineralization. If the future results from this location are positive, the mineralization may extend further east and west (not shown above).

The conductor within ROI-3 has completely disappeared. There is a weak conductive zone only at the western extension. Since the conductivity decreased with depth it is probably a surficial conductor.

The conductivity at ROI-5 also decreased with depth. It was less than 100 Ω·m in the near-surface (Figure 121) but it is more than 200 Ω·m at mid-depth. Therefore, this might be a weak conductor in the near-surface due to an alteration. This possible alteration should be investigated further to observe if it is associated with Ni-Cu mineralization.

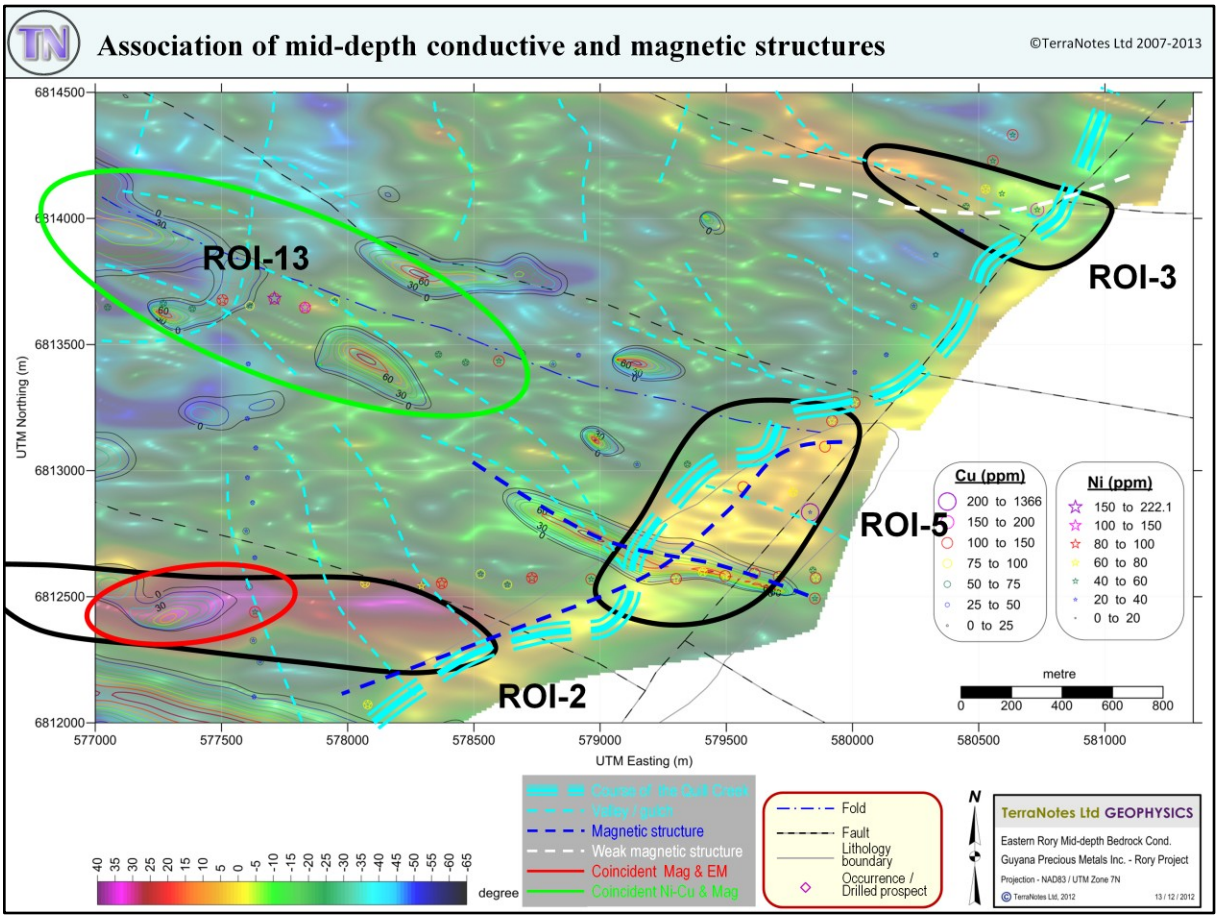


Figure 123. The mid-depth EM amplification map of Area 2. The Ni and Cu anomalies in soil are overlaid on the map as stars and circles, respectively (please refer to the legend at the bottom of the figure). The contours indicate the high magnetic anomalies of the all magnetic structures map. The thin gray polygons indicate the boundaries of the geological formations. The dashed black lines indicate the faults/shears and the dashed blue lines indicate fold axes. The thick black polygons indicate ROI-2, -3, and -5 within Area 2. The thick cyan line indicates the course of Quill Creek and the thin dashed cyan lines mark significant valleys that have been observed on the DTM map. The red ellipse indicates the weak magnetic anomaly within ROI-2. The dashed white line indicates a very weak magnetic trend within ROI-3 and the dashed blue lines indicate weak magnetic trends in ROI-5.

In the map above, everything above 0° degree is conductive. A 45° anomaly indicates a medium strength conductor and a 90° anomaly indicates very good conductor.

Main Findings

This map suggests a medium strength conductor at ROI-2 since it is close to 45°, and very weak conductors at ROI-3 and ROI-5 since they are just above 0°.

All the ROI show some elevated Ni and Cu anomalies in soil.

The green ellipse shows additional Ni and Cu anomalies near the weak magnetic anomalies in the north (ROI-13). There is also a embayment-like magnetic structure at this end. This region shows a similar characteristics to ROI-11 as it does show high resistivity and it could be its southeastern extension. If the future results from ROI-11 are positive, the same mineralization may extend beneath this area (green ellipse).



TerraNotes Ltd GEOPHYSICS

©TerraNotes Ltd 2007-2013

Conclusions & Recommendations

Conclusions

©TerraNotes Ltd 2007-2013

- High magnetic anomalies were mapped using the final corrected magnetic field and were interpreted as the ultramafic rocks and the gabbro intrusion.
- Weak magnetic anomalies were enhanced with the amplification techniques and were all identified in the interpretation section. Most of these anomalies were marked as mafic rocks of the Nicolai formation or as conduit/feeder zones.
- The contact zones of all the magnetic structures were delineated since the contacts are very important to reveal the possible Ni-Cu-PGE mineralization zones.
- All the EM conductors were identified with the raw and amplified EM maps. These EM results were integrated both visually and mathematically with the topography and magnetic maps. As a result of this procedure, strong bedrock conductors were separated from the near-surface weak conductors.
- Coincident magnetic and conductive zones were selected as the high priority targets for Ni-Cu-PGE mineralization because of their similar characteristics to the Wellgreen deposit.
- Cu and Ni anomalies in soil were overlaid on the geophysical maps and the high magnetic zones in the northern Rory and gabbroic intrusion area are found to be interesting for further exploration. Since there are no coinciding conductors, these high magnetic anomalies are selected as secondary targets.
- A total of sixteen (16) Regions of Interest (ROI) are selected for further exploration. These ROIs are classified into two groups: 1) the first nine are the cyan group and they are conductive ROI, and 2) the second seven are green group and they are magnetic ROI.
- Outside the Rory claim group, 5 EM anomalies and two magnetic anomalies are selected as further ROI in Wellgreen and Arch properties.
- The ROI-1 and the ROI-2 are selected as the most important coincident magnetic and EM anomalies. Close-up maps and interpretations were given in the vicinity of these ROI.

Recommendations

©TerraNotes Ltd 2007-2013

- Further geological, geochemical and groundtruthing survey could be performed on the coincident conductive and magnetic regions of interest (ROI-1 and -2).
- Further soil geochemistry overlays should be done for the full interpretation and assessment of the distal/proximal mineralization zones.
- The integrated products of soil geochemistry such as chalcophile index and/or geochemistry ratios should be calculated and overlaid on the geophysical maps to better characterize the sulphide mineralization.
- Deep penetrating EM methods should be deployed particularly on the Ni and Cu rich, resistive and magnetic anomalies (ROI-10 – 16). Magnetic and EM modelling and inversion procedures should be performed for these data before further work.
- If any drill holes exist in the future, correlation between Diamond Drill Holes core analyses and geophysical data should be performed to extend the known mineralization zones of interest. The results of the DDH (such as mineralization, alteration, lithology and structures such as faults and shear zones) can be overlaid on these geophysical maps to extend the zones of interest defined by the DDH analyses.
- Additional geophysical, geological, geochemical and drill hole data could be used in the next phase of the TerraNotes Workflow™, which is highly recommended to re-produce maps of very detailed, localized magnetic and electromagnetic anomalies for each ROI. These maps will also delineate the contacts, possible localized fractures, faults and shears. Such highly detailed maps may be crucial in the design of the drilling grid and the placement of collars.

Copyright

©TerraNotes Ltd 2007-2013

© 2007-2012 TerraNotes Ltd

This Document for Review and its content are protected by Canadian and international copyright law. The copyright owner is TerraNotes Ltd.

The Company cited on the Cover Page of this Document is allowed to publish excerpts from this Document to include in News Releases, Property Assessment filings, Corporate Web Site and Corporate Literature as per signed agreement.

Disclaimer

©TerraNotes Ltd 2007-2013

This report has been prepared exclusively for Guyana Precious Metals Inc. It is not intended for public information. The report reflects the professional opinion of TerraNotes Ltd. based on the data and information provided by Guyana Precious Metals Inc. TerraNotes Ltd. will not assume or otherwise accept responsibility or liability for losses incurred by Guyana Precious Metals Inc. or other parties as a result of the circulation, publication, reproduction, use of or reliance on this report contrary to the provisions discussed in this paragraph.

As per Agreement between Guyana Precious Metals Inc. and TerraNotes Ltd. pertaining to this project, Guyana Precious Metals Inc. understands and agrees that it is quite possible that errors and omissions may occur in data input and/or programming to convert the data in the form desired, and Guyana Precious Metals Inc. further understands and agrees that the data may not meet user's standards as to accuracy or completeness; notwithstanding, Guyana Precious Metals Inc. agrees to take the data "as is", fully expecting that there may well be errors and omissions in the data obtained from TerraNotes Ltd.

TerraNotes Ltd. has checked with sources believed to be reliable in their efforts to provide information that is accurate, comprehensive, and timely at the date of publication. However, human error and changes may occur. Guyana Precious Metals Inc. further understands that TerraNotes Ltd. has produced this document in good faith with the information available at the date of production of this report and makes absolutely no warranty whatsoever, whether expressed or implied, as to the accuracy, thoroughness, value, quality, validity, suitability, condition, or fitness for a particular purpose of the data or any programming used to obtain the data, nor as to whether the data is error-free, up-to-date, complete or based upon accurate meaningful facts.



©TerraNotes Ltd 2007-2013

APPENDIX A

Separation of Magnetic Field

Regional and Local

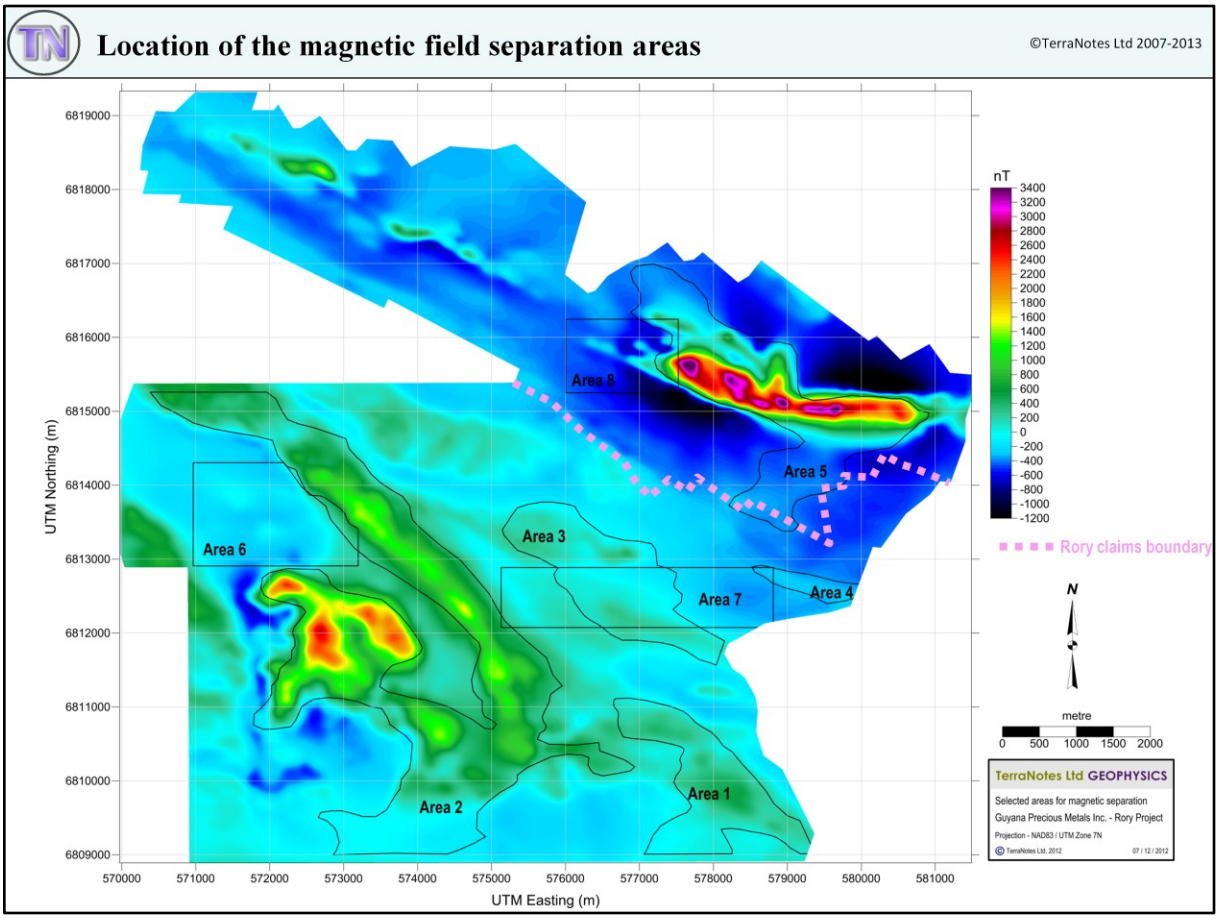


Figure A-1. The final corrected magnetic field with the boundaries of the selected areas for magnetic field separation procedure. The black polygons indicate those boundaries. The pink dotted line approximately separates the Rory claims from the other claims.

Main Findings

Local magnetic field and regional magnetic field are calculated for each area (black polygon) and the results are demonstrated in the following figures.

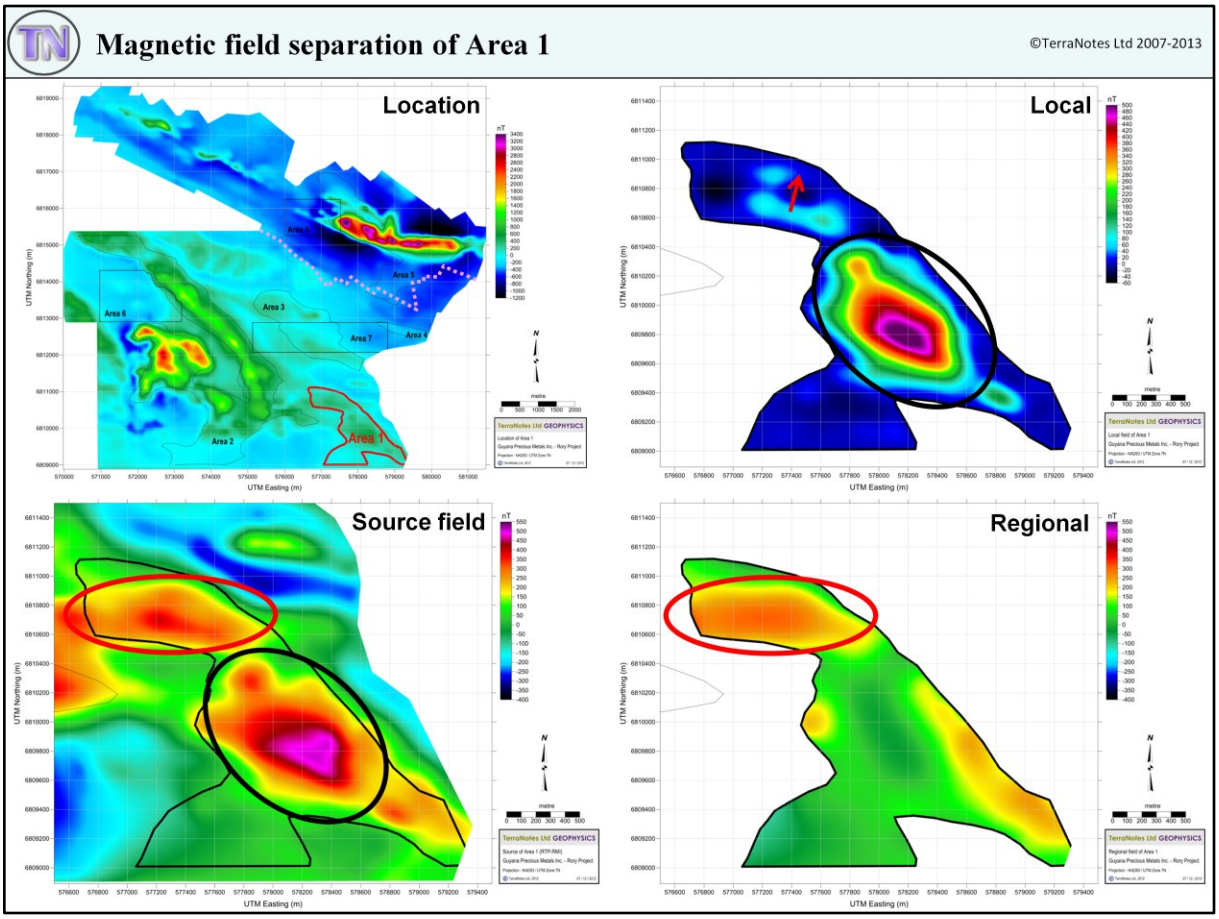


Figure A-2. The top left panel is the same map as Figure A-1 with the Area 1 boundary highlighted with the thick red polygon. The bottom left panel is the zoomed-in map of Area 1 and the thick black polygon shows the area of the source field for the magnetic field separation calculation. The top right panel is the local magnetic field calculated from the source field (bottom left panel) and the bottom right panel is the regional magnetic field calculated from the source field (bottom left panel).

Main Findings

As seen in the above map, Area 1 has moderate magnetic intensity anomalies at the southeast part of the Rory claims. When it was separated into the regional and local field, it was observed that the northern anomaly is more regional and deeper, whereas the southern anomaly is more local and shallow.

The black ellipse shows the local magnetic anomaly with 550 nT intensity. This could be a priority target within Area 1 in terms of magnetic strength but please note that there is an EM anomaly associated with this Area.

The red ellipse encompasses the regional and deeper magnetic anomaly. In the local field map, the only visible anomaly is in its southern part, which may suggest a dipping to the N-NE (see red arrow).

Please note that magnetic field separation algorithm is still in development and is not entirely validated. The reader should be cautious while applying these interpretation to their work.

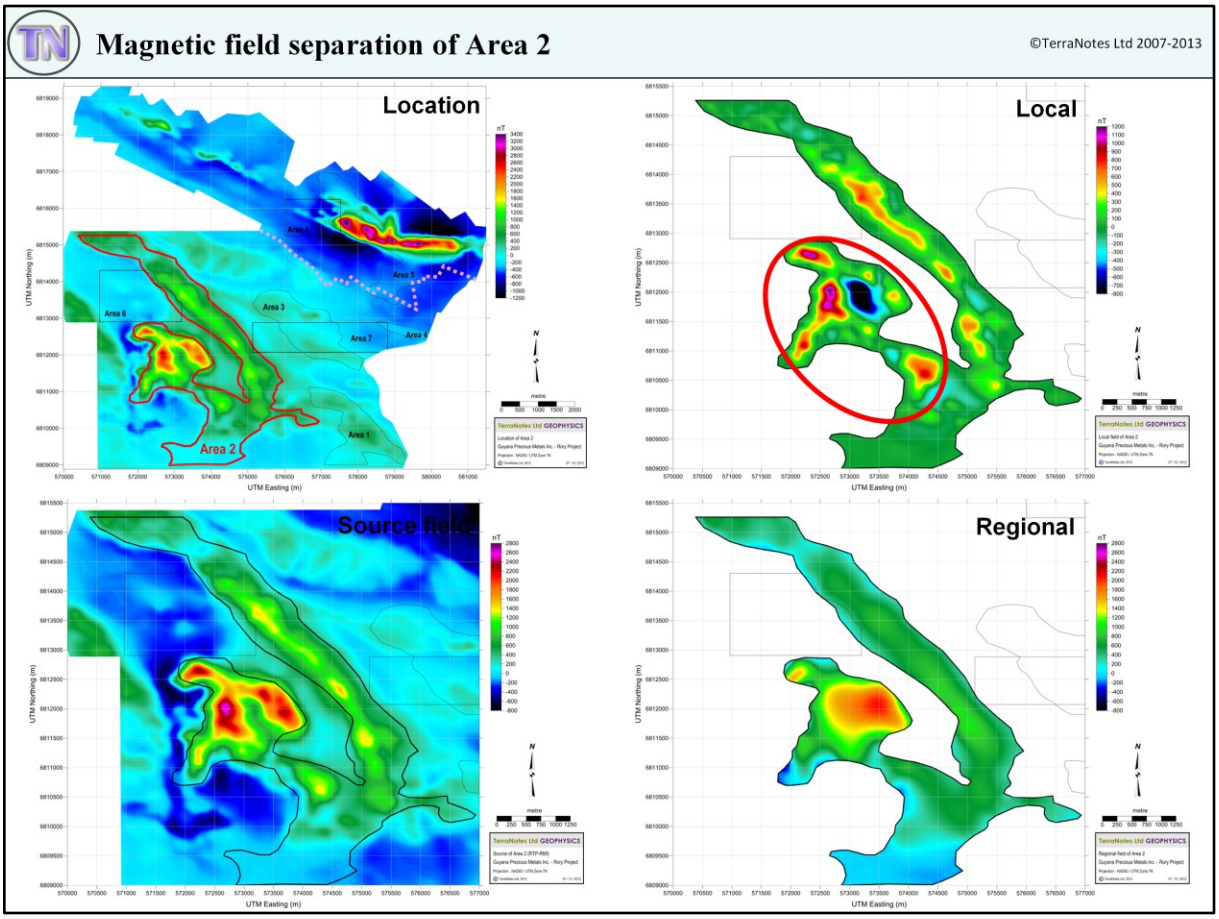


Figure A-3. The top left panel is the same map as Figure A-1 with the Area 2 boundary highlighted with the thick red polygon. The bottom left panel is the zoomed-in map of Area 2 and the thick black polygon shows the area of the source field for the magnetic field separation calculation. The top right panel is the local magnetic field calculated from the source field (bottom left panel) and the bottom right panel is the regional magnetic field calculated from the source field (bottom left panel).

Main Findings

Area 2 has strong magnetic intensity anomalies and it can be observed on both regional and local fields. This observation may suggest that these anomalies start near the surface and extend to the deeper parts of the claim group.

The red ellipse indicates the near surface variations within the Kluane Range Plutonic Suites (EKK). Please note that these variations could be due to more mafic to ultramafic rocks such as gabbro.

Please note that magnetic field separation algorithm is still in development and is not entirely validated. The reader should be cautious while applying these interpretation to their work.

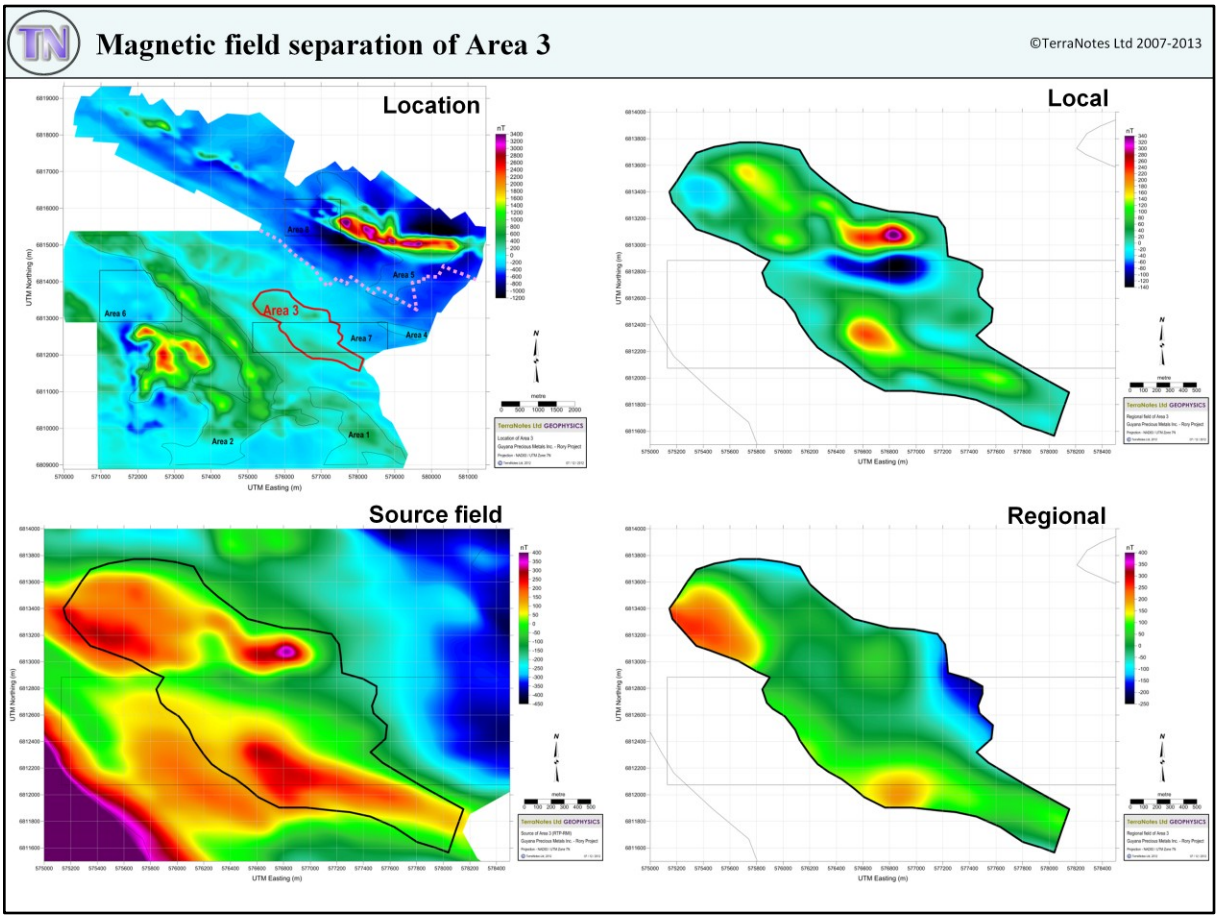


Figure A-4. The top left panel is the same map as Figure A-1 with the Area 3 boundary highlighted with the thick red polygon. The bottom left panel is the zoomed-in map of Area 3 and the thick black polygon shows the area of the source field for the magnetic field separation calculation. The top right panel is the local magnetic field calculated from the source field (bottom left panel) and the bottom right panel is the regional magnetic field calculated from the source field (bottom left panel).

Main Findings

Area 3 has intermediate magnetic intensities and the anomalies can be seen on both local and regional magnetic fields. Therefore, these anomalies also start at near-surface and they extend to deeper parts.

The local magnetic highs and lows could be used and modelled for further exploration.

The observed shift between the local and regional magnetic anomalies may suggest a dipping to the south.

Please note that magnetic field separation algorithm is still in development and is not entirely validated. The reader should be cautious while applying these interpretation to their work.

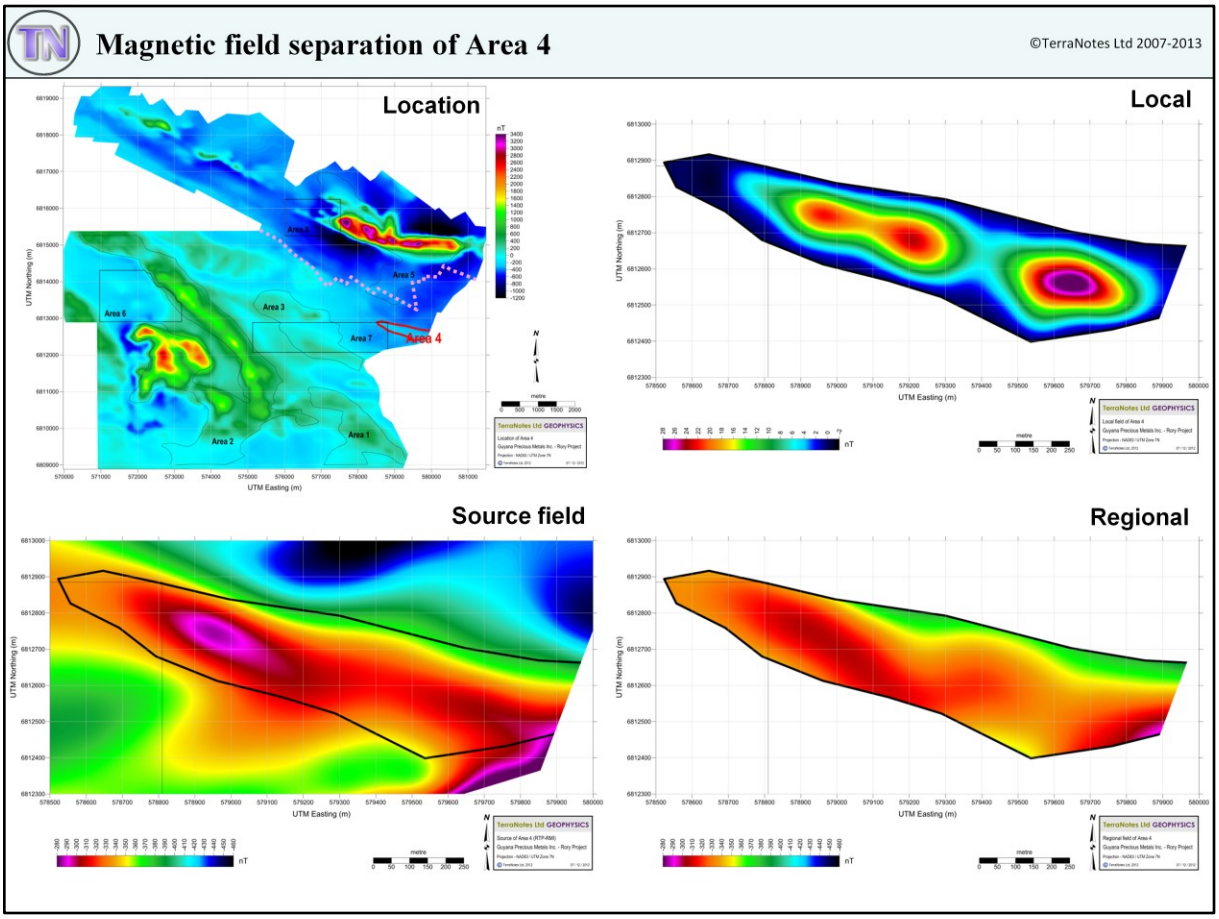


Figure A-5. The top left panel is the same map as Figure A-1 with the Area 4 boundary highlighted with the thick red polygon. The bottom left panel is the zoomed-in map of Area 4 and the thick black polygon shows the area of the source field for the magnetic field separation calculation. The top right panel is the local magnetic field calculated from the source field (bottom left panel) and the bottom right panel is the regional magnetic field calculated from the source field (bottom left panel).

Main Findings

Area 4 is a small scale, weak magnetic anomaly with negative intensities on the residual map (see source field).

This weak anomaly also extends deeper but the local field map gives the detailed structure at near-surface.

Please note that magnetic field separation algorithm is still in development and is not entirely validated. The reader should be cautious while applying these interpretation to their work.

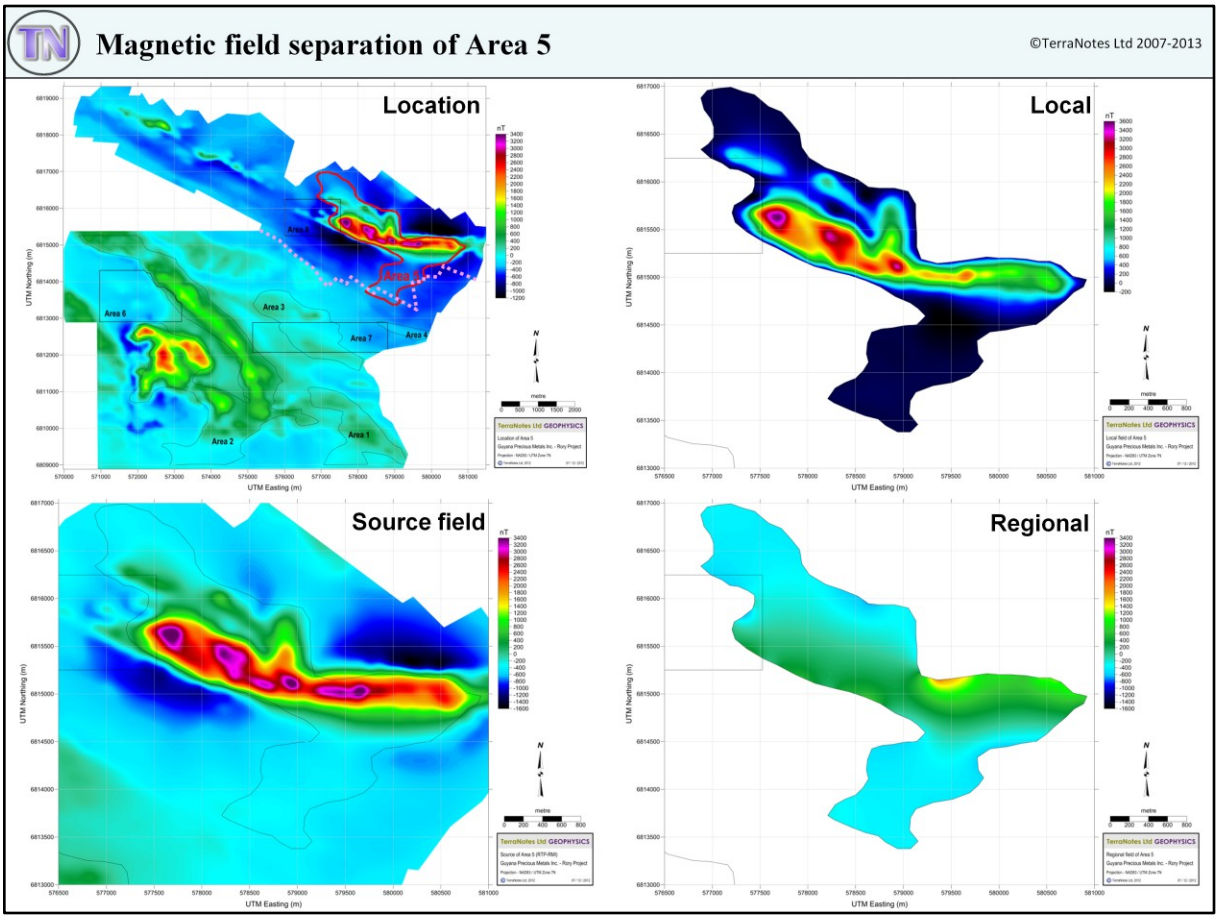


Figure A-6. The top left panel is the same map as Figure A-1 with the Area 5 boundary highlighted with the thick red polygon. The bottom left panel is the zoomed-in map of Area 5 and the thick black polygon shows the area of the source field for the magnetic field separation calculation. The top right panel is the local magnetic field calculated from the source field (bottom left panel) and the bottom right panel is the regional magnetic field calculated from the source field (bottom left panel).

Main Findings

Area 5 has the strongest magnetic anomaly in the survey area, and it is due to the ultramafic rocks which are also associated with the Wellgreen mineralization.

The local part of anomaly is very strong, it shows that the ultramafic rocks are near the surface.

The regional part has more intermediate magnetic intensities indicating that it extends deeper but not very deep. The ultramafic rocks at this location probably overly the Skolai formation.

Please note that Anomaly A is observed in this area. Hence the modelling work of the local field may help to understand the underground structure better and will allow more accurate selection of drill hole targets.

Please note that magnetic field separation algorithm is still in development and is not entirely validated. The reader should be cautious while applying these interpretation to their work.

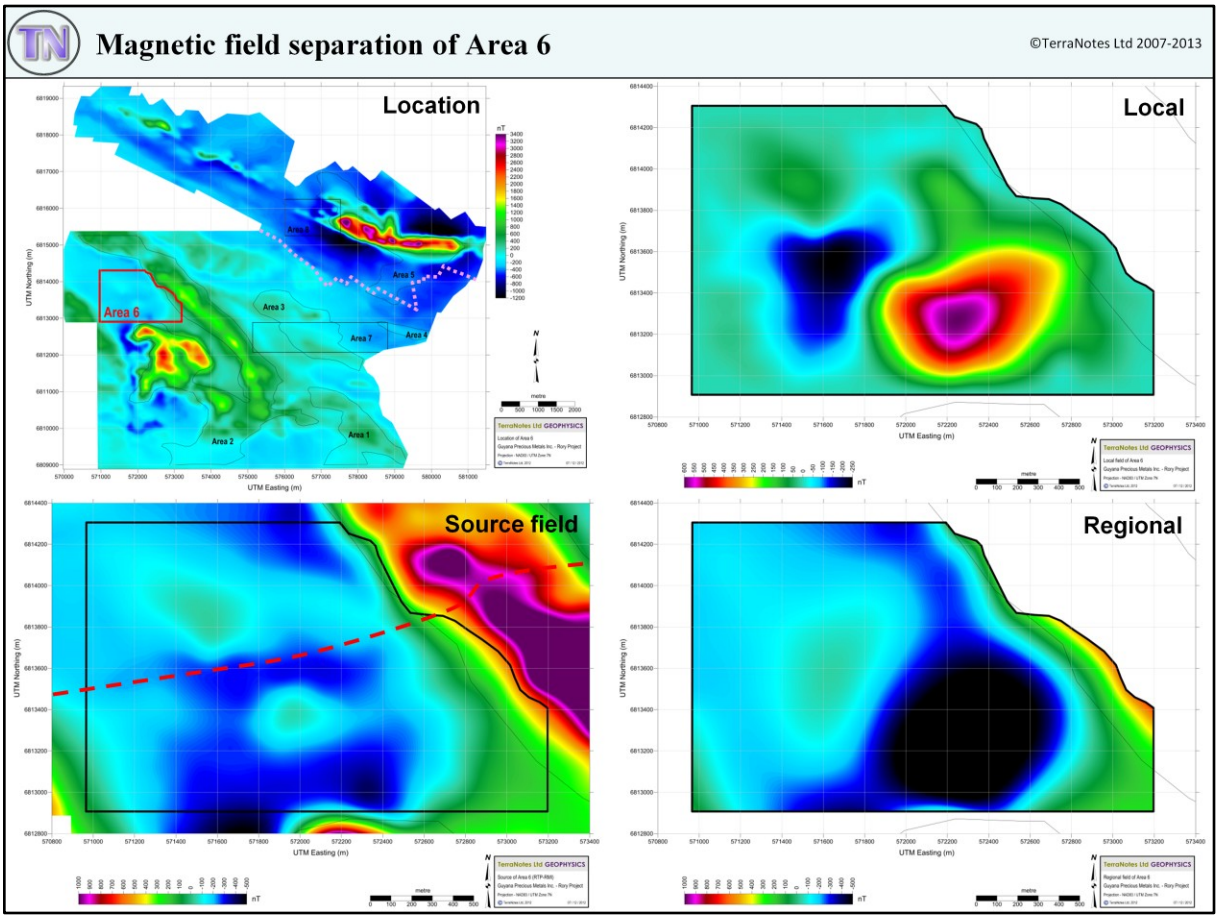


Figure A-7. The top left panel is the same map as Figure A-1 with the Area 6 boundary highlighted with the thick red polygon. The bottom left panel is the zoomed-in map of Area 6 and the thick black polygon shows the area of the source field for the magnetic field separation calculation. The top right panel is the local magnetic field calculated from the source field (bottom left panel) and the bottom right panel is the regional magnetic field calculated from the source field (bottom left panel).

Main Findings

Area 6 has a very weak magnetic anomaly (just above zero) but it is coincident with the conductive Anomaly B.

It shows that the magnetic anomaly was split into two pieces due to the E-W trending fault-like structures as it was marked with red dashed line.

The local magnetic anomaly is unexpectedly high and large in the south. The reason for this is that the regional anomaly has one large low in the southeast and one large intermediate high in the northwest. This may suggest a strong mineralization in the southeast and a thicker mineralization in the northwest.

On the other hand, this weak anomaly is situated in between the two strong magnetic field zones in the south and northeast (as shown in Area 2). Hence, the result may be influenced by these nearby strong anomalies and it exhibits the artifacts due to strong anomalies. We strongly recommend validating this calculation with further calculations before it is used for further modelling.

Please note that magnetic field separation algorithm is still in development and is not entirely validated. The reader should be cautious while applying these interpretation to their work.

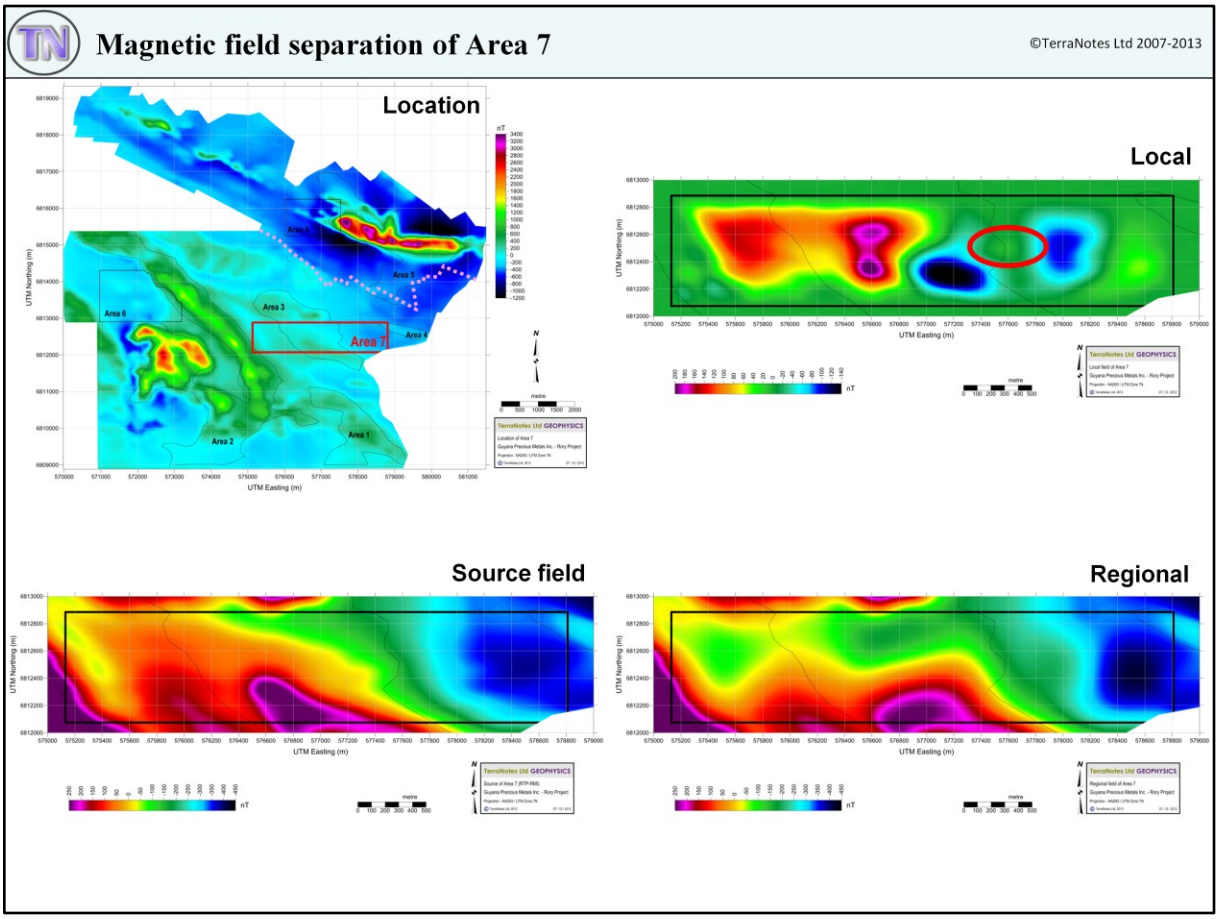


Figure A-8. The top left panel is the same map as Figure A-1 with the Area 7 boundary highlighted with the thick red polygon. The bottom left panel is the zoomed-in map of Area 7 and the thick black polygon shows the area of the source field for the magnetic field separation calculation. The top right panel is the local magnetic field calculated from the source field (bottom left panel) and the bottom right panel is the regional magnetic field calculated from the source field (bottom left panel).

Main Findings

According to the results given above, the western part has regionally high magnetic intensities whereas the eastern part has low intensities. We have expected to see an E-W trending local anomaly which would coincide with the conductive Anomaly E but this magnetic anomaly is not very strong.

The red ellipse above shows the weak local magnetic anomaly that coincides with the strongest part of the conductive Anomaly E.

A detailed ground geophysical survey (Magnetic and EM), along with the geology and geochemistry is recommended for this target to understand its nature and to select drill targets at this location.

Please note that magnetic field separation algorithm is still in development and is not entirely validated. The reader should be cautious while applying these interpretation to their work.

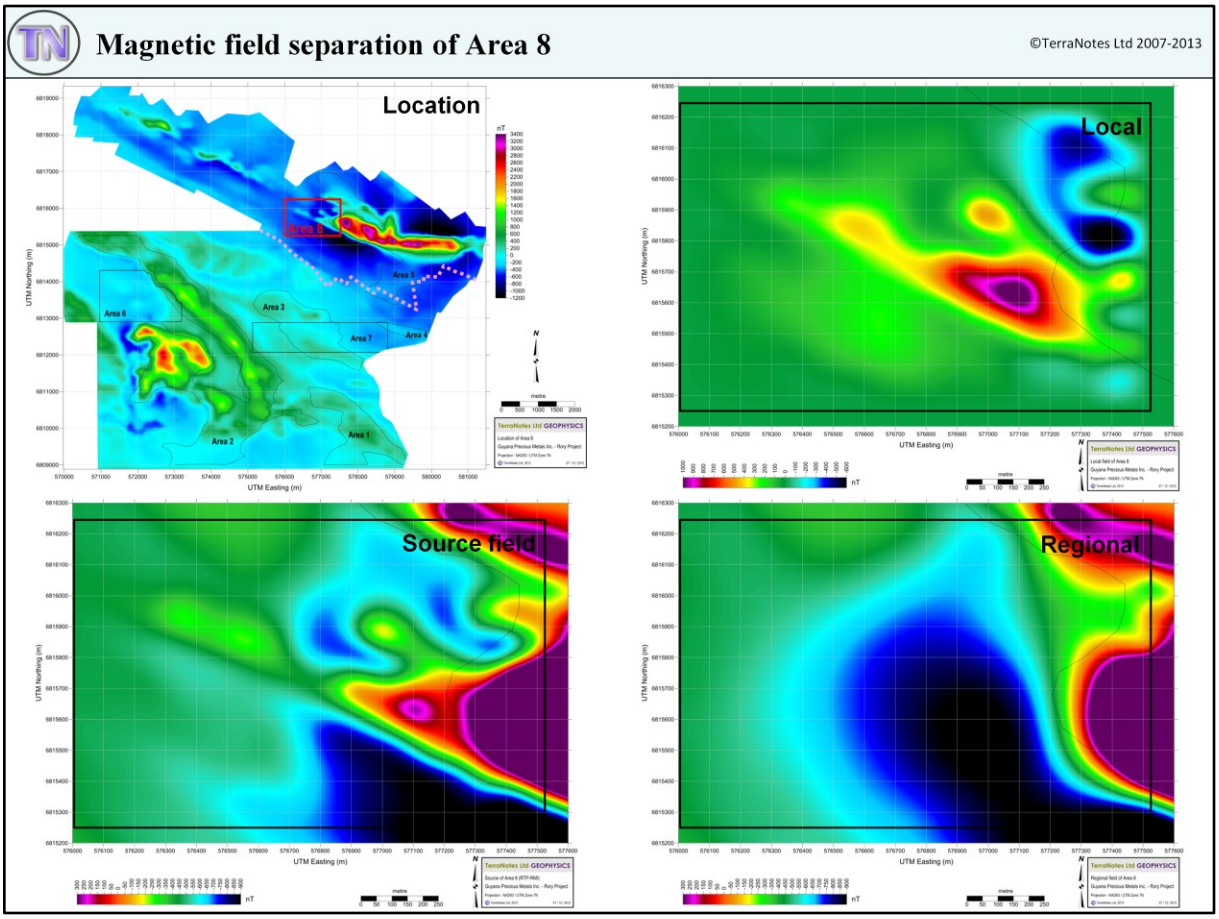


Figure A-9. The top left panel is the same map as Figure A-1 with the Area 8 boundary highlighted with the thick red polygon. The bottom left panel is the zoomed-in map of Area 8 and the thick black polygon shows the area of the source field for the magnetic field separation calculation. The top right panel is the local magnetic field calculated from the source field (bottom left panel) and the bottom right panel is the regional magnetic field calculated from the source field (bottom left panel).

Main Findings

Area 8 coincides with the conductive Anomaly A' at the western tip of the ultramafic structures. As can be observed from the local and regional magnetic field maps, the magnetic anomalies in this area are local, near-surface magnetic anomalies. Therefore, magnetic modelling of the local field would be very helpful to understand the underground structures, and the drill holes can be selected after integrating the magnetic modelling results with the EM anomalies.

Please note that magnetic field separation algorithm is still in development and is not entirely validated. The reader should be cautious while applying these interpretation to their work.



©TerraNotes Ltd 2007-2013

APPENDIX B

List of Figures

Name	Type	Size	Date modified
00-Rory_claim_from_Gov.jpg	JPG File	347 KB	24/05/2012 10:30 AM
00-Rory_claim_from_Gov+Cu.jpg	JPG File	9,109 KB	23/11/2012 9:49 AM
00-Rory_claim_from_Gov+Ni.jpg	JPG File	9,107 KB	23/11/2012 9:49 AM
00-Rory_Google_Earth.jpg	JPG File	510 KB	06/09/2012 2:59 PM
00-Rory_Google_Earth_zoom.jpg	JPG File	408 KB	06/09/2012 2:38 PM
01-Rory_property_location.png	PNG File	7,681 KB	22/11/2012 1:11 PM
02-GEOLOGY_withLegend.png	PNG File	4,609 KB	15/11/2012 10:06 AM
02-GEOLOGY_withLegend+flightline.png	PNG File	5,705 KB	15/11/2012 10:05 AM
03-Rory_DEM.jpg	JPG File	3,958 KB	17/05/2012 1:59 PM
03-Rory_DEM_2.jpg	JPG File	8,989 KB	26/11/2012 11:03 AM
03-Rory_DEM_comparison.jpg	JPG File	7,719 KB	26/11/2012 11:23 AM
04-Rory_DTM.jpg	JPG File	6,666 KB	10/09/2012 9:53 AM
04-Rory_DTM2.jpg	JPG File	6,666 KB	10/09/2012 9:52 AM
05-Rory_TMI.jpg	JPG File	7,471 KB	10/09/2012 10:15 AM
06-Rory_IGRF_&_Elevation_Corr.jpg	JPG File	7,469 KB	10/09/2012 10:25 AM
07-Rory_RMI.jpg	JPG File	7,459 KB	10/09/2012 10:27 AM
08a-Rory_RTP.jpg	JPG File	6,513 KB	10/09/2012 10:40 AM
08b-Rory_RTP.jpg	JPG File	6,104 KB	10/09/2012 10:43 AM
08c-Rory_RTP_histEq.jpg	JPG File	9,762 KB	10/09/2012 11:10 AM
08d-Rory_RTP_3D.jpg	JPG File	7,753 KB	27/11/2012 11:44 AM
09-Rory_PseudoGravity.jpg	JPG File	8,894 KB	10/09/2012 11:17 AM
10-Rory_RTP_VA1.jpg	JPG File	7,618 KB	10/09/2012 11:43 AM
11-Rory_RTP_VA2.jpg	JPG File	8,036 KB	10/09/2012 11:44 AM
12-Rory_RTP_VA3.jpg	JPG File	8,653 KB	10/09/2012 11:46 AM
13-Rory_RTP_VA4.jpg	JPG File	8,145 KB	10/09/2012 11:47 AM
14-Rory_HA_N-S.jpg	JPG File	7,606 KB	10/09/2012 11:49 AM
15-Rory_HA_E-W.jpg	JPG File	7,681 KB	10/09/2012 11:50 AM
16-Rory_HA_NW-SE.jpg	JPG File	7,825 KB	10/09/2012 11:52 AM
17-Rory_HA_NE-SW.jpg	JPG File	7,763 KB	10/09/2012 11:58 AM
18-Rory_RHA.jpg	JPG File	7,739 KB	10/09/2012 12:08 PM
19-Rory_THA.jpg	JPG File	8,453 KB	10/09/2012 12:10 PM
20-Rory_MHA.jpg	JPG File	8,545 KB	10/09/2012 12:11 PM
21-Rory_FMA.jpg	JPG File	7,584 KB	10/09/2012 12:24 PM
22-Rory_FMAA.jpg	JPG File	7,476 KB	10/09/2012 12:23 PM
23a-Rory_Block_Amp.jpg	JPG File	9,247 KB	10/09/2012 12:31 PM
23b-Rory_Block_Amp.jpg	JPG File	7,483 KB	10/09/2012 12:32 PM
23c-Rory_Block_Amp.jpg	JPG File	6,570 KB	10/09/2012 1:03 PM
24-Rory_Dir_Dev.jpg	JPG File	9,041 KB	10/09/2012 12:34 PM
25-Rory_E-W_Dir_Dev.jpg	JPG File	8,684 KB	10/09/2012 12:35 PM
26-Rory_N-S_Dir_Dev.jpg	JPG File	8,626 KB	10/09/2012 12:48 PM
27a-Rory_Edge_Enhancement.jpg	JPG File	10,451 KB	10/09/2012 12:57 PM
27b-Rory_Edge_Enhancement.jpg	JPG File	7,830 KB	10/09/2012 12:57 PM
28-Rory_Contact_Enhancement.jpg	JPG File	8,820 KB	26/11/2012 11:32 AM
E01-Rory_inphase-coplanar_56000Hz.jpg	JPG File	7,769 KB	10/09/2012 2:27 PM
E02-Rory_inphase-coplanar_7200Hz.jpg	JPG File	7,150 KB	10/09/2012 2:28 PM
E03-Rory_inphase-coaxial_5500Hz.jpg	JPG File	7,390 KB	10/09/2012 2:33 PM
E04-Rory_inphase-coaxial_1000Hz.jpg	JPG File	7,350 KB	10/09/2012 5:38 PM
E05-Rory_inphase-coplanar_900Hz.jpg	JPG File	7,057 KB	10/09/2012 2:31 PM
E06-Rory_quadrature-coplanar_56000Hz.jpg	JPG File	8,139 KB	27/11/2012 4:55 PM
E07-Rory_quadrature-coplanar_7200Hz.jpg	JPG File	7,623 KB	27/11/2012 4:56 PM
E08-Rory_quadrature-coaxial_5500Hz.jpg	JPG File	7,750 KB	27/11/2012 4:56 PM
E09-Rory_quadrature-coaxial_1000Hz.jpg	JPG File	7,352 KB	27/11/2012 4:57 PM
E10-Rory_quadrature-coplanar_900Hz.jpg	JPG File	6,892 KB	27/11/2012 4:58 PM
E11a-AppRes_56000Hz.jpg	JPG File	9,501 KB	10/09/2012 5:56 PM
E11b-LogAppRes_56000Hz.jpg	JPG File	7,952 KB	10/09/2012 6:01 PM
E12a-AppRes_7200Hz.jpg	JPG File	9,239 KB	10/09/2012 6:05 PM
E12b-LogAppRes_7200Hz.jpg	JPG File	8,398 KB	10/09/2012 6:04 PM
E13a-AppRes_900Hz.jpg	JPG File	8,708 KB	10/09/2012 6:04 PM
E13b-LogAppRes_900Hz.jpg	JPG File	8,157 KB	10/09/2012 6:04 PM
E14-AppDepth_56000Hz.jpg	JPG File	7,105 KB	20/11/2012 10:28 AM
E15-AppDepth_7200Hz.jpg	JPG File	7,270 KB	20/11/2012 10:28 AM
E16-AppDepth_900Hz.jpg	JPG File	6,871 KB	20/11/2012 10:28 AM
EMP01-DIFI_CX5500-CP7200.png	PNG File	6,856 KB	22/11/2012 12:03 PM
EMP02-DIFI_CX1000-CP900.png	PNG File	8,023 KB	22/11/2012 12:00 PM
EMP03-DIFQ_CX5500-CP7200.png	PNG File	6,870 KB	22/11/2012 12:06 PM
EMP04-DIFQ_CX1000-CP900.png	PNG File	7,154 KB	22/11/2012 12:08 PM
EMP05-RATI_CX5500-CP7200.png	PNG File	7,078 KB	22/11/2012 12:27 PM
EMP06-RATI_CX1000-CP900.png	PNG File	7,429 KB	22/11/2012 12:29 PM
EMP07-PHA56000.png	PNG File	8,129 KB	22/11/2012 12:41 PM
EMP08-PHA7200.png	PNG File	8,488 KB	22/11/2012 12:43 PM
EMP09-PHA5500.png	PNG File	9,019 KB	22/11/2012 12:49 PM
EMP10-PHA1000.png	PNG File	9,057 KB	22/11/2012 12:56 PM
EMP10-PHA1000_2.png	PNG File	9,260 KB	22/11/2012 12:54 PM
EMP11-PHA900.png	PNG File	8,785 KB	22/11/2012 12:45 PM
EMP11-PHA900_2.png	PNG File	9,107 KB	22/11/2012 12:47 PM
EMP12-Susceptibility_Effect_DIFI_CX1000-CP900.png	PNG File	7,368 KB	28/11/2012 4:49 PM
I3D-01_DTM.jpg	JPG File	1,132 KB	06/12/2012 12:25 PM
I3D-02_DTM_with_AppRes7200.jpg	JPG File	1,129 KB	06/12/2012 12:26 PM
I3D-03_DTM_with_AppRes900.jpg	JPG File	1,026 KB	06/12/2012 12:27 PM
I3D-04_DTM_with_PHA1000.jpg	JPG File	1,154 KB	06/12/2012 12:28 PM

Name	Type	Size	Date modified
3D-05_DTM_with_VA1.jpg	JPG File	1,194 KB	06/12/2012 12:28 PM
3D-06_DTM_with_DirDev.jpg	JPG File	1,487 KB	06/12/2012 12:29 PM
3D-07_VA1.jpg	JPG File	1,170 KB	06/12/2012 12:33 PM
3D-08_VA1_with_AppRes7200.jpg	JPG File	1,126 KB	06/12/2012 12:35 PM
3D-09_VA1_with_AppRes900.jpg	JPG File	1,069 KB	06/12/2012 12:34 PM
3D-10_VA1_with_PHA1000.jpg	JPG File	1,143 KB	06/12/2012 12:36 PM
3D-11_DD.jpg	JPG File	1,368 KB	06/12/2012 12:38 PM
3D-12_DD_with_AppRes7200.jpg	JPG File	1,071 KB	06/12/2012 1:37 PM
3D-13_DD_with_AppRes900.jpg	JPG File	1,048 KB	06/12/2012 1:40 PM
3D-14_DD_with_PHA1000.jpg	JPG File	1,096 KB	06/12/2012 1:41 PM
O00-Rory_Cu.png	PNG File	4,318 KB	04/12/2012 3:29 PM
O00-Rory_Ni.png	PNG File	3,596 KB	04/12/2012 3:27 PM
O01-Rory_Geol+Cu.png	PNG File	2,534 KB	15/11/2012 4:02 PM
O01-Rory_Geol+Ni.png	PNG File	2,521 KB	15/11/2012 4:14 PM
O02-Rory_DEM+Cu.png	PNG File	7,423 KB	15/11/2012 3:58 PM
O02-Rory_DEM+Ni.png	PNG File	7,414 KB	15/11/2012 3:53 PM
O03-Rory_RTP+Cu.png	PNG File	5,785 KB	15/11/2012 3:01 PM
O03-Rory_RTP+Cu_grouped.png	PNG File	5,741 KB	15/11/2012 2:57 PM
O03-Rory_RTP+Ni.png	PNG File	5,774 KB	15/11/2012 2:45 PM
O04-Rory_VA1+Cu.png	PNG File	9,289 KB	15/11/2012 3:33 PM
O04-Rory_VA1+Ni.png	PNG File	9,284 KB	15/11/2012 3:05 PM
O05-Rory_FMA+Cu.png	PNG File	8,043 KB	15/11/2012 3:31 PM
O05-Rory_FMA+Ni.png	PNG File	8,037 KB	15/11/2012 3:27 PM
O06-Rory_DirDev+Cu.png	PNG File	10,409 KB	15/11/2012 3:36 PM
O06-Rory_DirDev+Ni.png	PNG File	10,411 KB	15/11/2012 3:43 PM
O07-Rory_AppRes7200+Cu.png	PNG File	10,300 KB	04/12/2012 9:51 AM
O07-Rory_AppRes7200+Ni.png	PNG File	10,295 KB	04/12/2012 9:53 AM
O08-Rory_AppRes900+Cu.png	PNG File	10,748 KB	04/12/2012 9:49 AM
O08-Rory_AppRes900+Ni.png	PNG File	10,746 KB	15/11/2012 4:46 PM
Rory_Interpretation_Google_Earth_EMjpeg.jpg	JPG File	367 KB	21/11/2012 10:02 AM
RRS-01_RMI_Selected_areas_for separation.png	PNG File	4,403 KB	07/12/2012 2:11 PM
RRS-02_Location_of_AREA_1.png	PNG File	4,391 KB	07/12/2012 10:23 AM
RRS-03_Location_of_AREA_2.png	PNG File	4,309 KB	07/12/2012 10:26 AM
RRS-04_Location_of_AREA_3.png	PNG File	4,402 KB	07/12/2012 10:27 AM
RRS-05_Location_of_AREA_4.png	PNG File	4,407 KB	07/12/2012 10:28 AM
RRS-06_Location_of_AREA_5.png	PNG File	4,365 KB	07/12/2012 10:30 AM
RRS-07_Location_of_AREA_6.png	PNG File	4,390 KB	07/12/2012 10:32 AM
RRS-08_Location_of_AREA_7.png	PNG File	4,391 KB	07/12/2012 10:33 AM
RRS-09_Location_of_AREA_8.png	PNG File	4,394 KB	07/12/2012 10:40 AM
RRS-10_Sep_Area_1_Source.png	PNG File	3,784 KB	07/12/2012 11:12 AM
RRS-11_Sep_Area_1_Regional.png	PNG File	1,336 KB	07/12/2012 3:34 PM
RRS-12_Sep_Area_1_Local.png	PNG File	2,170 KB	07/12/2012 3:34 PM
RRS-13_Sep_Area_2_Source.png	PNG File	5,122 KB	07/12/2012 11:11 AM
RRS-14_Sep_Area_2_Regional.png	PNG File	1,944 KB	07/12/2012 3:54 PM
RRS-15_Sep_Area_2_Local.png	PNG File	2,605 KB	07/12/2012 3:52 PM
RRS-16_Sep_Area_3_Source.png	PNG File	4,930 KB	07/12/2012 4:01 PM
RRS-17_Sep_Area_3_Regional.png	PNG File	1,808 KB	07/12/2012 4:02 PM
RRS-18_Sep_Area_3_Local.png	PNG File	2,654 KB	07/12/2012 4:05 PM
RRS-19_Sep_Area_4_Source.png	PNG File	2,701 KB	07/12/2012 4:11 PM
RRS-20_Sep_Area_4_Regional.png	PNG File	1,118 KB	07/12/2012 4:11 PM
RRS-21_Sep_Area_4_Local.png	PNG File	2,131 KB	07/12/2012 4:13 PM
RRS-22_Sep_Area_5_Source.png	PNG File	3,222 KB	07/12/2012 11:33 AM
RRS-23_Sep_Area_5_Regional.png	PNG File	1,004 KB	07/12/2012 4:16 PM
RRS-24_Sep_Area_5_Local.png	PNG File	2,104 KB	07/12/2012 4:17 PM
RRS-25_Sep_Area_6_Source.png	PNG File	3,866 KB	07/12/2012 11:47 AM
RRS-26_Sep_Area_6_Regional.png	PNG File	2,050 KB	07/12/2012 4:19 PM
RRS-27_Sep_Area_6_Local.png	PNG File	2,549 KB	07/12/2012 4:21 PM
RRS-28_Sep_Area_7_Source.png	PNG File	2,116 KB	07/12/2012 11:55 AM
RRS-29_Sep_Area_7_Regional.png	PNG File	2,095 KB	07/12/2012 11:57 AM
RRS-30_Sep_Area_7_Local.png	PNG File	1,839 KB	07/12/2012 11:56 AM
RRS-31_Sep_Area_8_Source.png	PNG File	4,111 KB	07/12/2012 12:09 PM
RRS-32_Sep_Area_8_Regional.png	PNG File	3,160 KB	07/12/2012 12:05 PM
RRS-33_Sep_Area_8_Local.png	PNG File	2,866 KB	07/12/2012 12:17 PM
RT01_DTM_RTP_AR7200.png	PNG File	4,999 KB	21/11/2012 1:25 PM
RT02_DTM_RTP_AR900.png	PNG File	4,674 KB	21/11/2012 4:13 PM
RT03_DTM_VA1_AR7200.png	PNG File	5,496 KB	21/11/2012 4:16 PM
RT04_DTM_VA1_AR900.png	PNG File	5,197 KB	21/11/2012 4:19 PM
RT04_DTM_VA1_AR900_CMY.png	PNG File	4,830 KB	21/11/2012 5:08 PM
RT05_DTM_FMAA_AR7200.png	PNG File	5,638 KB	21/11/2012 4:22 PM
RT06_DTM_FMAA_AR900.png	PNG File	5,343 KB	21/11/2012 4:26 PM
RT06_DTM_FMAA_AR900_CMY.png	PNG File	4,959 KB	21/11/2012 5:07 PM
RT07_DTM_DirDev_AR7200.png	PNG File	12,140 KB	21/11/2012 4:29 PM
RT08_DTM_DirDev_AR900.png	PNG File	12,084 KB	21/11/2012 4:31 PM
RT10_VA1_FMAA_AR7200.png	PNG File	5,576 KB	21/11/2012 4:39 PM
RT10_VA1_FMAA_AR7200_CMY.png	PNG File	9,594 KB	29/11/2012 11:39 AM
RT11_VA1_FMAA_AR900.png	PNG File	5,324 KB	21/11/2012 4:33 PM
RT11_VA1_FMAA_AR900_CMY.png	PNG File	5,116 KB	21/11/2012 5:10 PM
RT12_VA1_DD_AR7200.png	PNG File	12,020 KB	21/11/2012 4:43 PM
RT12_VA1_DD_AR7200_CMY.png	PNG File	9,673 KB	21/11/2012 5:14 PM
RT13_VA1_DD_AR900.png	PNG File	11,977 KB	21/11/2012 4:43 PM
RT13_VA1_DD_AR900_CMY.png	PNG File	9,529 KB	21/11/2012 5:14 PM

Name	Type	Size	Date modified
RT14_DTM_AR7200_AR900_CMY.png	PNG File	4,667 KB	21/11/2012 5:15 PM
RT15_VA1_AR7200_AR900.png	PNG File	5,241 KB	21/11/2012 4:52 PM
RT15_VA1_AR7200_AR900_CMY.png	PNG File	5,002 KB	21/11/2012 5:16 PM
RT16_FMAA_AR7200_AR900.png	PNG File	5,295 KB	21/11/2012 4:54 PM
RT16_FMAA_AR7200_AR900_CMY.png	PNG File	5,080 KB	21/11/2012 5:18 PM
RT17_DD_AR7200_AR900.png	PNG File	9,752 KB	21/11/2012 4:58 PM
RT17_DD_AR7200_AR900_CMY.png	PNG File	10,979 KB	21/11/2012 5:19 PM
RT18_1overDTM_DTM_AR900.png	PNG File	4,480 KB	21/11/2012 4:57 PM
RT18_1overDTM_DTM_AR900_CMY.png	PNG File	4,277 KB	21/11/2012 5:20 PM
RT19_1overRTP_RTP_AR900.png	PNG File	4,169 KB	21/11/2012 4:58 PM
RT19_1overRTP_RTP_AR900_CMY.png	PNG File	3,802 KB	21/11/2012 5:22 PM
RT20_1overVA1_VA1_AR900.png	PNG File	4,718 KB	21/11/2012 4:59 PM
RT20_1overVA1_VA1_AR900_CMY.png	PNG File	4,107 KB	21/11/2012 5:23 PM
RT21_1overDD_DD_AR900.png	PNG File	11,772 KB	21/11/2012 5:01 PM
RT21_1overDD_DD_AR900_CMY.png	PNG File	9,014 KB	21/11/2012 5:24 PM
RT22_DTM_VA1_PHA1000.png	PNG File	7,096 KB	29/11/2012 2:14 PM
RT22_DTM_VA1_PHA1000_CMY.png	PNG File	7,688 KB	29/11/2012 2:16 PM
RT23_DTM_DD_PHA1000.png	PNG File	12,513 KB	29/11/2012 2:25 PM
RT23_DTM_DD_PHA1000_CMY.png	PNG File	10,877 KB	29/11/2012 2:19 PM
RT24_VA1_DD_PHA1000.png	PNG File	12,408 KB	29/11/2012 2:24 PM
RT24_VA1_DD_PHA1000_CMY.png	PNG File	10,863 KB	29/11/2012 2:24 PM
RT25_DTM_AR900_PHA1000.png	PNG File	6,149 KB	21/12/2012 4:58 PM
RT25_DTM_AR900_PHA1000_CMY.png	PNG File	6,833 KB	21/12/2012 5:00 PM
RT26_VA1_AR900_PHA1000.png	PNG File	7,011 KB	21/12/2012 5:16 PM
RT26_VA1_AR900_PHA1000_CMY.png	PNG File	7,753 KB	21/12/2012 5:17 PM
RT27_DD_AR900_PHA1000.png	PNG File	10,708 KB	21/12/2012 5:19 PM
RT27_DD_AR900_PHA1000_CMY.png	PNG File	11,581 KB	21/12/2012 5:21 PM
RT28_1overDD_DD_PHA1000.png	PNG File	12,209 KB	29/11/2012 2:32 PM
RT28_1overDD_DD_PHA1000_CMY.png	PNG File	10,309 KB	29/11/2012 2:33 PM
RTr01_DTM_Cu_Ni.png	PNG File	3,154 KB	13/12/2012 3:22 PM
RTr01_DTM_Cu_Ni_CMY.png	PNG File	3,338 KB	22/11/2012 11:18 AM
RTr02_RTP_Cu_Ni.png	PNG File	3,891 KB	22/11/2012 10:07 AM
RTr02_RTP_Cu_Ni_CMY.png	PNG File	3,963 KB	22/11/2012 11:15 AM
RTr03_VA1_Cu_Ni.png	PNG File	4,333 KB	22/11/2012 10:09 AM
RTr03_VA1_Cu_Ni_CMY.png	PNG File	4,535 KB	22/11/2012 11:13 AM
RTr04_FMAA_Cu_Ni.png	PNG File	4,362 KB	22/11/2012 10:09 AM
RTr04_FMAA_Cu_Ni_CMY.png	PNG File	4,607 KB	22/11/2012 11:04 AM
RTr05_DD_Cu_Ni.png	PNG File	8,947 KB	22/11/2012 10:13 AM
RTr05_DD_Cu_Ni_CMY.png	PNG File	10,532 KB	22/11/2012 11:02 AM
RTr06_LAC7200_Cu_Ni.png	PNG File	3,607 KB	22/11/2012 10:11 AM
RTr06_LAC7200_Cu_Ni_CMY.png	PNG File	3,568 KB	22/11/2012 11:00 AM
RTr07_LAC900_Cu_Ni.png	PNG File	3,465 KB	22/11/2012 10:13 AM
RTr07_LAC900_Cu_Ni_CMY.png	PNG File	3,374 KB	22/11/2012 10:59 AM
RTr08_LAC7200_LAC900_Ni.png	PNG File	3,547 KB	22/11/2012 10:14 AM
RTr08_LAC7200_LAC900_Ni_CMY.png	PNG File	3,551 KB	22/11/2012 10:57 AM
RTr09_LAC7200_LAC900_Cu.png	PNG File	3,655 KB	22/11/2012 10:52 AM
RTr09_LAC7200_LAC900_Cu_CMY.png	PNG File	3,694 KB	22/11/2012 10:54 AM
RTr10_DD_LAC900_Ni.png	PNG File	9,049 KB	22/11/2012 10:16 AM
RTr10_DD_LAC900_Ni_CMY.png	PNG File	10,615 KB	22/11/2012 10:58 AM
RTr11_DD_LAC900_Cu.png	PNG File	9,101 KB	22/11/2012 10:54 AM
RTr11_DD_LAC900_Cu_CMY.png	PNG File	10,635 KB	22/11/2012 10:56 AM
Z101_DTM_west.png	PNG File	6,508 KB	12/12/2012 4:50 PM
Z102_RMI_nTL_west.png	PNG File	7,856 KB	12/12/2012 4:56 PM
Z102_RMI_nTL_west_2.png	PNG File	7,063 KB	12/12/2012 4:54 PM
Z102_RTP_west.png	PNG File	6,210 KB	12/12/2012 4:57 PM
Z103_VA1_west.png	PNG File	7,568 KB	12/12/2012 4:59 PM
Z104_E-W_amp_west.png	PNG File	7,735 KB	12/12/2012 5:00 PM
Z105_N-S_amp_west.png	PNG File	8,638 KB	12/12/2012 5:02 PM
Z106_FMAA_west.png	PNG File	6,634 KB	12/12/2012 5:04 PM
Z107_DD_west.png	PNG File	9,137 KB	12/12/2012 5:06 PM
Z108_LAR56000_west.png	PNG File	9,111 KB	12/12/2012 5:08 PM
Z109_LAR7200_west.png	PNG File	9,528 KB	12/12/2012 5:10 PM
Z110_LAR900_west.png	PNG File	9,528 KB	12/12/2012 5:12 PM
Z110_LAR900_west+Ni_Cu.png	PNG File	6,561 KB	12/12/2012 5:39 PM
Z110_LAR900_west+Ni_Cu+DirDev.png	PNG File	9,820 KB	12/12/2012 5:37 PM
Z110_LAR900_west+Ni_Cu+DirDev2.png	PNG File	9,497 KB	13/12/2012 5:25 PM
Z111_PHA1000_west+Ni_Cu+DirDev.png	PNG File	8,521 KB	12/12/2012 5:25 PM
Z111_PHA1000_west+Ni_Cu+DirDev_wTL.png	PNG File	10,253 KB	12/12/2012 5:47 PM
Z301_DTM_east.png	PNG File	5,977 KB	12/12/2012 12:29 PM
Z302_RTP_east.png	PNG File	4,803 KB	12/12/2012 12:29 PM
Z303_VA1_east.png	PNG File	6,512 KB	12/12/2012 12:30 PM
Z304_E-W_amp_east.png	PNG File	7,032 KB	12/12/2012 12:30 PM
Z305_N-S_amp_east.png	PNG File	6,995 KB	12/12/2012 12:31 PM
Z306_FMAA_east.png	PNG File	7,019 KB	12/12/2012 12:32 PM
Z307_DD_east.png	PNG File	6,614 KB	12/12/2012 12:36 PM
Z308_LAR56000_east.png	PNG File	8,380 KB	12/12/2012 12:36 PM
Z309_LAR7200_east.png	PNG File	8,702 KB	12/12/2012 12:48 PM
Z310_LAR900_east.png	PNG File	8,120 KB	12/12/2012 12:46 PM
Z310_LAR900_east+Ni_Cu.png	PNG File	7,732 KB	13/12/2012 5:13 PM
Z310_LAR900_east+Ni_Cu+DirDev.png	PNG File	4,766 KB	14/12/2012 9:31 AM
Z311_PHA1000_east+Ni_Cu+DirDev.png	PNG File	6,182 KB	13/12/2012 5:37 PM



©TerraNotes Ltd 2007-2013

APPENDIX C

List of Claims

List of claims

©TerraNotes Ltd 2007-2013

District	GrantNumber	RegType	ClaimName	ClaimNbr	Claim Owner	OperationRecordingDate	StakingDate	ClaimExpiryDate	Status	NTS MapNumber	NonStdSize	Ops Number
Whitehorse	YC65957	Quartz	RORY	1	Coronation Minerals Inc - 100%	03/10/2007	01/10/2007	03/10/2013	Active	115G05		500151838
Whitehorse	YC65958	Quartz	RORY	2	Coronation Minerals Inc - 100%	03/10/2007	01/10/2007	03/10/2013	Active	115G05		500151839
Whitehorse	YC65959	Quartz	RORY	3	Coronation Minerals Inc - 100%	03/10/2007	01/10/2007	03/10/2013	Active	115G05		500151840
Whitehorse	YC65960	Quartz	RORY	4	Coronation Minerals Inc - 100%	03/10/2007	01/10/2007	03/10/2013	Active	115G05		500151841
Whitehorse	YC65961	Quartz	RORY	5	Coronation Minerals Inc - 100%	03/10/2007	01/10/2007	03/10/2013	Active	115G05		500151842
Whitehorse	YC65962	Quartz	RORY	6	Coronation Minerals Inc - 100%	03/10/2007	01/10/2007	03/10/2013	Active	115G05		500151843
Whitehorse	YC65963	Quartz	RORY	7	Coronation Minerals Inc - 100%	03/10/2007	01/10/2007	03/10/2013	Active	115G05		500151844
Whitehorse	YC65964	Quartz	RORY	8	Coronation Minerals Inc - 100%	03/10/2007	01/10/2007	03/10/2013	Active	115G05		500151845
Whitehorse	YC65965	Quartz	RORY	9	Coronation Minerals Inc - 100%	03/10/2007	01/10/2007	03/10/2013	Active	115G05		500151846
Whitehorse	YC65966	Quartz	RORY	10	Coronation Minerals Inc - 100%	03/10/2007	01/10/2007	03/10/2013	Active	115G05		500151847
Whitehorse	YC65967	Quartz	RORY	11	Coronation Minerals Inc - 100%	03/10/2007	01/10/2007	03/10/2013	Active	115G05		500151876
Whitehorse	YC65968	Quartz	RORY	12	Coronation Minerals Inc - 100%	03/10/2007	01/10/2007	03/10/2013	Active	115G05		500151877
Whitehorse	YC65969	Quartz	RORY	13	Coronation Minerals Inc - 100%	03/10/2007	01/10/2007	03/10/2013	Active	115G05		500151878
Whitehorse	YC65970	Quartz	RORY	14	Coronation Minerals Inc - 100%	03/10/2007	01/10/2007	03/10/2013	Active	115G05		500151879
Whitehorse	YC65971	Quartz	RORY	15	Coronation Minerals Inc - 100%	03/10/2007	01/10/2007	03/10/2013	Active	115G05		500151880
Whitehorse	YC65972	Quartz	RORY	16	Coronation Minerals Inc - 100%	03/10/2007	01/10/2007	03/10/2013	Active	115G05		500151881
Whitehorse	YC65973	Quartz	RORY	17	Coronation Minerals Inc - 100%	03/10/2007	01/10/2007	03/10/2013	Active	115G05		500151882
Whitehorse	YC65974	Quartz	RORY	18	Coronation Minerals Inc - 100%	03/10/2007	01/10/2007	03/10/2013	Active	115G05		500151883
Whitehorse	YC65975	Quartz	RORY	19	Coronation Minerals Inc - 100%	03/10/2007	01/10/2007	03/10/2013	Active	115G05		500151884
Whitehorse	YC65976	Quartz	RORY	20	Coronation Minerals Inc - 100%	03/10/2007	01/10/2007	03/10/2013	Active	115G05		500151885
Whitehorse	YC65977	Quartz	RORY	21	Coronation Minerals Inc - 100%	03/10/2007	01/10/2007	03/10/2013	Active	115G05		500151886
Whitehorse	YC65978	Quartz	RORY	22	Coronation Minerals Inc - 100%	03/10/2007	01/10/2007	03/10/2013	Active	115G05		500151887
Whitehorse	YC65979	Quartz	RORY	23	Coronation Minerals Inc - 100%	03/10/2007	01/10/2007	03/10/2013	Active	115G05		500151888
Whitehorse	YC65980	Quartz	RORY	24	Coronation Minerals Inc - 100%	03/10/2007	01/10/2007	03/10/2013	Active	115G05		500151889
Whitehorse	YC65981	Quartz	RORY	25	Coronation Minerals Inc - 100%	03/10/2007	01/10/2007	03/10/2013	Active	115G05		500151890
Whitehorse	YC65982	Quartz	RORY	26	Coronation Minerals Inc - 100%	03/10/2007	01/10/2007	03/10/2013	Active	115G05		500151891
Whitehorse	YC65983	Quartz	RORY	27	Coronation Minerals Inc - 100%	03/10/2007	01/10/2007	03/10/2013	Active	115G05		500151892
Whitehorse	YC65984	Quartz	RORY	28	Coronation Minerals Inc - 100%	03/10/2007	01/10/2007	03/10/2013	Active	115G05		500151893
Whitehorse	YC65985	Quartz	RORY	29	Coronation Minerals Inc - 100%	03/10/2007	01/10/2007	03/10/2013	Active	115G05		500151894
Whitehorse	YC65986	Quartz	RORY	30	Coronation Minerals Inc - 100%	03/10/2007	01/10/2007	03/10/2013	Active	115G05		500151895
Whitehorse	YC65987	Quartz	RORY	31	Coronation Minerals Inc - 100%	03/10/2007	01/10/2007	03/10/2013	Active	115G05		500151896
Whitehorse	YC65988	Quartz	RORY	32	Coronation Minerals Inc - 100%	03/10/2007	01/10/2007	03/10/2013	Active	115G05		500151897
Whitehorse	YC65989	Quartz	RORY	33	Coronation Minerals Inc - 100%	03/10/2007	01/10/2007	03/10/2013	Active	115G05		500151898
Whitehorse	YC65990	Quartz	RORY	34	Coronation Minerals Inc - 100%	03/10/2007	01/10/2007	03/10/2013	Active	115G05		500151899
Whitehorse	YC65991	Quartz	RORY	35	Coronation Minerals Inc - 100%	03/10/2007	01/10/2007	03/10/2013	Active	115G05		500151900
Whitehorse	YC65992	Quartz	RORY	36	Coronation Minerals Inc - 100%	03/10/2007	01/10/2007	03/10/2013	Active	115G05		500151901
Whitehorse	YC65993	Quartz	RORY	37	Coronation Minerals Inc - 100%	03/10/2007	01/10/2007	03/10/2013	Active	115G05		500151902
Whitehorse	YC65994	Quartz	RORY	38	Coronation Minerals Inc - 100%	03/10/2007	01/10/2007	03/10/2013	Active	115G05		500151903
Whitehorse	YC65995	Quartz	RORY	39	Coronation Minerals Inc - 100%	03/10/2007	01/10/2007	03/10/2013	Active	115G05		500151932
Whitehorse	YC65996	Quartz	RORY	40	Coronation Minerals Inc - 100%	03/10/2007	01/10/2007	03/10/2013	Active	115G05		500151933
Whitehorse	YC65997	Quartz	RORY	41	Coronation Minerals Inc - 100%	03/10/2007	01/10/2007	03/10/2013	Active	115G05		500151934
Whitehorse	YC65998	Quartz	RORY	42	Coronation Minerals Inc - 100%	03/10/2007	01/10/2007	03/10/2013	Active	115G05		500151935
Whitehorse	YC65999	Quartz	RORY	43	Coronation Minerals Inc - 100%	03/10/2007	01/10/2007	03/10/2013	Active	115G05		500151936
Whitehorse	YC66000	Quartz	RORY	44	Coronation Minerals Inc - 100%	03/10/2007	01/10/2007	03/10/2013	Active	115G05		500151937
Whitehorse	YC66001	Quartz	RORY	45	Coronation Minerals Inc - 100%	03/10/2007	01/10/2007	03/10/2013	Active	115G05		500151938
Whitehorse	YC66002	Quartz	RORY	46	Coronation Minerals Inc - 100%	03/10/2007	01/10/2007	03/10/2013	Active	115G05		500151939
Whitehorse	YC66003	Quartz	RORY	47	Coronation Minerals Inc - 100%	03/10/2007	01/10/2007	03/10/2013	Active	115G05		500151940
Whitehorse	YC66004	Quartz	RORY	48	Coronation Minerals Inc - 100%	03/10/2007	01/10/2007	03/10/2013	Active	115G05		500151941
Whitehorse	YC66005	Quartz	RORY	49	Coronation Minerals Inc - 100%	03/10/2007	01/10/2007	03/10/2013	Active	115G05		500151942
Whitehorse	YC66006	Quartz	RORY	50	Coronation Minerals Inc - 100%	03/10/2007	01/10/2007	03/10/2013	Active	115G05		500151943
Whitehorse	YC66007	Quartz	RORY	51	Coronation Minerals Inc - 100%	03/10/2007	01/10/2007	03/10/2013	Active	115G05		500151944
Whitehorse	YC66008	Quartz	RORY	52	Coronation Minerals Inc - 100%	03/10/2007	01/10/2007	03/10/2013	Active	115G05		500151945
Whitehorse	YC66009	Quartz	RORY	53	Coronation Minerals Inc - 100%	03/10/2007	01/10/2007	03/10/2013	Active	115G05		500151946
Whitehorse	YC66010	Quartz	RORY	54	Coronation Minerals Inc - 100%	03/10/2007	01/10/2007	03/10/2013	Active	115G05		500151947
Whitehorse	YC66011	Quartz	RORY	55	Coronation Minerals Inc - 100%	03/10/2007	01/10/2007	03/10/2013	Active	115G05		500151948
Whitehorse	YC66012	Quartz	RORY	56	Coronation Minerals Inc - 100%	03/10/2007	01/10/2007	03/10/2013	Active	115G05		500151949
Whitehorse	YC66013	Quartz	RORY	57	Coronation Minerals Inc - 100%	03/10/2007	01/10/2007	03/10/2013	Active	115G05		500151950
Whitehorse	YC66014	Quartz	RORY	58	Coronation Minerals Inc - 100%	03/10/2007	01/10/2007	03/10/2013	Active	115G05		500151951
Whitehorse	YC66015	Quartz	RORY	59	Coronation Minerals Inc - 100%	03/10/2007	01/10/2007	03/10/2013	Active	115G05		500151952
Whitehorse	YC66016	Quartz	RORY	60	Coronation Minerals Inc - 100%	03/10/2007	01/10/2007	03/10/2013	Active	115G05		500151953
Whitehorse	YC66017	Quartz	RORY	61	Coronation Minerals Inc - 100%	03/10/2007	01/10/2007	03/10/2013	Active	115G05		500151954
Whitehorse	YC66018	Quartz	RORY	62	Coronation Minerals Inc - 100%	03/10/2007	01/10/2007	03/10/2013	Active	115G05		500151955
Whitehorse	YC66019	Quartz	RORY	63	Coronation Minerals Inc - 100%	03/10/2007	01/10/2007	03/10/2013	Active	115G05		500151956
Whitehorse	YC66020	Quartz	RORY	64	Coronation Minerals Inc - 100%	03/10/2007	01/10/2007	03/10/2013	Active	115G05		500151957
Whitehorse	YC66021	Quartz	RORY	65	Coronation Minerals Inc - 100%	03/10/2007	01/10/2007	03/10/2013	Active	115G05		500151958
Whitehorse	YC66022	Quartz	RORY	66	Coronation Minerals Inc - 100%	03/10/2007	01/10/2007	03/10/2013	Active	115G05		500151959
Whitehorse	YC66023	Quartz	RORY	67	Coronation Minerals Inc - 100%	03/10/2007	01/10/2007	03/10/2013	Active	115G05		500151988
Whitehorse	YC66024	Quartz	RORY	68	Coronation Minerals Inc - 100%	03/10/2007	01/10/2007	03/10/2013	Active	115G05		500151989
Whitehorse	YC66025	Quartz	RORY	69	Coronation Minerals Inc - 100%	03/10/2007	01/10/2007	03/10/2013	Active	115G05		500151990
Whitehorse	YC66026	Quartz	RORY	70	Coronation Minerals Inc - 100%	03/10/2007	01/10/2007	03/10/2013	Active	115G05		500151991
Whitehorse	YC66027	Quartz	RORY	71	Coronation Minerals Inc - 100%	03/10/2007	01/10/2007	03/10/2013	Active	115G05		500151992
Whitehorse	YC66028	Quartz	RORY	72	Coronation Minerals Inc - 100%	03/10/2007	01/10/2007	03/10/2013	Active	115G05		500151993
Whitehorse	YC66029	Quartz	RORY	73	Coronation Minerals Inc - 100%	03/10/2007	01/10/2007	03/10/2013	Active	115G05		500151994
Whitehorse	YC66030	Quartz	RORY	74	Coronation Minerals Inc - 100%	03/10/2007	01/10/2007	03/10/2013	Active	115G05		500151995
Whitehorse	YC66031	Quartz	RORY	75	Coronation Minerals Inc - 100%	03/10/2007	01/10/2007	03/10/2013	Active	115G05		500151996
Whitehorse	YC66032	Quartz	RORY	76	Coronation Minerals Inc - 100%	03/10/2007	01/10/2007	03/10/2013	Active	115G05		500151997
Whitehorse	YC66033	Quartz	RORY	77	Coronation Minerals Inc - 100%	03/10/2007	01/10/2007	03/10/2013	Active	115G05		500151998
Whitehorse	YC66034	Quartz	RORY	78	Coronation Minerals Inc - 100%	03/10/2007	01/10/2007	03/10/2013	Active	115G05		500151999
Whitehorse	YC66035	Quartz	RORY	79	Coronation Minerals Inc - 100%	03/10/2007	01/10/2007	03/10/2013	Active	115G05		500152000
Whitehorse	YC66036	Quartz	RORY	80	Coronation Minerals Inc - 100%	03/10/2007	01/10/2007	03/10/2013	Active	115G05		500152001
Whitehorse	YC66037	Quartz	RORY	81	Coronation Minerals Inc - 100%	03/10/2007	01/10/2007	03/10/2013	Active	115G05		500152002
Whitehorse	YC66038	Quartz	RORY	82	Coronation Minerals Inc - 100%	03/10/2007	01/10/2007	03/10/2013	Active	115G05		500152003
Whitehorse	YC66039	Quartz	RORY	83	Coronation Minerals Inc - 100%	03/10/2007	01/10/2007	03/10/2013	Active	115G05		500152004
Whitehorse	YC66040	Quartz	RORY	84	Coronation Minerals Inc - 100%	03/10/2007	01/10/2007	03/10/2013	Active	115G05		500152005
Whitehorse	YC66041	Quartz	RORY	85	Coronation Minerals Inc - 100%	03/10/2007	01/10/2007	03/10/2013	Active	115G05		500152006
Whitehorse	YC66042	Quartz	RORY	86	Coronation Minerals Inc - 100%	03/10/2007	01/10/2007	03/10/2013	Active	115G05		500152007
Whitehorse	YC66043	Quartz	RORY	87	Coronation Minerals Inc - 100%	03/10/2007	01/10/2007	03/10/2013	Active	115G05		500152008
Whitehorse	YC66044	Quartz	RORY	88	Coronation Minerals Inc - 100%	03/10/2007	01/10/2007	03/10/2013	Active	115G05		500152009
Whitehorse	YC66045	Quartz	RORY	89	Coronation Minerals Inc - 100%	03/10/2007	01/10/2007	03/10/2013	Active	115G05		500152010
Whitehorse	YC66046	Quartz	RORY	90	Coronation Minerals Inc - 100%	03/10/2007	01/10/2007	03/10/2013	Active	115G05		500152011

Source: Yukon Geological Survey (http://mapservices.gov.yk.ca/YGS/WebMap.aspx

List of claims

©TerraNotes Ltd 2007-2013

District	GrantNumber	RegType	ClaimName	ClaimNbr	Claim Owner	OperationRecordingDate	StakingDate	ClaimExpiryDate	Status	NTS MapNumber	NonStdSize	Ops Number
Whitehorse	YC66047	Quartz	RORY	91	Coronation Minerals Inc - 100%	03/10/2007	01/10/2007	03/10/2013	Active	115G05		500152012
Whitehorse	YC66048	Quartz	RORY	92	Coronation Minerals Inc - 100%	03/10/2007	01/10/2007	03/10/2013	Active	115G05		500152013
Whitehorse	YC66049	Quartz	RORY	93	Coronation Minerals Inc - 100%	03/10/2007	01/10/2007	03/10/2013	Active	115G05		500152014
Whitehorse	YC66050	Quartz	RORY	94	Coronation Minerals Inc - 100%	03/10/2007	01/10/2007	03/10/2013	Active	115G05		500152015
Whitehorse	YC66051	Quartz	RORY	95	Coronation Minerals Inc - 100%	03/10/2007	30/09/2007	03/10/2013	Active	115G05		500152067
Whitehorse	YC66052	Quartz	RORY	96	Coronation Minerals Inc - 100%	03/10/2007	30/09/2007	03/10/2013	Active	115G05		500152068
Whitehorse	YC66053	Quartz	RORY	97	Coronation Minerals Inc - 100%	03/10/2007	30/09/2007	03/10/2013	Active	115G05		500152069
Whitehorse	YC66054	Quartz	RORY	98	Coronation Minerals Inc - 100%	03/10/2007	30/09/2007	03/10/2013	Active	115G05		500152070
Whitehorse	YC66055	Quartz	RORY	99	Coronation Minerals Inc - 100%	03/10/2007	30/09/2007	03/10/2013	Active	115G05		500152071
Whitehorse	YC66056	Quartz	RORY	100	Coronation Minerals Inc - 100%	03/10/2007	30/09/2007	03/10/2013	Active	115G05		500152072
Whitehorse	YC66057	Quartz	RORY	101	Coronation Minerals Inc - 100%	03/10/2007	30/09/2007	03/10/2013	Active	115G05		500152073
Whitehorse	YC66058	Quartz	RORY	102	Coronation Minerals Inc - 100%	03/10/2007	30/09/2007	03/10/2013	Active	115G05		500152074
Whitehorse	YC66059	Quartz	RORY	103	Coronation Minerals Inc - 100%	03/10/2007	30/09/2007	03/10/2013	Active	115G05		500152075
Whitehorse	YC66060	Quartz	RORY	104	Coronation Minerals Inc - 100%	03/10/2007	30/09/2007	03/10/2013	Active	115G05		500152076
Whitehorse	YC66061	Quartz	RORY	105	Coronation Minerals Inc - 100%	03/10/2007	30/09/2007	03/10/2013	Active	115G05		500152077
Whitehorse	YC66062	Quartz	RORY	106	Coronation Minerals Inc - 100%	03/10/2007	30/09/2007	03/10/2013	Active	115G05		500152078
Whitehorse	YC66063	Quartz	RORY	107	Coronation Minerals Inc - 100%	03/10/2007	30/09/2007	03/10/2013	Active	115G05		500152079
Whitehorse	YC66064	Quartz	RORY	108	Coronation Minerals Inc - 100%	03/10/2007	30/09/2007	03/10/2013	Active	115G05		500152080
Whitehorse	YC66065	Quartz	RORY	109	Coronation Minerals Inc - 100%	03/10/2007	30/09/2007	03/10/2013	Active	115G05		500152081
Whitehorse	YC66066	Quartz	RORY	110	Coronation Minerals Inc - 100%	03/10/2007	30/09/2007	03/10/2013	Active	115G05		500152082
Whitehorse	YC66067	Quartz	RORY	111	Coronation Minerals Inc - 100%	03/10/2007	30/09/2007	03/10/2013	Active	115G05		500152083
Whitehorse	YC66068	Quartz	RORY	112	Coronation Minerals Inc - 100%	03/10/2007	30/09/2007	03/10/2013	Active	115G05		500152084
Whitehorse	YC66069	Quartz	RORY	113	Coronation Minerals Inc - 100%	03/10/2007	30/09/2007	03/10/2013	Active	115G05		500152085
Whitehorse	YC66070	Quartz	RORY	114	Coronation Minerals Inc - 100%	03/10/2007	30/09/2007	03/10/2013	Active	115G05		500152086
Whitehorse	YC66071	Quartz	RORY	115	Coronation Minerals Inc - 100%	03/10/2007	30/09/2007	03/10/2013	Active	115G05		500152087
Whitehorse	YC66072	Quartz	RORY	116	Coronation Minerals Inc - 100%	03/10/2007	30/09/2007	03/10/2013	Active	115G05		500152088
Whitehorse	YC66073	Quartz	RORY	117	Coronation Minerals Inc - 100%	03/10/2007	30/09/2007	03/10/2013	Active	115G05		500152089
Whitehorse	YC66074	Quartz	RORY	118	Coronation Minerals Inc - 100%	03/10/2007	30/09/2007	03/10/2013	Active	115G05		500152090
Whitehorse	YC66075	Quartz	RORY	119	Coronation Minerals Inc - 100%	03/10/2007	30/09/2007	03/10/2013	Active	115G05		500152091
Whitehorse	YC66076	Quartz	RORY	120	Coronation Minerals Inc - 100%	03/10/2007	30/09/2007	03/10/2013	Active	115G05		500152092
Whitehorse	YC66077	Quartz	RORY	121	Coronation Minerals Inc - 100%	03/10/2007	30/09/2007	03/10/2013	Active	115G05		500152093
Whitehorse	YC66078	Quartz	RORY	122	Coronation Minerals Inc - 100%	03/10/2007	30/09/2007	03/10/2013	Active	115G05		500152094
Whitehorse	YC66079	Quartz	RORY	123	Coronation Minerals Inc - 100%	03/10/2007	30/09/2007	03/10/2013	Active	115G05		500152123
Whitehorse	YC66080	Quartz	RORY	124	Coronation Minerals Inc - 100%	03/10/2007	30/09/2007	03/10/2013	Active	115G05		500152124
Whitehorse	YC66081	Quartz	RORY	125	Coronation Minerals Inc - 100%	03/10/2007	30/09/2007	03/10/2013	Active	115G05		500152125
Whitehorse	YC66082	Quartz	RORY	126	Coronation Minerals Inc - 100%	03/10/2007	30/09/2007	03/10/2013	Active	115G05		500152126
Whitehorse	YC66083	Quartz	RORY	127	Coronation Minerals Inc - 100%	03/10/2007	30/09/2007	03/10/2013	Active	115G05		500152127
Whitehorse	YC66084	Quartz	RORY	128	Coronation Minerals Inc - 100%	03/10/2007	30/09/2007	03/10/2013	Active	115G05		500152128
Whitehorse	YC66085	Quartz	RORY	129	Coronation Minerals Inc - 100%	03/10/2007	30/09/2007	03/10/2013	Active	115G05		500152129
Whitehorse	YC66086	Quartz	RORY	130	Coronation Minerals Inc - 100%	03/10/2007	30/09/2007	03/10/2013	Active	115G05		500152130
Whitehorse	YC66087	Quartz	RORY	131	Coronation Minerals Inc - 100%	03/10/2007	30/09/2007	03/10/2013	Active	115G05		500152131
Whitehorse	YC66088	Quartz	RORY	132	Coronation Minerals Inc - 100%	03/10/2007	30/09/2007	03/10/2013	Active	115G05		500152132
Whitehorse	YC66089	Quartz	RORY	133	Coronation Minerals Inc - 100%	03/10/2007	30/09/2007	03/10/2013	Active	115G05		500152133
Whitehorse	YC66090	Quartz	RORY	134	Coronation Minerals Inc - 100%	03/10/2007	30/09/2007	03/10/2013	Active	115G05		500152134
Whitehorse	YC66091	Quartz	RORY	135	Coronation Minerals Inc - 100%	03/10/2007	30/09/2007	03/10/2013	Active	115G05		500152135
Whitehorse	YC66092	Quartz	RORY	136	Coronation Minerals Inc - 100%	03/10/2007	30/09/2007	03/10/2013	Active	115G05		500152136
Whitehorse	YC66093	Quartz	RORY	137	Coronation Minerals Inc - 100%	03/10/2007	30/09/2007	03/10/2013	Active	115G05		500152137
Whitehorse	YC66094	Quartz	RORY	138	Coronation Minerals Inc - 100%	03/10/2007	30/09/2007	03/10/2013	Active	115G05		500152138
Whitehorse	YC66095	Quartz	RORY	139	Coronation Minerals Inc - 100%	03/10/2007	30/09/2007	03/10/2013	Active	115G05		500152139
Whitehorse	YC66096	Quartz	RORY	140	Coronation Minerals Inc - 100%	03/10/2007	30/09/2007	03/10/2013	Active	115G05		500152140
Whitehorse	YC66097	Quartz	RORY	141	Coronation Minerals Inc - 100%	03/10/2007	30/09/2007	03/10/2013	Active	115G05		500152141
Whitehorse	YC66098	Quartz	RORY	142	Coronation Minerals Inc - 100%	03/10/2007	30/09/2007	03/10/2013	Active	115G05		500152142
Whitehorse	YC66099	Quartz	RORY	143	Coronation Minerals Inc - 100%	03/10/2007	30/09/2007	03/10/2013	Active	115G05		500152143
Whitehorse	YC66100	Quartz	RORY	144	Coronation Minerals Inc - 100%	03/10/2007	30/09/2007	03/10/2013	Active	115G05		500152144
Whitehorse	YC66101	Quartz	RORY	145	Coronation Minerals Inc - 100%	03/10/2007	30/09/2007	03/10/2013	Active	115G05		500152145
Whitehorse	YC66102	Quartz	RORY	146	Coronation Minerals Inc - 100%	03/10/2007	30/09/2007	03/10/2013	Active	115G05		500152146
Whitehorse	YC66103	Quartz	RORY	147	Coronation Minerals Inc - 100%	03/10/2007	30/09/2007	03/10/2013	Active	115G05		500152147
Whitehorse	YC66104	Quartz	RORY	148	Coronation Minerals Inc - 100%	03/10/2007	30/09/2007	03/10/2013	Active	115G05		500152148
Whitehorse	YC66105	Quartz	RORY	149	Coronation Minerals Inc - 100%	03/10/2007	30/09/2007	03/10/2013	Active	115G05		500152149
Whitehorse	YC66106	Quartz	RORY	150	Coronation Minerals Inc - 100%	03/10/2007	30/09/2007	03/10/2013	Active	115G05		500152150
Whitehorse	YC66107	Quartz	RORY	151	Coronation Minerals Inc - 100%	03/10/2007	30/09/2007	03/10/2013	Active	115G05		500152179
Whitehorse	YC66108	Quartz	RORY	152	Coronation Minerals Inc - 100%	03/10/2007	30/09/2007	03/10/2013	Active	115G05		500152180
Whitehorse	YC66109	Quartz	RORY	153	Coronation Minerals Inc - 100%	03/10/2007	30/09/2007	03/10/2013	Active	115G05		500152181
Whitehorse	YC66110	Quartz	RORY	154	Coronation Minerals Inc - 100%	03/10/2007	30/09/2007	03/10/2013	Active	115G05		500152182
Whitehorse	YC66111	Quartz	RORY	155	Coronation Minerals Inc - 100%	03/10/2007	30/09/2007	03/10/2013	Active	115G05		500152183
Whitehorse	YC66112	Quartz	RORY	156	Coronation Minerals Inc - 100%	03/10/2007	30/09/2007	03/10/2013	Active	115G05		500152184
Whitehorse	YC66113	Quartz	RORY	157	Coronation Minerals Inc - 100%	03/10/2007	30/09/2007	03/10/2013	Active	115G05		500152185
Whitehorse	YC66114	Quartz	RORY	158	Coronation Minerals Inc - 100%	03/10/2007	30/09/2007	03/10/2013	Active	115G05		500152186
Whitehorse	YC66115	Quartz	RORY	159	Coronation Minerals Inc - 100%	03/10/2007	30/09/2007	03/10/2013	Active	115G05		500152187
Whitehorse	YC66116	Quartz	RORY	160	Coronation Minerals Inc - 100%	03/10/2007	30/09/2007	03/10/2013	Active	115G05		500152188
Whitehorse	YC66117	Quartz	RORY	161	Coronation Minerals Inc - 100%	03/10/2007	30/09/2007	03/10/2013	Active	115G05		500152189
Whitehorse	YC66118	Quartz	RORY	162	Coronation Minerals Inc - 100%	03/10/2007	30/09/2007	03/10/2013	Active	115G05		500152190
Whitehorse	YC66119	Quartz	RORY	163	Coronation Minerals Inc - 100%	03/10/2007	30/09/2007	03/10/2013	Active	115G05		500152191
Whitehorse	YC66120	Quartz	RORY	164	Coronation Minerals Inc - 100%	03/10/2007	30/09/2007	03/10/2013	Active	115G05		500152192
Whitehorse	YC66121	Quartz	RORY	165	Coronation Minerals Inc - 100%	03/10/2007	30/09/2007	03/10/2013	Active	115G05		500152193
Whitehorse	YC66122	Quartz	RORY	166	Coronation Minerals Inc - 100%	03/10/2007	30/09/2007	03/10/2013	Active	115G05		500152194
Whitehorse	YC66123	Quartz	RORY	167	Coronation Minerals Inc - 100%	03/10/2007	30/09/2007	03/10/2013	Active	115G05		500152195
Whitehorse	YC66124	Quartz	RORY	168	Coronation Minerals Inc - 100%	03/10/2007	30/09/2007	03/10/2013	Active	115G05		500152196
Whitehorse	YC66125	Quartz	RORY	169	Coronation Minerals Inc - 100%	03/10/2007	30/09/2007	03/10/2013	Active	115G05		500152197
Whitehorse	YC66126	Quartz	RORY	170	Coronation Minerals Inc - 100%	03/10/2007	30/09/2007	03/10/2013	Active	115G05		500152198
Whitehorse	YC66127	Quartz	RORY	171	Coronation Minerals Inc - 100%	03/10/2007	30/09/2007	03/10/2013	Active	115G05		500152199
Whitehorse	YC66128	Quartz	RORY	172	Coronation Minerals Inc - 100%	03/10/2007	30/09/2007	03/10/2013	Active	115G05		500152200
Whitehorse	YC66129	Quartz	RORY	173	Coronation Minerals Inc - 100%	03/10/2007	30/09/2007	03/10/2013	Active	115G05		500152201
Whitehorse	YC66130	Quartz	RORY	174	Coronation Minerals Inc - 100%	03/10/2007	30/09/2007	03/10/2013	Active	115G05		500152202
Whitehorse	YC66131	Quartz	RORY	175	Coronation Minerals Inc - 100%	03/10/2007	30/09/2007	03/10/2013	Active	115G05		500152203
Whitehorse	YC66132	Quartz	RORY	176	Coronation Minerals Inc - 100%	03/10/2007	30/09/2007	03/10/2013	Active	115G05		500152204
Whitehorse	YC66133	Quartz	RORY	177	Coronation Minerals Inc - 100%	03/10/2007	30/09/2007	03/10/2013	Active	115G05		500152205
Whitehorse	YC66134	Quartz	RORY	178	Coronation Minerals Inc - 100%	03/10/2007	30/09/2007	03/10/2013	Active	115G05		500152206
Whitehorse	YC66135	Quartz	RORY	179	Coronation Minerals Inc - 100%	03/10/2007	30/09/2007	03/10/2013	Active	115G05		500152232
Whitehorse	YC66136	Quartz	RORY	180	Coronation Minerals Inc - 100%	03/10/2007	30/09/2007	03/10/2013	Active	115G05		500152233

Source: Yukon Geological Survey (http://mapservices.gov.yk.ca/YGS/WebMap.aspx

List of claims

©TerraNotes Ltd 2007-2013

District	GrantNumber	RegType	ClaimName	ClaimNbr	Claim Owner	OperationRecordingDate	StakingDate	ClaimExpiryDate	Status	NTS MapNumber	NonStdSize	Ops Number
Whitehorse	YC66137	Quartz	RORY	181	Coronation Minerals Inc - 100%	03/10/2007	30/09/2007	03/10/2013	Active	115G05		500152234
Whitehorse	YC66138	Quartz	RORY	182	Coronation Minerals Inc - 100%	03/10/2007	30/09/2007	03/10/2013	Active	115G05		500152235
Whitehorse	YC66139	Quartz	RORY	183	Coronation Minerals Inc - 100%	03/10/2007	30/09/2007	03/10/2013	Active	115G05		500152236
Whitehorse	YC66140	Quartz	RORY	184	Coronation Minerals Inc - 100%	03/10/2007	30/09/2007	03/10/2013	Active	115G05		500152237
Whitehorse	YC66141	Quartz	RORY	185	Coronation Minerals Inc - 100%	03/10/2007	30/09/2007	03/10/2013	Active	115G05		500152238
Whitehorse	YC66142	Quartz	RORY	186	Coronation Minerals Inc - 100%	03/10/2007	30/09/2007	03/10/2013	Active	115G05		500152239
Whitehorse	YC66143	Quartz	RORY	187	Coronation Minerals Inc - 100%	03/10/2007	30/09/2007	03/10/2013	Active	115G05		500152240
Whitehorse	YC66144	Quartz	RORY	188	Coronation Minerals Inc - 100%	03/10/2007	30/09/2007	03/10/2013	Active	115G05		500152241
Whitehorse	YC66145	Quartz	RORY	189	Coronation Minerals Inc - 100%	03/10/2007	30/09/2007	03/10/2013	Active	115G05		500152242
Whitehorse	YC66146	Quartz	RORY	190	Coronation Minerals Inc - 100%	03/10/2007	30/09/2007	03/10/2013	Active	115G05		500152243
Whitehorse	YC66147	Quartz	RORY	191	Coronation Minerals Inc - 100%	03/10/2007	30/09/2007	03/10/2013	Active	115G05		500152244
Whitehorse	YC66148	Quartz	RORY	192	Coronation Minerals Inc - 100%	03/10/2007	30/09/2007	03/10/2013	Active	115G05		500152245
Whitehorse	YC66149	Quartz	RORY	193	Coronation Minerals Inc - 100%	03/10/2007	30/09/2007	03/10/2013	Active	115G05		500152246
Whitehorse	YC66150	Quartz	RORY	194	Coronation Minerals Inc - 100%	03/10/2007	30/09/2007	03/10/2013	Active	115G05		500152247
Whitehorse	YC66151	Quartz	RORY	195	Coronation Minerals Inc - 100%	03/10/2007	30/09/2007	03/10/2013	Active	115G05		500152248
Whitehorse	YC66152	Quartz	RORY	196	Coronation Minerals Inc - 100%	03/10/2007	30/09/2007	03/10/2013	Active	115G05		500152249
Whitehorse	YC66153	Quartz	RORY	197	Coronation Minerals Inc - 100%	03/10/2007	30/09/2007	03/10/2013	Active	115G05		500152250
Whitehorse	YC66154	Quartz	RORY	198	Coronation Minerals Inc - 100%	03/10/2007	30/09/2007	03/10/2013	Active	115G05		500152251
Whitehorse	YC66155	Quartz	RORY	199	Coronation Minerals Inc - 100%	03/10/2007	30/09/2007	03/10/2013	Active	115G05		500152252
Whitehorse	YC66156	Quartz	RORY	200	Coronation Minerals Inc - 100%	03/10/2007	30/09/2007	03/10/2013	Active	115G05		500152253
Whitehorse	YC66157	Quartz	RORY	201	Coronation Minerals Inc - 100%	03/10/2007	30/09/2007	03/10/2013	Active	115G05		500152254
Whitehorse	YC66158	Quartz	RORY	202	Coronation Minerals Inc - 100%	03/10/2007	30/09/2007	03/10/2013	Active	115G05		500152255
Whitehorse	YC66159	Quartz	RORY	203	Coronation Minerals Inc - 100%	03/10/2007	30/09/2007	03/10/2013	Active	115G05		500152256
Whitehorse	YC66160	Quartz	RORY	204	Coronation Minerals Inc - 100%	03/10/2007	30/09/2007	03/10/2013	Active	115G05		500152281
Whitehorse	YC66161	Quartz	RORY	205	Coronation Minerals Inc - 100%	03/10/2007	30/09/2007	03/10/2013	Active	115G05		500152282
Whitehorse	YC66162	Quartz	RORY	206	Coronation Minerals Inc - 100%	03/10/2007	30/09/2007	03/10/2013	Active	115G05		500152283
Whitehorse	YC66163	Quartz	RORY	207	Coronation Minerals Inc - 100%	03/10/2007	30/09/2007	03/10/2013	Active	115G05		500152284
Whitehorse	YC66164	Quartz	RORY	208	Coronation Minerals Inc - 100%	03/10/2007	30/09/2007	03/10/2013	Active	115G05		500152285
Whitehorse	YC66165	Quartz	RORY	209	Coronation Minerals Inc - 100%	03/10/2007	30/09/2007	03/10/2013	Active	115G05		500152286
Whitehorse	YC66166	Quartz	RORY	210	Coronation Minerals Inc - 100%	03/10/2007	30/09/2007	03/10/2013	Active	115G05		500152287
Whitehorse	YC66167	Quartz	RORY	211	Coronation Minerals Inc - 100%	03/10/2007	30/09/2007	03/10/2013	Active	115G05		500152288
Whitehorse	YC66168	Quartz	RORY	212	Coronation Minerals Inc - 100%	03/10/2007	30/09/2007	03/10/2013	Active	115G05		500152289
Whitehorse	YC66169	Quartz	RORY	213	Coronation Minerals Inc - 100%	03/10/2007	30/09/2007	03/10/2013	Active	115G05		500152290
Whitehorse	YC66170	Quartz	RORY	214	Coronation Minerals Inc - 100%	03/10/2007	30/09/2007	03/10/2013	Active	115G05		500152291
Whitehorse	YC66171	Quartz	RORY	215	Coronation Minerals Inc - 100%	03/10/2007	30/09/2007	03/10/2013	Active	115G05		500152292
Whitehorse	YC66172	Quartz	RORY	216	Coronation Minerals Inc - 100%	03/10/2007	30/09/2007	03/10/2013	Active	115G05		500152293
Whitehorse	YC66173	Quartz	RORY	217	Coronation Minerals Inc - 100%	03/10/2007	30/09/2007	03/10/2013	Active	115G05		500152294
Whitehorse	YC66174	Quartz	RORY	218	Coronation Minerals Inc - 100%	03/10/2007	30/09/2007	03/10/2013	Active	115G05		500152295
Whitehorse	YC66175	Quartz	RORY	219	Coronation Minerals Inc - 100%	03/10/2007	30/09/2007	03/10/2013	Active	115G05		500152296
Whitehorse	YC66176	Quartz	RORY	220	Coronation Minerals Inc - 100%	03/10/2007	30/09/2007	03/10/2013	Active	115G05		500152297
Whitehorse	YC66177	Quartz	RORY	221	Coronation Minerals Inc - 100%	03/10/2007	30/09/2007	03/10/2013	Active	115G05		500152298
Whitehorse	YC66178	Quartz	RORY	222	Coronation Minerals Inc - 100%	03/10/2007	30/09/2007	03/10/2013	Active	115G05		500152299
Whitehorse	YC66179	Quartz	RORY	223	Coronation Minerals Inc - 100%	03/10/2007	30/09/2007	03/10/2013	Active	115G05		500152300
Whitehorse	YC66180	Quartz	RORY	224	Coronation Minerals Inc - 100%	03/10/2007	30/09/2007	03/10/2013	Active	115G05		500152301
Whitehorse	YC66181	Quartz	RORY	225	Coronation Minerals Inc - 100%	03/10/2007	30/09/2007	03/10/2013	Active	115G05		500152302
Whitehorse	YC66182	Quartz	RORY	226	Coronation Minerals Inc - 100%	03/10/2007	30/09/2007	03/10/2013	Active	115G05		500152303
Whitehorse	YC66183	Quartz	RORY	227	Coronation Minerals Inc - 100%	03/10/2007	30/09/2007	03/10/2013	Active	115G05		500152304
Whitehorse	YC66184	Quartz	RORY	228	Coronation Minerals Inc - 100%	03/10/2007	30/09/2007	03/10/2013	Active	115G05		500152318
Whitehorse	YC66185	Quartz	RORY	229	Coronation Minerals Inc - 100%	03/10/2007	30/09/2007	03/10/2013	Active	115G05		500152319
Whitehorse	YC66186	Quartz	RORY	230	Coronation Minerals Inc - 100%	03/10/2007	30/09/2007	03/10/2013	Active	115G05		500152320
Whitehorse	YC66187	Quartz	RORY	231	Coronation Minerals Inc - 100%	03/10/2007	30/09/2007	03/10/2013	Active	115G05		500152321
Whitehorse	YC66188	Quartz	RORY	232	Coronation Minerals Inc - 100%	03/10/2007	30/09/2007	03/10/2013	Active	115G05		500152322
Whitehorse	YC66189	Quartz	RORY	233	Coronation Minerals Inc - 100%	03/10/2007	30/09/2007	03/10/2013	Active	115G05		500152323
Whitehorse	YC66190	Quartz	RORY	234	Coronation Minerals Inc - 100%	03/10/2007	30/09/2007	03/10/2013	Active	115G05		500152324
Whitehorse	YC66191	Quartz	RORY	235	Coronation Minerals Inc - 100%	03/10/2007	30/09/2007	03/10/2013	Active	115G05		500152325
Whitehorse	YC66192	Quartz	RORY	236	Coronation Minerals Inc - 100%	03/10/2007	30/09/2007	03/10/2013	Active	115G05		500152326
Whitehorse	YC66193	Quartz	RORY	237	Coronation Minerals Inc - 100%	03/10/2007	30/09/2007	03/10/2013	Active	115G05		500152327
Whitehorse	YC66194	Quartz	RORY	238	Coronation Minerals Inc - 100%	03/10/2007	30/09/2007	03/10/2013	Active	115G05		500152328
Whitehorse	YC66195	Quartz	RORY	239	Coronation Minerals Inc - 100%	03/10/2007	30/09/2007	03/10/2013	Active	115G05		500152329
Whitehorse	YC66196	Quartz	RORY	240	Coronation Minerals Inc - 100%	03/10/2007	30/09/2007	03/10/2013	Active	115G05		500152330
Whitehorse	YC66197	Quartz	RORY	241	Coronation Minerals Inc - 100%	03/10/2007	30/09/2007	03/10/2013	Active	115G05		500152359
Whitehorse	YC66198	Quartz	RORY	242	Coronation Minerals Inc - 100%	03/10/2007	30/09/2007	03/10/2013	Active	115G05		500152360
Whitehorse	YC66199	Quartz	RORY	243	Coronation Minerals Inc - 100%	03/10/2007	30/09/2007	03/10/2013	Active	115G05		500152361
Whitehorse	YC66200	Quartz	RORY	244	Coronation Minerals Inc - 100%	03/10/2007	30/09/2007	03/10/2013	Active	115G05		500152362
Whitehorse	YC66201	Quartz	RORY	245	Coronation Minerals Inc - 100%	03/10/2007	30/09/2007	03/10/2013	Active	115G05		500152363
Whitehorse	YC66202	Quartz	RORY	246	Coronation Minerals Inc - 100%	03/10/2007	30/09/2007	03/10/2013	Active	115G05		500152364
Whitehorse	YC66203	Quartz	RORY	247	Coronation Minerals Inc - 100%	03/10/2007	30/09/2007	03/10/2013	Active	115G05		500152365
Whitehorse	YC66204	Quartz	RORY	248	Coronation Minerals Inc - 100%	03/10/2007	30/09/2007	03/10/2013	Active	115G05		500152366
Whitehorse	YC66205	Quartz	RORY	249	Coronation Minerals Inc - 100%	03/10/2007	30/09/2007	03/10/2013	Active	115G05		500152367
Whitehorse	YC66206	Quartz	RORY	250	Coronation Minerals Inc - 100%	03/10/2007	30/09/2007	03/10/2013	Active	115G05		500152368
Whitehorse	YC66207	Quartz	RORY	251	Coronation Minerals Inc - 100%	03/10/2007	30/09/2007	03/10/2013	Active	115G05		500152369
Whitehorse	YC66208	Quartz	RORY	252	Coronation Minerals Inc - 100%	03/10/2007	30/09/2007	03/10/2013	Active	115G05		500152370
Whitehorse	YC66209	Quartz	RORY	253	Coronation Minerals Inc - 100%	03/10/2007	30/09/2007	03/10/2013	Active	115G05		500152371
Whitehorse	YC66210	Quartz	RORY	254	Coronation Minerals Inc - 100%	03/10/2007	30/09/2007	03/10/2013	Active	115G05		500152372
Whitehorse	YC66211	Quartz	RORY	255	Coronation Minerals Inc - 100%	03/10/2007	30/09/2007	03/10/2013	Active	115G05		500152373
Whitehorse	YC66212	Quartz	RORY	256	Coronation Minerals Inc - 100%	03/10/2007	30/09/2007	03/10/2013	Active	115G05	Partial Qz fr (<25 acres)	500152374
Whitehorse	YC66213	Quartz	RORY	257	Coronation Minerals Inc - 100%	03/10/2007	30/09/2007	03/10/2013	Active	115G05		500152375
Whitehorse	YC66214	Quartz	RORY	258	Coronation Minerals Inc - 100%	03/10/2007	30/09/2007	03/10/2013	Active	115G05		500152376
Whitehorse	YC66215	Quartz	RORY	259	Coronation Minerals Inc - 100%	03/10/2007	30/09/2007	03/10/2013	Active	115G05		500152377
Whitehorse	YC66216	Quartz	RORY	260	Coronation Minerals Inc - 100%	03/10/2007	30/09/2007	03/10/2013	Active	115G05		500152378
Whitehorse	YC66217	Quartz	RORY	261	Coronation Minerals Inc - 100%	03/10/2007	30/09/2007	03/10/2013	Active	115G05		500152379
Whitehorse	YC66218	Quartz	RORY	262	Coronation Minerals Inc - 100%	03/10/2007	30/09/2007	03/10/2013	Active	115G05		500152380
Whitehorse	YC66219	Quartz	RORY	263	Coronation Minerals Inc - 100%	03/10/2007	30/09/2007	03/10/2013	Active	115G05		500152381
Whitehorse	YC66220	Quartz	RORY	264	Coronation Minerals Inc - 100%	03/10/2007	30/09/2007	03/10/2013	Active	115G06	Full Qz fr. (25+ acres)	500152382
Whitehorse	YC66221	Quartz	RORY	265	Coronation Minerals Inc - 100%	03/10/2007	30/09/2007	03/10/2013	Active	115G05	Partial Qz fr. (<25 acres)	500152383

Source: Yukon Geological Survey (http://mapservices.gov.yk.ca/YGS/WebMap.aspx

Certificate of Qualified Person

©TerraNotes Ltd 2007-2013

VOLKAN TUNCER, P.GEO.

I, Volkan Tuncer, P.Geo., residing at 85 Thorncliffe Park Drive Suite 515, Toronto, Ontario, do hereby certify that:

1. I am currently performing consulting geophysics to the mining and mineral exploration industry and I am currently under contract as a Chief Geophysicist with TerraNotes Ltd. with an office address of

25 Adelaide Street East, Suite 1040, Toronto, ON, Canada, M5C 3A1

2. This certificate applies to the report titles "*Geophysical Interpretation of the Rory Claim Group, Yukon*" with an effective date of Jan 03,2013.

3. I graduated from Istanbul University, Istanbul, Turkey, with B.Sc. degree in Geophysical Engineering in 1999. I received an M.Sc. degree from Istanbul Technical University, Geophysical Engineering Department, Istanbul, Turkey, in 2003 and another M.Sc. degree in Geophysics from, University of Alberta, Edmonton, Alberta, Canada in 2007. I have worked as a geophysicist for a total of 13 years since obtaining my B.Sc. degree. I am a practicing member of APEGGA (Member Number 95445) since 2008 and APGO (Registration Number 1976) since 2011.

I have read the definition of "qualified person" set out in National Instrument 43-101and certify that, by reason of my education, affiliation with professional associations (as defined in NI 43-101) and past relevant work experience. I fulfill the requirements to be a "qualified person" for the purposes of NI 43-101.

My relevant work experience for the purpose of this report.

Trainee Geophysicist, Yertek Mühendislik Araştırma ve Sondaj San. Tic. Ltd. Şti., 1999

Contract Geophysicist, Renteks, 2000-2003

Teaching and Research Assistant, Physics (Geophysical Sciences) Department, University of Alberta, 2003-2007

Geophysicist in Training, TerraNotes Ltd., 2007-2008.

Manager Geophysicist, TerraNotes Ltd., 2008-2010

Chief Geophysicist, TerraNotes Ltd., since 2010.

4. I have not visited the Rory claim group that is subject to this report.

5. I am responsible for authoring of the entire report.

6. I have not had prior involvement with the Rory claim group that is subject to this report.

Effective Date: Jan 03, 2012

SIGNED AND STAMPED

_____

Volkan Tuncer, P. Geo.